Nanostructuration of epoxy networks by using polyhedral oligomeric silsesquioxanes POSS and its copolymers

Jiangfeng Chen

N° d'ordre 2012-ISAL-0049 Année 2012

Thèse

présentée devant

l'Institut National des Sciences Appliquées de Lyon

pour obtenir

le grade de Docteur

École Doctorale : Matériaux de Lyon
Spécialité : Matériaux Polymères et Composites

par

Jiangfeng CHEN

Nanostructuration of Epoxy Networks by Using Polyhedral Oligomeric Silsesquioxanes POSS and Its Copolymers

---

Soutenue 8 Juin 2012 devant la Commission d'Examen :

JURY

Prof. LU	Canzhong	Fujian Institute of Structure of Matter, CAS	– Rapporteur
Prof. CHEN	Xudong	Sun Yat-sen University	– Rapporteur
Prof.GERARD	Jean-François	INSA Lyon	–Directrice de thèse
Prof DAI	Lizong	Xiamen University	– Directrice de thèse
Prof. Wu	Huihuang	Xiamen University	– Examinateur
Dr. XU	Yiting	Xiamen University	– Examinateur

INSA Direction de la Recherche - Ecoles Doctorales – Quinquennal 2011-2015

SIGLE	ECOLE DOCTORALE	NOM ET COORDONNEES DU RESPONSABLE
CHIMIE	**CHIMIE DE LYON** http://www.edchimie-lyon.fr M. Jean Marc LANCELIN Insa : R. GOURDON	M. Jean Marc LANCELIN Université Claude Bernard Lyon 1 Bât CPE 43 bd du 11 novembre 1918 69622 VILLEURBANNE Cedex Tél : 04.72.43 13 95 Fax : lancelin@hikari.cpe.fr
E.E.A.	**ELECTRONIQUE, ELECTROTECHNIQUE, AUTOMATIQUE** http://edeea.ec-lyon.fr Secrétariat : M.C. HAVGOUDOUKIAN eea@ec-lyon.fr	M. Gérard SCORLETTI Ecole Centrale de Lyon 36 avenue Guy de Collongue 69134 ECULLY Tél : 04.72.18 60 97 Fax : 04 78 43 37 17 Gerard.scorletti@ec-lyon.fr
E2M2	**EVOLUTION, ECOSYSTEME, MICROBIOLOGIE, MODELISATION** http://e2m2.universite-lyon.fr **Insa : H. CHARLES**	Mme Gudrun BORNETTE CNRS UMR 5023 LEHNA Université Claude Bernard Lyon 1 Bât Forel 43 bd du 11 novembre 1918 69622 VILLEURBANNE Cédex Tél : 04.72.43.12.94 e2m2@biomserv.univ-lyon1.fr
EDISS	**INTERDISCIPLINAIRE SCIENCES-SANTE** Sec : Safia Boudjema M. Didier REVEL Insa : M. LAGARDE	M. Didier REVEL Hôpital Cardiologique de Lyon Bâtiment Central 28 Avenue Doyen Lépine 69500 BRON Tél : 04.72.68 49 09 Fax :04 72 35 49 16 Didier.revel@creatis.uni-lyon1.fr
INFOMATHS	**INFORMATIQUE ET MATHEMATIQUES** http://infomaths.univ-lyon1.fr	M. Johannes KELLENDONK Université Claude Bernard Lyon 1 INFOMATHS Bâtiment Braconnier 43 bd du 11 novembre 1918 69622 VILLEURBANNE Cedex Tél : 04.72. 44.82.94 Fax 04 72 43 16 87 infomaths@univ-lyon1.fr
Matériaux	**MATERIAUX DE LYON** Secrétariat : M. LABOUNE PM : 71.70 –Fax : 87.12 Bat. Saint Exupéry Ed.materiaux@insa-lyon.fr	M. Jean Yves BUFFIERE INSA de Lyon MATEIS Bâtiment Saint Exupéry 7 avenue Jean Capelle 69621 VILLEURBANNE Cédex Tél : 04.72.43 83 18 Fax 04 72 43 85 28 Jean-yves.buffiere@insa-lyon.fr
MEGA	**MECANIQUE, ENERGETIQUE, GENIE CIVIL, ACOUSTIQUE** M. Jean Louis GUYADER Secrétariat : M. LABOUNE PM : 71.70 –Fax : 87.12	M. Jean Louis GUYADER INSA de Lyon Laboratoire de Vibrations et Acoustique Bâtiment Antoine de Saint Exupéry 25 bis avenue Jean Capelle 69621 VILLEURBANNE Cedex Tél :04.72.18.71.70 Fax : 04 72 43 72 37 mega@lva.insa-lyon.fr
ScSo	**ScSo*** M. OBADIA Lionel Insa : J.Y. TOUSSAINT	M. OBADIA Lionel Université Lyon 2 86 rue Pasteur 69365 LYON Cedex 07 Tél : 04.78.69.72.76 Fax : 04.37.28.04.48 Lionel.Obadia@univ-lyon2.fr

*ScSo : Histoire, Geographie, Aménagement, Urbanisme, Archéologie, Science politique, Sociologie, Anthropologie

Acknowlegements

I wish to express my sincere appreciation to those who have contributed to this thesis and supported me in one way or the other during this amazing journey.

First of all, I am pleased to thank my supervisors at the Laboratory of Macromolecular Materials of the INSA-Lyon, Jean-François Gérard and Jocelyne Galy, for having followed me attentively while at the same time trusting me and leaving me free to try different ideas and experiments. It was only due to their valuable guidance, cheerful enthusiasm and ever-friendly nature that I was able to complete my research work in a respectable manner. I am also grateful to the supervisor Professor DAI Lizong at Xiamen University for his detailed and constructive comments, and for his important support throughout this work. Their willingness to dialogueand their support in hard moments are something I will always remember. Merci beaucoup!

Many people on the faculty and staff of LMM/IMP assisted and encouraged me in various ways during my course of studies. I am especially grateful to Profs. Jean-Pierre Pascault, Alain Rousseau, Francoise Fenouillot, Jerome Dupue, Julien Bernard, Daniel Portinha and Etienne Fleury for all that they have taught me, for their valuable advices and friendly helps.

International exchanged PhD students often talk about loneliness during the course of their study but this is something which I never experienced at LMM/IMP.About my stay in Lyon, Arnaud, Cecile, Elsa, Redha, Nadia, Emily and Estella (translation from French, suggestions about all the practical aspects of living in France…Merci bien!), Pierre Alcouffe for the TEM pictures shown in this manuscript, Ruben Vera (UCBL-Lyon) for the WAXS experiments are also gratefully acknowledged to have shared with me great moments. I am also grateful for the hospitality and support of Hynek and Du Xian, our hiking experiences around Lyon and Grenoble are the treasure of my live. Special thanks to Antonella of kind helps, "Big thank you"!

Heartfelt thanks goes to Professor Xu Yiting, Luo Weiang, Zeng Birong, Liu Xinyu for kind helps. I will never forget their supports and for providing me numerous insipirations. I

would also like to take this opportunity to thank Professor Zhou Yousi, Dong Yanming, Lin Guoliang, for their very helpful comments and suggestions.

The members of Fujian Provence Key Lab of Fireproofing Materials in Xiamen University have contributed immensely to my personal and professional time at Xiamen University. The group has been a source of friendships as well as good advice and collaboration. I am especially grateful for the members who stuck it out in grad school with me: Lei guangcai, Deng Yuanming, Zheng Yifang, Peng Xiaoliang, Yangcangjie, Ma Yingying etc.

I would like to thank my parents, who through my childhood and study career had always encouraged me to follow my heart and inquisitive mind in any direction this took me. I would like to thank my wife Sarah whose faithful support during the stages of this Ph.D. is so appreciated. She has been a constant source of strength and inspiration. There were times during the past years when everything seemed hopeless and I didn't have any hope. Thank you sooo much !!!

Table of Contents

General Introductions

Hybrid Inorganic/Organic (*I/O*) polymeric materials are attracting a wide interest because they combine some excellent features of polymer (low density and easiness of synthesis-processing, high plasticity) with the ones of the inorganic materials (like high modulus and hardness, flame resistant and barrier properties).

Polyhedral oligomeric silsesquioxanes (POSS) as building blocks, because of the unique structure of the POSS macromer, is a well defined cluster with an inorganic silica-like core surrounded by eight organic corner groups. It is considered as the minimum silicate precursors, which forms silica after fully oxidation. POSS is incorporated into polymers to overcome the shortage of traditional composites which can't be dispersed in molecular lever in materials.

In the first dissetion, a new analogue of amino POSS (denoted as POSSMOCA) was synthesized via addition reaction, which was potential to be utilized in polymers and coating, such as polyurea and nylon. It was characterized by NMR, FTIR. The prereaction temperature was determined by DSC through heating the blend of POSSMOCA and epoxy precursors DGEBA. Introduced into epoxy network by the active amino group, POSSMOCA improved the thermostability, based on the synergic effect of silicon, nitrogen and halogen in POSSMOCA. It was worthy notifying that amorphous POSSMOCA, with a polar side chain and patterned POSS head, crystallized in epoxy network. A mechanism was hypothesized called as “Destructive Reaction-Induced Crystallization”, which explained the phenomena reliably. It would be meaningful to design new materials and develop new functional materials such as pH sensitive materials.

Epoxy/polyhedral oligomeric silsesquioxanes (POSS) hybrid composites were prepared from prereaction between trifunctional isobutyl- silsesquioxane trisilanol (POSS-OH) and diglycidyl ether of bisphenol A (DGEBA) via the reaction between silanol and the oxirane group. Three kinds of catalysts were utilized to facilitate the ring opening reaction. It was found that the incorporation of POSS-OH into epoxy allowed the incompleted condensed POSS cage linking to the DGEBA, and forming a spheral nanostructure in TEM by POSS cage as the crosslinking point. To reveal the mechanism of POSS silanol-epoxy ring open reaction, SEC and DSC was employed, finding epoxy homopolymerization by the condensation of POSS. It broke the balance

of epoxy with curing agent leading to glass transition temperature decreases dramatically, owing to the presence of POSS silanol.

A dioester terminated macro-initiator PGMA was homopolymerized via Reversible Addition-Fragmentation Transfer Polymerization utilizing CDB as a chain transferring agent. Then the second POSS block was copolymerized with PGMA macroinitiator. These epoxide POSS copolymers were characterized by Fourier transform infrared spectroscopy (FTIR), size exclusion chromatography (SEC), differential scanning calorimetric (DSC), thermal gravimetric analysis (TGA) and X ray diffraction (XRD). It was easy to tail the compatibility of the epoxide block copolymer with a matrix, through prereaction with monomer. Our block copolymer was possible to structure a nanophase easily in UV curing resins, optical waveguide devices.

Partial compatible POSS copolymers, such as poly methacrylate isobutyl/cyclohexyl POSS-co-methyl methacrylate random, diblock and triple-block copolymers, were characterized by fourier transform infrared spectroscopy (FTIR), size exclusion chromatography (SEC), differential scanning calorimetric (DSC) , thermal gravimetric analysis (TGA) and X ray diffraction (XRD). It was found that Tg decreased with the increase of POSS content, which was resulted from the declined molar mass and the free volumn of POSS. Compared with the isobutyl and cyclohexyl vertex group of POSS, the strong interaction of cyclohexyl lead to a higher Tg than that of isobutyl POSS. From the cloud point testing, the reation induced phase separation took place in the POSS-PMMA random copolymers. The thermostability of network introduced POSS copolymer was characterized, the silicate protective layer formed after flammation. From the reology of POSS copolymer modified DGEBA/MDEA, the dilution effect was influenced by the reaction induced phase separation. The dynamic of DGEBA/MDEA reation was determined by DSC, the dilution effect of POSS copolymers changed with the POSS loading in copolymers. *Tg* of epoxy at different conversion, was characterized and simulated with Couchman equation. In the composites, *Tg* was fitted with Gordon-Taylor equation and Kwei equation, which reflectd the interaction between modifier and DGEBA/MEDA/ epoxy/amine oligomers.

Chapter 1 Bibliographic review about POSS-based copolymers and nanocomposites

Hybrid materials generally consist of two molecular level dispersed organic and inorganic components. From the term early definition, hybrid materials was considered as mixtures of two or more materials with new properties created by new electron orbitals formed between each material.[1] There are two elements in the term: interaction between components and new properties different from component to component.

1.1 Polyhedral Oligomeric Silsesquioxanes, POSS

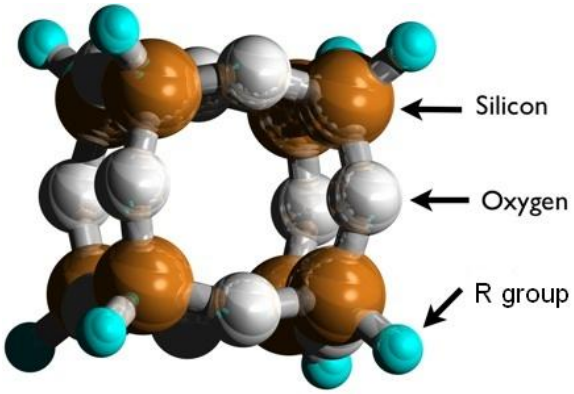

Figure 1.1. Polyhedral Oligomeric Silsesquioxanes

POSS is the acronym of Polyhedral Oligomeric Silsesquioxanes, referring to all structures with the empirical formula RSiO1.5, (Figure 1.1) where R is hydrogen or any alkyl, alkylene, aryl, arylene, or organofunctional derivative of alkyl, alkylene, aryl, or arylene groups[2]. The term "*silsesqui*" is referred to the ratio of the silicon and oxygen atoms, i.e. Si:O = 1:1.5. It is an incompletely oxided silicate compare with the formula of SiO_2. When the vertex group of POSS is oxided such as inflammation or oxygen-plasma, silica is obtained so that the POSS is viewed as a precursor of ceramic or "preceramic" [3]. Oligomeric silsesquioxanes with different molecular architectures, are shown as examples in the Figure 1.2[2]: Therefore, from POSS, it is able to create higher dimensionality through aggregation or crystallization of POSS macromers in the polymer matrix to build 1–3-dimensional scaffolds[4, 5].

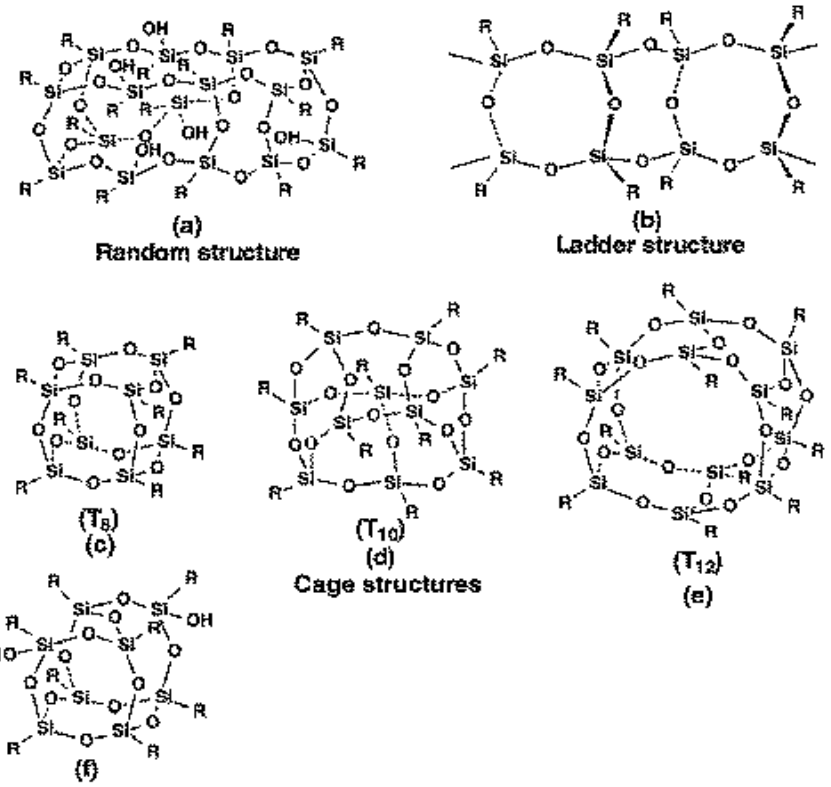

Figure 1.2 Structure of silsesquioxane

POSS molecules with a T_8 cubic inorganic core composed of silicon-oxygen ($R_8Si_8O_{12}$) are the most prevalent system studied; although the Q_8 structure ($R_8Si_8O_{20}$) has also attracted significant attention. Here, "*T*" and "*Q*" refer to conventional nomenclature from silicon nuclear magnetic resonance (NMR) literature, with *T* and *Q* referring to silicon atoms bonded to three or four oxygen atoms, respectively[6]. POSS cage could be described as three different bonding topology in bulk according to their reactive functionality: star (triple and above functionality), beadlike (difunctionality) and hang (monofunctionality) (Figure 1.3). However, the separated POSS point is difficult to be observed in bulk because the agglomeration is caused easily owing to the nanosize effect.

POSS structures were reported in 1946 Scott paper on completely condensed POSS cages. The major POSS manufactory marked the start-up of Hybrid Plastics in Fountain Valley, CA, was set up in the fall of 1998. It was funded by the Air Force Office of Scientific Research which enacts an excellent model to transit the collaboration of government–academic to the commercial sector. Besides Hybrid Plastics, Aldrich also supplies POSS laboratory reagent, but not so much as the

former. The research and commercialization of POSS started not early in China. As far as we know, Amwest Company was the only commercial organization which produces POSS monomer in China and provides Oct-vinyl, methyl, hydrogen, phenyl POSS.

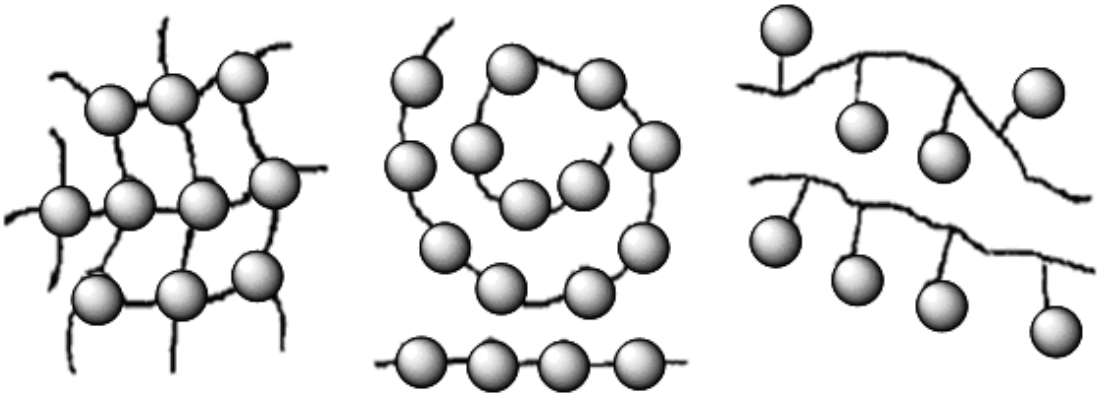

Figure 1.3 The topology of POSS in bulk via chemical bonding.

**In reality, the number of functionality decides the topology as a star-like (triple funcitional), bead (difunctional) and hanging (monofunctional).*

1.2 Preparation of POSS macromolecule

1.2.1.Metal coordinating polymerization

Carbon-based polymers offer fascinating perspectives and an enormous potential to improve the capacity of macromolecular materials with new dynamic properties. The preparation of polyhedral oligomeric metallasilsesquioxanes (POMSS) as a structural or functional model of silica supported metal catalyst attracts attentions. When metal coordinate with two POSS cage regularly, rather end-capping with one POSS cage, a novel linear polymer can be polymerized through the coordinating bond using POSS as the linkers and metal atoms as the nodes.(Figure 1.4)

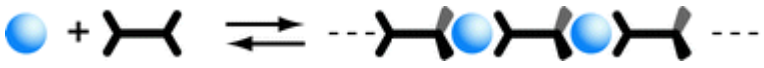

Figure 1.4 the mechanism of metal coordinating polymerization.

- *metal atom as the nodes and monomer as linkers.*

Hay[7] reacted titanium(*IV*) isopropoxide with a dilute THF solution containing a stoichiometric amount of Phenyl POSS tetrasilanol under a nitrogen atmosphere(Figure 1.5). The product was sparingly soluble or insoluble in common organic solvents. There was a large T_3 peak at-79.1 ppm and a much smaller T_2 peak at -70.2 ppm in solid-state ^{29}Si NMR spectrum. The smaller T_2 resonance was ascribed to silanol silicons on the end of the polymer chain, whereas the large T_3 resonance corresponded to the remaining internal silicones within the coordination polymer. The estimated number averaged degree of polymerization was 40, calculated from integrated ratio between the T_3 and T_2 silicon. Some soluble in acetone was characterized by MALDITOF, Four major fragments at 5562.03 m/z, 4449.51 m/z, 3335.73 m/z, and 2223.26 m/z were detected under positive ion conditions. These showed a good agreement with small oligomers, having the general formula $((C_6H_5)_8Si_8O_{14}Ti)_n$ (n=5, 4, 3, 2) with all four species having lost three or four H^+.

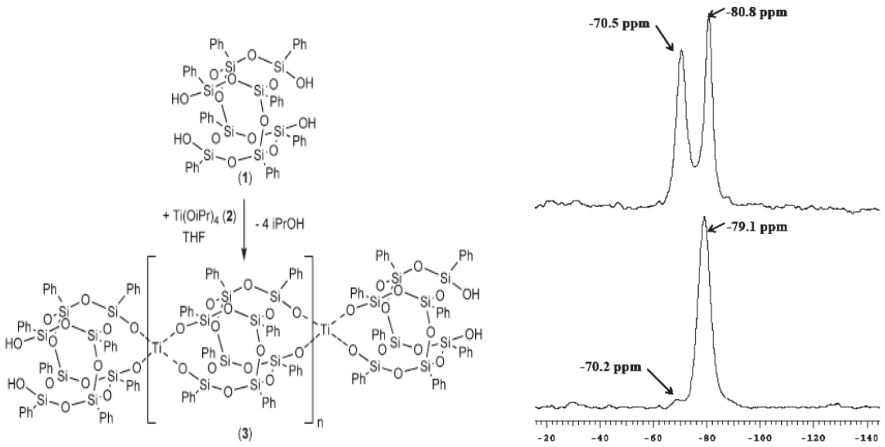

Figure 1.5 Metal coordinating polymerization of POSS

***** *Linear POSS-Ti polymer fabricated by POSS as linkers and Ti atom as nodes. In the ^{29}Si NMR, DP was calculated from the ratio of -70.2 ppm (silanol silicon on the end of chain) and -79.1 ppm (the remaining internal silicone). [7]*

1.2.2.Random radical polymerization

As other commercial polymer materials, the most common and useful method for synthesizing polymers is free radical polymerization. Unsaturated functional POSS was introduced into polymer via the radical polymerization frequently, homopolymerization and copolymerization, to tune the performance and compatibility

of POSS polymer. Many monomers bearing carbon double bond were polymerized via free radical polymerization, such as vinyl pyrrolidone[8, 9] ethylene[9] propylene[10], styrene,[11] methacrylate,[12-14] acrylate[14], norbornene[15]

When it own two or more functional groups for polymerization, a network is obtained, with multifunctional POSS as curing point. However, it is difficult to arrive the fully conversion of POSS, considering its steric hinderance. Yang[8] copolymerized a series of poly(vinyl pyrrolidone-co-octavinyl polyhedral oligomeric silsesquioxanes) (PVP-POSS) organic-inorganic hybrid nanocomposites containing different percentages of POSS via free radical polymerization. The average numbers of reacted vinyl groups for octavinyl-POSS macromer are calculated to be 5–7, which depends on POSS feed ratios. It is to conclude that the improvements in thermal properties (*Tg* and *Tdec*) resulted from crosslinking structure and dipole–dipole interaction between POSS cores and PVP carbonyl groups.

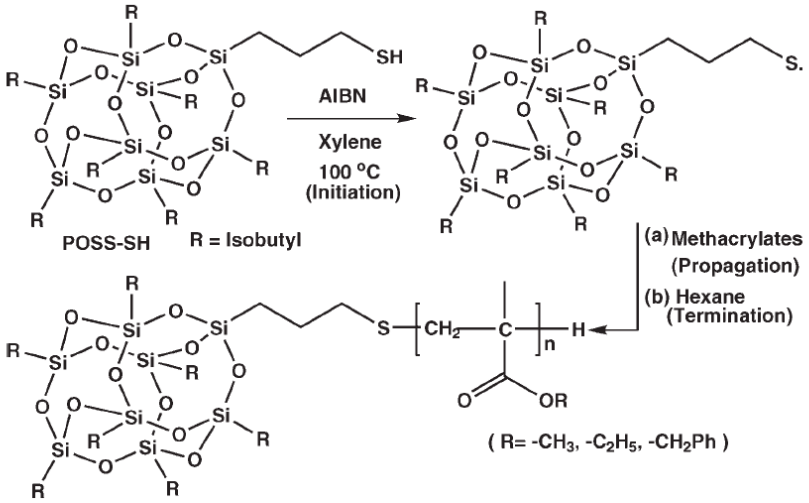

Figure 1.6 Mercaptan POSS compounds as radical chain transfer agents controlled the degree of polymerization and obtain POSS endcapping polymer.

Xu et al[16, 17]prepared copolymers of Poly-(vinylpyrrolidoneco-isobutylstyryl-POSS) and poly (acetoxystyrene-coisobutylstyryl-POSS) using a conventional free radical polymerization technique. The interaction between POSS and polar comonomer was characterized, which was positive to the performance of polymer. Mercaptan-based compounds as radical chain transfer agents was well established as a method to control the degree of polymerization or to terminate growing chains [18]. Katol[19]synthesized Polyhedral oligomeric silsesquioxanes (POSS)-polymethacrylate hybrids, such as POSS-poly(methyl methacrylate) (POSS-PMMA), POSS-poly(ethyl methacrylate) (POSS-PEMA), and POSS-poly(benzyl methacrylate)

(POSS-PBzMA) with controllable molecular weights and low polydispersities by thiol-mediated radical polymerization at elevated temperature, mediated with POSS-SH(Figure 1.6). In our opinion, it is dubiously that the decreased *Tg* of copolymer was conclude to the POSS content, because the *Mn* decreases obviously (from 26k D to 5K D). POSS-PMMA hybrid material showed physical aging[20] properties through annealing.

Besides the solution polymerization, the emulsion polymerization and the bulk polymerization were attested as efficient methods to synthesize POSS containing polymer. It was possible to fabricate POSS into polymer via hydrolysis of silane monomer for instance, a series of trimethoxysilylpropyl methacrylate copolymer latexes, with good film-forming behavior either[21]. In this case, the trimethoxysilylpropyl methacrylate co-unit may be considered as the sol-gel-type precursor of a multifunctional POSS. Valter Castelvetro[22] described POSS emulsion and miniemulsion free radical polymerization in details. It is observed that the highly water-insoluble POSS would be inefficient in supporting both particle nucleation and particle growth in emulsion polymerization, leading to lower conversion of POSS. The introduction of POSS nanoparticles linked to the macromolecules caused an increase of both modulus and tensile strength of the nanocomposite sheets prepared by casting, as well as a net reduction of the elongation at break.

To polymerize POSS containing polymer in bulk, the temperature higher than melting point of POSS monomer was chosen to change the solid powder to a liquid phase as Figure 1.7. The wide molecular weight distribution of products was a demerit of bulk polymerization (*PDI*>3.7) .

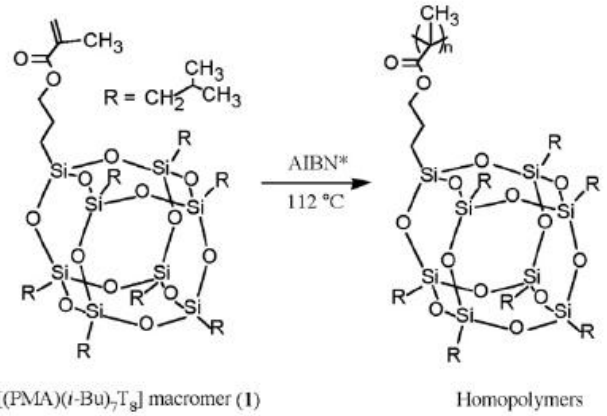

Figure 1.7 POSS homopolymer was synthesized via bulk polymerization, at elevated temperature higher than melting point.

1.2.3. Ring-opening metathesis polymerization

Kwon et al[23] used cyclopentyl-POSS-norbornene (POSS-NBE) monomer as the first block in the block copolymer. Living poly(POSS-NBE) with controlled molecular weight and narrow molecular weight distribution was produced in the presence of catalyst $RuCl_2(=CHPh)(PCy_3)_2$. Then, poly(POSS-NBE-b-MTD) copolymers were successfully prepared, in which sequential monomer addition of methyltetracyclododecene(MTD) to end living poly(POSS-NBE) chain was utilized to achieve quantitative crossover efficiency(Figure 1.8).

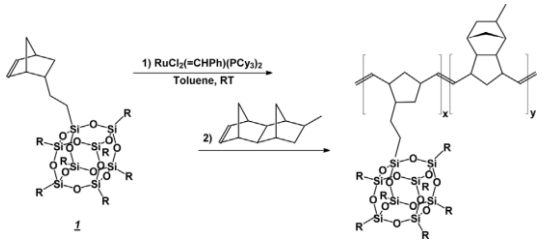

Figure 1.8 Ring-opening metathesis polymerization of norbornene POSS.[23]

1.2.4. "Grafting"

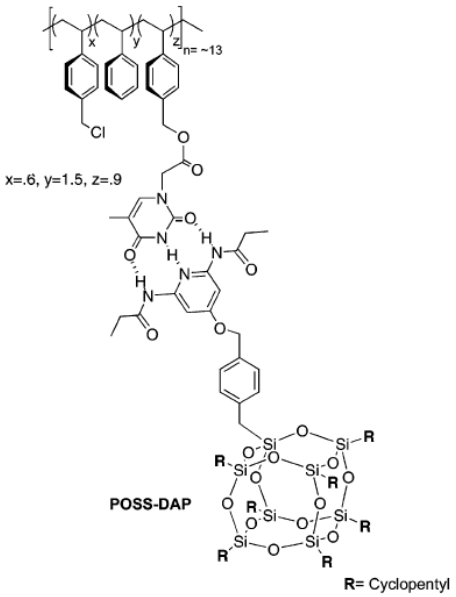

Figure 1.9 In"plug and play" method, POSS is grafted to the polystyrene mainchain efficiently. **[24]**

Considering the steric hinderance of POSS, conversion of monomer and the degree of polymerization is limited. Grafting reaction via the polyaddition, polycondensation or hydrogen bonding breaks the limitation of radical polymerization

efficiently. It is one of the hottest research areas of POSS containing polymer. Haddad et al[25] functionalized the triblock copolymer of polystyrene-butadiene-polystyrene (SBS) grafting polyhedral oligomeric silsesquioxane (POSS) molecules by the hydrosilation between the block copolymer and POSS molecule.

Using "plug and play" tailored polymeric systems (Figure 1.9), the efficiency and specificity of interactions between polymers and guests can be tailored through choice of recognition element. Cyclopentyl-POSS-diaminopyridine (POSS-DAP) was synthesized in one step via substitution of 4-hydroxydiamidopyridine with cyclopentyl-POSS-benzyl chloride. Via hydrogen bonding, the grafting reaction took place between the diamidopyridine-functionalized POSS monomer (POSSDAP) and thymine-functionalized copolymer[24].

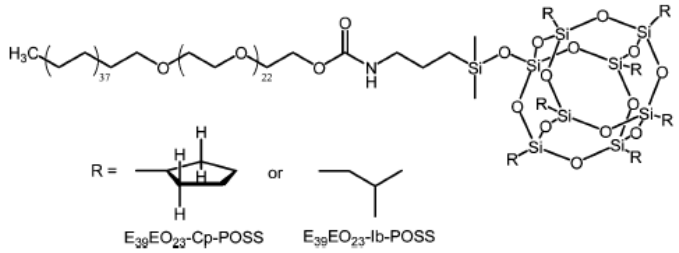

Figure 1.10 Isocyanate-Cp-POSS and Isocyanate-iBu-POSS were graft to a hydroxyl terminated block copolymer**. [26]**

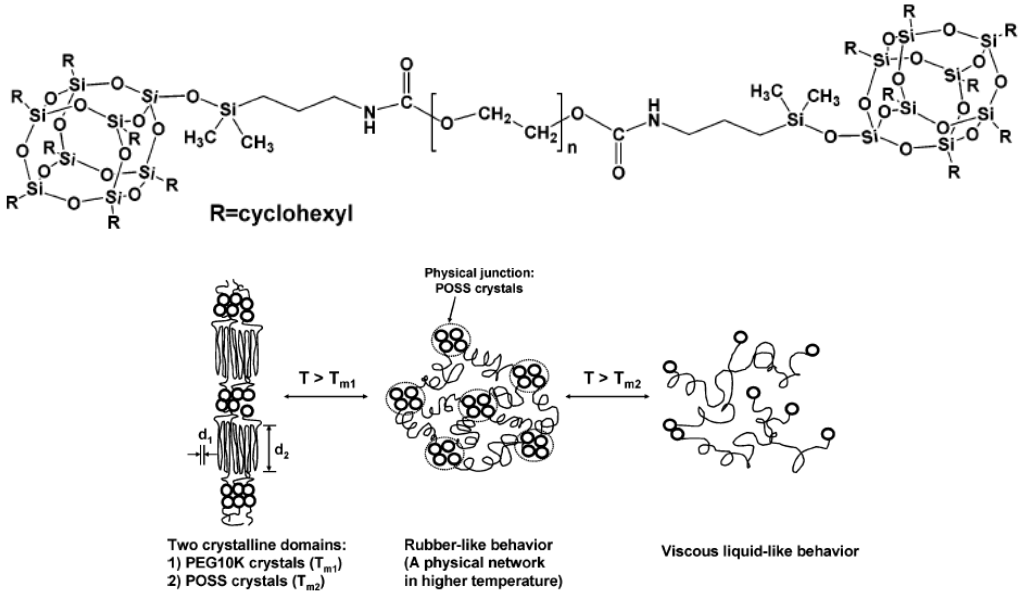

Figure 1.11 POSS end-capping PEG, which performances two metling stages because of PEG and POSS with metling temperatures.

Isocyanatopropyl dimethylsilycyclohexyl-POSS grafted to Poly(ethylene glycol) was prepared by Mather[26],[27](Figure 1.10). It was proposed that at low temperature, both PEO (as folded lamellae) and POSS (as self-aggregates) crystalline phases coexist as a solid. Above the melting point of the PEO crystallites, the PEO crystalline phase disappeared while POSS crystallites, acting as physical cross-linking sites, preserved solid rheological character. Finally, with increasing the temperature above an order-disorder transition, the amphiphilic POSS telechelics becomes fluid (Figure 1.11). Via the polycondensation reaction, POSS as a hydroxyl resource reacted with the comonomer was introduced into PET[28-30], PC[31, 32] efficiently.

1.2.5 Ring open polymerization

Yoshiki Chujo[33] synthesized the hybrid micelles derived from CubePOZO with both seven hydrophobic cyclopentyl groups of POSS and polyoxazoline (POZO) , which played a role of a hydrophilic segment by ring opening reaction initiated by I-POSS (Figure 1.12).

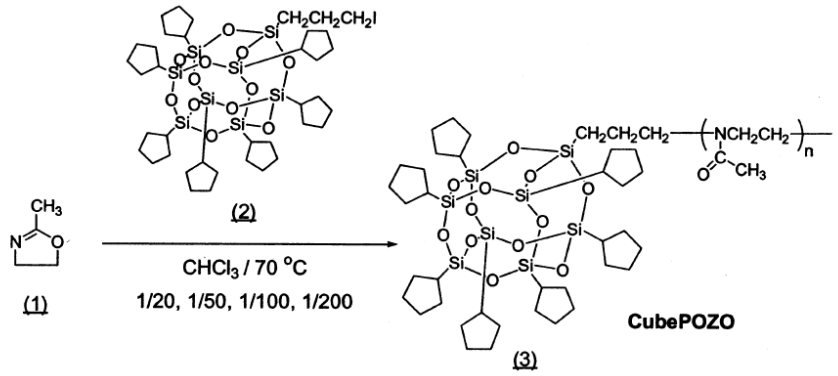

Figure 1.12 I-POSS initiated oxazoline ring opening polymerization. [33]

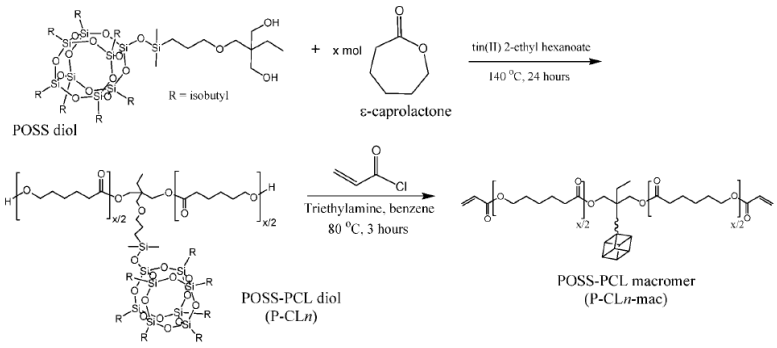

Figure 1.13 POSS diol as a difunctional initiator to synthesize polycaprolactone which is photocurable by the end-capping carbon double bond. **[34]**

Lee et al[34] used the POSS diol as a difunctional initiator, synthesized a biodegradable telechelics polycaprolactone. End-capping unsaturated carbon double bond, it was photocured by photoradical generator (2,2-dimethoxy-2-phenylacetophenone). There were double network after photocuring, the physical curing part of POSS and chemical curing part of photoradical generator (Figure 1.13).

Zheng[35] used 3-hydroxypropylheptaphenyl polyhedral oligomeric silsesquioxane (POSS) as the initiator for the ring-opening polymerization of ε-caprolactone (CL) to prepare the POSS-capped polycaprolactone catalyzed by stannous(*II*) octanoate ($Sn(Oct)_2$). When it was introduced into DGEBA/MOCA thermosetting matrix, compared to the binary blends of epoxy with PCL, there was less PCL chains that was mixed with epoxy matrix in the nanocomposites; i.e., the plasticization of PCL chains on the epoxy matrix would be effectively weakened, and thus the higher *Tg*'s of epoxy matrix were exhibited(Figure 1.14).

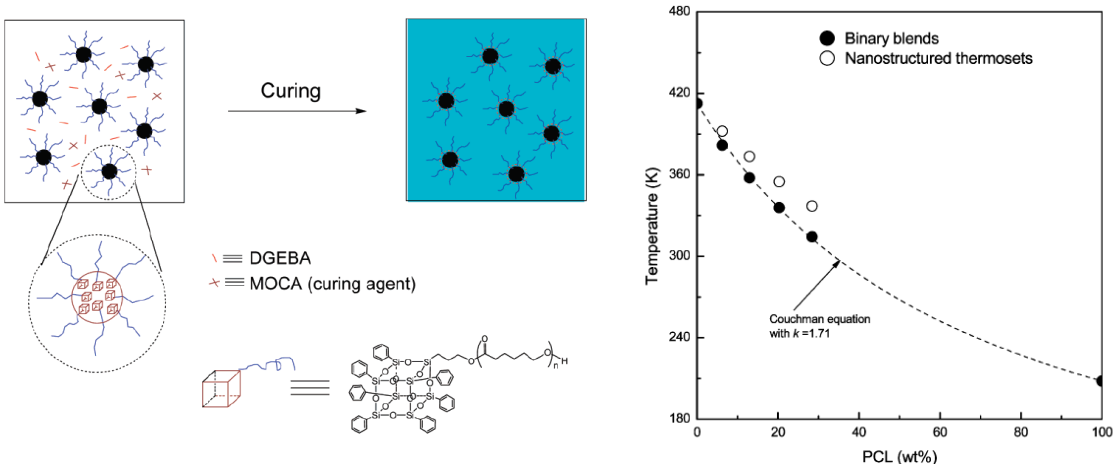

Figure 1.14 Polycaprolactone initiated by hydroxyl end POSS

** Catalyzed with tin catalyst，which self-assembled into micelle and constrained the plasticizer effect of thermoplastic chain. [35]*

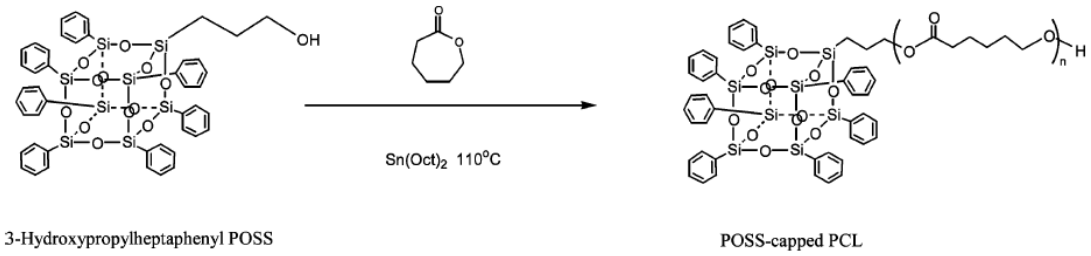

Figure 1.15 Polycaprolactone was initiated by hydroxyl POSS and catalyzed with $Sn(Oct)_2$. [36]

Ni et al[36] fabricated a supramolecular inclusion complexes (*ICs*) using the above POSS-capped PCL(Figure 1.15) and α-cyclodextrin (*α*-CD). Because of the presence of the bulky silsesquioxane terminal group, the inclusion complexation between *α*-CD and the POSS-capped PCL was carried out, only with a single end of a PCL chain threading inside the cavity of *α*-CD (-cyclodextrin). The inclusion of POSS depends on the length of PCL chain. When the PCL chains were shorter (e.g., for the POSS-capped PCL of *Mn* = 1720 or 2490), the efficiency of the inclusion complexation decreased, which could be attributed to the lower mobility of the bulky POSS groups which restrict the motion of the PCL chain.

Poly(butylene terephthalate) (PBT) is an important semicrystalline engineering thermoplastic with many valuable properties including a high rate of crystallization, good solvent resistance, thermal stability, and excellent processing properties. Wu[37] prepared a (PBT)/(POSS) nanocomposites by ring-opening polymerization of cyclic poly(butylene terephthalate) initiated by functionalized POSS, which played the role of nucleating agent in the process of crystallization of PBT(Figure 1.16)

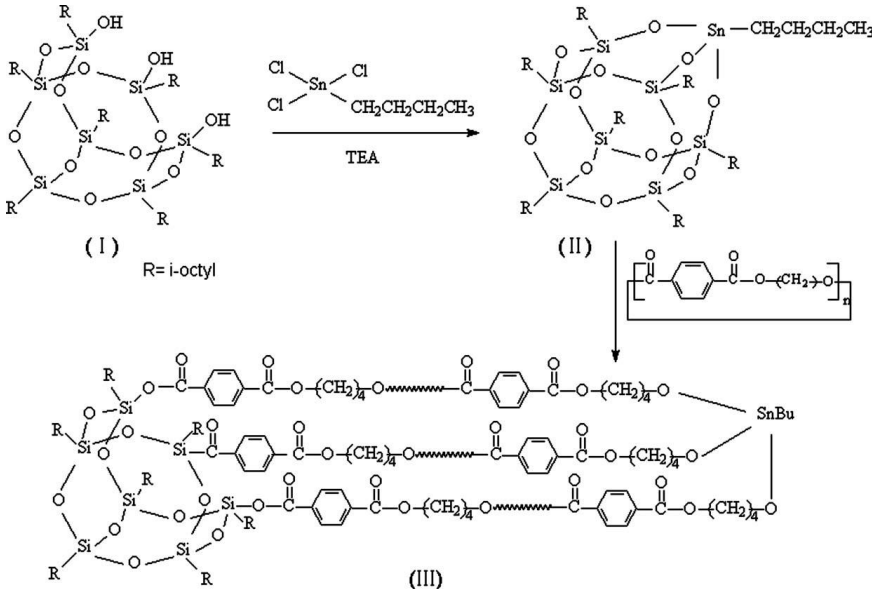

Figure 1.16 (PBT)/ (POSS) nanocomposites

**synthesized by ring-opening polymerization of cyclic poly(butylene terephthalate) initiated by functionalized POSS.[37]*

1.2.6 Controllable polymerization

I. Atom transfer radical polymerization (ATRP): Atom transfer radical polymerization (ATRP) had attracted the most attentions of POSS polymer controllable polymerization. Reagent with a halogen atom such as (Br, Cl) initiated the polymerization of methacrylate POSS effectively. Linear[38], star[39], branching[40] polymers containing POSS were successfully synthesized via ATRP. Matyjaszewski et al. synthesized ((MA-POSS)-co-BA-co-(MA-POSS) block copolymers by the ATRP of methacrylate functionalized POSS monomers [41]. The limited *DP* of pMA-POSS by ATRP is relatively low, about 15. Because the active center of ATRP is the chelating metal ion, which is of huge volume, moreover the steric hinderance of POSS center as a side group for methacrylate monomer. Successfully, POSS with halogen atom was utilized as initiator of ATRP. For instance, Fei[42] synthesized a block copolymer containging PMMA and PS diblock, initiated by *1*-chlorine-*3,5,7,9,11,13,15*-cyclopentyl polyhedral oligomeric silsesquioxane (POSS-Cl) with CuCl/ bipyridine. Ohno et al[43] used incompletely condensed POSS to synthesize a ATRP initiator with 2-bromoisobutyl group and chlorosulfonyl group, providing tadpole-shaped polymers with an "inorganic head" of POSS and an "organic tail".

II. Live anion polymerization: The live anion polymerization is viewed as another method to synthesized POSS-containing block copolymer and further overcome the limitation of other methods such as ATRP, leading to a well-defined hierarchical structure containing POSS sheets in polymer films.

The pioneer work was initiated by Hayakawa et al[44]. In 2008, two kinds of POSS-containing BCP's, namely PMMA-b-PMAPOSS and PS-b-PMAPOSS, were synthesized by living anionic polymerization. *Sec*-BuLi initiator and the living chain of polystyrene (PS) are highly reactive reagents and selectively attack carbonyl groups. High *DP* of POSS chain $DP_{(PMMA\text{-}b\text{-}PMAPOSS)}$=30 and $DP_{(PS\text{-}b\text{-}PMAPOSS)}$ =21 was successfully obtained which is higher than the limitation of *DP* by ATRP(*DP*=16). After that, POSS-MMA, POSS-St copolymers with high DP(PS_{69}-b-$PMAPOSS_{47}$, $PMMA_{41}$-b-$PMAPOSS_{29}$) were synthesized by anion polymerization [45]. The high DP functional POSS macroinitiator was achieved with a Molar Mass of 92500 (DP=98). PS_{52}-b-$PMAPOSS_9$. $PMMA_{450}$-b-$PMAPOSS_7$ and PS_{587}-b-$PMAPOSS_4$ with a PMAPOSS volume fraction of 13% and 4%, respectively, show

spherical PMAPOSS morphologies. Well-defined lamellar structures were observed for the $PMMA_{262}$-b-$PMAPOSS_{23}$ and PS_{266}-b-$PMAPOSS_{20}$ with PMAPOSS volume fractions of 44% and 37%, respectively. For the $PMMA_{52}$-b-$PMAPOSS_{18}$ and PS_{52}-b-$PMAPOSS_{9}$ with PMAPOSS volume fraction of 77% and 58%, respectively, cylindrical morphology was observed (Figure 1.17).

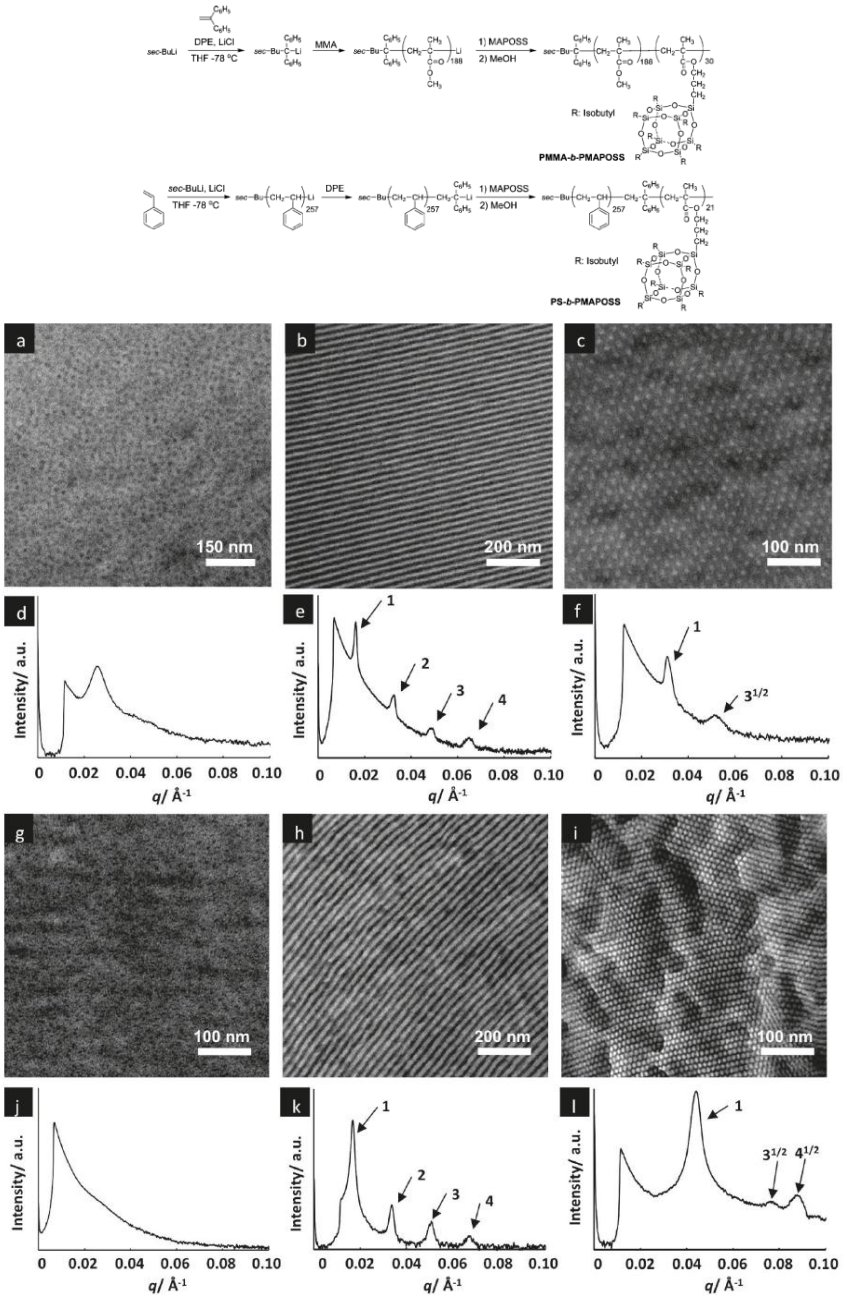

Figure 1.17 The protocol of live anion polymerization of POSS.

**TEM and TSAXS profiles of (a, d) PMMA450-b-PMAPOSS7, (b, e) PMMA262-b-PMAPOSS23, (c, f) PMMA52-b-PMAPOSS18, (g, j)PS587-b-PMAPOSS4, (h, k) PS266-b-PMAPOSS20, and (i, l)*

III. Reversible addition-fragmentation transfer polymerization *RAFT*: Reversible addition-fragmentation transfer polymerization(*RAFT*), as a novel living radical polymerization technique, has attracted great attentions, as it can be applied to a wide range of monomers containing a carboxyl[46-48], amino[49] and ionic group[50], and lower requirement of polymerization medium such as aqueous solution[51].

Zhang Weian synthesized the first POSS *RAFT* agent, "tadpole-shaped" POSS and it was empolyed in synthesis of POSS end-capping polymer. Monofunctional POSS molecule was used as an initiator with a topology of "tadpole-shaped". This chain transfering reagent was used to produce tadpole-shaped organic/inorganic hybrid Poly(N-isopropylacrylamide) (PNIPAM) [52], which exhibited a change in volume in response to external temperature changes[53].

Moreover, Polystyrene homopolymer and Polystyrene-methyl acrylate block copolymer were synthesized via the POSS bearing chain transferring agent[54]. Poly(tert-butyl acrylate) was prepared by *RAFT* polymerization of tert-butyl acrylate (tBA) using a POSS-containing chain transfer agent (*CTA*) [55]. POSS-PtBA was further hydrolyzed into amphiphilic, tadpole-shaped poly(acrylic acid) (POSSPAA). The *z*-average hydrodynamic radius decreased when *pH* decreased from 8.5 to 4, due to protonation and the resulting contraction of the PAA chains (Figure 1.18).

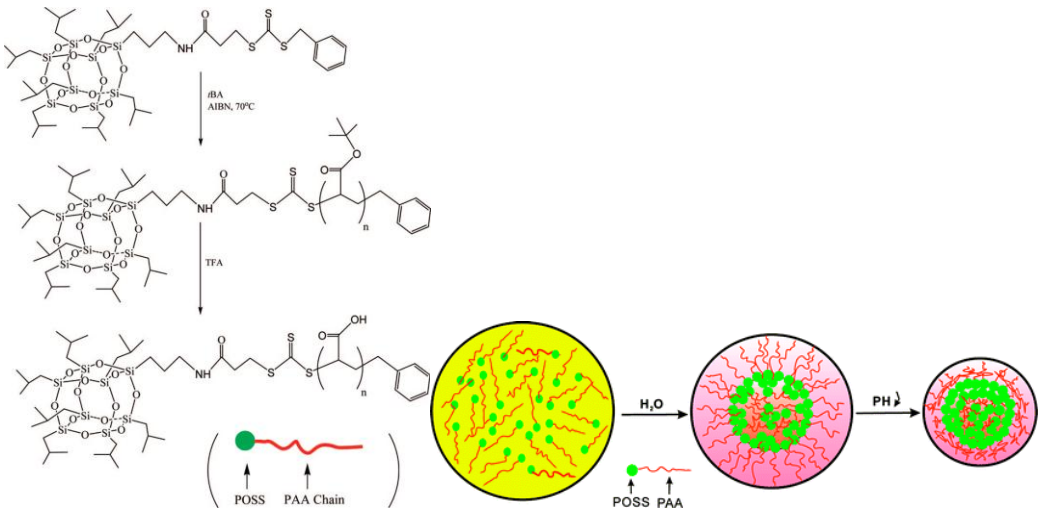

Figure 1.18 Tadpole-shaped POSS RAFT reagent and its application in POSS-(polyacrylate acid)PAA ph sensitive assembly.

Recently, Zhang[56] synthesized an alkyne-functionalized ATRP initiator and RAFT agent and applied them into the preparation of alkyne-terminal poly(methyl

methacrylate) and polystyrene. The tadpole-shaped POSS-containing hybrid polymers were easily obtained by the click reaction with an azido-functional POSS molecule (Figure 1.19).

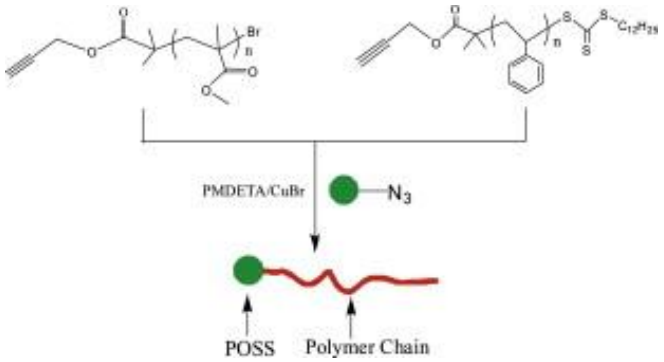

Figure 1.19 The integration of ATRP/RAFT with click chemistry via alkyne-functionalized ATRP initiator and RAFT agent with azido-functional POSS.

1.3 POSS hybrid nanostructural epoxy

Epoxy network is brittle with poor fracture toughness, poor resistance to crack propagation, and low impact strength. Thermoplastics-modified epoxies[57-59] were widely described in the literature, aiming at toughening the network and improving its impact properties. The fracture energy of cured epoxy resins is lower than do thermoplastics and other high-performance materials[60].

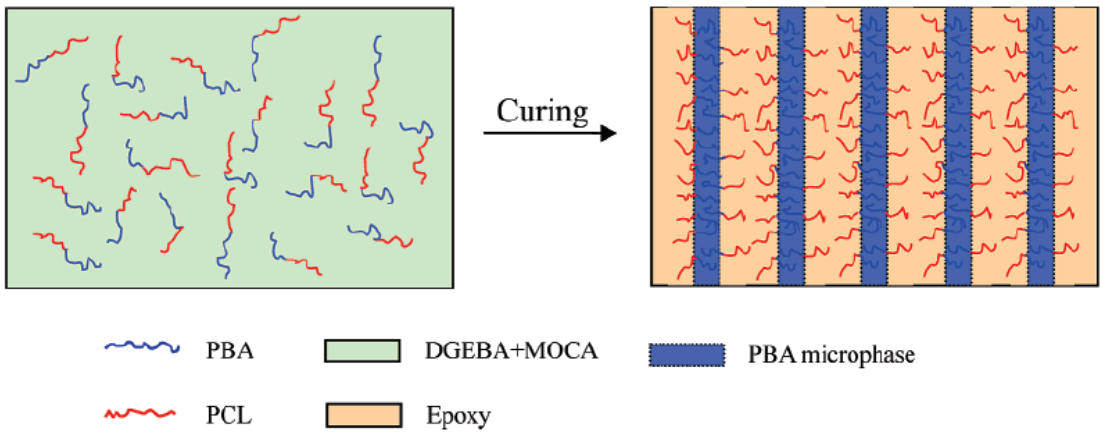

Figure 1.20 Toughen of epoxy by thermoplastic polymer with reaction-induced phase separation [61]

Because the epoxide network is brittle, introduction of soft dispersed phase improves the properties of strength at break. Recently, the formation of nanostructures in the multi-component thermosets is expected to optimize the interactions between

the thermosetting matrixes efficiently and the modifiers, thus the mechanical properties of materials have been significantly improved. This has been called " toughening by nanostructures "[62, 63](Figure 1.20).

The nanostructuration of epoxy aims at that final structure enhances more or less the toughness properties and meanwhile maintain favorable properties, such as *Tg* and stiffness. The introduction of a rigid thermoplastic polymer overcomes the modulus reduction of epoxy modified by thermoplastics[64]. Besides the linear, hyperbranching polymer is introduced into epoxy widely, whose mechanical performance is close to that of linear polymer, but morphology is exceptional porous in some case[65]. Reactive copolymer modified epoxy attracted attentions in the last decades. It is possible to employ reactive regent [66] as demonstrated by J.P Pascault in methylmethacrylate and N,N-dimethylacrylamide modified epoxy. This result was correlated with both the change of morphology induced by reactive blending with a decrease of size to nanoscale and an increase of the adhesion between the two phases. Valéry Rebizant[67] reported that reactive/nonreactive block copolymers nanostructurated block copolymer toughening effectively in DDS and MDA curing epoxy.

1.3.1 POSS modified epoxy

I.Physical blend:POSS as an inert epoxy modifier to nanostructurate an epoxy matrix has been studied for a decade[68], while the dispersion of POSS was a great challenge in the modification process. Physical mixing is a method easily to carry on; however, POSS remains undispersed or dispersed inhomogeneously even tending to agglomerate in the mixing system. In most cases, such POSS-based materials have very poor physical properties and a gradient composition over film thickness. Compared to the bulk material, the surface of POSS-based materials is enriched with POSS cages [69, 70]. The tendency of POSS agglomeration and enrichment in the surface is associated with the poor compatibility of POSS with most of the polymers, which is due to the nature of the organic ligands (isobutyl or cyclohexyl), and the tendency to self-association in the case of strongly interactive ligands such as phenyl rings [71]. For instance, as a small molecular modifier Octaphenyl POSS and Octanitrophenyl POSS were prepared and added[72] into DGEBA/DDM to nanosturcturate epoxy. All the samples before curing are homogenous and transparent. The Octaphenyl POSS without covalent bonding with matrix, formed

macroscale phase separation, namely the "reaction-induced phase separation", which was different from the curing POSS. The thermostability of Octaphenyl POSS was higher than that of Octanitrophenyl POSS, which was proposed that gaseous fragments from segmental decomposition could be suppressed by well-dispersed POSS cubes at the molecular level. According to the theory of "similarity and intermiscibility", the dispersion of POSS in epoxy matrix depends on the "fitness" between vertex group and matrix. Li and coworkers investigated the compatibility of epoxy with POSS, and found out that the epoxy/POSS blends exhibited good miscibility only at a low content (POSS% ≤ 10 *wt* %), while exhibited phase separation when the POSS content was 15%[68].

II.Epoxide POSS as a precusor[73]: Using reactive POSS to modify the epoxy network is one of in-depth strategies, because the epoxy-philic chain could be obtained through the covalent bond between POSS and matrix. Based on the fact that the reaction of epoxy and curing agent is stepwise, once the reactive POSS was incorporated into oligomer of epoxy, obtaining an epoxy-philic tail, and then the POSS will be partial compatible with epoxy network. It would be possible for POSS nanophase disperse into epoxy homogenously. There are two kinds of reactive POSSs utilized frequently: i) epoxy bearing POSS, ii) ring open reagent POSS.

As far as the epoxy bearing POSS is concerned, they can be classified into two kinds. The one is derived from the synthesis of POSS and the other is from the grafting of epoxy monomers. POSS can be monofunctional, octafunctional or multifunctional according to the number of functionality groups.

In the pioneer works by Zhang and Laine, silsesquioxanes were used as synthetic platforms in the functionalization of POSS with epoxy groups[74]. Mya[75] et al studied the addition of octafunctional epoxy POSS to a commercial epoxy system. It was observed that a strong suppression and even disappearance of the *tan δ* peak, due to the reduction of the overall segmental motion. Huang[76] used the same type of POSS to synthesize the epoxy network with a glass transition temperature higher than 400 °C.

Gao et al[77] synthesized the POSS epoxy resin (GM-POSS) based on 3-glycidyloxypropyl- trimethoxysilane (GTMS) and Me triethoxysilane (MTES) by hydrolytic condensation (Figure 1.22). The product was a blend of the majority of *T8* and *T9* and some amount of *T10*. GM-POSS was co-cured bisphenol A (BPA)-based epoxy resin with 3-methyl-tetrahydrophthalic anhydride (MeTHPA).

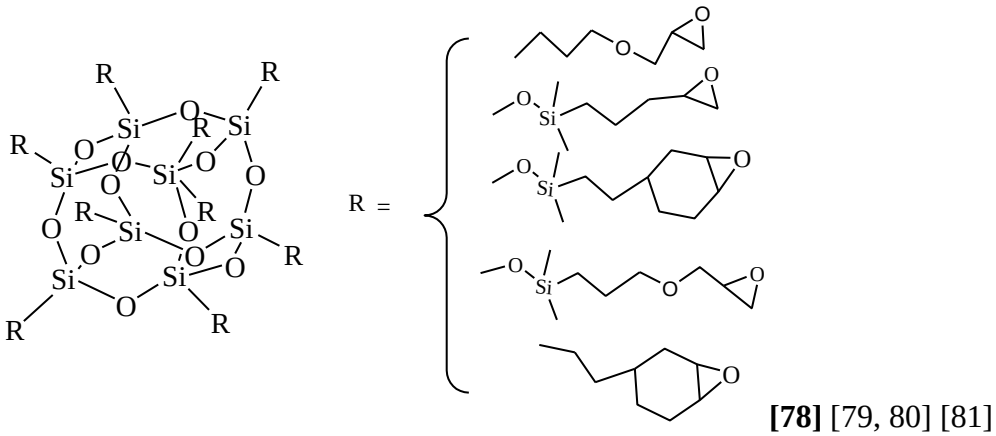

[78] [79, 80] [81]

Octa-epoxy POSS

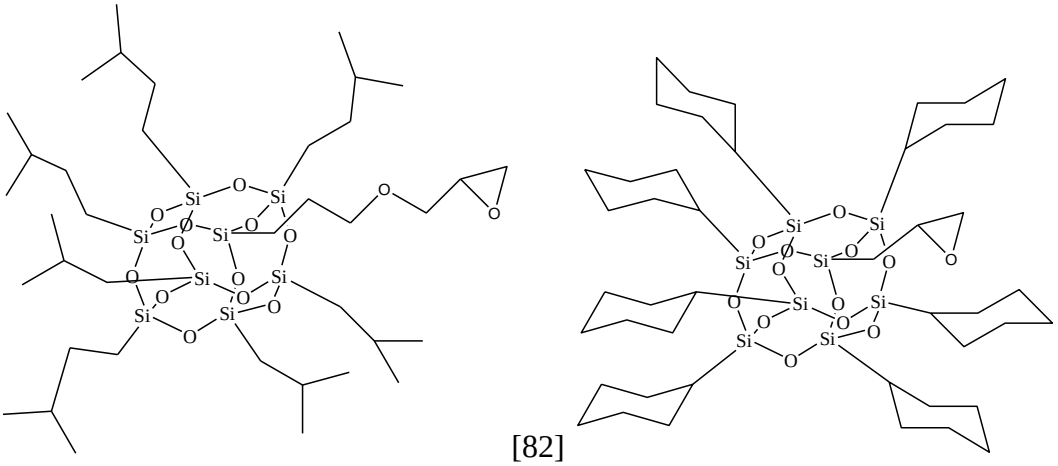

[82]

Mono-epoxy POSS[83]

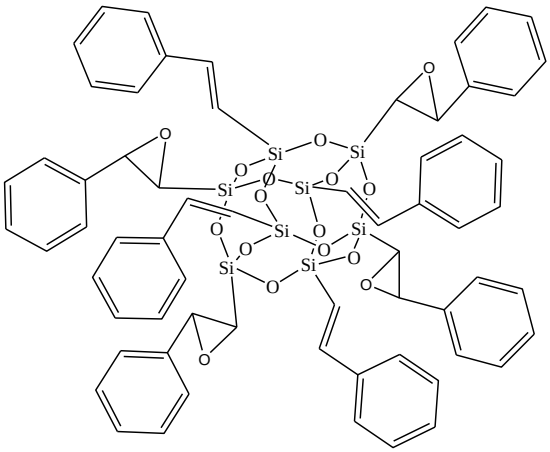

multifunctional[68]

Figure 1.21 Octa-, mono-, multifunctional epoxy POSS

By grafting reaction, it is possible to design the structure of POSS which can not be achieved by hydrolysis. Chiu[84] synthesized a POSS modified DGEBA precursor

(denoted as IPEP) via adding hydroxyl and isocyanate POSS (Figure 1.23). After an addition reaction occured, the wave numbers at 1716 and 1105 cm^{-1} appeared in FTIR, which were the characteristic peaks of C=O bonding and saturated easter group connecting the urethane chain. The curing activation energies increased slightly as the IPEP content increased.

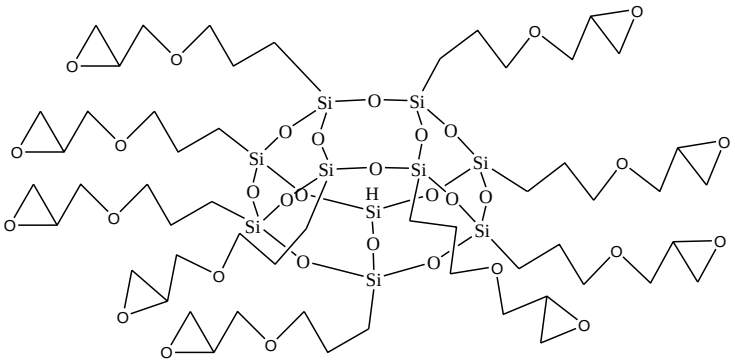

Figure 1.22 T10 epoxy-POSS[77]

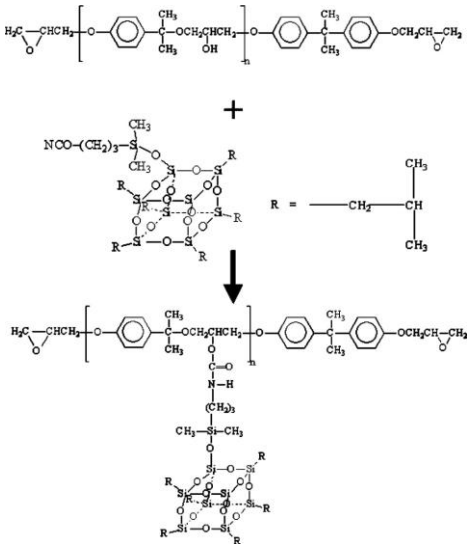

Figure 1.23 POSS-NCO grafted to DGEBA precusor. [84]

Wu et al[85] synthesized a functional POSS (NPOSS) with two epoxy ring groups via the reaction between trisilanolisobutyl-POSS and triglycidyl isocyanurate, and then cured it with epoxy network(Figure 1.24).

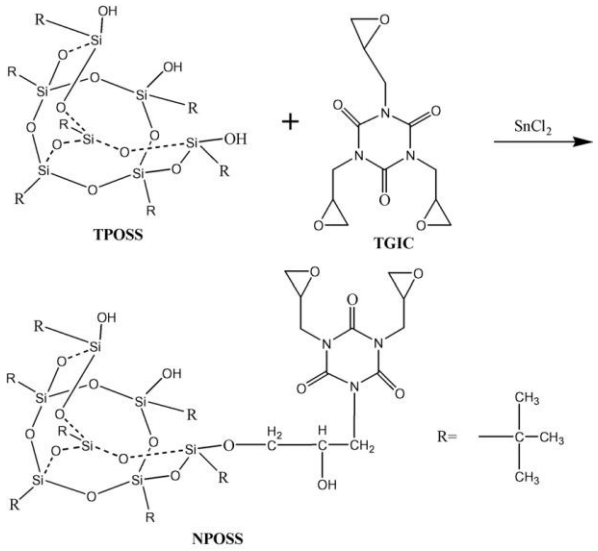

Figure 1.24 Reaction between trisilanolisobutyl-POSS (TPOSS) and triglycidyl isocyanurate (TGIC) .

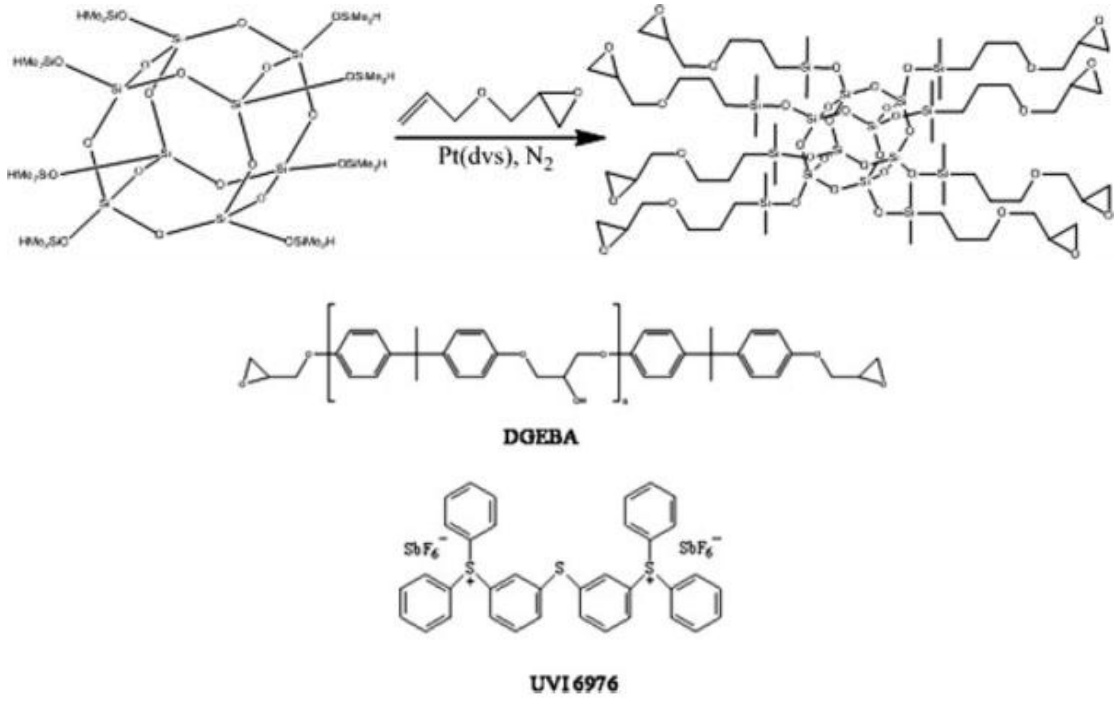

Figure 1.25 Functional POSS as an epoxy source is photocured by UV initiator. [86]

The multi-epoxy functional POSS is an efficient epoxy material in the photopolymerization. Huang et al [86] prepared octakis(glycidylsiloxy)octa-silsesquioxane(OG) and diglycidyl ether of bisphenol A by irradiating the sample at a distance of 10 cm for 60 min at room temperature(Figure 1.25). The UV-cured sample was then heated (postcured) at 160 °C for 2 h. *Tg* increased upon increasing the OG content; For example, *Tg* of the epoxy/POSS nanocomposite featuring an OG content

of 20 phr was 142.8 °C, significantly higher than that of the neat epoxy(125 °C). Because the damping properties were provided by the ratio of the viscous and elastic components, it was surmised that a reduced peak height was associated with a lower segmental mobility and fewer relaxation species. Therefore, it was indicative of stronger bonding for the epoxy/POSS nanocomposites (Figure 1.26).

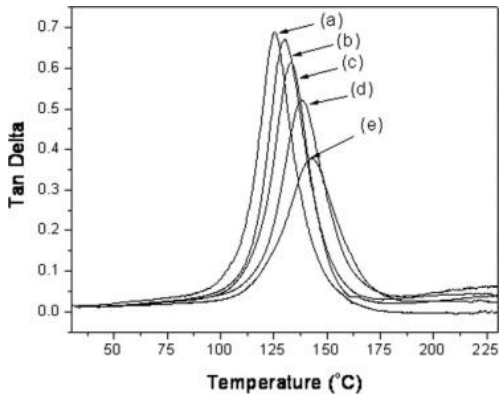

Figure 1.26 Plots of *tan* δ of the epoxy/POSS nanocomposites

** OG contents of (a) 0, (b) 2, (c) 5 (d) 10, and (e) 20 phr. [86]*

III. POSS containing curing agent is deeply stuidied, especially for those bearing reactive amino group, aiming to disperse homogenously in the matrix. In this case, the POSS−POSS interaction is the main factor controlling the network structure[73]. Matejka [87]investigated the distribution of POSS in network, which depended on the ratio of resin, curing agent and POSS. For instance, stoichiometric *O–I* networks or those with relatively small excess of amine regularly arranged silsesquioxane cluster junctions interlinked by the organic chains of amine. At deficiency of amine, the cylinders become interconnected, at last a percolation threshold to form the silsesquioxane network.

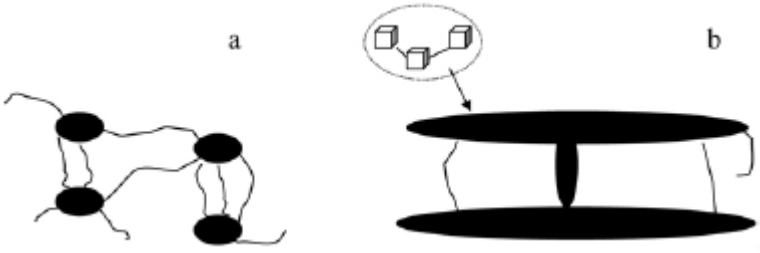

Figure 1.27 The topology of POSS agglomerate in matrix. a. in stoichiometric, b. at deficiency of amine.

Cook et al[88]evaluated chemical structure and cage structure of the POSS incorporated into epoxy, and indicated a enhanced dispersion for N-phenylaminopropyl substituted POSS in comparison to aminopropylphenyl POSS. The more highly dispersed POSS was expected to yield enhanced surface and mechanical properties. Moreover, N-phenylaminopropyl groups, had better interaction with the epoxy matrix than that of the glycidyl-POSS containing.[89]

Octa(aminpropyl)silsesquioxane $(NH_2CH_2CH_2CH_2)_8Si_8O_{12}$ (POSS-NH_2), containing eight amine groups on the vertexes, was used as the curing agent for epoxy resin (DGEBA) by Zhang et al[90]. It was observed that the river-like structure and the fiber-like pulling out morphology in the composites. This effect could absorb large amounts of breaking energy. As a result, the impact strength was improved. *Td* of DGEBA/POSS system (519 °C) was 160 °C higher than that of DGEBA/DDS system (359 °C). It also can be seen that the char residues of the POSS/epoxy system (30.35%) was 17.21% higher than that of DDS/epoxy (13.14%).

Octa(3-chloroammoniumpropyl)octasilsesquioxane(OCAPS) is a quaternary ammonium functionalised POSS synthesized by Perrin et al [91], which is water soluble. It also possesses a latent amine functionality that should be more reactive than the aromatic amino groups of Octa(aminophenyl)silsesquioxane. A series of nanocomposites DGEBA/Jeffamine-T403/OCAPS with 0, 2, 5 and 7.5 wt% of OCAPS were prepared at a stoichiometric ratio of functional groups *R*(NH/epoxy) = 1. Alkyl ammonium ions catalyzes both epoxy homopolymerisation[92] and epoxy–curing agent[93] reactions. The mechanism of epoxy homopolymerisation catalyzed by the acidic protons of primary ammonium is shown in *Eqs.*(1)–(3),

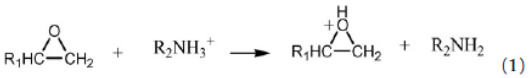
(1)

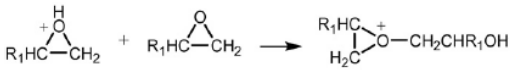
(2)

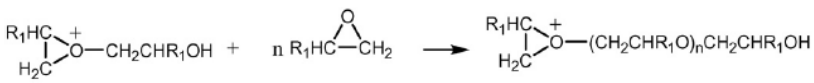

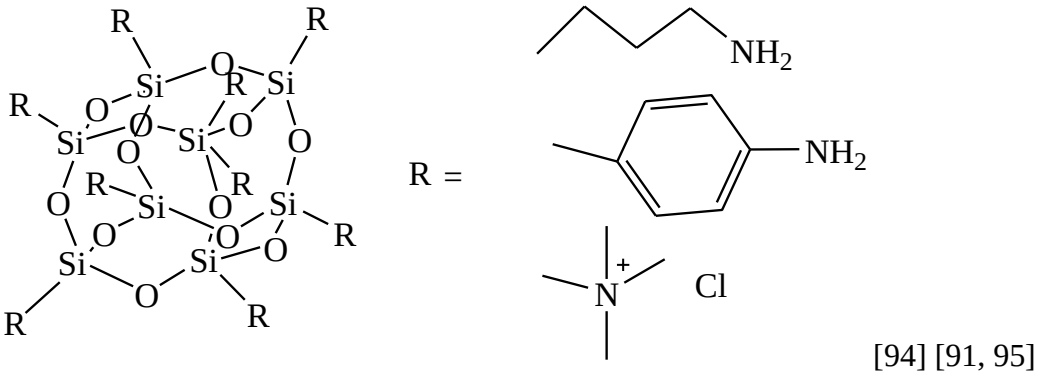

[94] [91, 95]

Figure 1.28 amino functional POSS.

Because the latent curing POSS doesn't connect to epoxy directly, the poor compatibility led to the aggregation of POSS in epoxy matrix, failed to fabricate a nanosubject into epoxy.

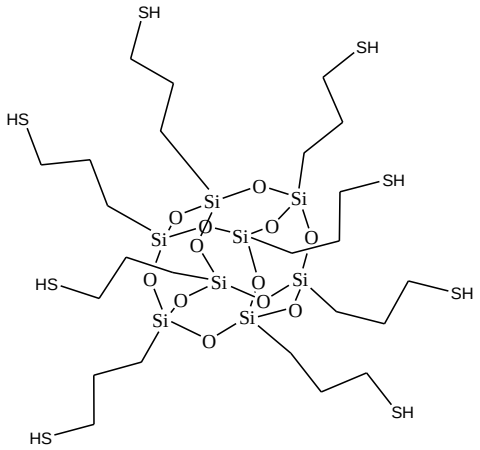

Figure 1.29 Octa-mercaptopropyl POSS[96]

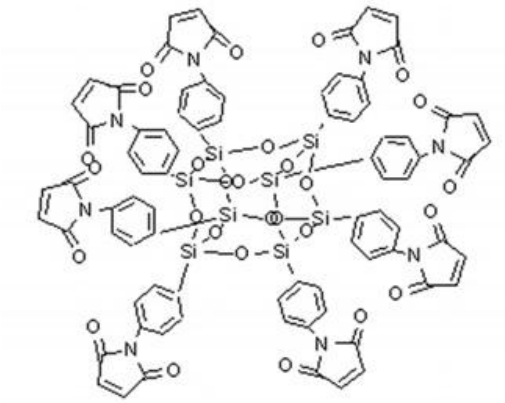

Figure 1.30 Octa-maleimide POSS. [97]

Fu et al [96] synthesized mercaptopropyl group via the hydrolytic condensation of mercaptopropyl triethoxysilane(see Figure 1.29) in an ethanol solution catalyzed by concentrated hydrochloric acid and was used to modify epoxy–amine networks by a cocuring reaction with DGEBA.

Jothibasu[97] et al synthesized octafunctionalized POSS maleimide precursor (OMPS), however, it was not an direct curing reagent for epoxy resin(Figure 1.30). Aspartimide was formed after the reaction between the amino groups of DDM and the maleimide double bonds through Michael addition (Figure 1.31). For DDM, the residual tail of amine reacted with epoxy, which will facilitate the fine dispersion of POSS macromer in the composite system[98]. When the contents of POSS were less than 5wt%, the nanocomposites enhanced glass transition temperatures (*Tg*) in comparison with the neat epoxy.

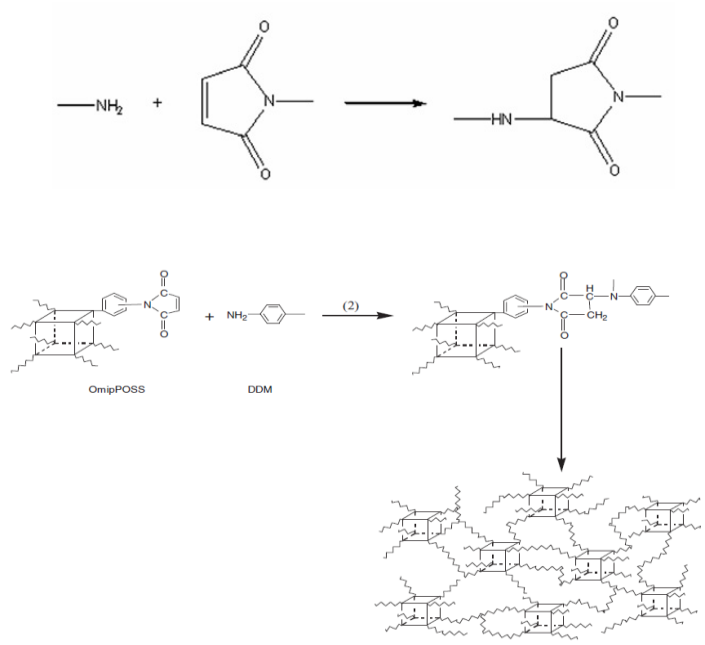

Figure 1.31 Octa-maleimide POSS nanobuilding in epoxy matrix via the addition between maleimide and amino group.

Xu et al [99]synthesized monofunctional-anhydride polyhedral oligomeric silsesquioxane AH-POSS reacting with DGEBA(Figure 1.32). The result of pre-reaction between AH-POSS and DGEBA was also confirmed by GPC. Two shifts were observed, indicating the formation of higher molecular mass unites, attributing to AH-POSS bonded one or two DGEBA chains.

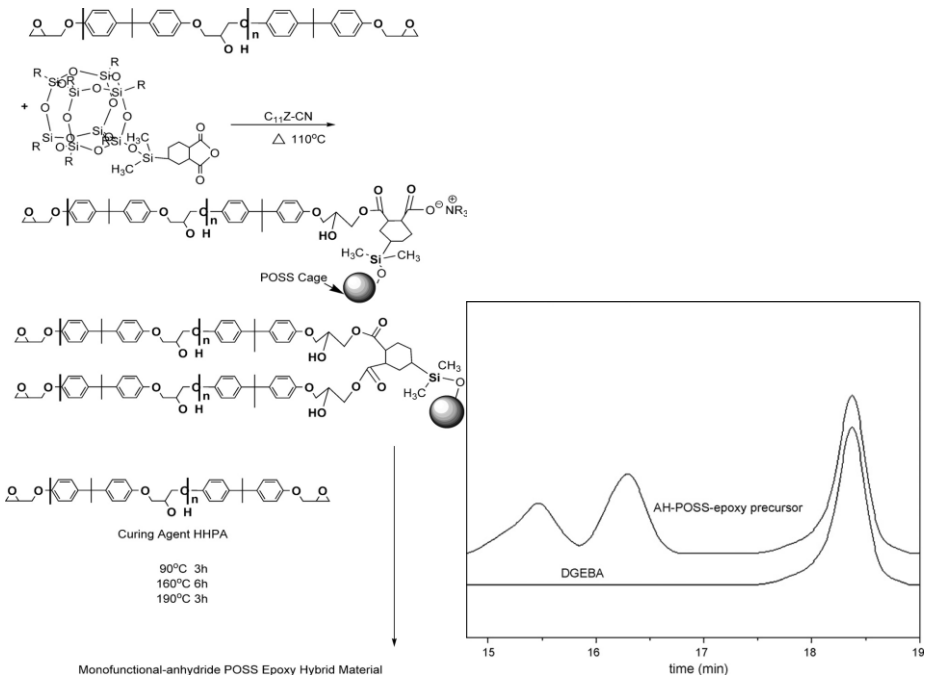

Figure 1.32 Anhydride POSS and its nanobuilding in epoxy matrix. [99]

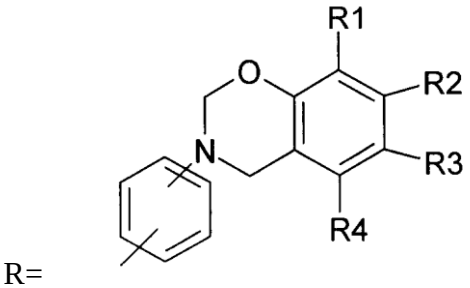

R=

Figure 1.33 Vertex group for benzoxazine-containing Silsesquioxanes. [100]

Yu et al prepared benzoxazine-containing silsesquioxanes[100]: $(RSiO_{1.5})_n$(Figure 1.33), wherein *n* = 6, 8, or 12, R1-4 = H or C1-10 alkyl, allyl, vinyl, by condensation ring-formation reaction of primary amine-containing. Phenyl silsesquioxane, phenol, and aldehydrate was at a molar ratio of 1-15 : 1 : 2-4. As a curing agent for epoxy, benzoxazine-containing silsesquioxanes improved the thermostability.

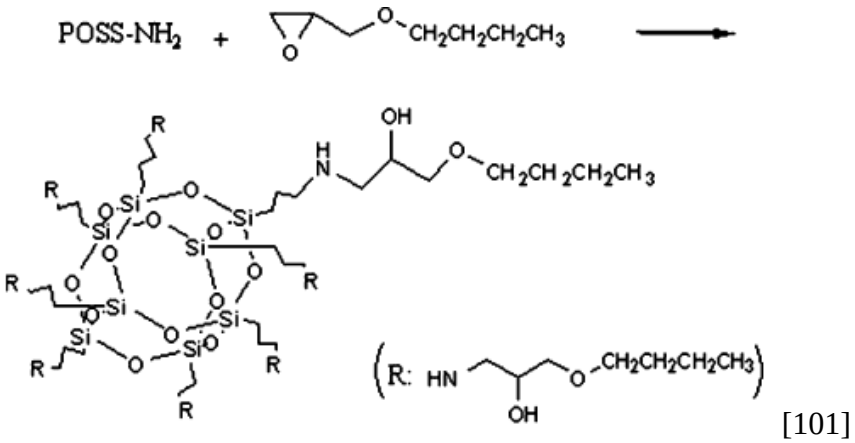

[101]

Figure 1.34 Hydroxyl and imino functional POSS as a curing agent.

Ni et al[101] synthesized a reactive POSS bearing hydroxyl and amino group via (γ-aminopropylsilsesquioxane) reacting with n-butyl glycidyl ether(Figure 1.34). The hybrids were added into epoxy resin for improving mechanic and thermal properties of the epoxy resin. The impact strength and thermal properties of the epoxy resin were greatly enhanced by adding the inorganic/organic hybrid material to the system, which could be ascribed to the high curing density of POSS.

Compared with the general epoxy precursor, epoxy bearing POSS has a lower reactivity because of the steric hindrance. Moreover, the reaction induced phase separation of POSS leads to the decrease of conversion and *Tg*[102]. Pre-reaction between the POSS epoxy precursor and the curing agent made a complete reaction and a homogenous phase, which was fulfilled by Gerard[103] and Lu[102]. In some molecular POSS epoxy resin an autocatalytic behavior occurred in the overall curing process, for instance a system cured by 4,4'-Diaminodiphenylsulfone (DDS) [104]. Zhang et al [105]calculated the activation energies of curing for DGEBA with 10%wt octa(aminopropyl)silsesquioxanes, and the results were 60.01 and 64.89 kJ/mol according to the Kissinger and Flynn-Wall-Ozawa methods, respectively. The corresponding activation energies obtained of curing for neat epoxy are 55.67 and 58.33 kJ/mol, respectively. It confirmed that the reactivity of the hybrid resin system containing POSS was lower than the pristine epoxy resin.

Linseed oil as one of the cheapest and most abundant biological feedstocks available in large quantities is of low toxicity and inherent biodegradability. Lligadas et al[106] obtained a POSS epoxy modified epoxide linseed oil(ELO), catalyzed by the latent catalyst(Figure 1.35).

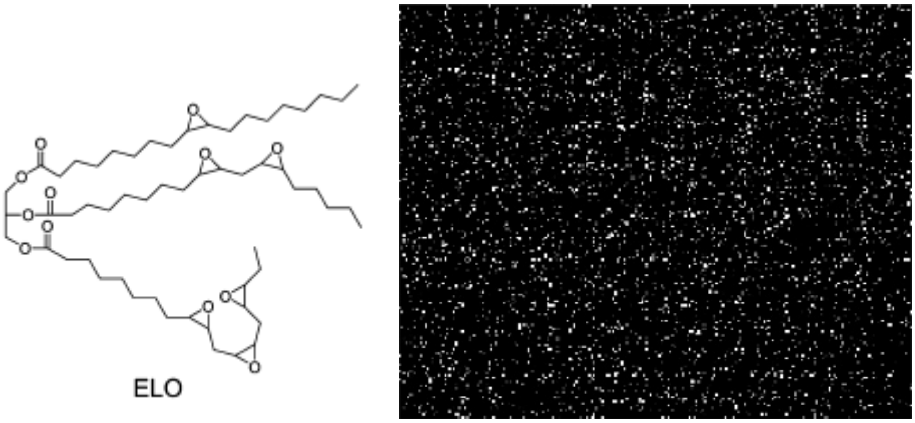

Figure 1.35 SEM-EDX Si-mapping micrograph of a cross section of ELO 5 wt % G-POSS nanocomposite.

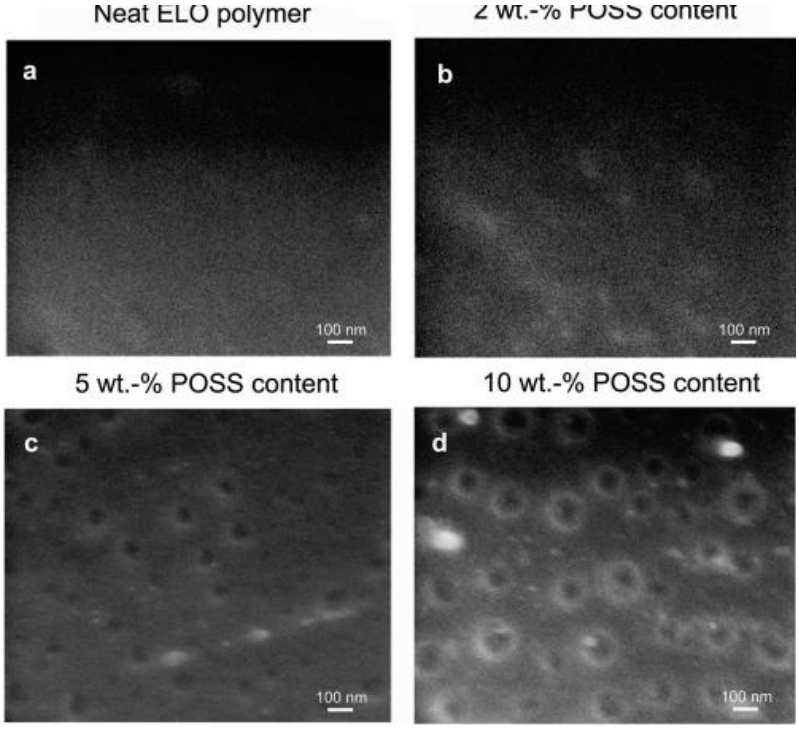

Figure 1.36 SEM cross-sectional micrographs of ELO polymer (a) and ELO nanocomposites containing G-POSS: 2 wt % (b), 5 wt % (c), and 10 wt % (d)

Homogenous dispersion of POSS was characterized from EDX Si mapping of all of the composites. The white particles as POSS-enriched regions, were uniformly dispersed in the cross-sectional surfaces. Nano-spherical particles (40-50 nm in diameter) uniformly dispersed at a low POSS loading, and some aggregation (80-150 nm in diameter) occured in 10 wt % containing composite. It was assumed that the reactivity of epoxy POSS should be lower than that of ELO, due to the steric hindrance and phase separation of POSS rich domains occuring at low conversions (Figure 1.36).

For a blend, strong particle-matrix interactions are important to build nanostructures in a polymer matrix. Such interactions are likely a key to the preparation of stable POSS nanocomposites of engineering plastics, which possess enhanced properties. Schiraldi et al[107] employed POSS into a series of nanocomposites such as cellulose propionate, polycarbonate, poly(ethylene-co-norbornene) and so on. The nanobuilt composites are amorphous, transparent. Trisilanol isooctyl POSS with cellulose propionate exhibited both high clarity and enhanced thermo-mechanical properties, because of strong interact between nanoparticle and matrix.

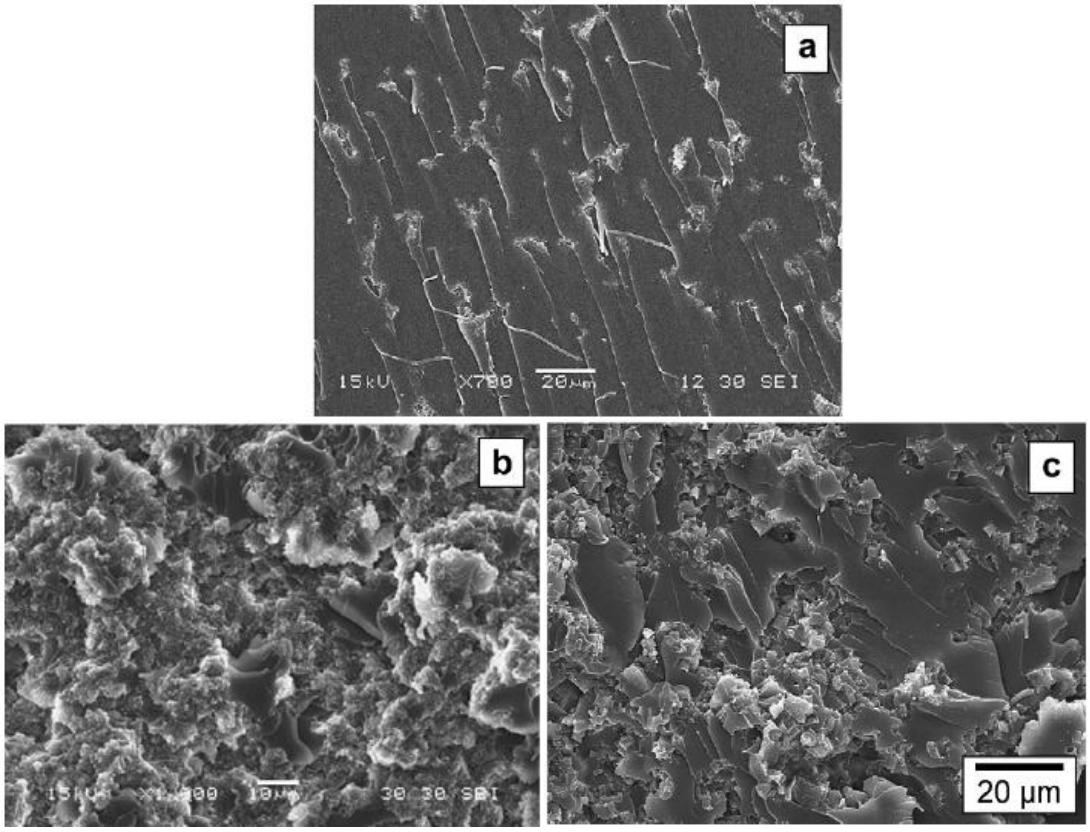

Figure 1.37 SEM micrographs of final morphologies generated in DGEBA–MDEA epoxy networks modified with POSS (3.7 inorganic wt%): (a) pre-reacted Gly-iBu POSS. (b) pre-reacted Gly-Ph POSS (c) non reactive OctaPh POSS.

The vertex group of POSS determines the morphology, which decides the polarity and interaction with the matrix. Zucchi et al[103] compared the phase separation of monoepoxide isobutyl POSS and phenyl POSS. The isobutyl POSS led to the formation of irregular POSS aggregation composed by a set of small individual domains. Phenyl POSS sample had a more complex morphology, composed by a smooth phase, assigned to the epoxy amine matrix, and a rough phase (largest area),

thought to be the POSS-rich phase. It means the better compatibility of the phenyl ligands with the epoxy-amine components compared with the isobutyl ligands. And the pre-reaction of POSS increase the compatibility with matrix obviously (Figure 1.37).

Compared to neat epoxy, the fracture surfaces of the nanocomposites of octa-epoxycyclohexyl POSS showed considerably different fractographic features(Figure 1.38) [108]. Generally, adding POSS into the epoxy matrix results in a much rougher fracture surface, which increased with higher POSS content. Besides the rougher fracture surface, there are many small smooth zones. These smooth zones nucleated in the material at areas of localized deformation and, in the center of each partly oval-shaped zone, a second-phased particle can be observed. During the failure process, the crack propagation changed direction as it crossed second-phased particles. The pinning effect prevent crack opening. When second-phased parties were few and widely spaced, the cracks propagated longer before coalescing, resulting in a fracture surface with large smooth zones. Smaller zones were formed when many second-phased particles were produced. The size of smooth zones decreased with increasing POSS weight fractions. The path of the crack tip was distorted because of more second-phased particles, which made crack propagation more difficult. Fewer smooth zones and more surface roughness implied that the number of second-phased particles increased with increasing POSS content.

In generally, the mechanism of phase formation of POSS modified epoxy was based on a typical liquid-liquid phase separation induced by polymerization. In recent, Di Luca et al[109] prepared a cured epoxy which exhibited a dual dispersion of POSS crystalline platelets and spherical domains rich in POSS. The C-L equilibrium between pure crystalline POSS and the solution was calculated from the classic equations developed by Flory and extended to a polydispersal solvent using the Flory-Huggins model(Figure 1.39).

It is observed that the river-like structure and the fiber-like pulling out morphology form in the composite (Figure 1.40) [110]. As a result, the impact strength is improved. It indicates that the inorganic-organic materials possess excellent toughness POSS containing. Fiber-like fracture zones and toughening whorls absorb large amount of impact energy when break happens[110].

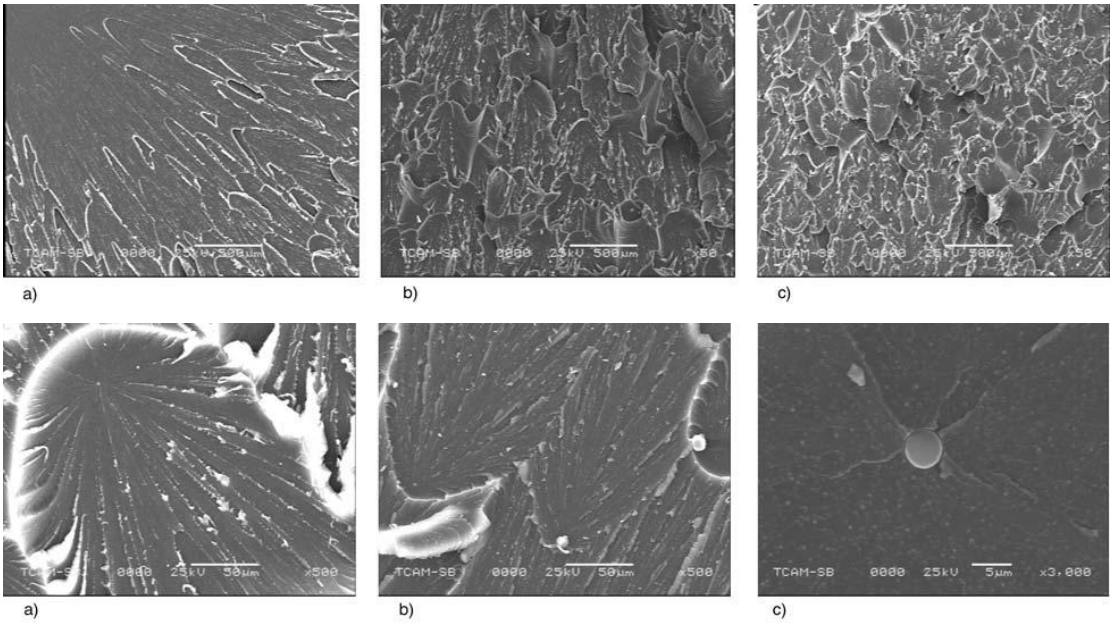

Figure 1.38 Fracture surface of neat and nanophased epoxy (a-neat epoxy, b-1 wt%POSS/epoxy and c-5 wt%POSS/epoxy

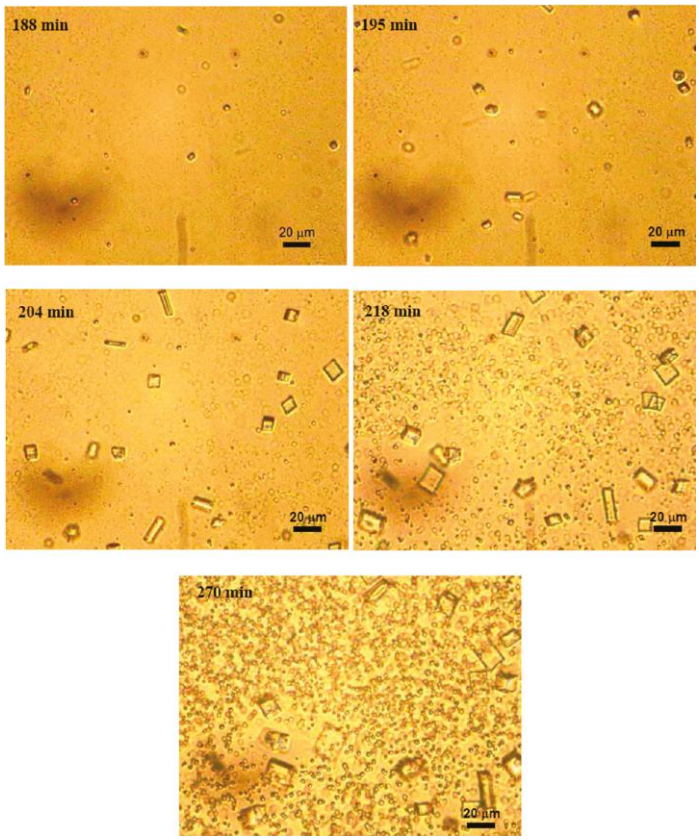

Figure 1.39 Sequence of the evolution of morphologies observed by TOM in a POSS-DGEBA/MDEA blend with 5 wt % POSS cured at 115 °C.

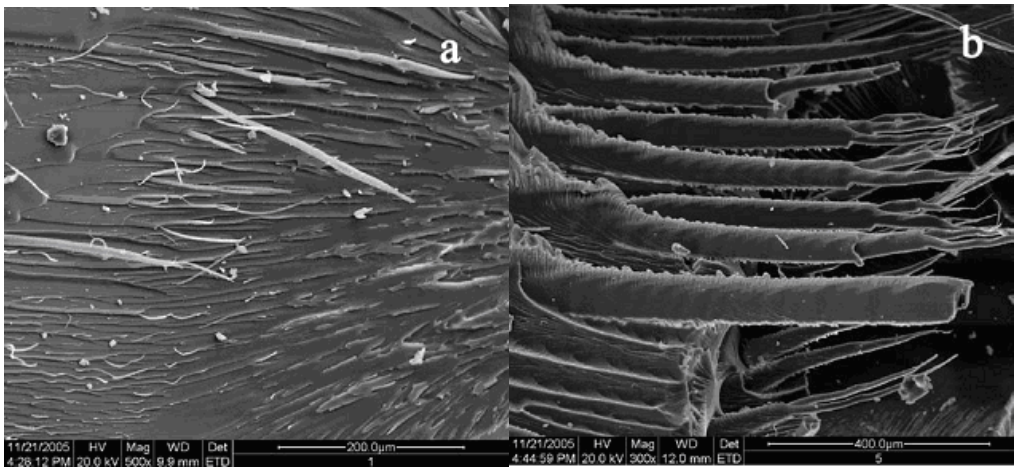

Figure 1.40 The river-like structure and the fiber-like pulling out morphology in the composite

1.3 Properties of POSS modified epoxy

1.3.1 Thermostability

To understand the thermostability and fire retardency of POSS, it is necessary to introduce the method of evaluation. Evaluating from thermogravimetric analysis, some points are frequently utilized: the temperature of 5% weight loss, T5 (denoted as initial thermodegradation temperature usually), the mid-point temperature of the degradation (T50) and the temperature of maximum degradation rate from the differential thermogravimetric Td[85]. The char production is a key parameter to evaluate the thermostability, because the char of POSS ceases the transmission of oxygen and the release of fragment, furthermore protects the matrix away from high temperature.

The apparent decomposition temperature T_A, heat-resistant index T_{zg} could be determined from the TGA thermograms. T_A and T_{zg} were determined by a cut-line (CL) method according to JB2624-7945 and calculated with the following equations:

$$T_A = (10C - 3B)/7 \qquad T_{zg} = (T_A + B)/2x$$

Where B and C are the temperatures at which 50% weight loss (T50) and 15% weight loss (T15) occur, respectively, and x is the functionality index. x is 2.37 for the epoxy compounds when the epoxy content is above 50%, and it is 2.14 for the no-epoxy compounds when the epoxy content is below 50%[96].

The integral procedure decomposition temperature (*IPDT*) is calculated by $\mathrm{IPDT}\,(^{\circ}\mathrm{C}) = A * K * (T_f - T_i) + T_i$.

T_i is the initial experimental temperature, and T_f is the final experimental temperature (Figure 1.41). *A* and *K* can be calculated by the following equations:

$$A = \frac{S_1 + S_2}{S_1 + S_2 + S_3}$$

$$K = \frac{S_1 + S_2}{S_1}.$$

The *IPDT* can provide the information of the fraction of volatile of polymeric materials generated as well as the inherent thermal stability of polymers.

It was shown that the effectiveness of POSS enhanced the properties of polymer in nanocomposites or created new properties such as fire retardancy[111], primarily depended on the degree of dispersion and distribution of the POSS cages in the polymer matrix and on type of orgnic, substituent of the silicon atoms of the POSS cage.[112]

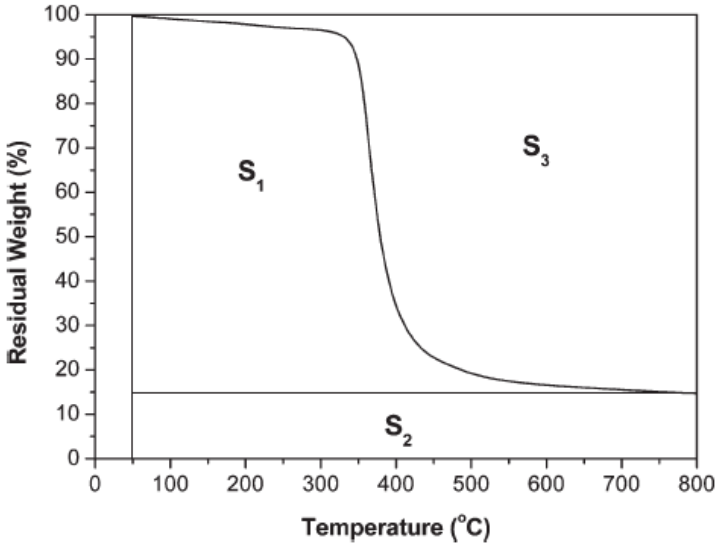

Figure 1.41 The *IPDT* curve by TGA measurement.

An anaerobic adhesive was obtained by using epoxy acrylates as the unsaturated monomers. POSS and N-p-tolylmaleimide (NPTMI) as the high temperature resistant modifier, the shear strength retention ratio was about 75% at 200 °C[113]. O-cresol formaldehyde epoxy acrylate (o-CFEAR) as adhesive modified with POSS, showed that shear strength of the anaerobic adhesive was 15.3 MPa, and was conserved about 87% compared with temperature at 200 °C and 96 h[114]. Other properties desired in

high use temperature resin including heat distortion and flammability characteristics, permeability, optical properties, texture, feel and durability were possible to be improved by coupling with POSS. [115] Blending POSS (15wt%) into epoxy vinyl ester (EVE) resins reduced smoke, heat release rate (*HRR*), and increased ignition time obviously[116].

Zhang et al[117] built a POSS resin/glass fiber composites, PM 1287, with a bucky paper which was prepared by grinding single-walled carbon nanotubes (SWNT). The shielding of SWNT improved fire, smoke, and toxicity performance of the POSS resin/glass fiber composites. Pittman et al[118] reported that carbon nanofiber/phenolic resin composites and nanofiber/POSS/phenolic materials had excellent high temperature erosion resistance either.

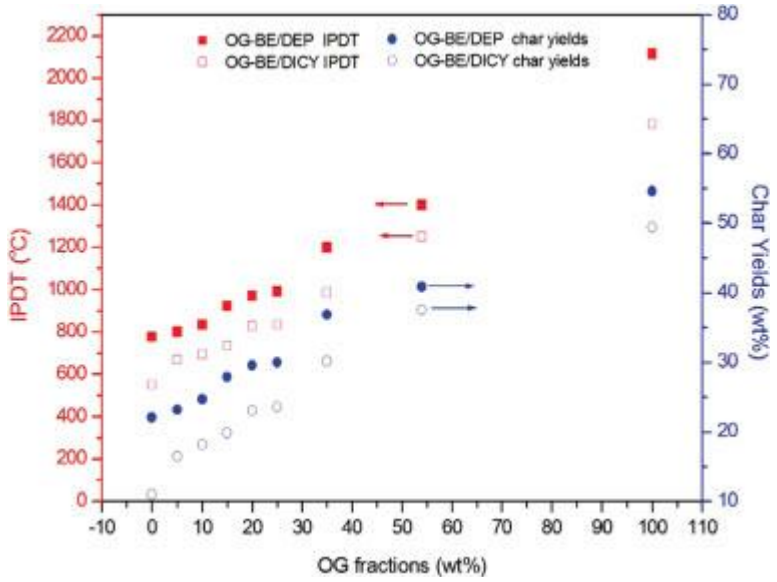

Figure 1.42 The relationship between POSS loading and *IPDT*.

Liu et al[119] utilized octakis(glycidyldimethylsiloxy)octasilsesquioxane (OG) and diglycidyl ether of bisphenol A(Figure 1.42), which were cured with small-molecule curing agents of diethylphosphite (DEP) and dicyandiamide (DICY), to nanosturcturate epoxy. The phosphonate group in DEP was a char-formation promoter. The relatively high char yields and high *IPDT* values were reasonable. POSS addition to epoxy resins significantly increased their char yields and *IPDT* values. High char yields correspond to reduced amounts of volatile and combustible compounds evolving from the thermal degradation processes and improved flammability. The curing density is important for the POSS modified epoxy, Fu et al reported that the values of *IPDT*, T_A, and T_{zg} increased with the addition of mercapto-

POSS first, attained a maximum when the POSS content was 10%, and then decreased modestly indeed with the POSS content further increasing. T_{max} decreased slightly for all POSS/DGEBA hybrids. This may be explained as follows: an increasing amount of mercapto-POSS decreased the polymer's crosslink density.

The parameter used to measure the flame retardancy of a compound is *LOI*. The char yields can be linearly related to *LOI* values using the Van Krevelen linear correlation:

$$LOI \times 100 = 17.5 + 0.4 \times CR$$

Where CR is the char residue obtained in argon atmosphere. The sample with POSS generally showed a higher *LOI* than matrix, such as loading 2.5wt% of octa-epoxy POSS exhibited a value of *LOI* of 25.4%, slightly higher than that obtained for the mixture without silsesquioxane, 24.3%[78]. This fact indicated that the silsesquioxane influenced the combustion of an epoxy/amine mixture by acting as a retardant agent, but not in the expected extension.

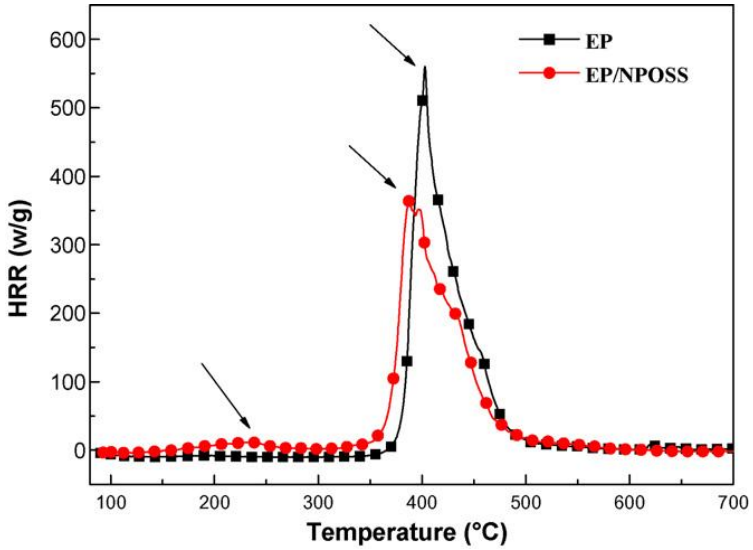

Figure 1.43 The *HRR* peak decreases when introducting POSS.

Combustion calorimeter is a widely used thermal analysis method to measure chemical properties related to fire. In general, the peak *HRR* was reduced incorporated with POSS means a slower degradation in POSS modified epoxy. As the following results from Wu[85](Figure 1.43), it can be concluded that the incorporation of POSS into the epoxy was beneficial for improving the flame retardancy of epoxy.

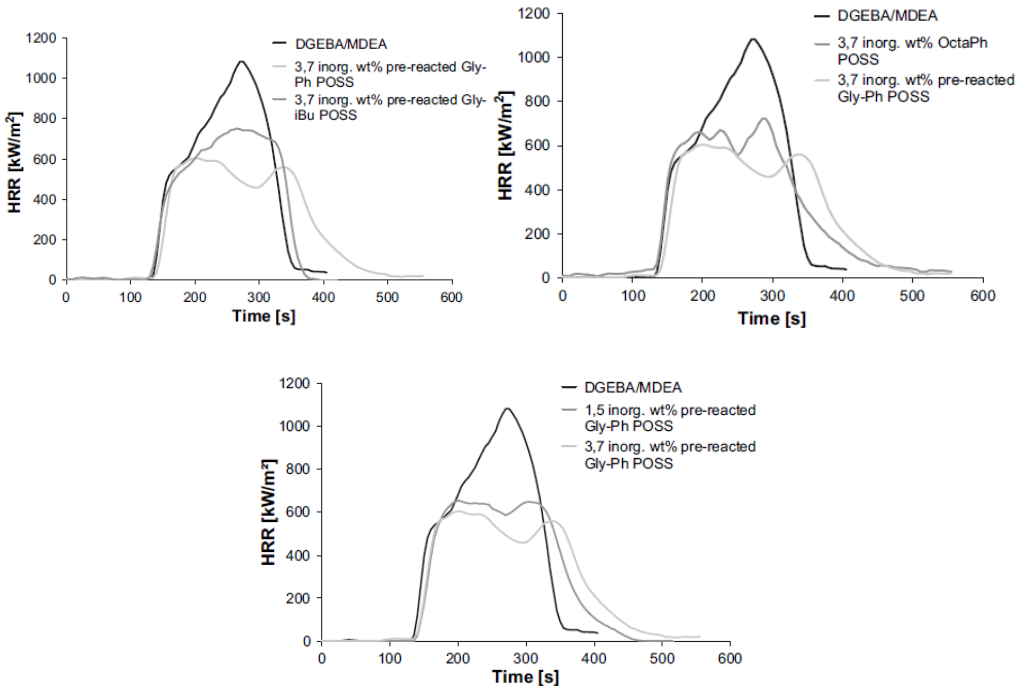

Figure 1.44 Heat release rate (*HRR*) as a function of time for epoxy networks containing different amount of pre-reacted Gly-Ph POSS: Effect of POSS content.

The morphology influences the heat release rate (*HRR*), because of POSS as a non-halogen fire retardant, the homo-dispersion improves its efficiency. The addition of POSS in epoxy/POSS would accelerate the char formation, resulting in the reduction of the *HRR*. As Franchini reported[120], 3.7 wt% of non reactive octaphenyl POSS and pre-reacted glycidyl-phenyl POSS incorporated into DGEBA(Figure 1.44). When the POSS bearing epoxy group are pre-reacted, they act as a kind of surfactant where the POSS/epoxy balance facilitates the homogeneous distribution of the POSS-rich domains within the matrix. A more homogeneous distribution of POSS molecules inside the epoxy network as a nanomodifier, the *HRR* will be smaller meaning a better fire retardency. Wu et al[121] observed the addition of POSS reduced the peak *HRR* of epoxy from 883 to 777 kW/m^{-2}(Figure 1.45). Epoxy/POSS including Al acetylacetonate, which was an acidic catalyst, had lower peak release rate (590 kW/m^2) and the second peak *HRR* disappeared. Because the presence of Al assisted char formation more efficienlyt and thermo-stably than the epoxy/POSS and neat epoxy samples.

The smoke is fatal when gets fire, so the reduction of smoke release is meaningful to evaluate the fire retardant. The lower smoke production was related to the more aromatic specimen left in the carbonaceous layer, which led to higher char

yield. The introduction of POSS, the CO and CO_2 release peak in the curve of epoxy/POSS decreased in the combustion(Figure 1.46) [121]. These enhancements on reducing toxic character in the combustion properties improved the fire safety performance.

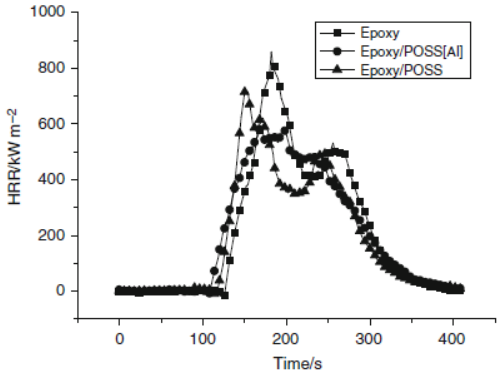

Figure 1.45 The *HRR* results of epoxy, epoxy/POSS, and epoxy/POSS[Al]

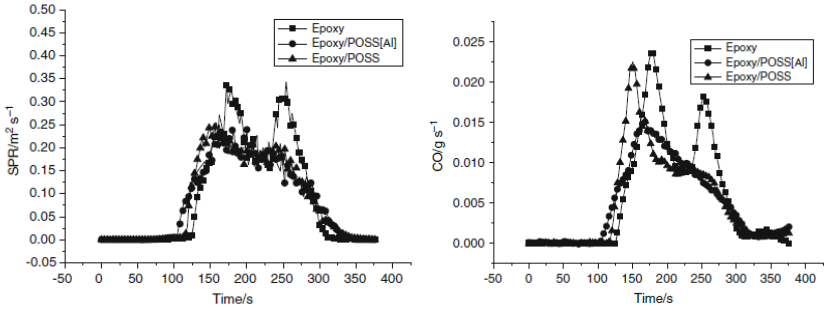

Figure 1.46 Smoke production and CO concentration during combustion of epoxy, epoxy/POSS.

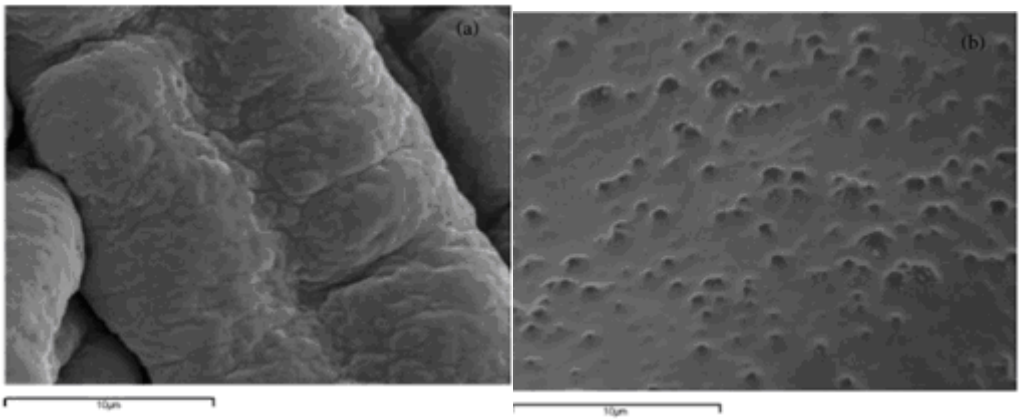

Figure 1.47 Compact outside layer and alveolate insider layer formed after flammation of POSS nanocomposites.

Compact silica layer formed after flammation is important for thermostability. In case, the inner surface was alveolate and the outer one was closed. This kind of char structure slowed down the transfer of gases and mass during the burning process. Thick char became a better thermal insulating layer, which underwent slow oxidative degradation and prevented heat reaching the remaining polymer(Figure 1.47). It was believed that this carbonaceous (Si–O–C) layer with SiO_2-like species could act as an insulator and a barrier to mass transport on heating[122]122]. The vertex group is possible to form different char morphology, which performed different thermostability. A solid sponge-like structure(Figure 1.48) formed after burining in presence of isobutyl containing POSS clusters modified epoxy.[120]

The char layer generated is thought to act as a barrier for both heat flow and mass transport, familiar with intumescent flame-retardant coatings. The differences are due to the intrinsic stability of the organic group and the compressed evaporation of phenyl group POSS[120].

Charring of the epoxy network takes place in air at a higher yield due to catalysis by oxygen. The vertex groups determine the interaction among POSSs and influence the bulk properties. For instance, the cyclopentylPOSS (Cp) cylinders have a diameter of 6 nm and cyclohexylPOSS (Cy) cylinders have a diameter of 12 nm [123]. Also, the Cp cylinders were about 36 nm long while the Cy cylinders were 62 nm long. The net result is that seven times as much POSS is tied up in each cylinder in the Cy case when compared to the Cp case. The morphology of residue may be related to the sizes of the POSS particles dispersed in matrix. There were a lot of holes on the carbonaceous residue left by epoxy/POSS. As a latent catalyst, Al acetylacetonate accelerated epoxy to leave a compact and uniform char layer, which acted as barrier more effectively than the char from epoxy/POSS.[121]

Figure 1.48 A solid sponge-like structure in presence of isobutyl containing POSS.

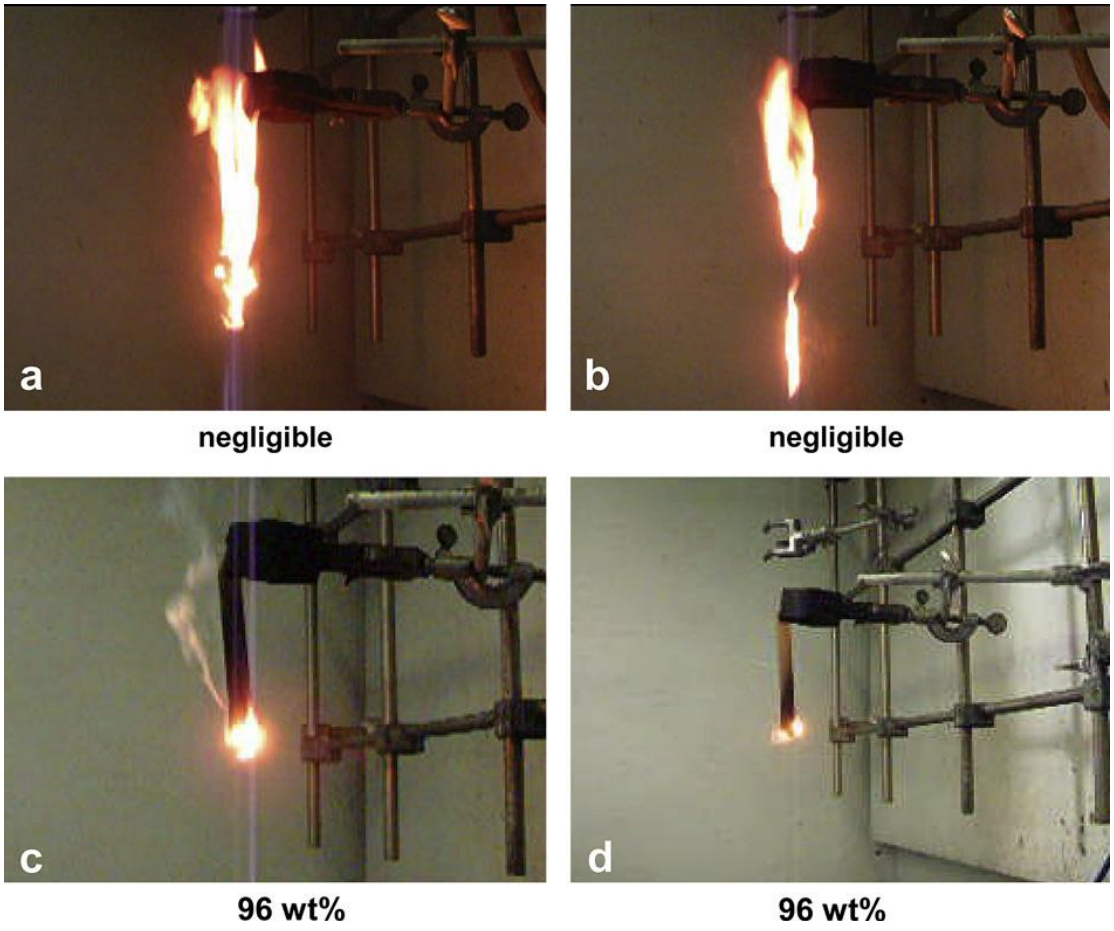

Figure 1.49 Vertical test pictures and the corresponding residual weight: (a) neat epoxy matrix, (b) 3.7 wt% pre-reacted glycidyl-isobutyl POSS, (c) 3.7 wt% pre-reacted glycidyl-phenylPOSS and (d) 3.7 wt% non reactive OctaPh POSS.

When UL94 vertical burning tests had also been carried out, neat epoxy network and the network containing POSS bearing isobutyl ligands exhibited the worst results, in which all these materials burned until clamps with release of incandescent drops. And the samples bearing phenyl group POSS showed self extinguish flames(Figure 1.49).

To understand the mechanism of thermo degradation involving POSS, Wu et al [85] employed the FTIR spectra to trace the process(Figure 1.50). The main products of the thermal decomposition of epoxy were compounds containing –OH (such as H_2O, phenol), CO_2, CO, hydrocarbons, compounds containing carbonyl, compounds containing aromatic ring, etc. The pyrolysis byproducts for epoxy at the beginning (from about 20.0 min) were mainly composed of H_2O, CO_2, etc. With the increase of temperature (above 30.0 min), CO, hydrocarbons, compounds containing carbonyl and aromatic ring, etc. were released. The evolved gas analysis for EP/NPOSS exhibited characteristic bands of compounds containing -OH group, methylsubstituted

compounds, CO_2, CO, compounds containing carbonyl, compounds containing aromatic ring, hydrocarbons, etc. It can be drawn that the pyrolysis products for POSS/epoxy at the beginning (from about 15.2 min) were mainly composed of compounds containing carbonyl and aromatic ring and hydrocarbons. Then, methyl-substituted compounds, compounds containing carbonyl and aromatic ring, etc. were released. The evolved gas products for epoxy were different from that of epoxy/POSS.

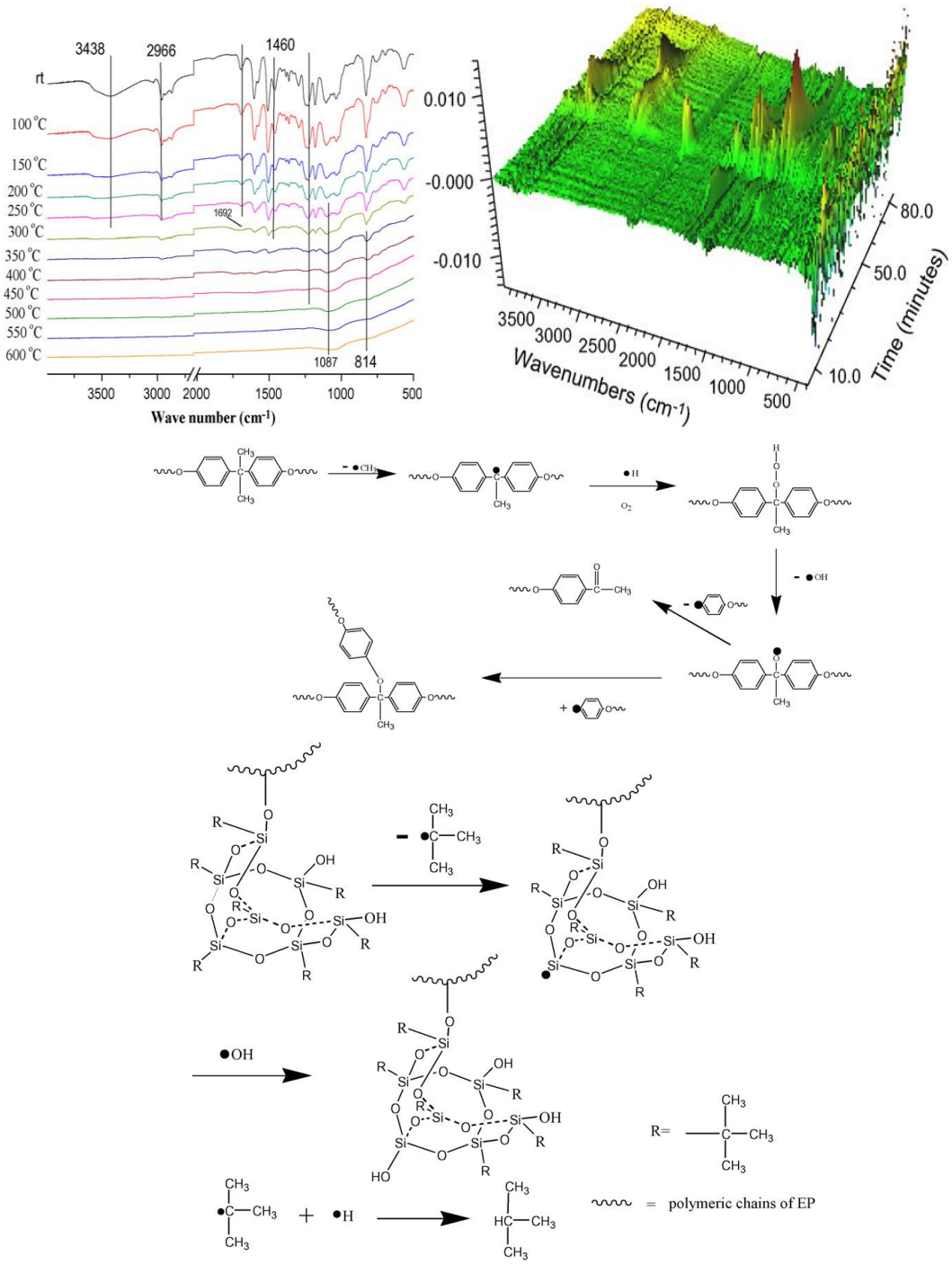

Figure 1.50 TG-FTIR of POSS epoxy composites and its proposed mechanism.

The main evolved gas products of epoxy were composed of small molecule, such as CO_2 and CO. In another aspect, epoxy/POSS released mainly methyl-substituted, carbonyl and aromatic ring. It was ascribed to that the presence of POSS retarded the movement and destruction of the main chain of epoxy during its thermal degradation. It tended to form polyaromatic substituted phenols with the degradation $-CH_2$, $-CH_3$. The isobutyl radical could capture the hydrogen radical and the silicon radical of POSS could capture the hydroxy radical. As a result, POSS could played a role of radical trap via the consuming of highly reactive hydrogen and hydroxy radicals. It was interesting to retard further thermal degradation of underlying materials.

About the thermodegradation of POSS modified epoxy, Wu et al [124]divided the thermodegradation into two steps: First, degradation was observed at low temperature with production of alkyl group species from polymer backbone and formation carbonaceous compounds. It worked as physical barrier to protect substrates from fire via reducing the energy and mass transfer between substrates and heat source (fire). In the second step, at high temperature, the carbonaceous compounds were oxidized and volatilized. Since the second stage of mass loss of an epoxy resin in air was related to the oxidation of the residual formed from thermal decomposition of the resin, the nano-additives acted as a thermal insulating material to the residual, because of their excellent oxidation resistance and reaction to fire.

Wang et al[125] postulated that the oxidation of Octa vinyl POSS was oxidated to form acetaldehyde and carbon dioxide. The cage of POSS, which could be seen as a radical trapper (Figure 1.51), could react with pyrolysis radicals and form the branched and crosslinked intermediate siloxane products which resulted in the enhancement of thermostability.

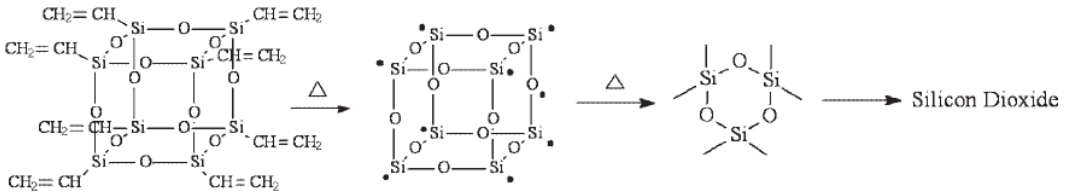

Figure 1.51 POSS pyrolysis as a radical trapper.

The high char yields also implied that relatively small amounts of volatile small molecules were released under thermal decomposition. The percentage of POSS and

the vertex group influence *Tg* and *Td* obviously. In cyclohexyl and cyclopentyl POSS copolymerized with 4-methylstyrene copolymers, when at low content of POSS, (1 mol% of the POSS), *Tg* and *Td* of copolymers were lower than poly(4-methylstyrene). However, as the mole percent of POSS increased to 9%, the copolymers exhibited higher values of *Tg* and *Td* **[123].**

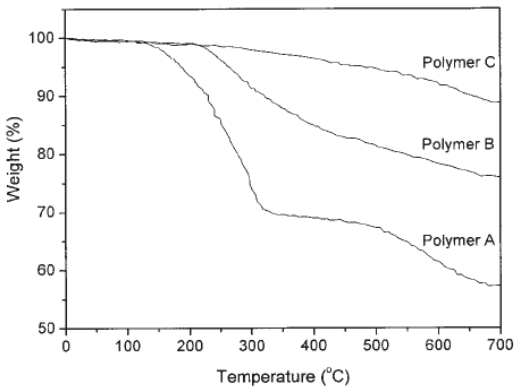

Figure 1.52 POSS epoxy composites cured by ethylenediamine(polymer A), 1,3-propanediamine(polymer B) and 1,4-butanediamin(polymer C).

It was worthy noticing that the higher molecular tension resulted from the short organic tethers between the bulky POSS cages. Xu et al[126] observed the POSS cured by ethylenediamine, 1,4-butanediamin and 1,3-propanediamine. The thermo decomposition of copolymer became stable with the increase of curing agent molecular length, *Ti* at 136.5°C, *Td* at 180°C for ethylenediamine cured, *Ti* at 225.0°C, *Td* at 255°C for 1,3-propanediamine cured, and *Ti* at 282.5°C, *Td* at 460.0°C for 1,4-butanediamin cured(Figure 1.52).

1.3.2 The influence of *Tg*

Tg of the POSS hybrid copolymers is influenced by the following factors: (1) a role of diluents on reducing the self-association of the matrix; (2) a strong interaction between the POSS siloxane and the matrix. For instance, in polar monomer such as vinylpyrrolidone,[127] the strong dipole-dipole interactions existed between siloxane of POSS and carbonyl group of PVP and enhanced the *Tg*. To certain the interactions, FTIR and NMR were usually employed, because the interactions reassign the bond from the original state. (3) physical aggregation of nanoscale POSS; (4) POSS hinder the motion of chain[128]; (5) POSS reduce the crosslinking density[101]; (6) branching effect, on the dimension of the reptation tube, was shown in (Figure 1.53).

Presuming that the dynamics of the present random copolymers followed the tube model, the resultant average tube diameter would increase because of the presence of the pendent isobutyl POSS molecules and consequently the lower entanglement density. (7) Li et al [68] recently reported an aliphatic epoxy composite with a multifunctional POSS. It was found that the epoxy/POSS 75/25 (wt) composite exhibited much lower *Tg* than the control epoxy. They argued that the *Tg* depression could be germane incomplete curing reaction of epoxy due to the inclusion of POSS cages.

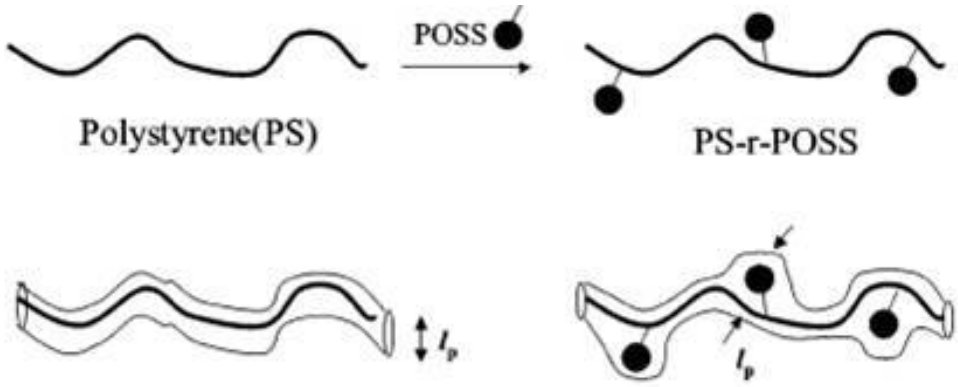

Figure 1.53 Schematically drawing the effect of the pendent POSS group on the PS chain topoloty and the resultant tube dimension.

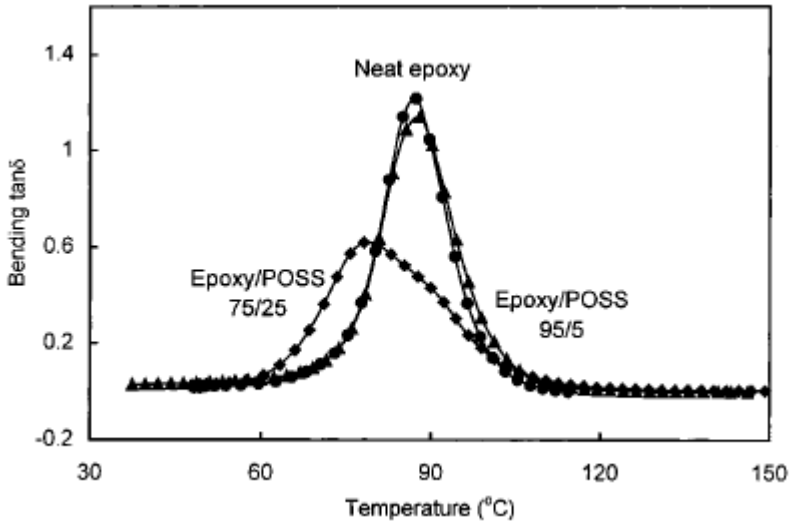

Figure 1.54 Bending *tan δ* vs temperature curves of epoxy resin and its epoxy/POSS 95/5 and 75/25 (*wt/wt*) composites after final curing at 120 °C/25 h.

(8) The interaction between vertex groups. Wu et al[129] investigated the thermal and linear rheological behavior of polystyrene (PS)-based random copolymers incorporating POSS with three kinds of vertex groups: isobutyl (iBu), cyclopentyl

(Cp), and cyclohexyl (Cy). The weak iBuPOSS-PS segment interaction resulted in a phenomena that glass transition temperature (*Tg*) monotonically decreased with increasing iBuPOSS content. Conversely, the strong CpPOSS/CyPOSS-PS segment interaction resulted in glass transition enhancement, though with complex dependence in the CyPOSS case.

(9) Incompletely conversion of POSS took place in POSS bearing epoxy group which had low reactivity compared with the one of epoxy precursor.[102, 103] Gerard obtained a more homodispersed POSS particle in pre-action of epoxy POSS with curing agent amine. The non-reacted epoxy POSS led to a dispersion of spherical particles with sizes in the range of the micrometers concluded to RIPS related with the incomplete conversion of POSS[103]. The steric effect of epoxy group was considered as an important effect slowing down the reactivity of POSS precursor. Li[68] incorporated POSS epoxy precursor into Epoxy. In those composites, epoxy groups in this POSS macromer were disubstituted with a large phenyl ring. Thus, SN2 substitution by amine with epoxy ring-open, should be slower than the same reaction on the neat epoxy molecules. This could lead to a smaller fraction of the POSS epoxy groups participating in the cure. As a result, the cross-linking density in epoxy/POSS 75/25 was less than that in neat epoxy and decreased the *Tg* of composites(Figure 1.54). The annealing at high temperature, *Tg* would increased because of removing the residual epoxy in POSS(Figure 1.55).

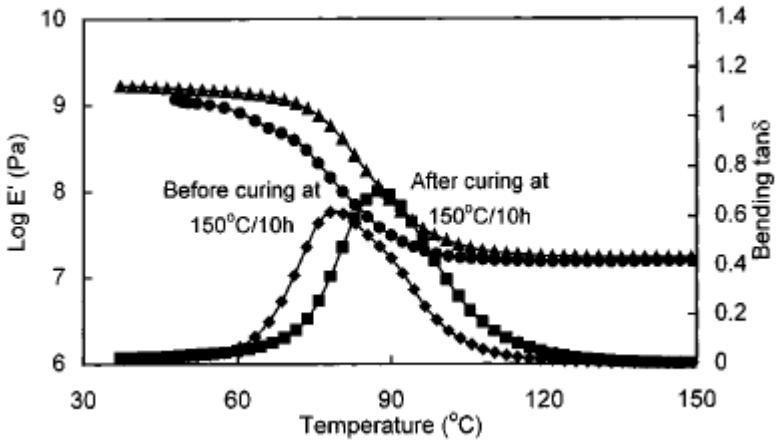

Figure 1.55 Bending modulus (*E'*) and *tan δ* vs temperature curves of epoxy/POSS 75/25 (*wt/wt*) composite before and after curing at 150 °C/10 h.

(10). oligomer of POSS decreased the curing density.When epoxy bearing POSS pre-reacted with curing agent to homodisperse, oligomer formed probably and decreased the curing density obviously, reflecting on the *Tg* decrease. After 10 min of

premixing, Lu[102] observed that a tail appeared on the high molecular weight side in GPC. This signified that reaction between HHPA and oxirane groups of POSS had formed significant amount of POSS dimers and trimers(Figure 1.56).

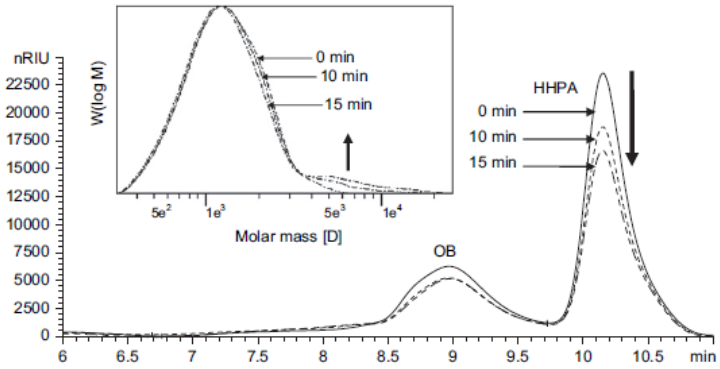

Figure 1.56 A tail appears on the high molecular weight side in GPC.

Expecting that the curing density was influenced by the molecular structure and length, Xu afforded a method as reference[130] to analyses the tether chain between epoxy bearing POSS and curing agent after reaction: the silica core of POSS cages were dissolved with HF and extracted for GC-MS analyses(Figure 1.57).

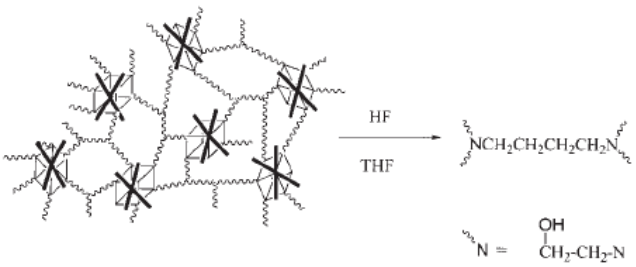

Figure 1.57 Preparation of real tethers by digestion of POSS with HF.

A single peak was observed in the GC chromatograms of both the model compound and the HF-digested hybrid polymer, which suggested that all epoxy rings reacted with the amino groups in the butanediamine molecules and, thus, that the butanediamine was completely tetrafunctional. In MS spectra, almost every peak in the MS spectra could be assigned to the corresponding fragment ion(Figure 1.58). Simultaneously, it also provided us with an easy method to the investigation of the tether structure between the POSS cubes in the hybrid polymers. From the above disscusion, it is difficult to conclude the effect of POSS into a model, so there are increased *Tg* [128] [131], compressed *Tg* [72], alternating *Tg* [10, 127, 132] of composites obtained.

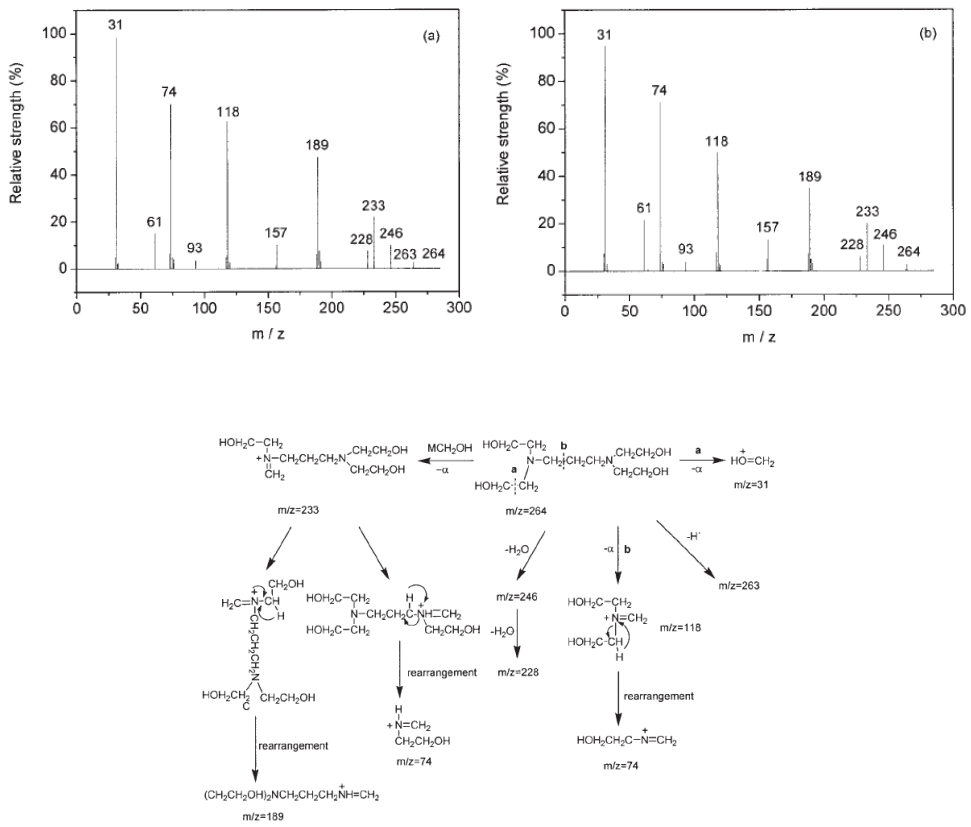

Figure 1.58 MS spectra of (a) model and (b) real tethers

The aim of this work

The aim of this work is to nanostructure POSS into epoxy networks, via physical blend or chemical bonding. POSS doesn't distribute homogeneously and tends to agglomerate in composites. Phase separation frequently occurs between POSS and monomer(s) before and during polymerization depending on the chemical nature and functionality of the organic ligands in POSS cages. It is observed that the POSS-based composite has ultra low friction and gradient distribution of POSS, which tends to enrich on the surface rather than inside [69, 70].

The ideal structure of POSS homogeneously dispersed in the matrix that is often desired, however frequently not achieved in practice due to the lack of compatibility of POSS with the matrix. The silicon nature of POSS constrains its compatibility with the matrix, although it's switchable with the vertex group.

In Chapter 1 and Chapter 2, we attempted to fabricate a hybrid epoxy based on reactive POSS precusors. A new analogue of POSS (denoted as POSSMOCA), which had reactive amino group, was synthesized via addition reaction and could be utilized

in polymers and coating, such as polyurea and nylon. It was characterized by NMR, FTIR and Element Analysis. The prereaction temperature was determined by heating POSSMOCA and epoxy precursors DGEBA blend through DSC. After bonding into epoxy network, it improved the thermostability, based on the structural silicon, nitrogen and halogen in POSSMOCA. It is worthy notifying that amorphous POSSMOCA, which had a polar side chain and patterned POSS head, crystallized in epoxy network. To explain the result, a mechanism was hypothesized called as "Destructive Reaction-Induced Crystallization", which described the phenomena reliably: when two alignment parameters coexisted, it crystallized after vanishment of irregular motivation. It would be meaningful to design new materials and develop new functional materials such as pH sensitive materials.

Moreover, POSS-silanol structured a nanophase, based on a DGEBA prepolymer via using different organic metal compounds as catalysts. In this work, anhydride was considered as comonomer rather than a diamine due on the fact that anhydride gives a high thermal stability, lower toxicity, and shrinkage. Moreover, the dependence with stoichiometric ratio between of epoxy and anhydride is relatively not important compared with strictly stoichiometric amino hydrogen-to-epoxy in epoxy/amine systems. Aluminium acetylacetonate was reported to be an efficient catalyst for the POSS ring-opening reaction[133]. As similar metal-based complexes, two other catalysts based on Cu and Co were also considered to introduce POSS-OH in epoxy networks. To our knowledge these two catalysts were not already described to catalyze POSS-OH and epoxy reactions. Hybrid *O/I* were prepared with/without presence of moisture and a mechanism of reactions involved, i.e. competition between consumption of epoxy groups with anhydride and silanols is proposed.

Although the invariant polarity of POSS monomer, POSS is copolymerized, then different comonomer tunes its compatibility with DGEBA network. For instance, the compatibility of block copolymer depends on the curing agent and epoxy precursors, PMMA is of heterogeneous with DGEBA/4,4'-diaminodiphenyl sulfone (DDS) or 4,4'-methylene dianiline (MDA), however homogenous with DGEBA 4,4'-methylenebis(3-chloro2,6-diethylaniline) [134]. There are a few POSS copolymers were synthesized and obtain a nanostructure in epoxy network. Zheng et al[35] synthesized a POSS-capped PCL via ring-opening polymerization of ε-caprolactone with 3-hydroxypropylheptaphenyl POSS as the initiator, which is incorporated into epoxy resin to obtain hybrid thermosets. Zeng et al [135] synthesized hepta(3,3,3-

trifluoropropyl) polyhedral oligomeric silsesquioxane (POSS)-capped poly(epsilon-caprolactone) (POSS-capped PCL) was synthesized via the ring-opening reaction of F-caprolactone, which was initiated by 3-hydroxypropylhepta(3,3,3-trifluoropropyl) POSS with stannous (*II*) octanoate [$Sn(Oct)_2$] as the catalyst. Then the epoxy is cured in present of POSS copolymer via selfassembling in network.

In Chapter 4, PGMA was homopolymerized via reversible addition-fragmentation transfer polymerization utilizing CDB as a chain transferring agent, to obtain a dioester terminated macro-initiator. Then the second POSS block was polymerized with PGMA macroinitiator at different ratio. Epoxide group in GMA was be prereacted by the curing reagent MDEA, then connected into the epoxy networks. We supposed that the curable POSS block copolymer self-assembled into micelle and formed POSS core/intercrossing GMA-MDEA corona in the epoxy base. PA, PAI, PU, PC, PET and PUA are possible to nanostructurate via this “bottom-up” method via the reactive POSS block copolymer. Because the epoxide group has universal ring open agent, for instance acid, amine, anhydride, isocyanates and coordinating polymer. It is easy to tail the compatibility of the reactive block copolymer bearing epoxide group with a step-growth polymerization matrix. For instance, it could be prereacted with multi-hydroxyl agent, then nanobuilt in multi-isocynate component. Our block copolymer could structure a nanophase easily in UV curing resins, optical waveguide devices.

In order to fabricate a hybrid epoxy network, POSS-PMMA copolymers were blent with the DGEBA/MDEA and were characterized its performances in Chapter 5. Owing to the hydrogen bonding between PMMA with DGEBA/MDEA, POSS-PMMA built different morphologies, which depended on the POSS concentration and topology of POSS-MMA copolymers. To avoid the POSS copolymer aggregates before curing, POSS polymers were dispersed into DGEBA precursor and obtain a homogenous stable mixture, namely prepreparation. Even it’s compatible with the precursor, it aggregates resulting from the entropy of mixture decrease with the conversion of precursor, which means the reaction induced phase separation.

Chapter 2 Synthesis of POSSMOCA and its nanobuilding in epoxy

2.1 Brief introduction of reactive POSSMOCA and its composite

Using reactive POSS to modify the epoxy network is one of effective strategies, because the epoxy-philic chain could be obtained through the covalent bond between POSS and matrix. Based on the fact that the reaction of epoxy and curing agent is stepwise, once the reactive POSS was incorporated into oligomer of epoxy, obtaining an epoxy-philic tail, and then the POSS will be partial compatible with epoxy network. It would be possible for POSS nanophase disperse into epoxy homogenously. There have two kinds of reactive POSSs: i) epoxy bearing POSS, ii) ring open reagent POSS.

In our early research, POSS as a halogen-free fire retardant, its vertex groups determined the final properties of composites, such as better thermostability obtained by phenyl POSS via prereaction in the epoxy network [136].

Multi-elements synergetic fire-retardant attracts a lot of attentions, because the silicon forms char at high temperature, however the char evaporated[137, 138]. Al[139] , Ti and V complex [140] , carbon nanotube [117, 141] had synergetic effect with POSS and improved its fire, smoke, and toxicity performance. Synergetic effect in some cases was tunable via the compatibility between POSS and other elements in bulk. For instance, in PU/POSS nanocomposite, a Si-N synergetic system with poly(vinyl silsesquioxane) resulted in 50% reduction of the heat release rate (*HRR*) peak, whereas, octamethyl-POSS did not show any improvement in fire retardancy[142].

We synthesized an imcompletely condensated POSS analogue, a trifunctional amino-capped POSS, then characterized this amorphous POSS and introduced it into epoxy networks. Synthesized POSS with halogen may not only enhance the epoxy networks flame retardants, but also nanostructurate organic-inorganic hybrid materials in epoxy matrix, which was interested to be a hybrid nano-fire retardant.

2.2 The synthesis and characterization of POSSMOCA

2.2.1 The synthesis of POSSMOCA

2.2.1.1 Materials

Trisilanol phenylPOSS (SO1458) was obtained from HybridPlastics Co, which with three Si-OH group and seven phenyl vertex group. Toluene-2,4-diisocyanate (TDI, C.P.) was purchased from Sinoreagent Co. Tetrahydrofuran (THF, Sinoreagent Co., A.R.) was purified by stirring with KOH and then redistillation with Na fiber before using. 4, 4' methylene-bis-(ortho-chloroaniline) (MOCA, C.P.) was afforded by TAIWAN PU CO. Dimethyl sulfoxide (DMSO, Sinoreagent Co., A.R.) was distilled after stirring with CaH (Sinoreagent Co., A.R.). Acetonitrile (Xilong chemical Co.) and Dibutyltin dilaurate (DBTDL) were utilized as received. DER 332 (Dow Co.) and MDEA(Lonza Co.) formed the epoxy network.

2.2.1.2 Preparation of POSS-MOCA.

Protocol of POSSMOCA is shown as Scheme 2.1. TDI was dissolved in anhydrous THF in a sealed flask to obtain a 0.3 g/ml solution, then 1g/ml trisilanol POSS/THF solution were added into the TDI/THF solution dropwise in 3h with vigorouse agitation, (the molar ratio of trisilanol POSS to TDI was 1:1.5), then the mixture was injected by syringe into 0.2g/ml MOCA/THF in 1h. In the flask, some powder precipitated after the addition of MOCA, and then the reaction was processed for 2 h after dropping. The product was purified by dissolved into DMSO and precipitated in acetonitrile and THF. After dried in 60°C vacuum, the final product, POSSMOCA was obtained. The yeild of POSSMOCA was about 24%. No obvious melting transition of POSSMOCA was observed from the capillary tube testing.

2.2.1.3 Characterization of POSSMOCA

a.FTIR

The FTIR measurements were performed on a Fourier transform spectrometer (Nicolet Avatar 360) at room temperature. The samples were dispersed into KBr, measurements were recorded at a resolution of 4 cm^{-1}, 32 scans.

b.NMR

Bruker 300M Nulear Magnetic Resonance was employed to characterize the ^{1}HNMR and ^{13}CNMR. The samples were dissolved in *d*-chloroform and tetramethyl silicane was used as an interal reference.

c.Elemental Analysis

The Elemental Analysis was characterized via Vario EL III (Elementar Analysen Syetem GmbH Co).

d.DSC

A differential scanning calorimeter (DSC) (The Netzsch DSC 204, Netzsch Co.) was employed to research the crystallization of sample and the curing and the prereaction of POSS/epoxy in a nitrogen atmosphere. The sample was heated from ambient temperature to 250 °C at rate of 10 °C min^{-1}.

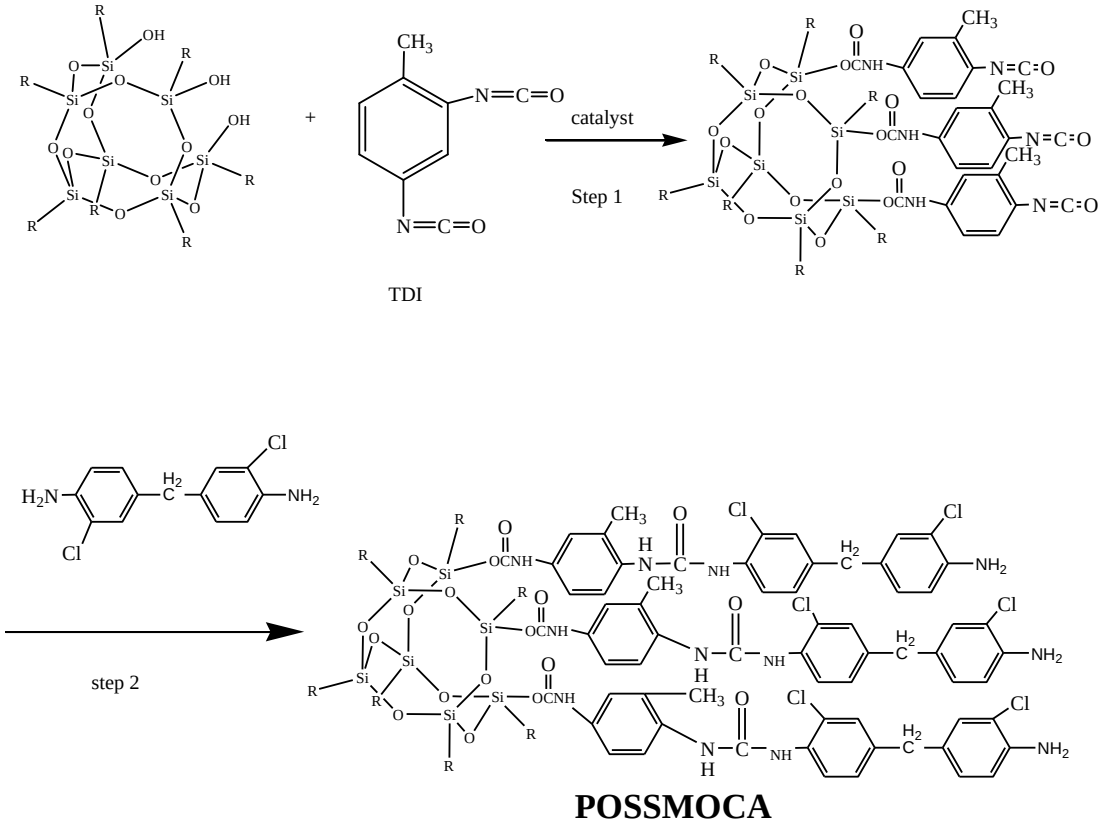

Scheme 2.1 The protocol to prepare POSSMOCA.

**R group= phenyl.*

2.2.2 Characterization of POSSMOCA

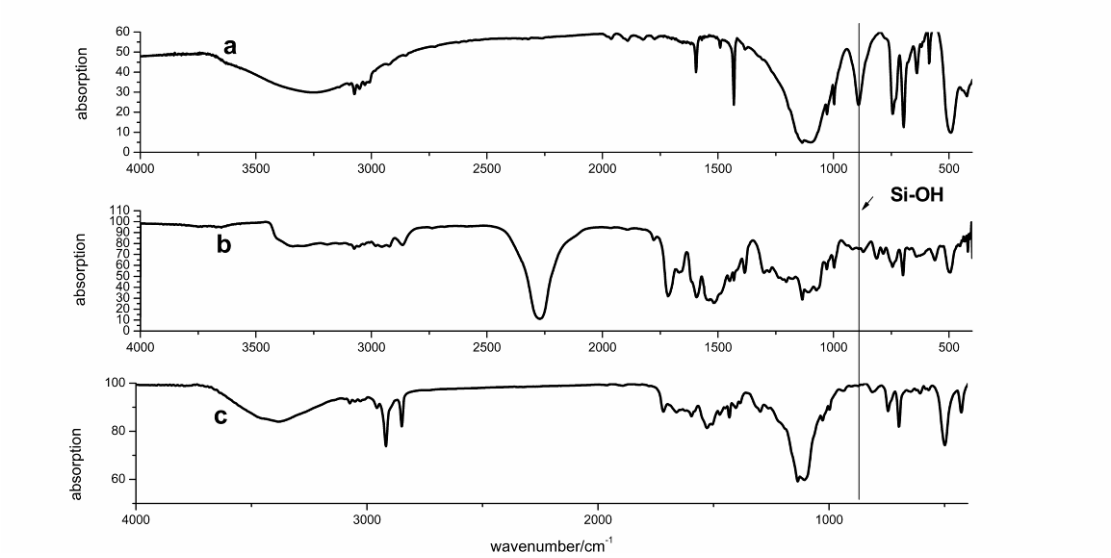

Figure 2.1 FTIR spectra of the products

**a. the raw material, POSS-OH, b. the product of step 1 of Scheme 2.1, to check the NCO-end intermediate. c. POSSMOCA*

FTIR was utilized to monitor the reaction between POSS-OH and TDI (Figure 2.1). Before reaction, a huge peak at 3356 cm^{-1} is described to the -OH in POSS cage incompletely condensated sketch. The hydroxyl group is reliable to react with the N=C=O group, for example the addition between polyols and polyisocyanate to prepare polyurethane[143]. Previously, Many reports confirmed the possiblity of reaction between the hydroxyl capping POSS and NCO reagent into a polymer base (polyurethane), which was a powerful method to obtain a nanomodified composite POSS under mild conditions.[144] Dibutyltin dilaurate (DBTDL) was affirmed as a high active catalyst for the addition reaction between N=C=O and hydroxyl[145]. Therefore, DBTDL was employed as a catalyst for the POSS-OH/TDI. After the addition reaction between –OH and N=C=O, the peak appears at 1715 cm^{-1} and 1592 cm^{-1} assigned to the C=O in carbamate, which is derived from addition of –OH and N=C=O. The active end capping N=C=O at 2276 cm^{-1} is able to react with $-NH_2$ in MOCA. After the second step, the end-capping N=C=O was indiscernible in the final products, POSSMOCA(Figure 2.1c). It is noticeable that the huge –OH peak at 3250 cm^{-1} is replaced by 3350 cm^{-1} and 3464 cm^{-1}, which is assigned to the $-NH_2$ and -NH group. 646 cm^{-1}, 1028 cm^{-1} are assigned to the C-Cl stretch in aromatic ring[146]. It is considered that the carbonyl group at 1685 cm^{-1} in hydrogen bonding environment probably[147]. The silanol group (Si-OH) is indiscernible in the sample b and final

product sample c indicating high conversion of Si-OH. Moreover, the result of element analysis is quite in accordance with the theoretical value (Calculated C 57.5%, H 4.11%, N 7.45%, O 12.77%, Experimental C 57.8%, H 4.01%, N 7.60%, O 12.86%,). Furthermore, the SEC spectrum of final product shows a mono-peak at about 2400, d=1.05 with PS standard, which is close to the POSSMOCA theoretical value (2255).

To confirm POSSMOCA, ^{1}HNMR and ^{13}CNMR were followed after the reaction. As shown in ^{1}HNMR (Figure 2.2), δ=9.08 and 9.06 ppm represent two kinds of N-H circumstances in carbamido. The former reflects with hydrogen in chloro-aromatic ring and the later reflects with the one in methyl-aromatic ring. δ=9.36 ppm is the N-H of carbamate, the integration of –NHCOO- should be a half of –NHCONH-, in accordance with the experiment. The peak at δ=6.5-8.9 ppm is assigned to the aromatic ring, and δ=3.73 ppm is characteristic of the $–CH_2$ group of MOCA units. $–CH_3$ and amino group appear at δ=2.20 ppm and 3.86 ppm respectively. In ^{13}CNMR of POSSMOCA (Figure 2.3), the chemical shift of δ=13.20 and 17.95 ppm are assigned to methyl and methylene group respectively. Since the carbamate (-NHCOO-) and carbamido (-NHCONH-) structures are introduced into the POSSMOCA by step-wise, they are decisive to confirm the validity of reactions. They were found at δ=153.21 and 152.98 ppm respectively and assure the reaction took place as designed.

Because of structure symmetry, POSS cage generally tends to crystallize. Its symmetric inorganic core is likely to pack regularly and form crystal such as hexagonal lattice or crystalline region, deriving from the strong dipole-dipole interaction between vertex groups[148]. The crystallization tendency would be enhanced in free POSS connecting with a polar end group[144, 149]. Even if the POSS connecting in the main chain of polymer with a strong restrict of macromolecular chain, it forms crystalline region generally[150]. The precursor POSS-OH crystallize with a very high degree of crystallinity and forms hexagonal lattice in the publishment[151]. However, it is interesting to observe that our product POSSMOCA is amphormous from XRD (Figure 2.8), there are few reports mentioned an amorphous POSS[152, 153].

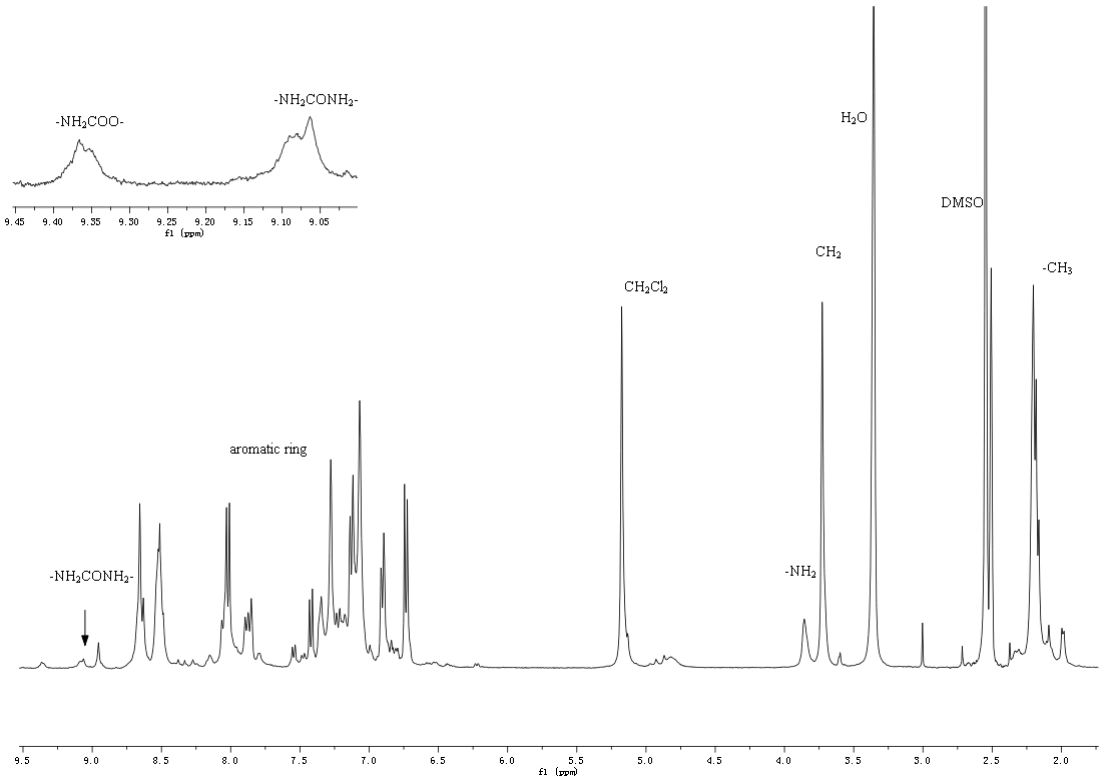

Figure 2.2 ^{1}HNMR spectra of POSSMOCA in *d*-DMSO.

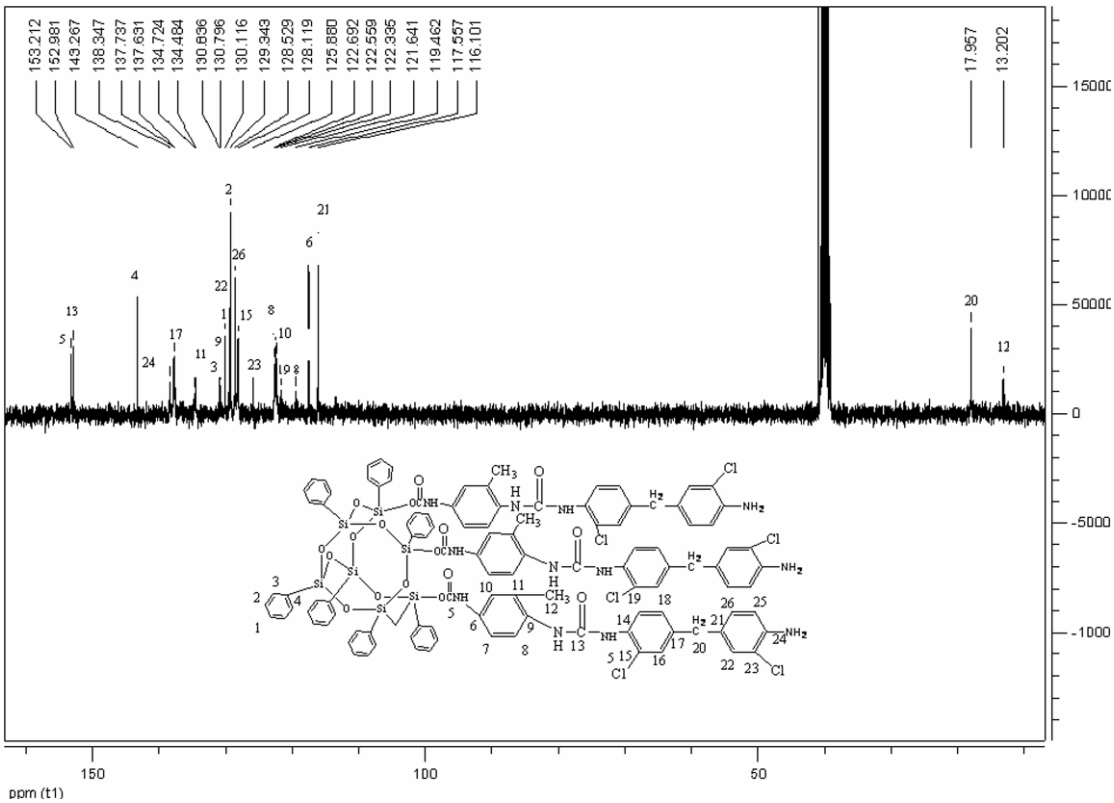

Figure 2.3 ^{13}CNMR spectrum of POSSMOCA in *d*-DMSO.

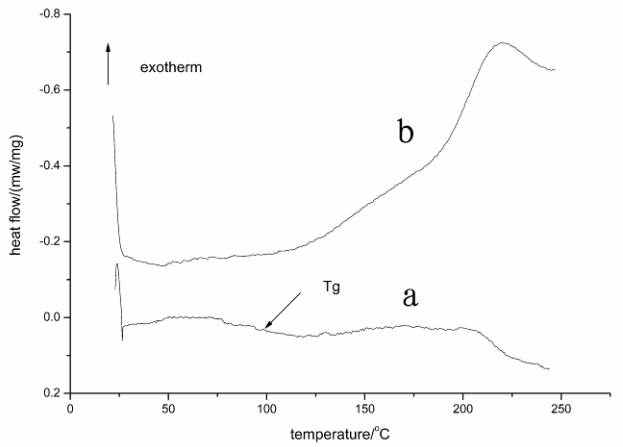

Figure 2.4 DSC spectra of POSSMOCA and POSSMOCA/DGEBA,
**a.POSSMOCA, Tg=93°C, b.POSSMOCA/DGEBA*

To assure its amorphous nature, DSC was utilized and no endothermic transition was observed obviously (Figure 2.4). It means non-crystalline of POSSMOCA, in accordance with the XRD result (Figure 2.8). The glass transitions is observed in the thermogram, which means to the vitrification of amorphous POSS analogue in accordance with the reference[152]. Besides calculating the degree of crystalline, DSC was usually employed to determine the exothermy of the reaction, for instance, epoxy ring-opening reaction involving generally exothermic 100–118 kJ/eq[91]. The end-capping NH_2 in POSSMOCA is reliable to open the epoxide ring effectively as other amine curing agents. In the blend of POSS/DGEBA, the onset temperature of ring opening reaction is observed at 120°C. The main exothermic transition takes place at the center of 219°C with a shoulder peak at 180°C. Whether pretreatment is processed plays an important role to the morphology and the mechanical properties[71]. In hybrid materials, the ideal structure consists in pendent POSS cages homogeneously dispersed in the network. If without pre-reaction, the POSS monomer tends to form agglomerate spontaneously, because of the incompatible nature between POSS and epoxy. Furthermore, when the curing reaction is processed, the phase separation appears at the beginning of reaction between epoxy and POSS[154]. With the procedure of pre-reaction, POSS tends to connect with the DEGBA precursor, and becomes partial compatible with epoxy because of the grafted DGEBA segment. It compresses a phase separation and is likely to a nano-phase separation which is close to the diameter of POSS molecular level. From the thermal trace, pre-reactive

temperature with mild rate at 190°C is reasonably determined, to link the POSS into DEGBA precursor.

2.3 POSSMOCA/DGEBA composite and its crystallization

2.3.1 Preparation of POSSMOCA/DGEBA composites

To achieve POSSMOCA hybrid materials, POSSMOCA was introduced into a DGEBA/MDEA network by pre-reaction. The pre-eaction was processed at 190 °C for 4 h. After that, the prereactd DGEBA was blend with a stoichiometric MDEA to obtain a transparent solution 90 °C for 20 min. The resulted mixture was poured into an aluminium model (1cm* 3cm), cured at 135°C for 4h and 190°C for 4h. The samples were stripped from the aluminium model and cut into desire size to characterize.

Measurement of composites

a.SEM

The morphology of POSS-containing epoxy hybrids was observed with a Philips XL 30 Scanning Electron Microscope (SEM). The samples were immersed in liquid nitrogen and fracture. The surfaces were etched in DMSO at room temperature for 30 min, because it is an excellent solvent to the un-reacted POSSMOCA. The etched specimens were dried to remove the solvent. After that, a gold coating of about 100 Å was sprayed on the fracture surface. Activation voltage of SEM observation is 20 kV.

b.XRD

The degree of crystalline was carried out by x-ray diffraction (XRD, Philips X'Pert Pro Super X-ray diffractometer, Cu Kα radiation, at a 2 °min^{-1} scan rate.

c.TGA

A Netzsch STA 409EP (Netzsch Co) Thermal Gravimetric Analyzer (TGA) was used to investigate the thermal stability of hybrid composites. The samples were heated from ambient temperature to 800°C in an air atmosphere. The heating rate of 10° C/min was used in all cases.

d.DMTA

Dynamic Mechanical Thermal Analysis (DMTA) was carried out on cured hybrid networks with a Rheometrics Solid Analyzer (RSA II) to obtain tensile dynamic mechanical spectra (storage modulus E', loss modulus E", and loss factor tan δ) between 25 and 220°C at a frequency of 1Hz in the linear viscoelastic domain.

Standard epoxy samples (1cm*3cm*2mm) obtained by cutting and polishing were used for DMTA analysis.

2.3.2 Characterization of POSS/MOCA composites

2.3.2.1 The morphology of POSSMOCA/DGEBA composites

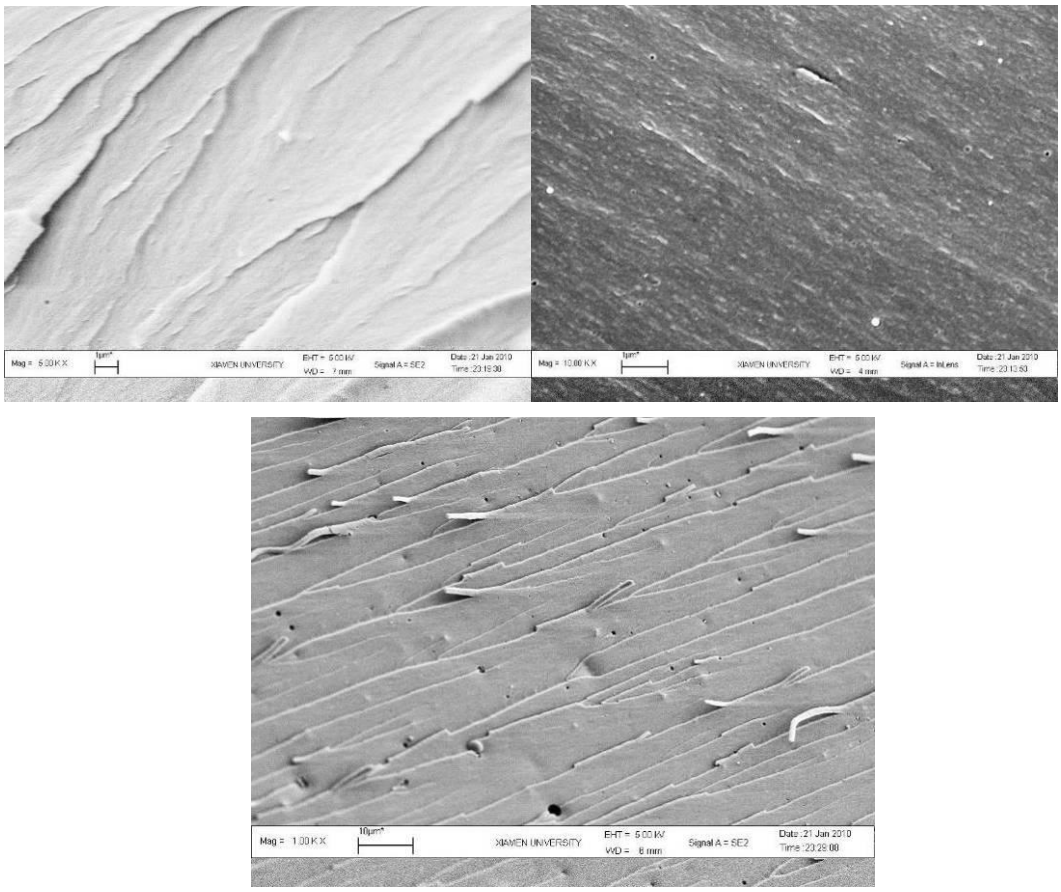

Figure 2.5 Morphology of POSSMOCA epoxy composite observed from SEM, a. 5%POSS, b.10%POSS, c. 20% POSS

After the pre-reaction, homogenous morphology is achieved in samples in Figure 2.5, in addition, there are some dots (50-80 nm) dispersed in the matrix. No big cavity is observed after etched by DMSO, which is an excellent solvent for POSSMOCA. It demonstrates the compatibility between POSSMOCA/DGEBA after pre-reaction. In our case, no micrometer scale POSSMOCA domain obviously disperses in the neat epoxy in low loading (Figure 2.5a, 2.5b). Whereas, besides the nanodomain as low loading, POSSMOCA enriches into microsphere with 1-2 μm diameter at a high loading (Figure 2.5, 20%wt). Some elapsed residual in the cavity (in Figure 2.5c), maybe a part of inner POSSMOCA is covered by reacted POSSMOCA which is

amphiphilic with epoxy matrix. The solid surface shrinks after the inside un-reacted POSSMOCA abstracted by the solvent. This microphase separation is related with the mechanical properties of final nanocomposites. After reaction with DGEBA, the end of tail, DGEBA group of POSSMOCA is compatible with the matrix resin and then is connected with the matrix with the curing reagent MDEA. However, the POSSMOCA structure, thanks to the strong polarity of carbamido and carbaminate group, is incompatible with the epoxy matrix. It forces the POSSMOCA self assemble to a nanoscale micelle or emulsion particle. Inside of the emulsion particle, the un-reacted POSSMOCA may be wrapped by the reacted POSSMOCA/DGEBA.

2.3.2.2 TGA of POSSMOCA and its composites

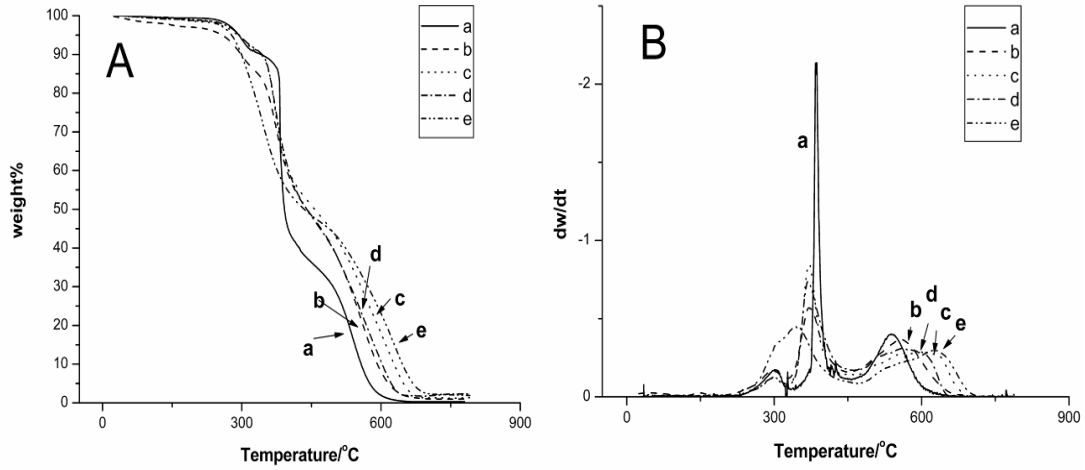

Figure 2.6 thermostability is characterized via TGA in the air, A. weight loss curve, B. differential TG

**a.neat epoxy, b. 5%POSSMOCA, c. 10%POSSMOCA, d. 20%POSSMOCA, e. POSSMOCA*

Epoxy because of the hydrocarbon nature is poor at flame retardancy. The halogen is widely utilized as a functional reagent of flame retardancy, even though it is hazard to the humanbeing's healthy and is forbidden to utilize in body touched materials. To approach high thermostability of polymer base materials, multicomponents fire retardants were employed, because the synergistic effect between components improves the flame retardance. It was found on Si, N, P, halogen, B and so on components [125, 155-157]. Here, POSS tends to formulate silica coating during combution, which protects the matrix inside far away oxidation by the air. It would cease the attack from the oxygen radical and the thermodegraded active radical, in the end to improve the utilized temperature of materials. Moreover,

low content Cl is introduced base on that the Cl atom quenches the active radical and compresses the probability of chain reaction[158].

The thermodegradation(Figure 2.6) consists of 2 steps in pure POSSMOCA: 250-470, 470-700 deriving from the long vertex group degradation and vaporization, then the formation of silica at higher temperature[159]. Three steps of thermodegradation take place in the neat epoxy network, familiar with the POSSMOCA composite. The step 1 is almost the same in the weight loss in differentiate TG curve, whereas the weight loss of step 2 for POSS modified epoxy samples are compressed compared with the neat epoxy, although with a lower degradation temperature. It could be assigned to the halogen stabilizing effect. The same improvements take place in the step 3; therewithal the composites with POSSMOCA have lower weight loss and better Td than the neat epoxy. It is reasonable to be assign to the POSS forming inorganic ceramic layer. It should be notified that the thermostability doesn't follow the increase of POSSMOCA in epoxy directly. The weight loss rate of 10% POSSMOCA loading sample is lower than 20% in step 2 and step 3. There are 50 º C improvements in Td of 10% loading sample then the one of 20% sample in step 3. That might derive from the POSSMOCA microscale phase separation in 20% loading sample, which has been discussed in the morphology part. However, frankly, the introduction of POSSMOCA doesn't improve that much, because of silica formation at higher temperature than the halogen degradation. It is a explanation for the limited halogen and Si synergistic effect and no surprisingly improvement.

2.3.2.3 Thermal dynamic properties of POSSMOCA composites

DMTA results are presented in Figure 2.7. The vitrification of POSS modified epoxy shows a boarder peak than the one of neat epoxy, which is correspondence with large free volume of POSS[160]. Decreasement of Tg with the addition from 5% to 10% demonstrates the enhanced plasticizer effect of POSS. However, at 20% loading, an increased T_α was oberserved, with a T_β at 141°C, which is assigned to the vitrification of the plasticized separated phase of POSS. From the view of reaction induced phase separation, POSS phase plays as a dilute phase at the continuous phase, whereas continuous phase contains less POSSMOCA. Getting a high Tg in macrophase separation composite than the one of nanocomposite is reasonable, due to a compress of plasticizer effect. The continuous phase appears similar DMTA result

to the neat epoxy. Contrarily, the separated phase, which contains high concentrated POSS namly a thick phase, follows the relationship of the compressed Tg with higher POSS loading.

Considering the volume and the stiffness of POSS cage, there is a controversy of POSS cage in the neat epoxy because it could be an interacting curing point and a high free volume plasticizer. It is inevitable to decrease the epoxide concentration when connecting POSS into epoxy matrix, namely a higher EEW, resulting in a lower cross-linking density generally. The suppression of epoxy density leads to chain motion easier and Tg decreasing. POSS cages occupy a chemical curing point between epoxy network chains because of its relatively high volume compared with epoxy unit. It directly results in low curing density and low Tg. Reflected by the low Tg from experiments, it is supposed that the homogenous dispersed POSS domain connecting into main chain efficiently decrease the difficulty of main chain's α transition. However, it is well known that the chain stiffness makes the chain segment motion difficult. The POSS cage, with hybrid nano silica core, is a rigid unit which improves the chain's rigidness. By covently bonding the POSS cage on the macromolecular network, some reports supported the improvement of chain rigidness[161], namely Tg elevating in the mixture. In our case, the POSS is covalently connected into the neat epoxy, at nanoscale (close to the POSS molecular size) via the reaction between amine group of POSSMOCA and epoxide groups of DGEBA. Therefore, POSS domain in the neat epoxy can be considered as homogeneously dispersed functional nanofiller covalently bonded in the matrix, which may improve the storage modules. From the view of POSS structure, a strong self aggregation tendency results from the incompatibility of POSS with neat epoxy, because of POSS-POSS interaction [162] and the high polarity of side chain. In the separation phase at high loading from SEM, POSS rich particles are assembled by several free POSS cages, larger than a POSS unite (1-3 nm). Therefore, POSS domain is a physical curing point in the network and forms a secondary bond interaction between each other. Moreover, in our case, a chemical curing point is attributed to the trifunctional POSSMOCA by covalent bonding to DGEBA after curing. Considering high polar subchain (NHCOO, NHCONH), it increases intermolecular interaction and is good for a higher working temperature[163]. Whereas, the large subchain tend to enlarge the distance of epoxy networks, resulting in the enhanced motion of

mainchain. It is difficult to conclude the effect of POSSMOCA to the thermal dynamic properties in composite, which is a multi-factor combined result.

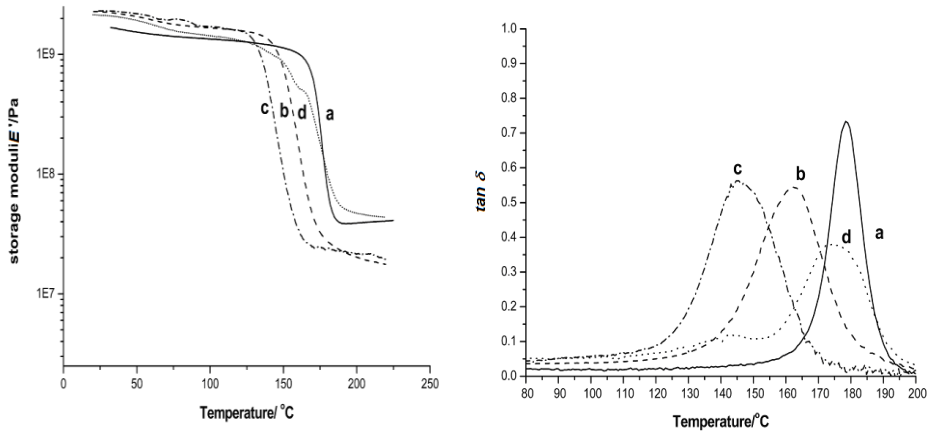

Figure 2.7 DMTA curves of POSSMOCA composite

**a. neat epoxy, b. 5%POSSMOCA, c. 10%POSSMOCA, d. 20% POSSMOCA*

2.3.3 Reaction induced crystallization

The degree of crystallinity can be determined by a variety of physical methods, for example, X-ray diffraction (XRD), differential scanning calorimetry (DSC), density measurement, infrared spectroscopy (IR), and nuclear magnetic resonance (NMR). In the present work, the degrees of crystallinity of POSSMOCA nanocomposites have been evaluated by XRD. $Xc = \frac{Ac}{Ac + Aa}$, Where *Xc* refers to the degree of crystallinity, *Ac* and *Aa* stand for the crystallized area and the amorphous area on the X-ray diffractogram, respectively.

In the spectra (figure 2.8), two distinct amorphous halos of POSSMOCA at 23.7 ° (d-spacing of ca. 0.38 nm) and 15.78 °(d-spacing of ca. 0.56 nm) to the Si–O–Si distance (d=ca. 0.31 nm) and the diameter of the POSS siloxane cage (d=0.54 nm), in accordance with the published amorphous samples[153]. Interestingly, POSSMOCA forms crystalline in epoxy resin. Besides the amorphous halo, a shoulder peak at 13.9°, which is assigned to the crystalline, forms after reaction in all composites (d=0.64 nm). CS Chem3D software (MM2 calculations) was used for molecular modeling to calculate the cube size as well, and the results were shown in Figure 2.9, showing good agreement with X-ray diffractogram. From the calculation, the end-to-end lengths of core framework to vertex group (Figure 2.9) are 0.64 nm for POSSMOCA,

which is in accordance with the experimental *d* value from XRD. The degree of crystalline is 0.17 when 5% POSSMOCA loading. The reacted POSSMOCA tends to assemble into a monolayer of POSS framework from the XRD spectra.

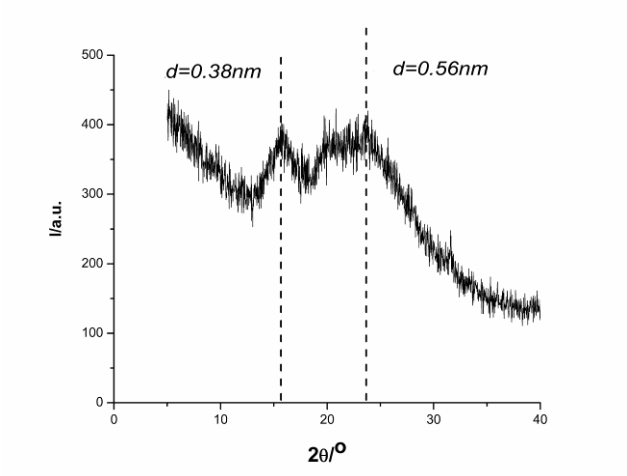

Figure 2.8. XRD spectra of amorphous POSSMOCA

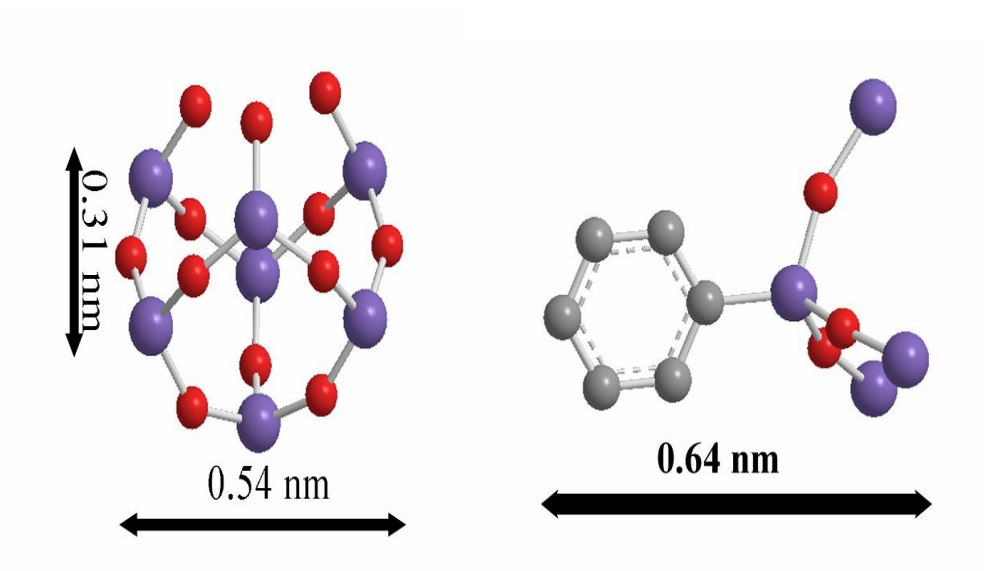

Figure 2.9 CS Chem3D software (*MM2* calculations) for molecular modeling to calculate the cube size and the framework of the POSS.

**red ball=O, purple ball=Si, gray ball=C.*

The steric hinderance is an important factor to noncrystalline in references[153]. The side chain of POSSMOCA, it is a stiff chain deriving from the plenty of phenyl π structure. Therefore, the motion of POSS becomes suppressed by the stiff side chain, because the molecular folding and rotation is constrained.

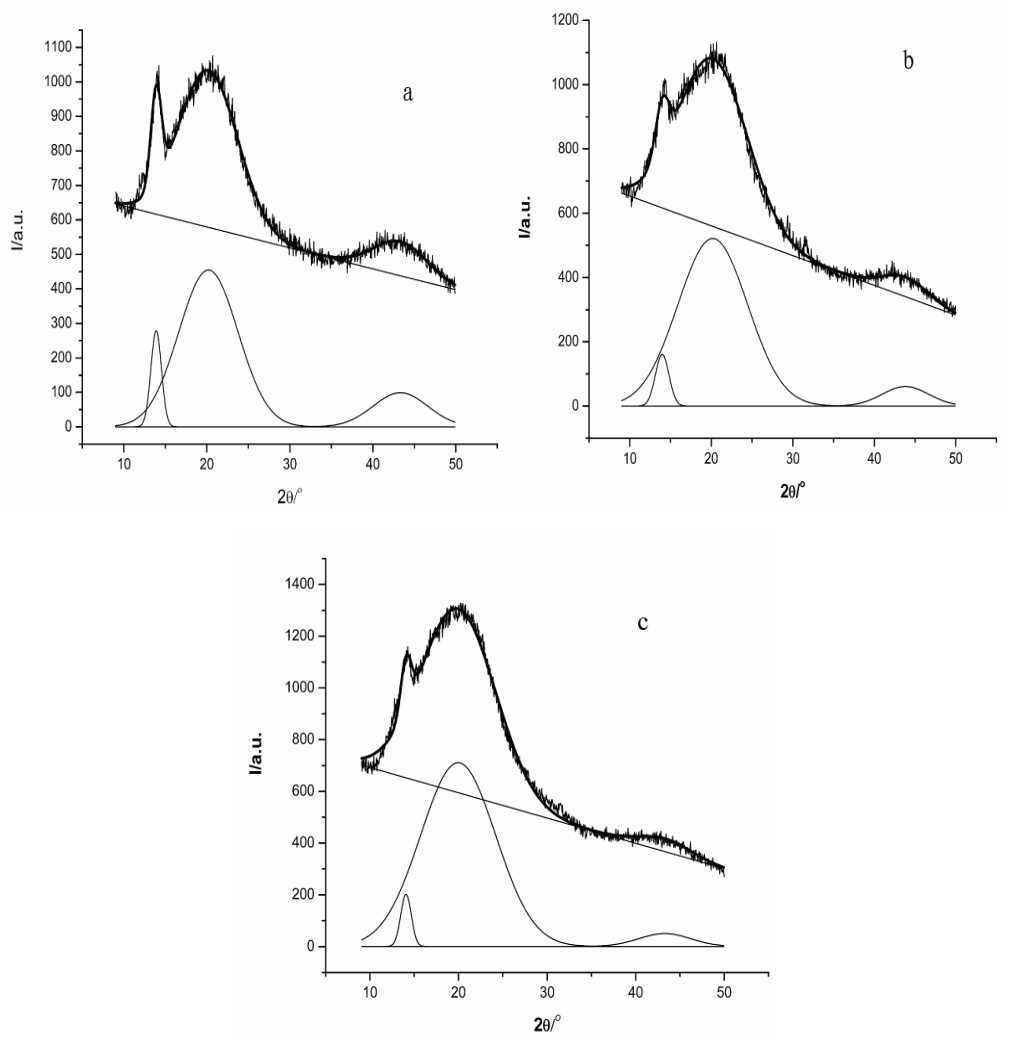

Figure 2.10 degree of crystalline is calculated from XRD spectra

** a. 5%POSSMOCA, b. 10%POSSMOCA, c. 20%POSSMOCA*

A larger active energy should be overcome with the chain stiffness, leading to a poor probability to form a fine crystalline. After the addition reaction between the aromatic epoxy precursor and POSSMOCA, the side chain aggrandizes compared with the original POSSMOCA subchain. It is probable to overcome a larger active energy and to rotate more difficult. In consequence, a smaller *Xc* should have achieved, rather than an increasing *Xc* in reality. It is not plausible to conclude directly that the amorphous POSSMOCA is caused by steric hinderance of side chain. Although the publications[152] focusing on the significant steric hinderance in amorphous POSS, maybe it is not a perfect interpretation of the amorphous phenomena in the case of hydrogen bonding interaction.

To understand the amphormous nature of POSSMOCA, a mechanism is hypothesized shown in Figure 2.10. The inorganic core tends to regularly arrange and crystallize; whereas the stronge polar structure, for instance, carbamido, carbaminate and amine group forms hydroxyl group easily, because the subchain of POSS cage is assymetrically dispersed nucleophilies (NH_2, NH) and electrophilic group (C=O).The end of subchain (NH_2) could interacts with C=O group of another subchain. The hydrogen bonding intermolecular and intramolecular organizes POSSMOCA into an irregular network; the inorganic core fails to forms a regular crystalline (Figure 2.10).

Hydrogen bond as a universal secondary bond interaction is decisive for the final properties of materials, especially their crystallinity[164, 165]. The existence of donor and acceptor in intermolecular hydrogen bond is a motivation of crystallization, increasing the strength of materials, for instance nylon. Hydrogen bonding strengthens the alignment of units, finally promoting the formation of crystalline. However, for a multi-components blend, the formation of intermolecular hydrogen bonds between the components usually induces miscibility. The interaction between components facilitates the motion in the matrix. For instance, polymer is plasticized by the small molecules[166], with an increase of the molecular motion, which leads to non-crystalline. Besides the effect of regular alignment, hydrogen bonds can also affect the crystalline polymorph form [167]. From the discussion above, it is deduced that the existence of hydrogen bond will promote to crystallize when the hydrogen bond assists to the arrangement and regularity. Considering the molecular configuration, the crystallization probably improves after the removement of irregular hydrogen bond. Moreover, the increase of crystallization is reasonable if there is another motivation to regular arrangement, such as the amphiphilic structure and π units stacking. With the amphiphilic structure, a self-assembly will take place in the interface or in the bulk of rich domaine, which will assist to arrangement and form a regular lattice or crystalline[168]. In this work, the amphiphilic structure is obtained, which contains DGEBA tail and POSS head after the prereaction. Namely, after the vanishment of irregular hydrogen bond, the self assembly would assist to form crystalline and obtain a crystalline structure instead of the original amorphous structure. It is in accordance with our experimental results.

From the discussion above, it is plausible to interpret that the hydrogen bond in POSSMOCA constrains the orientation and form a non-crystal state, because of the

irregular dispersed donor and acceptor in subchain. After pre-reaction, the amino hydrogen is consumed with DGEBA precursors, although with a larger steric hinderance than the original. A quasi-amphiphilic structure is obtained with POSS cage and DGEBA tail, which probably arranges into a regular structure and form a crystalline domaine. The dipole-dipole interact of POSS in the POSSMOCA is discernible and effective to form regular structure. From the morphology of nanocomposite, POSS possibly assembles in the surface of the nanoparticle and forms a regular POSS arrangement (Figure 2.11). With the increase of POSS content, the free POSS enters this nanophase and swells this particle as a swelling micelle mechanism in emulsion polymerization[169]. Inevitablely, the free POSS interacts with each other and interferes the regular arrangement of POSS on the micellar surface via hydrogen bonding, resulting in the decrease of crystallization directly.

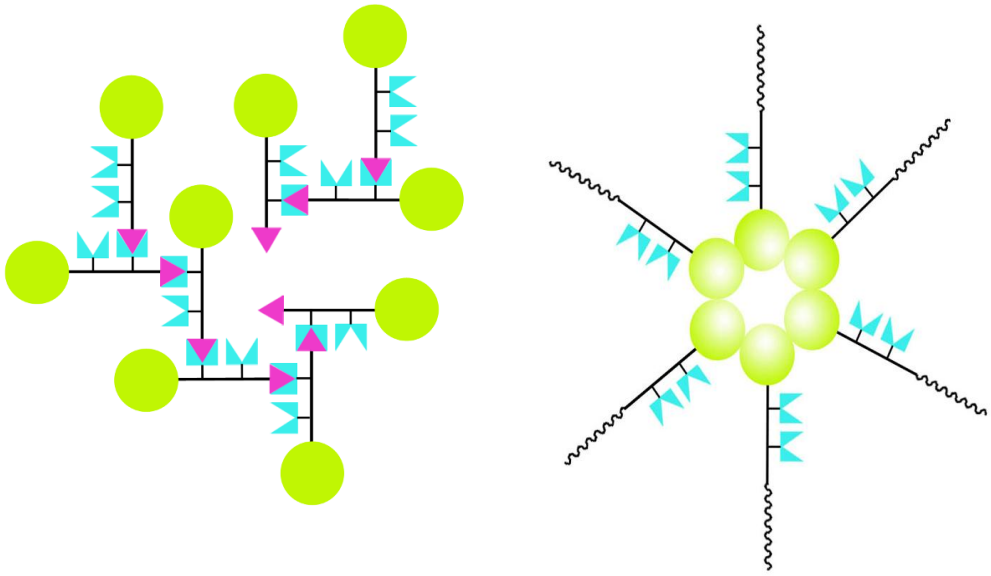

Figure 2.11 Effect of structural assymetric

**a.irregular hydrogen bond takes place, results in fail to arrange via POSS cage.b.after reaction, the hydrogen bond is vanished then POSS arranges into a micelle or a emulsion particle.*

Altogether, it could be explained by the reaction between the -NH_2 group and epoxy. The amino groups in POSSMOCA react with DGEBA, generating epoxy functionalized moities which could react with the curing reagent MDEA further. Generally, the POSS cages act as a trifunctional co-curing agent. The reaction between amino and epoxy groups compresses the interaction between amino groups in subchains, resulting in the regular arrangement of inorganic silsesquioxane core.

Conclusion

A new analogue of amino POSS, named POSSMOCA was synthesized and characterized. After reaction with epoxy by the active amino group, it improved the thermostability (about 50^{o}C in *T50* and more char production), because of the synergic fire-retardent effect between silicon, nitrogen and halogen

Compared with the neat epoxy, POSSMOCA modified samples had about twice glass state moduli as the one of neat epoxy. However, *Tg* decreased with the loading of POSSMOCA.

POSSMOCA successfully fabricated a nanophase separation (<100 nm) at a low POSSMOCA loading (<20%*wt*). However some POSSMOCA rich domains were larger than 1μm at a high POSSMOCA loading (20%*wt*).

It is worthy notifying that amorphous POSSMOCA crystallized in epoxy network, with a larger side chain via prereaction.

To explain the result, a mechanism was hypothesized called as "Destructive Reaction-Induced Crystallization". The hindrance of orientation (steric or dynamic) was compressed via reaction, and then the crystallization took place resulting from the regular pattern. In our case, the hindrance of orientation derived from the hydrogen bonding in the irregular subchain of POSSMOCA; after reaction with the epoxy precursors, -NH_2 group, the hydrogen bond acceptor and donor was consumed, it release the constrain of orientation; after that, the self-assembly of POSS analogue took place.

Chapter 3 Nanostructuration of POSS-OH into Epoxy and its mechanism

3.1 Brief introduction of reactive POSS modified Epoxy

There are many papers reporting the contribution of POSS to thermomechanical properties in such networks [74, 75, 130, 170-172]. These reports concluded that the addition of POSS into epoxy networks benefits to the stiffness and improves Tg, whereas contradictory results were also reported[173-175]. The understanding of POSS effects is still complex and some conclusions are achieved up to now: i/ phase separation could occur between POSS and monomers before or during polymerization depending on the chemical nature and functionality of the organic ligands of the POSS cages. The first case is related to the initial miscibility of the POSS[128, 176], whereas the latter case, denoted as a Reaction Induced Phase Separation, RIPS, results from the competition between polymerization reaction and thermodynamics of the system, i.e. entropy changes [103, 133]; ii/ a contribution of POSS cages to the free volume which reduced the crossling density21. iii/ Incompletely conversion of POSS takes place in POSS bearing epoxy group resulted from low reactivity compared with the one of epoxy precursor, which is possibly reacted incompletely in network. [102, 103] iv/ a diluent role of the POSS in reducing the self-association of the matrix[17, 177]; v/ the random dispersed POSS cage is familiar with a large side group as a intraplasticizer.[129, 132] vi/ the interaction of POSS cage and matrix in some cases[132] and the POSS volumetric hinderance to main chain molecular segments[178]. (iii-v leads to a decrease of Tg, however, vi strengthens Tg.)

One interesting route for insertion of nano-objects in epoxy networks is to consider incompletely condensed POSS cages. This compound possesses free silanols which can be used for coupling reaction. Lu[179] incorporated an incompletely condensed cyclohexyl-disilanol POSS into an epoxy-amine network, via a pre-reaction between silanol and oxirane ring using cobalt naphtenate as catalyst. The modified network exhibits slightly improved thermo-mechanical and fire-retardant properties, and increased Tg associated with a reduction of segmental mobility between crosslinks. Liu[133] introduced a phenyltrisilanol POSS into an epoxy-amine system via the same coupling reaction but catalyzed by aluminium triacetylacetonate. Homogeneous nanocomposites were obtained which display lower glass transition temperatures and storage moduli (both in the glassy and rubbery states) than the control epoxy. These results appear contradictory as one expects a lower decrease of Tg for trifunctional POSS-OH which acts as a crosslink whereas difunctional POSS-OH acts as a chain extender and contributes to lower significantly the crosslink density. The mechanism of condensation reactions between amine and epoxy groups is well understood whereas the reaction mechanisms between POSS-OH silanol and epoxy are not well documented. Therefore, the understanding of its mechanisms would be helpful to deeply explain the previous results and to design novel hybrid inorganic-organic epoxy networks.

The aim of this work is to introduce POSS silanols into an epoxy network, based on a DGEBA prepolymer and an anhydride curing agent, using three different metal complexes as catalysts. Anhydride was considered as comonomer rather than a diamine due to the fact that anhydride gives networks with high thermal stability, lower toxicity, and shrinkage. Moreover, the dependence with stoichiometric ratio between of epoxy and anhydride is not as important as compared with amino

hydrogen-to-epoxy ratio in epoxy/amine systems[180, 181]. The influence of water was studied through the preparation of hybrid O/I networks with/without water. The morphology and thermo-mechanical properties of the networks were investigated using electronic microscopy, dynamic mechanical analysis and thermogravimetric analysis.

3.2 Ring open reaction between POSS-OH and Epoxy

3.2.1. Preparation of POSS-OH Modified Epoxy

3.2.1.1 Materials

The diepoxy monomer was a diglycidyl ether of bisphenol A (DGEBA, DER332 from Dow Co.) with an epoxide equivalent weight of 173 g/mol. Hexahydrophthalic anhydride (HHPA, Alfa Aesar A Johnson Matthey Co.) was used as curing agent. 1-benzyl-2-phenyl imidazole (1B2PZ, Shikoku Chemicals Co.) was used as catalyst for the epoxy – anhydride reaction. Phenyl glycidyl ether (PGE, Alfa Aesar A Johnson Matthey Co.) was used for model reactions. Trisilanol isobutyl polyhedral oligomeric silsesquioxane (denoted POSS-OH, reference SO1450) was purchased from Hybrid Plastics Co. Aluminum triacetylacetonate ([Al], Aldrich Co.), cobalt isooctoate ([Co], Akzo Nobel Co.), and copper acetylacetonate ([Cu], Janssen Chemical Co.) were used as catalysts for the reaction between POSS-OH and DGEBA precursors. Zeolite (Sinoreagent Co.) was activated at 500 °C before using.

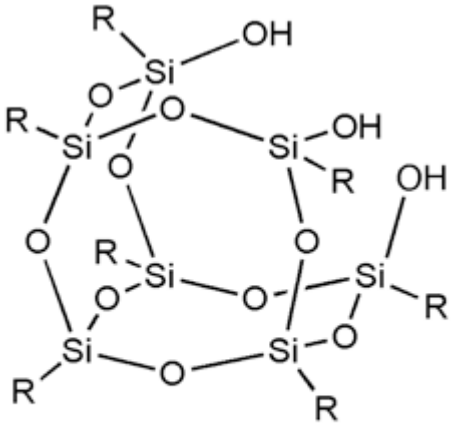

Scheme 3.1.Structure of trisilanol POSS (POSS-OH)

3.2.1.2 Experimental techniques

a. Fourier Transform Infra-Red spectroscopy(FTIR) measurements were performed on a Nicolet Avatar 360 at room temperature. To determine the molar mass, Size Exclusion Chromatography (SEC) was performed by using a Waters 510 pump with UV and refractive index detectors. THF was used as eluent at a 1 mL/min flow rate. Three columns (Waters HR1, HR2, and HR3) were used. Polystyrene (PS) standard was used for obtaining calibration curve. The ^{1}H NMR was employed on a Bruker 300M Nuclear Magnetic Resonance. The samples were dissolved in d-chloroform, and tetramethyl silane was used as an internal reference.

b. A differential scanning calorimeter (DSC) (TA Q1000, TA Instruments) was used under a nitrogen atmosphere to investigate the curing process of epoxy. Moreover, the influence of epoxide homopolymerization can be measured, which is derived from the pre-reaction of POSS-OH and DGEBA. The sample was heated from -60 to 350 °C at a rate of 10 $K \cdot min^{-1}$.

c. The morphology of POSS-OH-containing epoxy hybrids was observed with a Philips XL 30 Scanning Electron Microscope (SEM). The samples were immersed in liquid nitrogen and then fractured. The surfaces were etched in dichloromethane at room temperature for 30 min as it is an excellent solvent for the unreacted POSS-OH. After that, a gold coating was sprayed on the fracture surface. Activation voltage of SEM observation is 20 kV. Transmission electron microscopy (TEM) was performed on a Philips CM120 TEM at an acceleration voltage of 80 kV. Ultra-thin sections (ca. 70 nm in thickness) were cut using an ultramicrotome machine, and were placed on a 200 mesh copper grids for observation.

d. The Dynamic Mechanical Thermal Analysis (DMTA) was carried out on cured hybrid networks with a Rheometric Solid Analyzer (RSA II). To obtain dynamic mechanical spectra in tension mode (storage moduli E', loss moduli E", and loss factor tan δ), the samples were tested between 25 and 220 °C at a frequency of 1 Hz in the linear viscoelastic domain.

3.2.1.3 Model reaction of PGE and POSS-OH.

A series of model reactions between phenyl glycidyl ether (PGE) and POSS-OH (*n*(PGE):*n*(POSS-OH)=6:1) with catalyst (0.6 wt % of PGE) were undertaken to examine the ring-opening reaction between phenyl glycidyl ether (PGE) and POSS-

OH. The reactions were performed at different temperatures, depending on the miscibility of the components and the reactivity of the catalysts (the temperature of reaction was selected by heating was by heating the catalyst at 90, 120, 150, and 180 °C and observation of the transparency). The model compounds were denoted as PGE-POSS-*X*, where *X* is the type of catalysts. To investigate the reaction mechanism, the reaction products were characterized by using Fourier Transformed Infrared Spectroscopy (FTIR), Size Exclusion Chromtography (SEC), and NMR spectroscopy.

3.2.1.4 Synthesis of POSS-OH modified epoxy nanocomposites

DGEBA was mixed with proper amount of POSS-OH and 0.6 wt % catalyst at a given temperature, until obtaining a homogenous mixture. Afterward, HHPA and 1B2PZ were introduced into the mixture and mixed for 10 min at 80 °C. The molar ratio of HHPA with DGEBA was 0.9:1 with 2 wt % 1B2PZ. The curing protocol is at 90 °C for 3 h, 160 °C for 6 h, and at 190 °C for 3 h for post-cure. The final products were denoted as DGEBA-*w*POSS-*X* (*X* is the catalyst, *X*=M in POSS physical blending sample, *w* is the weight percent of POSS-OH). Besides, a sample was prepared to investigate the effect of moisture. DGEBA was kept in a flask under vacuum at 100 °C for 3 h, then cooled down to room temperature and mixed with catalyst and POSS. The mixture was kept in vacuum for 4 h. The reaction and curing conditions were the same as the ones mentioned previously. To get a fully cured network, i.e. all the epoxy groups in the system were reacted fully, the catalyst was excluded by mixing with a zeolite after the pre-reaction with catalyst, and then centrifuged, due to the fact that acetylactonate salts are easily adsorbed on the zeolite supermolecule cage.

3.2.1.5 Model systems involving DGEBA, POSS-OH, and Catalysts

The model reaction of stoichiometric systems DGEBA/POSS-OH/[Cu] was processed without anhydride curing agent and moisture as described as follows: POSS-OH after vacuumed was mixed with [Cu] and DGEBA in vacuum for 2 h, reacted at 150 °C for 30 min. Otherwise, the samples with water was prepared under ambient atmosphere and with water before reaction. The samples were denoted as POSS-*X* (-Vac), (*X* is the catalyst, Vac is prepared in vacuum). The resultants were characterized by FTIR, UV spectroscopy and ^{1}HNMR.

3.2.1.6 Synthesis of POSS-OH Modified Epoxy Nanocomposites

DGEBA, proper amount of POSS-OH and 0.6 wt % catalyst was mixed at a given temperature by using a mechanical stirrer until a homogenous mixture was achieved. Afterward, HHPA and 1B2PZ were introduced at 80 °C into the mixture and continue stirring for 10 min. The molar ratio of HHPA to DGEBA was 0.9:1, with 2 wt % 1B2PZ. The curing protocol was 90 °C, 3 h+160 °C, 6h, and post-cured at 190 °C for 3 h. The final products were denoted as DGEBA-*5*POSS-*X* (*X* is the catalyst, *X*=M in POSS physical blending sample, *5* is the weight percent of POSS-OH).

A sample was prepared to investigate the effect of the presence of moisture. DGEBA was kept under vacuum at 100 °C for 3 h, and then cooled down to room temperature and mixed with catalyst and POSS-OH. The mixture was kept in vacuum for 4 h. The reaction and curing conditions were the same as those mentioned before.

To get a fully cured network, i.e. systems for which all the epoxy groups have reacted, the metal catalyst was excluded by mixing with a zeolite after the reaction with catalyst, and then centrifuged, due to the fact that acetylacetonate salts are easily adsorbed on the zeolite supermolecule cage.

3.2.2 Silanol-epoxy model reaction between POSS-OH and PGE

In the model reaction, phenyl glycidyl ether (PGE) is used instead of DGEBA, Due to PEG is a mono-functional compound, gelation, i.e. 3D polymerization, can not occur. The molar ratio 3:1 for PGE: POSS-OH can be expected to be the ideal case as it corresponds to 1:1 for epoxy-to-silanol ratio(Figure 3.1).

The peak at 913 cm^{-1} is attributed to the epoxy group from PGE, the peak at 3400 cm^{-1} is attributed to stretching vibration of free silanol groups from POSS-OH; the peak at 1100 cm^{-1} is due to the vibration of Si-O-Si from the silsesquioxane cage and the peak at 1510 cm^{-1} is the stretching vibration of aromatic C=C from PGE. Additionally, free –OH at 3600 cm^{-1} appears which would be ascribed to the produced hydroxyl group after a hydroxyl group added to epoxide ring. It can be seen that the epoxy and hydroxyl peaks decrease after 30 min of reaction, which means that efficient ring opening reaction is carried out.

The conversion of epoxy groups (α), can be calculated according to the relative ratios of peak area between epoxy and phenyl (internal reference at 1600 cm^{-1}) (A_e, A_Φ) . It is calculated from the following expression:

$\alpha = 1 - (A_{ei}/ A_{\Phi i})/(A_{ef}/ A_{\Phi f})$,

(i is reference sample and f is the sample reacted with catalyst)

The results are reported in Figure 3.1. The conversions are in the same range, but the reaction of epoxy proceeds slightly faster when using [Cu] catalyst.

Table 3.1 Conversion of epoxy groups calibrated from FTIR

Catalyst	conversion (%)
[Al]	67
[Co]	62
[Cu]	74
Vac	89

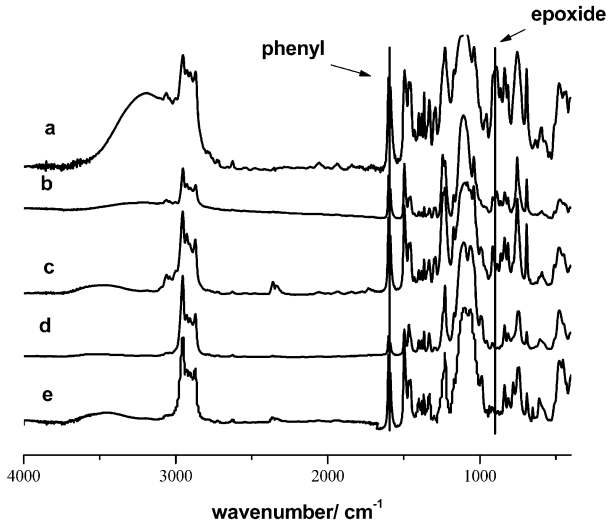

Figure 3.1 FTIR spectra of model reaction between POSS-OH and PGE

**without catalyst before pre-reaction (a), and after reaction PGE-POSS-Al (b), PGE-POSS-Co (c), PGE-POSS-Cu (d), PGE-POSS-Cu-Vac(e).*

The compound (PGE-POSS-Cu-Vac) prepared under vacuum without water has a high conversion of epoxy group as those obtained on the sample prepared under air. According to a previous work[133, 179], these results confirm that such types of metal catalysts are efficient compounds for promoting the reaction between POSS-OH and epoxy group. Indeed the epoxy peak is overlapped with other vibrations; the determination of the epoxy conversion is not of precision via FTIR.

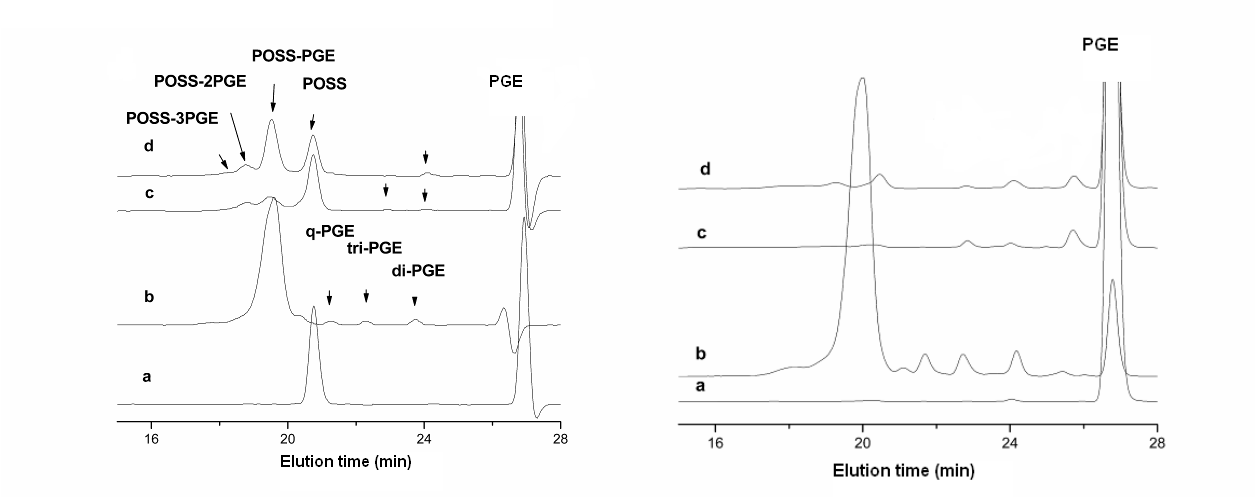

Figure 3.2 Chromatograms of model reaction products

** left: RI signal, right: UV detector.PGE -POSS with catalyst before reaction (a), and after 30 min of reaction PGE-POSS-Al at 120 °C (b), PGE-POSS-Co at 180 °C (c), PGE-POSS-Cu at 150 °C (d),*

Further evidence of the ring-opening reaction is provided from SEC results (Figure 3. 2). The chromatogram traces by ultra-violet spectrophotometer detector and refractive index detector are reported in Figure 3.2 In Figure 3.2A, the peaks at the elution times of 26.5 min and 20.5 min are attributed to PGE and POSS-OH, respectively. While in Figure 3.2 B, only the peak of PGE can be observed. The POSS-OH molecule does not show any UV signal because of the absence of chromophore group. Depending on the catalyst used in the systems, different reaction products can be observed. In the case of [Al] catalyst, a peak appears at a low elution time both on the RI and UV signals (te = 19.5 min, Figure 3.2). Three new peaks (te =22.8, 23.9 and 25.7 min) can also be observed. At the same time, the POSS peak disappears and the peak for residual PGE weakens obviously. The first peak is due to the addition of one to three molecules of PGE to POSS-OH, while the other three peaks are attributed to oligomers of PGE (dimer, trimer, etc…). There are different behaviors with the two other catalysts. On one hand, they do not promote the formation of PGE oligomers evidently; on the other hand, they are less active to catalyze the reaction between silanols and epoxy, despite the higher reaction temperature. In each case, amounts of residual POSS-OH and PGE are observed. The conversion of PGE, α, was calculated using the area of the UV signal of the chromatogram before reaction, A_{t0}, compared to the chromatogram after 30 min of reaction, A_t, as followed: $\alpha = 1 - A_t/A_{t0}$. The conversions are 80%, 20% and 50% for

[Al], [Co] and [Cu] metal catalyst, respectively. The relative activity is the highest for [Al] and lowest for [Co].

From the FTIR and SEC results, we are certain that the ring-opening reaction takes place. However, the conversions calculated from different methods are not consistent. Compared with the SEC, FTIR is influenced by the determination of baseline and the precision of peak separation, so it has a lower reliability than SEC.

The relative activity is the highest for [Al] and lowest for [Co] from figure 3.2. From Figure 3.3, a straight line is obtained and the dot is the experimental molar mass, when plotting ln M vs. elution time. It suggests the calculation of molar mass according to SEC is relieable and close to that of POSS species with different degrees of substitution and the oligomers of PGE. As a consequence, one can conclude that there is a good agreement between the theoretical molar masses and measurements from the calibration curve.

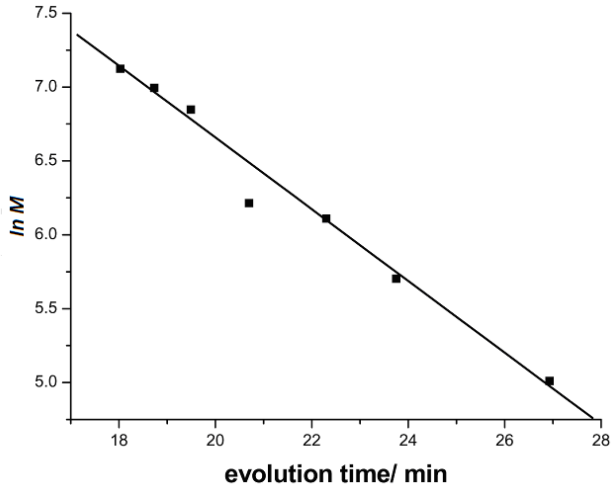

Figure 3.3 Correlation of *ln M* vs elution time, the experimental value showing in separated dots.

3.2.3 Nonstoichiometeric in POSS-OH modified epoxy nanocomposites

DGEBA was mixed with proper amount of POSS-OH and 0.6 wt % catalyst using a mechanical stirrer until obtaining a homogenous mixture, at a given temperature. Afterward, HHPA and 1B2PZ were introduced into the mixture at 80 °C and mixed for 10 min. The molar ratio of HHPA to DGEBA was 0.9:1, with 2 wt % 1B2PZ. The curing protocol was at 90 °C for 3 h, 160 °C for 6h, and at 190 °C for 3h for post-cure. The final products were denoted as DGEBA-*5*POSS-*X* (*X* is the

catalyst, *X*=M in POSS physical blending sample, *5* is the weight percent of POSS-OH).

A sample was prepared to investigate the effect of the presence of moisture. DGEBA was kept under vacuum at 100 °C for 3 h, then cooled down to room temperature and mixed with catalyst and POSS-OH. The mixture was kept in vacuum for 4 h. The reaction and curing conditions were the same as the ones mentioned previously.

To get a fully cured network, i.e. systems for which all the epoxy groups have reacted, the metal catalyst was excluded by mixing with a zeolite after the reaction with catalyst, and then centrifuged, due to the fact that acetylacetonate salts are easily adsorbed on the zeolite supermolecule cage.

DSC is usually used to determine the enthalpy of reaction for epoxy reactions which corresponds to 100–118 kJ/eq[91], and the corresponding conversion for a given time of reaction. Here, the same technique is considered for analysis the reaction between DGEBA, anhydride and POSS-OH. In our study, DSC is employed to analyze the difference in mechanism between the systems prepared via a pre-reaction between POSS and DGEBA, or via mixing POSS silanol and epoxy system. Three systems were compared: (1) The first system is the neat epoxy-anhydride matrix, i.e. DGEBA and HHPA combined with/without the organometallic compound (X = [Al], [Cu], or [Co]), denoted as DGEBA-X/(Neat) to study the influence of the catalyst on the epoxy-anhydride reaction; (2) The second one is the neat epoxy-anhydride and catalyst with mixing POSS, i.e. without pre- reaction, denoted as DGEBA-5POSS-X-M; (3) The third one is related to a pre-reaction of POSS-OH and the diepoxy mixture with the catalyst, denoted as DGEBA-5POSS-X. For all the systems, the epoxy-anhydride matrix is based on DGEBA, HHPA, and 1B2PZ at the same ratios. Thermograms shown in Figure 3.4, exhibit a single glass transition temperature, Tg, and two exothermic peaks. The exotherm at lower temperatures, denoted as Peak I, is known to be due to esterification whereas the exotherm at higher temperatures denoted as Peak II can be attributed to etherification reaction[182]. The reaction mechanism is illustrated in Figure 3.5.

There is no big change of the temperature and enthalpy of the exotherms with changing catalyst. It indicates that the metal catalyst doesn't accelerate the 3D polymerization crosslinking process in this reactive system, i.e. imidazole acts as catalyst. In the systems for which POSS-OH is introduced by introduced without any

pre-reaction (Figure 3.4B), there is no change compared to the reaction of the neat epoxy-anhydride system, except in the ratio of enthalpies of the two reactions. In the case of pre-reacted POSS-OH (Figure 3.4C) a decrease of reaction enthalpy (residual enthalpy is 40 % for [Co], 30 % for [Cu] and [Al] approximately) takes place. This phenomenon is expected as there is a consumption of epoxy species during pre-reaction of POSS-OH bearing silanols and epoxy prepolymer. In theory, three epoxy groups should be connected with each trisilanol POSS and considering the molar mass of trisilanol POSS-OH as well as the low amount used (5 wt% POSS-OH), only few epoxy groups condensed with silanols from POSS-OH. Therefore a decrease in the enthalpy of reaction of about 3% should be expected.

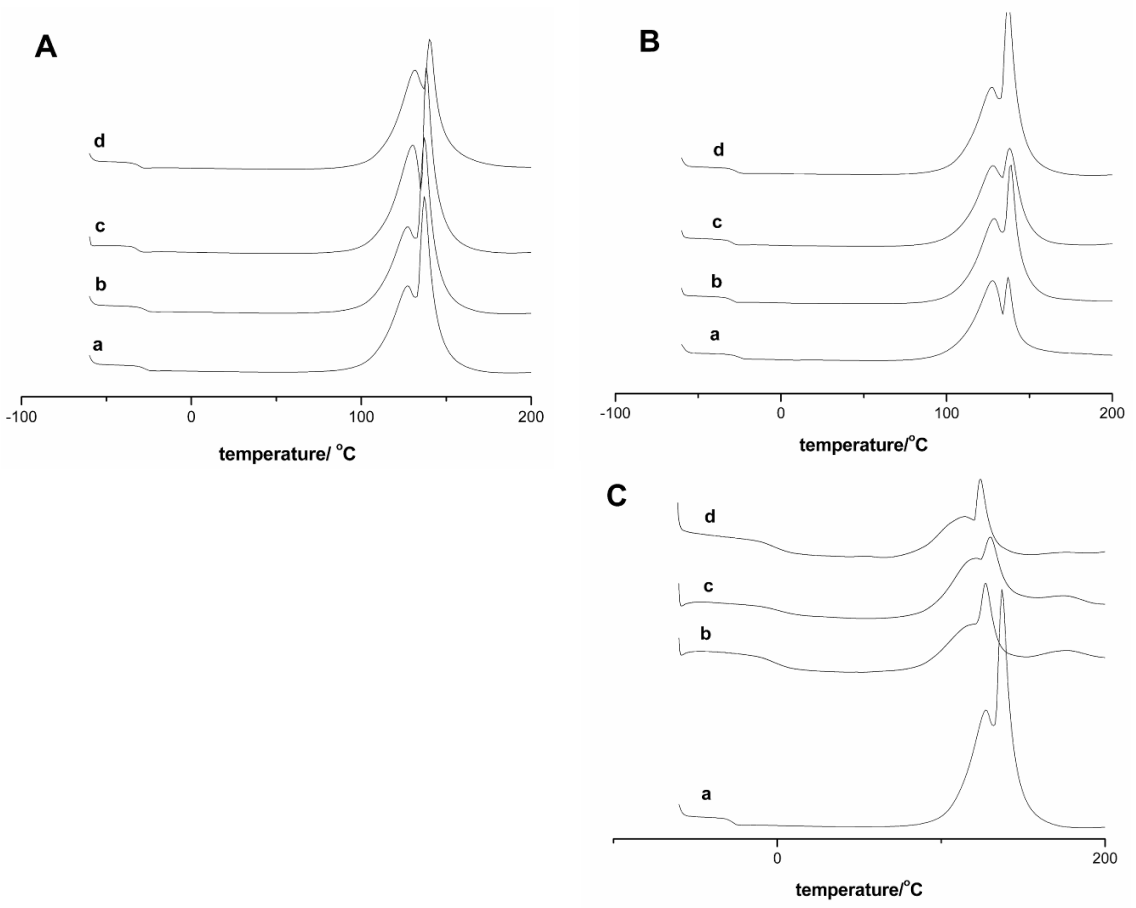

Figure 3.4 DSC traces of reactive systems

** (A) DGEBA-neat and DBEBA-X; (B) DGEBA-neat and DGEBA-5POSS-X-M; (C). DGEBA-neat and DGEBA-5POSS-X. Legends: (a) neat matrix, (b) X=[Al], (c) X=[Co], (d)X=[Cu]. (upward means heat release, heating rate: 10 K·min^{-1})*

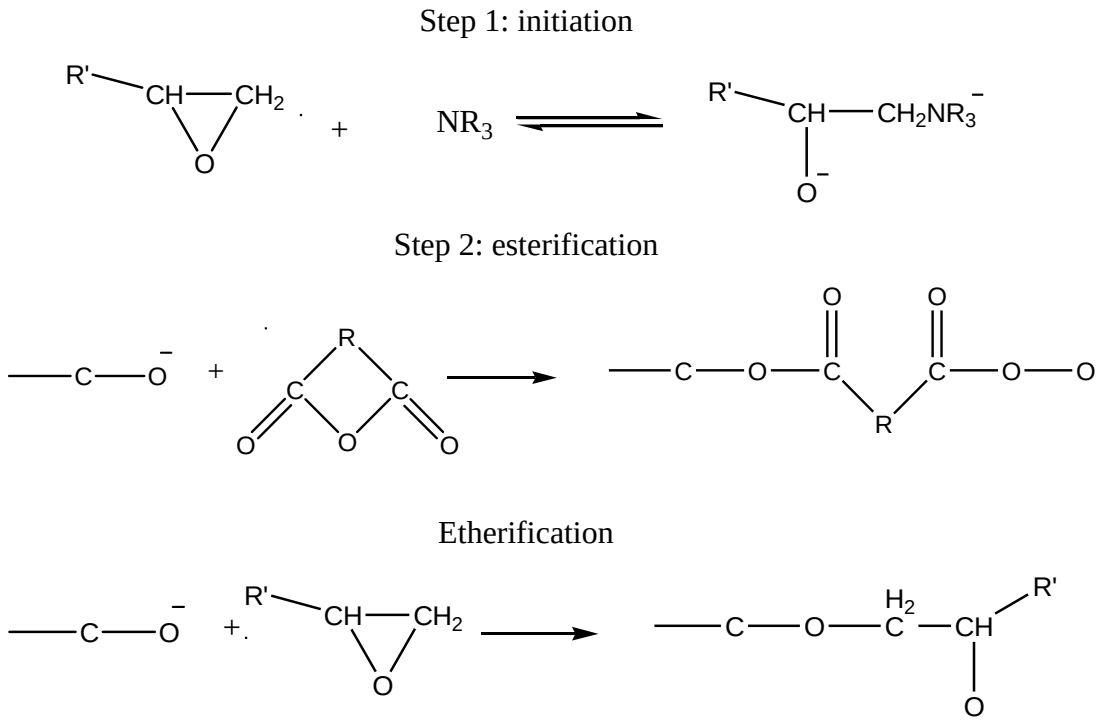

Figure 3.5 The mechanism of epoxy and anhydride with imidazole. [182]

The deviation could be assigned to the homopolymerization of epoxy precursors, in accordance with the conclusions from SEC. It is worthy to notice that the Tg_o of the samples after pre-reation deviates from that of the neat system, about twenty degrees higher. whereas for POSS-OH mixed with epoxy prepolymer without pre-reaction, Tg_o remains the same as in the neat epoxy system, due to the poor solubility of isobutyl trisilanol POSS-OH in DGEBA. The Tg increase in POSS-OH pre-reacted systems is another evidence, that trisilanol POSS-OH is covalently bonded to the DGEBA moieties leading to a reduction of the chain mobility. The formation of this adduct also improves the solubility of POSS in DGEBA and therefore leads to the insertion in the epoxy-anhydride network.

3.2.4 Inspect the epoxy concentration via ^{1}HNMR

The epoxide concentration were checked via ^{1}HNMR (Figure 3.6, 7, 8, 9) from the area of epoxide H (δ=3.54-3.57) and aroma (δ=7.02-7.36). In case the ratio of aromatic (*Aa*) and epoxide (*Ae*) before reaction is set as a reference, the epoxide group after prereaction could be calculated from the residual *Aa/Ae*. From ^{1}HNMR, the DGEBA precursor is almost unique, the hydrogen atom in the aromatic ring is divided into two groups equally (δ=7.09-7.16, 6.84-6.79 ppm). δ=2.71-2.77, 2.86-2.93, 3.30-

3.38 ppm is assigned to the hydrogen connecting with carbon atom in the epoxide group. The hydrogen in the carbon connecting with phenoxyl δ=3.98-3.91, 4.14-4.21 ppm. Theoretically, there is a relationship between the area of hydrogen in aromatic ring and epoxide ring, A (6.84-6.79) =2A (2.86-2.93), (A is the area). The conversion of DGEBA could be calculated as follows:

Conv.=A (2.86-2.93) /A (6.84-6.79)/0.5×100%

Considering the trifuncitional POSS-OH (the molar mass of POSS-OH, $F.W.$ =791.4), each hydroxyl should react with equal epoxy group. If m% POSS-OH was introduced into the composite, the theoretical conversion of DGEBA could be (100/173-3m/791.4)/(100/173), because of the epoxide equivalent weight is 173 g/eq. A large deviation to the theoretical value obtained demonstrates the homopolymerization of DGEBA with the POSS-OH and catalyst.

Table 3.2 The conversions of epoxide group are calculated from ^{1}HNMR

	In The Air atmosphere			vacuum
POSS	0.5%	3%	5%	5%
Residual Epoxy	94%(99.7)	88% (98.1%)	70%(96.7)	97%(96.7)

**Based on Figure 3.6, 3.7, 3.8, 3.9, and the theoretic values are shown in the parenthesis.*

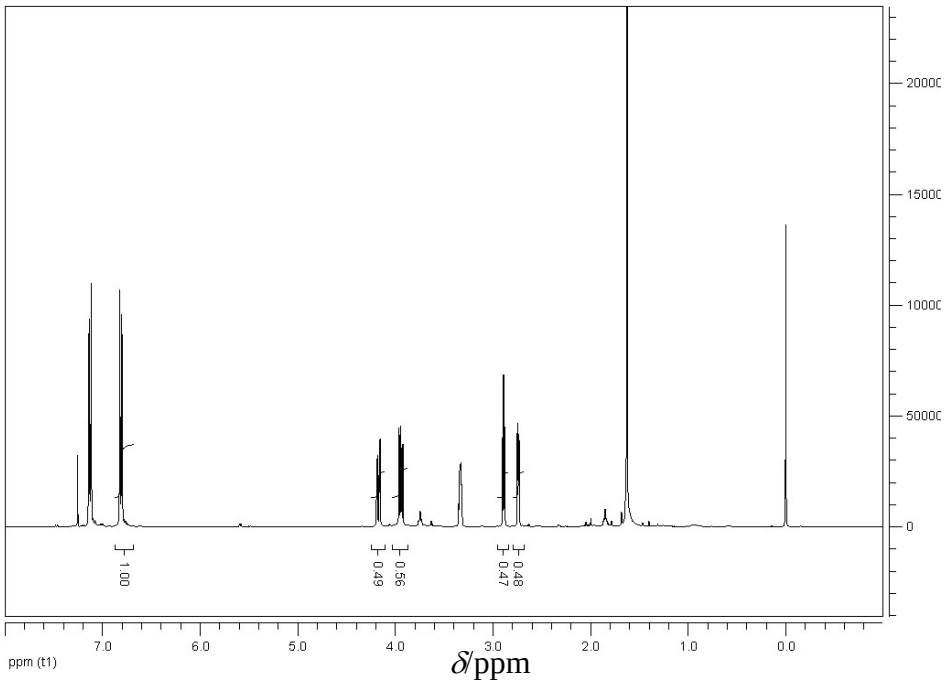

Figure 3.6 ^{1}HNMR of DGEBA-0.5POSS-Cu after prereaction.

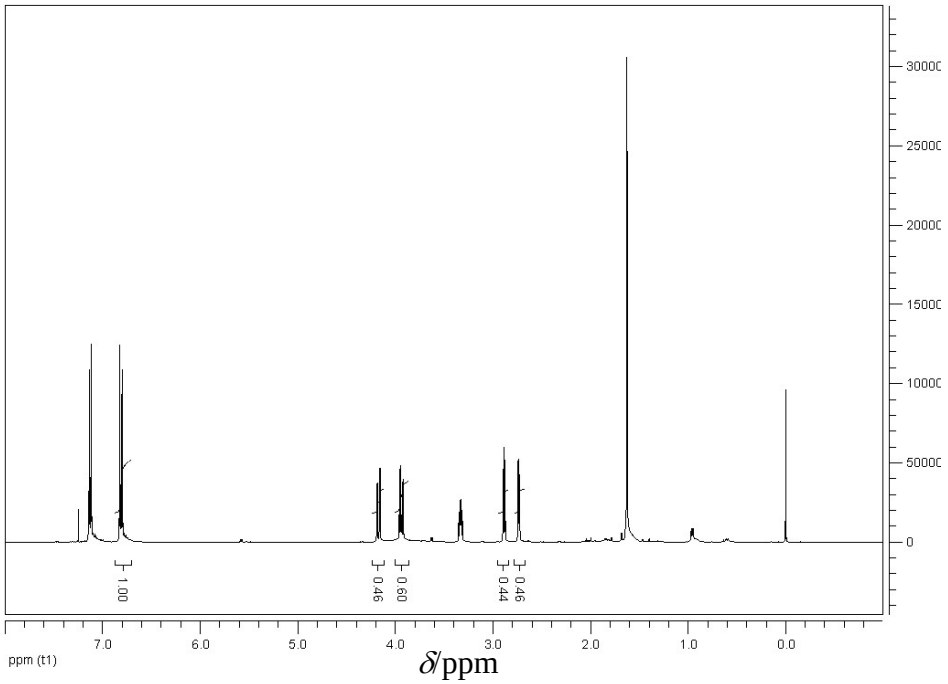

Figure 3.7 ^{1}HNMR of DGEBA-3POSS-Cu after prereaction

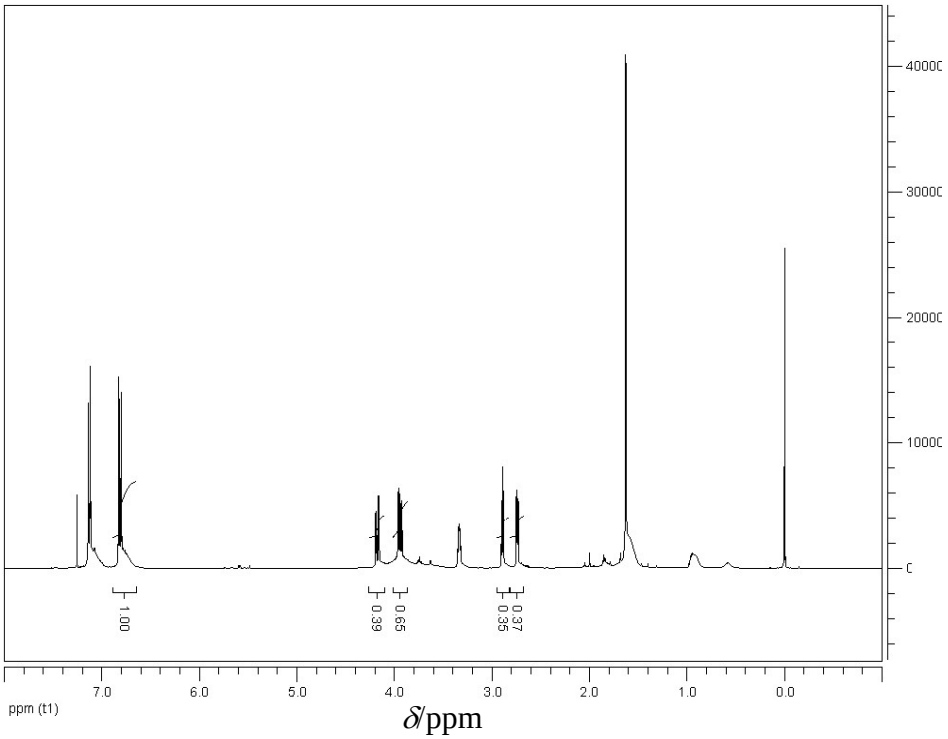

Figure 3.8 ^{1}HNMR of DGEBA-5POSS-Cu after prereaction

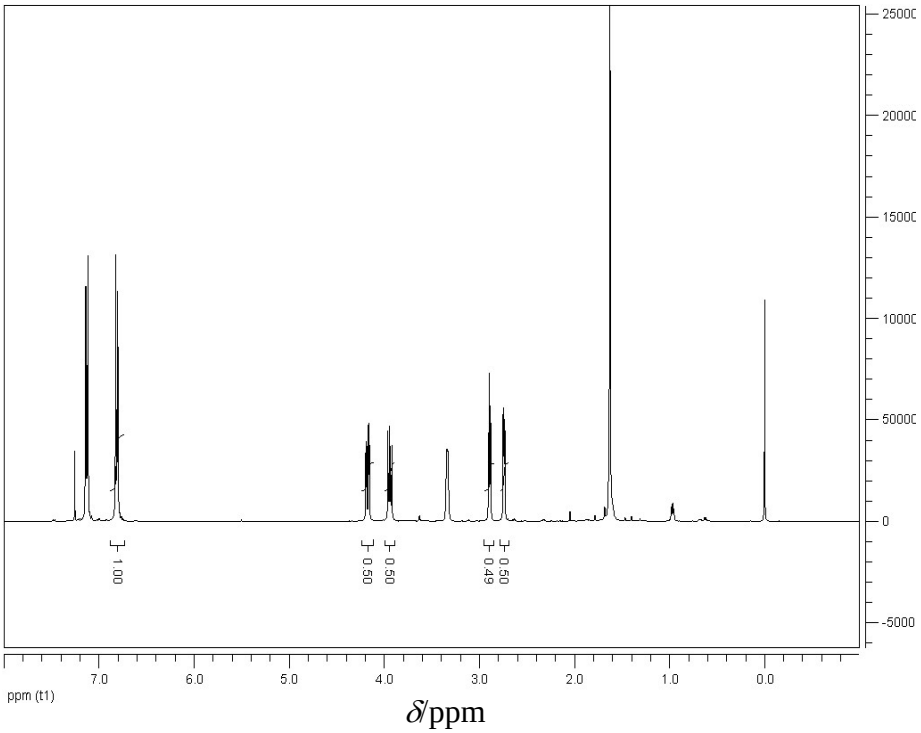

Figure 3.9 ^{1}HNMR of DGEBA-0.5POSS-Cu-Vac under vacuum after prereaction

3.3 Role of POSS-OH and water in the ring-opening reaction

3.3.1 Characterization of the POSS-OH ring open reaction with/without water.

In this work, the influence of water and the possible formation of by-products are considered. Oligomers which could be present in the final networks could act as plasticizers and lead to a decrease of Tg, not only the free volume increase introduced by the POSS cages as reported in the literature[21].

Free hydroxyl group in POSS-OH (δ=6.33 ppm) and CH_2-Si (δ=0.63-0.55 ppm) were shown in the following figures (Figure 3.10, 3.11, 3.12). Compared with the physical blend, –OH shifts to a high field (δ=6.0 ppm) and forms a new band at δ=-0.45 ppm, which is assigned to the coordination of -OH with catalyst. With the moisture, –OH shifts to a higher field (δ=5.3 ppm) and gains a similar band at δ=-0.45 ppm too. After the coordination, the electron density of hydrogen atom decreases which leads to the shielding effect of adjacent atom suppressed, the peak moved to low field. Here, the additional area of CH_2-Si appears at lower field is chosen as a scale to determine the coordination between Si-OH and catalyst.

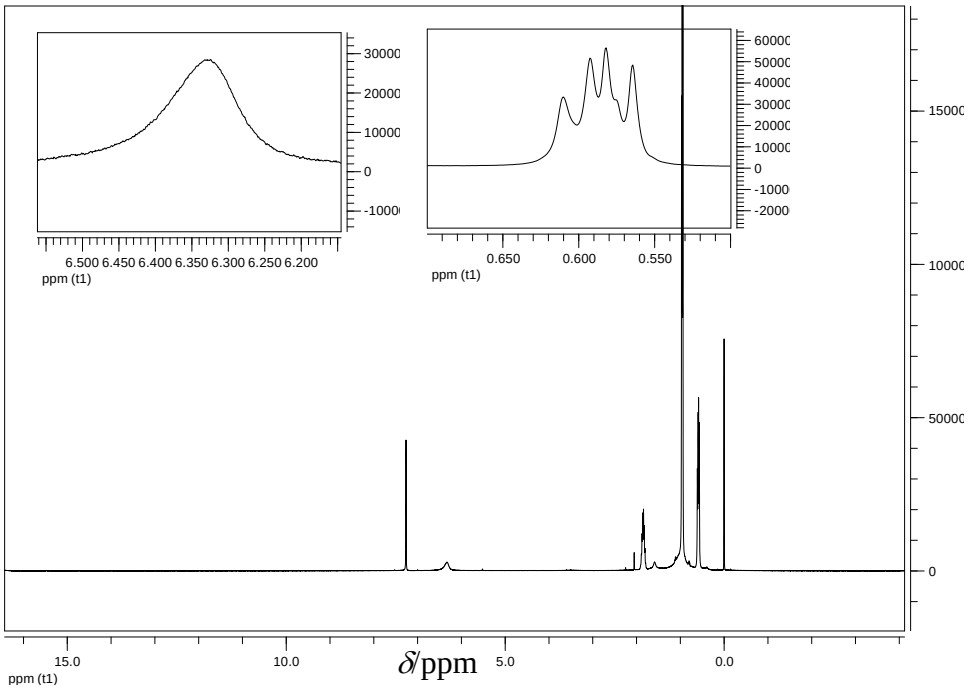

Figure 3.10 ^{1}HNMR of POSS-Cu physical blend before reaction

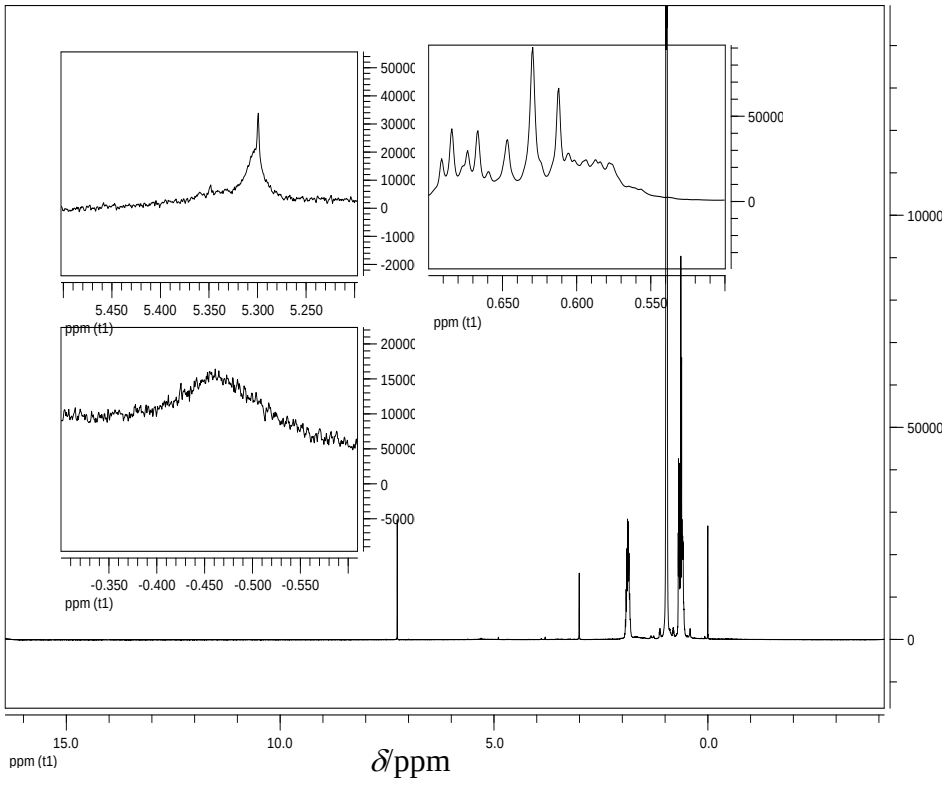

Figure3.11 ^{1}HNMR of POSS-Cu with moisture after reaction

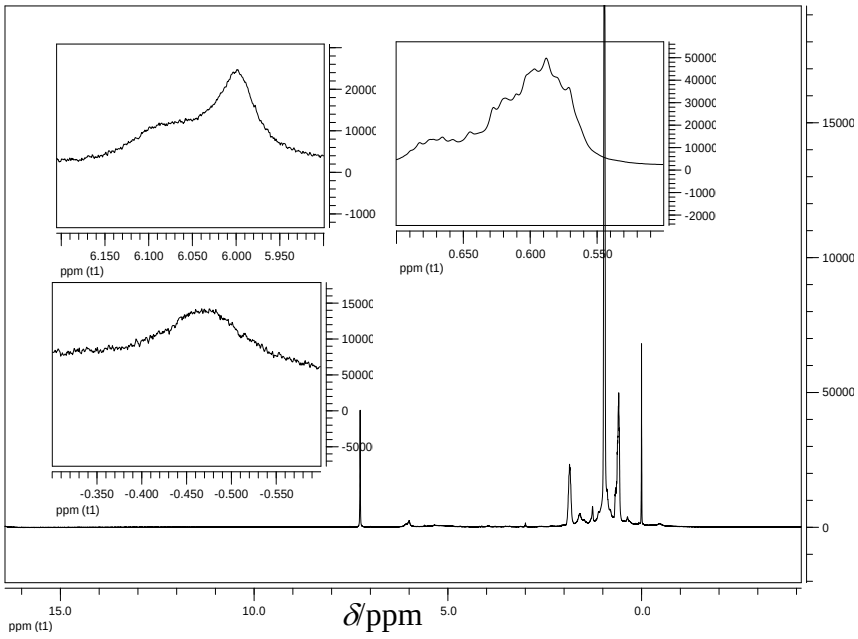

Figure 3.12 ^{1}HNMR of POSS-Cu-Vac in vacuum after reaction

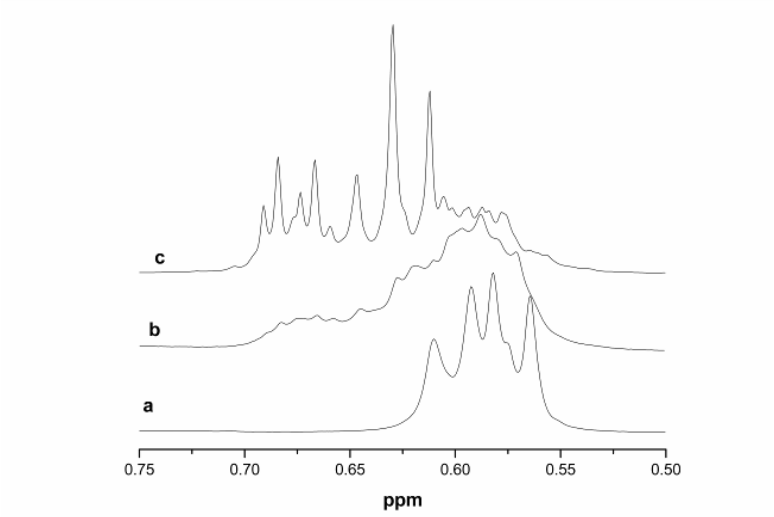

Figure 3.13 ^{1}HNMR spectra of -CH_2 region: (a) POSS-Cu before reaction; (b). POSS-Cu-Vac; (c) POSS-Cu- water.

Moreover, the part of CH_2-Si shifts to a low field besides the original peaks, which corresponds to the coordination of Si-OH to catalyst(Figure 3.13). The resonance peak of the proton from methylene group, HO-Si-CH_2-, is observed between 0.63 and 0.55 ppm before reaction (Figure 3.13a). The chemical signal of ^{1}HNMR is sensitive to the change of chemical environment, for example when coordination appears. In samples of POSS-Cu-water and POSS-Cu-Vac, there are additional peaks at δ=0.611-0.69 ppm (Figure 3.13b and c) compared with the system before reaction. These peaks are due to the coordination of Si-OH to the [Cu] catalyst.

The electron density of the hydrogen atom is decreased and the signal moves to a lower chemical shift.

3.3.2 Variety of bonding strenghth in catalyst.

3.3.2.1 Characterization of the coordination of water and POSS-OH with catalyst via ^{1}HNMR

To understand the mechanism between chelated compound and POSS system and the possible formation of by-products, samples with/without water were considered and characterized. In agreement with our FT-IR analyses, the similar infrared results[133] illustrates that the catalysts successfully facilitate the ring-opening reaction. Liu et al[133] proposed that the mechanism between oxirane and Si-OH is initiated by the formation of complex between oxirane and metal atom of catalyst. Templin et al[183] observed that the Al catalyst combined with silanol group can form an Al-O-Si active center to open the ring of the inorganic groups. However, there is also some different viewpoints about the mechanisms for the effect of silanol on epoxy ring-opening reaction. For instance, Fu et al[184] proposed that the phenyl silanol POSS-OH did not significantly affect the epoxy/amine curing reaction until the gelation stage from the FT-IR spectra. As observed in this work from ^{1}HNMR, using [Cu] as catalyst, the epoxy conversion deviates from the expected value determinated from the stoichiometric between epoxy and curing agent, one can observe that the residual epoxy is 70% in humidity less than the theoretical value (96.7%). However, when the reaction is done under vacuum, no deviation of epoxy conversion is shown. This is because the ligand is easily released from the acetylacetonate salt, the released ligand doesn't play a role to open epoxy ring at this low temperature. As a consequence, one can conclude that the mechanism of the ring-open reaction is influenced by the presence of water. This phenomenon was confirmed by ^{1}HNMR by introducing additional water.

3.3.2.2 FTIR and UV-vis characterizes the coordination between POSS-OH and catalyst

The above conclusions are in agreement with FTIR analyses (Figure 3.14). In fact, the C=O vibration of ligand acetylacetonate (acac) at 1,582 cm^{-1} in [Cu][185] (Figure 3.14a), shifts to 1,590 cm^{-1} in POSS-Cu-Vac (Figure 3.14b) after vacuum heating and 1,594 cm^{-1} in POSS-Cu- water (Figure 3.14c). In this interaction, the occupied orbital of the donor overlaps with the vacant orbital of the acceptor. The

probability of formation of this bond grows with increasing number of d electrons of the metal. Formation of π^* bonds with organic reagents is typical of Cu (II), which enables the electron density transfer. The coordination effect between –OH and Cu (II) weakens the bond of cupric and ligand, then the bond strength of C=O in ligand increases. The orbital overlap makes the electron transfer from the nonbonding p orbital of -OH to the vacant orbital of the 3d transition metal ion. It is well known that the frequency of vibration (ν) is proportional to square root of the strength (k), name $\nu \propto k^{1/2}$. When the coordination of cupric and –OH takes place, the blue shift of C=O vibration should be investigated.

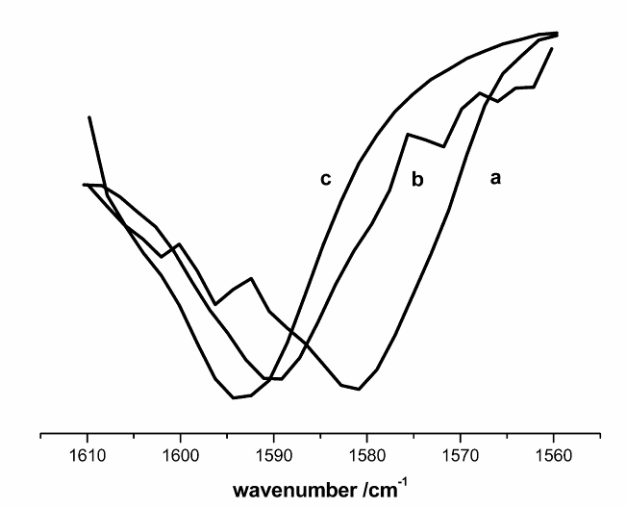

Figure 3.14 FTIR shifts of C=O vibration for: (a) POSS-OH; (b) POSS-Cu-Vac; (c) POSS-Cu

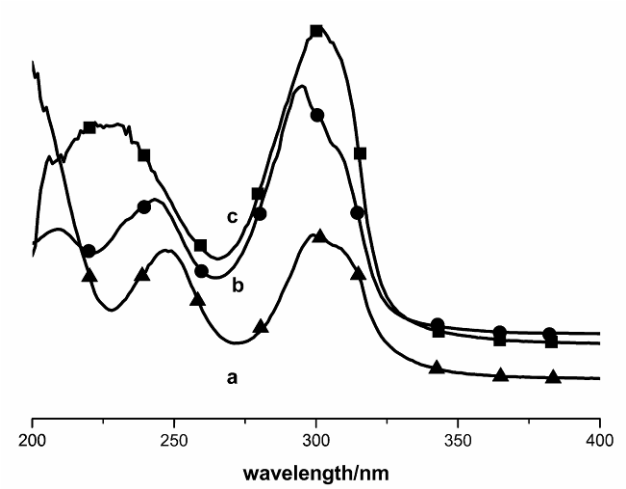

Figure 3.15 UV spectra of samples in hexane solution of (a) POSS-Cu before reaction; (b) POSS-Cu-Vac; (c) POSS-Cu with moisture.

In addition, UV spectra (Figure 3.15) of these compounds were also performed. The absorbance at 247 nm is assigned to the ligand to metal charge transfer [186](*LMCT* transition) and a blue shift to 240 nm and 223 nm is observed for the POSS-Cu-Vac and (POSS-Cu-water), respectively. It demonstrates that hydroxyl groups could be involved in the complex immobilization through hydrogen bonds with the delocalized π-system of the acetylacetonate ligand. The interaction enlarges the orbital symmetry and weakens the donation of ligand, which leads to a higher energy of *LMCT* band.

3.3.3 A mechanism of water catalyzed ring open reaction.

On the basis of above discussion, a mechanism can be proposed as follows: (1) with water, POSS-OH coordinates with the center ion which would facilitate the addition of epoxide because the bonding released via coordination, whereas with in the presence of water, the water molecule forms hydrogen bonds with ligand and assists the POSS-OH to form a hexatomic ring with the center ion; (2) or the water molecule coordinates with center ion from the axial vertical and assists POSS to form an intermediate. It decreases the probability of oxirane coordinate with metal and makes the termination Si-OH by epoxide difficult.

The efficient catalysis of the metal-O-Si coordinated state for epoxy homopolymerization is supported by Hayase[187] and Templin[183]. It is possible that Water stabilizes of metal-O-Si complex or forms an intermediate ceasing Si-OH coupled with the epoxide via steric hinderance. Polybutadiene epoxide[188] and cyclohexyl oxide[189] were researched and explained by the reaction model via the Brönster/Lewis acid model, considering acidic Si-OH. After the addition of water, the active point of Si-OH with epoxy coupling reaction is shielded from the axial direction. In case water coordinates with metal ion, the bond between H-O reduces and becomes easy to attack epoxide group, then initiates the homopolymerization based on the hydrogen released from water and will decrease the termination of homopolymerization by Si-OH/epoxide addition. While continuous consumption of epoxide group leads to a deviation of epoxy value and the formation of oligomers. However, it is difficult to conclude that the water stabilized POSS/catalyst is a reaction active center of the ring-opening reaction. It may play as an intermediate to

the real active center.–In a word, there are two possibilities: either the metal coordinates with oxygen atom of oxirane[190] or the -OH adds to oxirane directly because of acidity[179]. If this mechanism is involved, the networks prepared without presence of water should get a higher *Tg*. The effect of water o *Tg* n of the resulting POSS-OH modified epoxy-anhydride networks will be discussed in the following section.

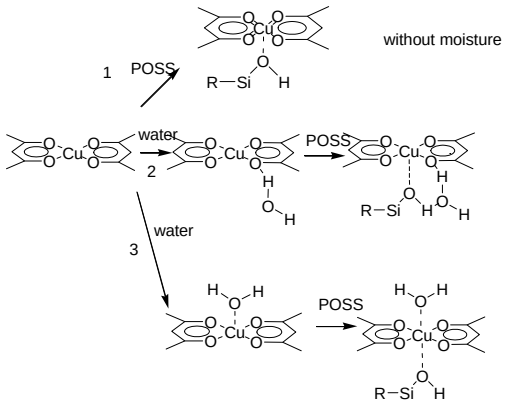

Scheme 3.2 Proposed interaction mechanism of POSS-OH and Cu-based catalyst

3.3.4 Comparation of composites prepared with/without moisture.

3.3.4.1 Morphology of POSS modified epoxy

Figure 3.16 shows the typical morphology obtained from scanning and transmission electron microscopies for *O/I* hybrid networks based on 5 wt% POSS-OH and synthesized either from pre-reaction of POSS-OH with catalyst or from direct mixing of POSS-OH without catalyst. In the first case, i.e. with a pre-reaction, the fracture surface of hybrid epoxy appears homogenous before (Figure 3.16a) and after (Figure 3.16c etching with chloroform. The micrographs show a brittle epoxy matrix. In the second case, i.e. for which POSS-OH is mixed directly without pre-reaction, some cavities (Figure 3.16b) are observed after etching with chloroform due to the extraction of the POSS phase which is poorly dispersed in the epoxy network and non-grafted to the epoxy network. POSS-OH displays a poor compatibility with DGEBA and a low reactivity of epoxy with POSS-OH without catalyst. After covalent bonding of POSS-OH to DGEBA, an amphiphilic structure of POSS-OH-modified DGEBA precursor is obtained. As a consequence, POSS-OH clusters assemble in 20 nm-diameter micelles (Figure 3.16d). When the POSS-OH amount increases up to 5% wt, besides the 20 nm-diameter POSS-OH micelles, larger POSS-

OH-rich structures (0.5-1 μm) can be observed (Figure 3.16e). These microstructures could be attributed to the agglomeration of unreacted POSS-OH, with reacted POSS-OH/DGEBA species acting as interfacial agent.

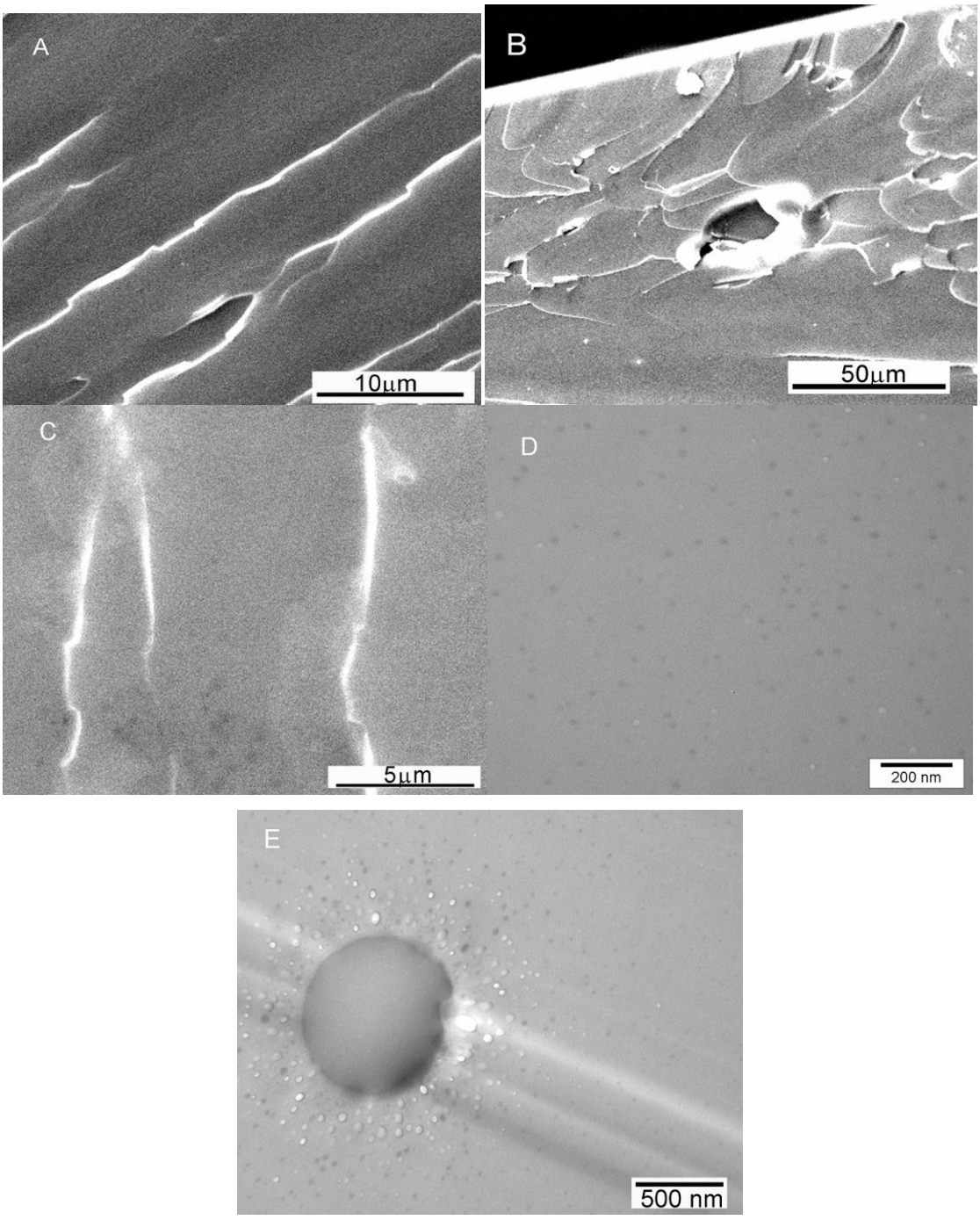

Figure 3.16 SEM and TEM micrographs of fracture surfaces of composites

**(a) the neat epoxy-anhydride network; (b) the epoxy-anhydride with POSS-OH introduced without any pre-reaction after etching, (c) the epoxy-anhydride with POSS-OH introduced with pre-reaction after etching; TEM micrographs of (d) hybrid epoxy network with POSS-OH introduced with a pre-reaction (3% wt. POSS-OH) and*

(e) hybrid epoxy network with POSS-OH introduced with a pre-reaction (5% wt. POSS-OH)– details of a POSS-OH-rich aggregate

3.3.4.2 Mechanical performance of POSS nanocomposites

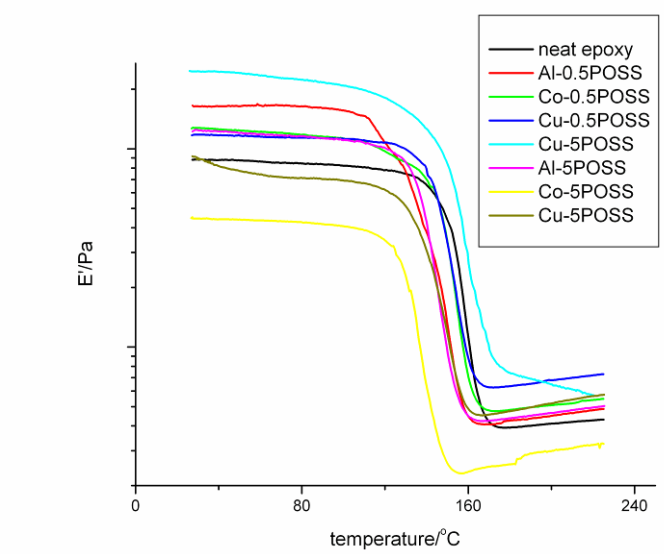

Figure 3.17 The storage moduli of neat epoxy and composite samples.

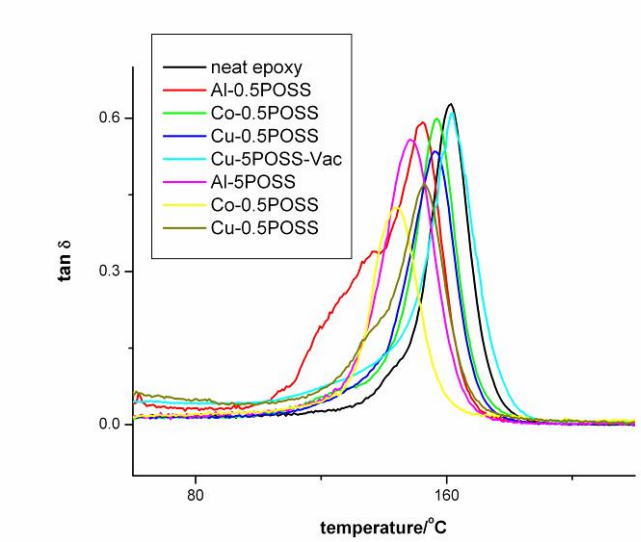

Figure 3.18 tanδ v.s. temperature of neat epoxy and composites.

Table 3.3 shows the thermomechanical properties of the cured neat epoxy and the epoxy modified by POSS with/without the use of metal catalysts according to Figure 3.17, 3.18. According to the accuracy of the measurements of storage modulus in the glassy state, *E'* for all the systems are very close and only *E'* at the rubbery plateau is reported. The major relaxation, denoted α relaxation, displayed on *tan* δ vs.

temperature, at 162 °C, is attributed to the glass transition of the neat epoxy network. For the hybrid prepared by mixing POSS without pre-reaction, which have POSS-OH as large micrometer size agglomerates, close values are observed for α relaxation temperature, *Tα*, as well as storage modulus in the rubbery state. In such a microcomposite POSS-OH acts as a filler of micrometer size and doesn't contribute to a change of the crosslinking density as it is not covalently attached to the epoxy network. However, the effect of the covalent bond results in a slight decrease of *Tα* (from 5 to 10 °C) even for very low amount of POSS-OH, while the rubbery modulus is improved to a limited extent. It means that the crosslink density in the hybrids is slightly higher than in the neat epoxy. As the POSS-OH used is trifunctional, it will act as a crosslinking agent only if the three silanols are able to react with the epoxy groups from DGEBA whereas if only two silanols react, the POSS-OH will act as a chain extender between crosslinks. Finally if only one silanols reacted, it may create dangling chain ends in the network. The network synthesized without moisture (DGEBA-5POSS-Cu-Vac) has very interesting characteristics as the glass transition temperature remains similar to the neat epoxy-anhydride matrix but with a higher rubbery modulus. However, in the cases of high POSS loading, storage modulus *E'* decreases dramatically, which can be assigned to the formation of micrometer-size POSS-OH agglomerates. (Figure 3.17, 3.18)

Table 3.3 Storage moduli, E' and α-relaxation temperatures, T

Sample	E'_r (MPa)	$T\alpha$ (°C)
Neat epoxy	43	162
DGEBA-5POSS-M	39	163
DGEBA-0.5POSS-Cu	72	152
DGEBA-0.5POSS-Al	54	157
DGEBA-0.5POSS-Co	48	156
DGEBA-5POSS-Cu-Vac	57	161

**associated to glass transition at 1 Hz of epoxy-anhydride networks modified or not with POSS-OH cured with/without catalyst.*

It is well known that the chain stiffness makes the motion of chain segment more difficult; the POSS-OH cage, with its hybrid nano silica core, is a rigid unit which may increase the chain rigidness. By connecting the POSS-OH cage on the

macromolecular network, some reports support the improvement of chain stiffness[128] [131], namely *Tg* (or Tα) increases compared with neat matrix. From electron microscopy, it was shown that the POSS-OH is organized in 20 nm diameter domains, corresponding to several POSS-OH units (1-3 nm). In this case, POSS-OH domain in the network can be considered as homogeneously dispersed functional nanofiller covalently bonded to the matrix, which can increase the storage moduli in the rubbery state. From the view of POSS-OH structure, a strong self-aggregation tendency results from the incompatibility of POSS with the neat epoxy, namely POSS-POSS interaction as suggested by Lichtenhan[162]. Therefore, POSS-OH domains act as physical crosslinks, with strong internal interactions, connected to the network. The strength of these physical interacting points, namely interaction between POSS units depends on the nature of organic ligands. Cyclohexyl, for instance, leads to stronger POSS-POSS interactions compared to isobutyl group.[191] Moreover, in our case, chemical crosslinks could be generated and are attributed to the trifunctional POSS-OH silanol, covalently bonded to DGEBA during curing.

In the epoxy network, there is a controversy about the influence of the POSS cage which is considered as an interacting crosslink and a plasticizer with high free volume. Interestingly, the epoxy reacted with POSS has fewer epoxide ring, namely a higher epoxy equivalent weight (eew), resulting in a lower crosslinking density. The decrease of the epoxy crosslink density leads to easiest chain motion and decreases Tg. From the values reported in Table 3.3, it seems that the effect of crosslink is not large, whereas the latter, the plasticizing effect introduced by POSS cage is even more important.

In addition, if the POSS crystallized in the domain, melting temperature (Tm) of POSS depends strongly on the nature of the POSS ligands. For instance, Tm of isobutyl POSS is lower than that of phenyl POSS. Therefore, the role of POSS in the composite is stepwise: the Tm of net POSS is close to 120 °C,[191] about 30 °C below Tg of the epoxy networks, so in between the melting point of POSS and Tg of epoxy networks the dispersed POSS rich domain becomes soft . In such case, the glassy epoxy disperses with soft nano-scale domain is similar to plastic modified by soft matter, such as epoxy modified by rubber. This comparison could assist us to understand the role of the plasticizer effect of POSS domains, whatever POSSs crystallize or not. In this way, the nanofiller deviate from a tough component to a soft component, along with the temperature field.

3.3.4.3 Thermostablity of hybrid composites

The thermostability which is a very important issue for the hybrid organic/inorganic materials was characterized using TGA in order to examine the influence of the presence of POSS-OH clusters in epoxy networks. Table 3.4 shows the initial decomposition temperature, *T5* (temperature at 5 wt% loss) and the char residue at 700 °C. These data were the results of TGA tests (Figure 3.19, 3.20).

Table 2.4 TGA results, tests under air at 10 K/min

Sample	*T5* (°C)	Char residue (wt%)
Neat epoxy	355	0
DGEBA-5POSS-M	367	3.3
DGEBA-5POSS-Cu	341	6.5
DGEBA-5POSS-Al	346	6.8
DGEBA-5POSS-Co	354	11

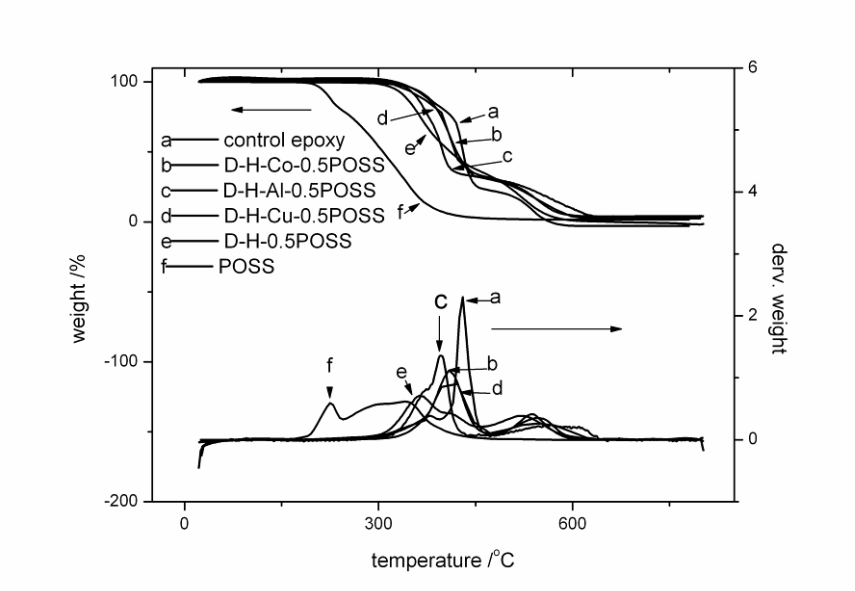

Figure 3.19 TGA trace of POSS and POSS composites in the air, heating rate=10 °C/min.

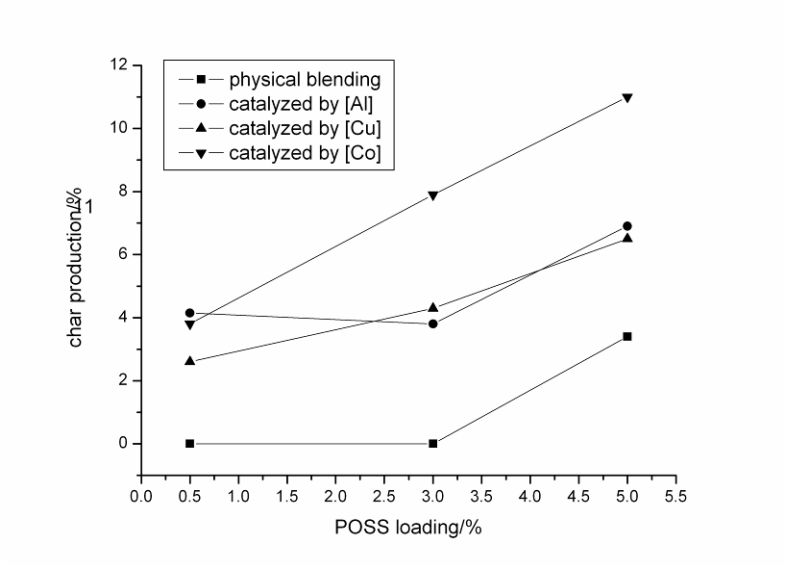

Figure 3.20 The char production at different POSS loading in epoxy

It is well known [192, 193] that there are three steps in the degradation process of epoxy networks under air: near 380 °C there is a dehydration mechanism, then the maximum rate of degradation takes place at 430 °C and complete oxidation-combustion takes place with maximum rate at 535 °C. The thermal stability of POSS clusters depend mainly on the type of organic groups surrounding the inorganic cage.

There is some controversy about employing POSS to improve the thermostability[15-16]. In general, the POSS is considered as a precursor of ceramic, thermostable silicate formed after fully thermooxided[159]. Ceramic preventing the inside oxidation further formed from POSS. The protection competes with the reaction of matrix thermodegradation, naturally leads to a higher char product in POSS hybrid materials. However, some researchers considered POSS had not made any contributions but breakages sometimes to the thermostabilty[69]. In the process of TGA, 3 reactions advance actually: thermoxidation, ash forming and volatilization, the last one is ignored generally. The lower char production is resulted from the volatilization prior to char production, which means POSS evaporation before forming a continuous film to protect the matrix. It is affirmed by Weickmann[69] that non char produced in the process of matrix thermodegradation. The evaporation has relationship with the vertex and the structure of POSS. Fina[194] concluded that POSS got more char and higher evaporation resistance with increasing molar mass. Here, POSS-OH leads to almost no residue (≈1.7%). Interesting, for POSS silanol,

structural rearrangements induced by sublimation at ambient pressure is not observed, which seems to be in conflict with the dehydrolysis of silanol at high temperature[3]. The POSS nanocomposite can combinate the performance of POSS and neat epoxy: 3 steps of thermodegradation with lower Td, (the peak of differential thermogravimetric curve, 410 °C for Co-0.5POSS, 394 °C for Al-0.5POSS and 420 °C for Cu-0.5POSS respectively). It is worthy of noticing that the organic metal catalyzing POSS nanocomposites have higher Td than the blended specimen. It is assumed that the nanoscale dispersion of POSS molecules in the matrices and their covalent bonding onto the network should contribute to the enhancement of Td. The ash production of neat POSS is relatively lower than the theoretical production (≈24%) which is assumed to the tendency of POSS evaporating.

It should be pointed out that the ash production of blend specimen is nearly 0% much lower than that of the nanocomposite samples, from 2.6 to 4.1% in practice (0.24% in theory). The result proves that POSS cages covalently bonded to epoxy networks hindered the POSS cage evaporating from the matrix compared with POSS blend specimen.

The char production (Figure 3.20) of the nanocomposites increases with the percent of POSS monotonously. It is believed that the ceramic coating which forms at a higher POSS content and resists the oxidation of main chain. It is interesting to investigate a higher char production of POSS modified epoxy than neat POSS.

Here, considering the few char of pure POSS and sharp peak of DTG (Figure 3.19), the only one step in TGA is attributed to the evaporation of POSS. In the physical blending specimen, it is assumed the POSS were thermooxidated or volatilized firstly at the temperature elevation resulting the first step of weight lose. Then channels, newly generated fracture arounding POSS cages after the combustion of side group, is utilized for oxygen transferring and fragments escaping. The effect of shortcut in energy and substance passing by is the reason why the improvement of thermostability can not fulfill by introducing of ceramic precursor, POSS. Td in POSS modified epoxy is higher than POSS blending specimen at the 0.5% POSS additive, demonstrating the covalent bonding restrained the hydrolysis and evaporation of POSS, however still less lower than that of neat epoxy. In addition, the increased Td for the nanocomposites could be resulted from the increased chain spacing because of POSS, which gives rise to a lower thermal conductivity.

It demonstrates that grafting POSS cage to epoxy-anhydride network has significant impacts on the thermomechanical and thermal stability behaviour. In such cases, one can demonstrate that for designing hybrid organic-inorganic (nano) materials, the most efficient route is to synthesize O/I materials[195], for which strong coupling is introduced between organic and inorganic phases from proper chemical interfacial reactions.

3.3.4.4 Crystallization of modified nanocomposites: X-ray diffraction of POSS

In the XRD spectra (Figure 3.21), a slight crystalline peak of POSS center at 7.2° in physical mixture. This peak corresponds to the strongest reflection of crystalline MA-POSS (101 hkl reflection associated to a characteristic distance of 1.12 nm)[196] . However, which is hardly to observe in the prereacted samples with catalyst. Because the crystallization increases with POSS content, there is low POSS loading in the samples, 5wt%, possible not very strong enough for clear diffraction signal.

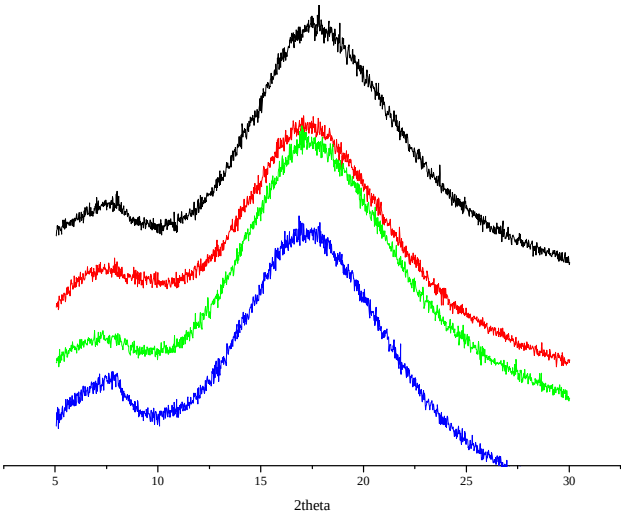

Figure 3.21 The XRD spectra of POSS modified composites.blue-5% POSS physical mixture, red-catalyzed by [Al], black catalyzed by [Cu], green- catalyzed by [Co]

3.3 Conclusion

In the present investigation the incorporation of trisilanol isobutyl POSS-OH into an epoxy-anhydride reactive systems, via the reaction between Si-OH and oxirane ring, was studied and various hybrid organic/inorganic nanomaterials were synthesized using an amount of 5 wt% POSS.

Using model compounds, FTIR spectroscopy and SEC demonstrated that the catalyst used has an influence on the reaction mechanism and that homopolymerisation of epoxy can occur. This result was confirmed by DSC on

DGEBA-anhydride-POSS-OH reactive systems which show an increase of the initial glass transition temperature and a huge decrease of the enthalpy of reaction, as soon as a pre-reaction between POSS-OH and DGEBA was done. It was also shown by NMR spectroscopy that the presence of residual water has an influence on the homopolymerisation reaction and a mechanism was proposed.

Crosslinks introduced by POSS-OH could be generated as far as a pre-reaction between epoxy prepolymer, DGEBA, and POSS-OH occurred. The analysis of morphologies on the hybrid materials was performed by Transmission Electron Microscopy and showed well dispersed POSS-OH 20 nm- nano-domains. By DMA a slight decrease of Tg was observed as compared to the neat network. Therefore the introduction of POSS to improve Tg is counterbalanced by the presence of epoxy oligomers obtained through homopolymerisation, which act as plasticizers. This phenomenon could explain some contradictory discussion on the influence of POSS-OH noticed in literature. POSS has also an influence on the formation of a char residue, even for a low amount of 5 wt %; better results were obtained by using phenyl rather than isobutyl ligands to delay the temperature of degradation.

Chapter 4 POSS-PGMA block copolymers and self assembly in epoxy

4.1 Brief introduction of POSS copolymer modified epoxy

The homogeneously dispersion of POSS with ideal structure in the matrix, which is quite desirable, is hard to be achieved in practice due to the poor compatibility of POSS with the matrix. Although it's tunable with the vertex group, the silicon nature of POSS considerably constrains its compatibility with the matrix. To overcome this difficulty, the introduction of amphiphilic POSS polymers acts as an effective tool to improve the compatibility of nanobuild hybrid polymers[35, 135]. Whereas, even if copolymer is compatible with the precusors, aggregation or phase separation may take place because of the decreased entropy of mixture when polymerization. Hence, for epoxy network, the compatibility of block copolymers (BCPs) depends on the curing agent and epoxy precursors. For instance, PMMA was incompatible with DGEBA/4,4'-diaminodiphenyl sulfone (DDS) or 4,4'-methylene dianiline (MDA) but compatible with DGEBA/ 3-chloro 2,6-diethylaniline (MCDEA) [134, 197]. Unfortunately, it means we were obliged to prepare various POSS polymers to satisfy the different base materials in general.

On the other hand, POSS based block copolymer have been synthesized via kinds of controllable polymerization, such as ATRP[41, 198], cationic polymerization[44, 45], ring-opening polymerization[23]. The large steric hindrance of POSS constrains the activity of monomer, leading to a lower degree of polymerization. In the case of ATRP, the limitation of DP is about 15 MA-POSS[41, 198]. The anionic polymerization overcomes the limitation of ATRP[45], yield the POSS based block copolymers with a narrow polydispersity. Xu[199] synthesized a brush based on PGMA grafting from a long poly-initiator poly(2-(2-bromoisobutyryloxy)ethyl methacrylate) (PBIEM) via ATRP, and covalently linked PGMA to POSS-SH by reaction with the epoxy groups. Recently, there are several publishcations of tadpole-shape POSS based polymers prepared via reversible addition-fragmentation transfer polymerization(RAFT)[52, 54-56].

Here, PGMA terminated dioester group was synthesized via RAFT polymerization utilizing CDB as chain transfer agent, and then the chain extension of

POSS monomer was preceeded with this macro-CTA. Because the epoxy group could react with many ring open agents, for instance acid, amine, anhydride, isocyanates and coordinating polymer. It is easy to tune the compatibility by prereaction with step-growth monomer and forms nanostructure. In this part, we employed this curable POSS block copolymer linking to the epoxy networks via the curing reagent MDEA. The reactive POSS would self-assemble into micelle and form POSS /intercrossing GMA core/shell nanostructure in the epoxy matrix. This reactive block POSS polymer was a promising candidate for bottom-up nanotechnology, since its morphology can be tuned by coupled with different step-growth polymerized monomers.

4.2 The synthesis of POSS-GMA block copolymer

4.2.1 Preparation of Initiator (cumyl dithiobenzoate)

4.2.1.1 Materials

The synthesis of RAFT initiator accord with the referenece, a high purity >99% measured from ^{1}HNMR. 2, 2-azobis (isobutyronitrile) (AIBN, 99%) was purchased from Sinoreagent and recrystallized twice from methanol. GMA was purified by passing through a column filled with basic Al_2O_3. Methacrylate isobutyl POSS from Hybrid Plastic Co. was utilized as received. THF was mixed with KOH 48 h, and then redistilled with the Na foil.

4.2.1.2 Experiments

a. Fourier Transform Infrared Spectroscopy (FTIR).

The sample of PGMA and POSS-PGMA copolymers are compress into pellets with KBr. The FTIR measurements were performed on a Fourier transform spectrometer (FTIR) at room temperature (25 °C).Measurements were recorded at a resolution of 2cm^{-1}, 64 scans.

b. Nuclear Magnetic Resonance Spectroscopy (NMR).

Nuclear Magnetic Resonance Spectroscopy, Varian Mercury Plus 400 MHz NMR spectrometer was utilized at 25°C to collect ^{1}HNMR. The samples were dissolved with deuterated chloroform, tetramethylsilane (TMS) as the internal reference.

c. Elemental Analysis

The Elemental Analysis was characterized via Vario EL Ⅲ(Elementar Analysen Syetem GmbH Co) .

d. Size exclusion chromatography (SEC).

SEC was performed in tetrahydrofuran using an Elite P230 pump, Shodex GPC KW-804L column and an Elite RI230 refractive index detector. Calculations of apparent molar mass were processed via the EC2000 software from based on linear polystyrene standards.

e. Thermal Gravimetric Analysis (TGA).

A TA Q10 thermal gravimetric analyzer (TGA) was used to investigate the thermal stability of hybrid composites. The samples (about 10 mg) were heated from ambient temperature to 800 °C in the air, heating rate of 10°C/min in all cases.

4.2.1.3 Preparation of CDB

Phenyl magnesium bromide was prepared from bromobenzene (62.8 g) and magnesium (10 g) in dry tetrahydrofuran (300 mL). Carbon disulfide (30.44 g) was added over l5 minutes whilst maintaining the reaction temperature at 40°C. The resultant dark brown mixture was added benzyl bromide (76.95 g) over 15 minutes. The reaction temperature was raised to 50 °C for a further 45 minutes. Ice water (1.5 L) was added and the organic products was extracted with diethyl ether (total 2L). The ethereal phase was washed with water (1L), brine (500 ml) and dried over anhydrous magnesium sulfate. After solvent removed and vacuum pumped, benzyl dithiobenzoate was obtained as red oil.

Dithiobenzoic acid (9.9 g), styrene (10 mL) and carbon tetrachloride (30 mL) were combined and the mixture heated at 70 for 4 hours. The resultant mixture was reduced to a crude oil, and then purified by column chromatography (aluminium oxide (activity III) petroleum spirit 40-60 °C eluent).

4.2.1.3 Characterization of CDB.

Vibration of C=S in FTIR is at 1046 cm^{-1} and 1223 cm^{-1}, in accordance with the reference. Moreover, the phenyl group is at >3000 cm^{-1} and its skeleton appears at 760, 695 cm^{-1}, representing mono-funtional phenyl group. The peaks at 1382 and 1362 cm^{-1} resulted from the -$C(CH_3)_2$, which is characteristic of CDB.(Figure 4.1)

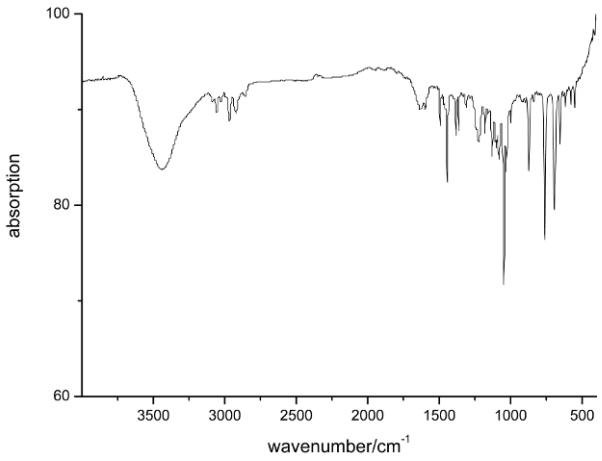

Figure 4.1 FTIR spectrum of CDB

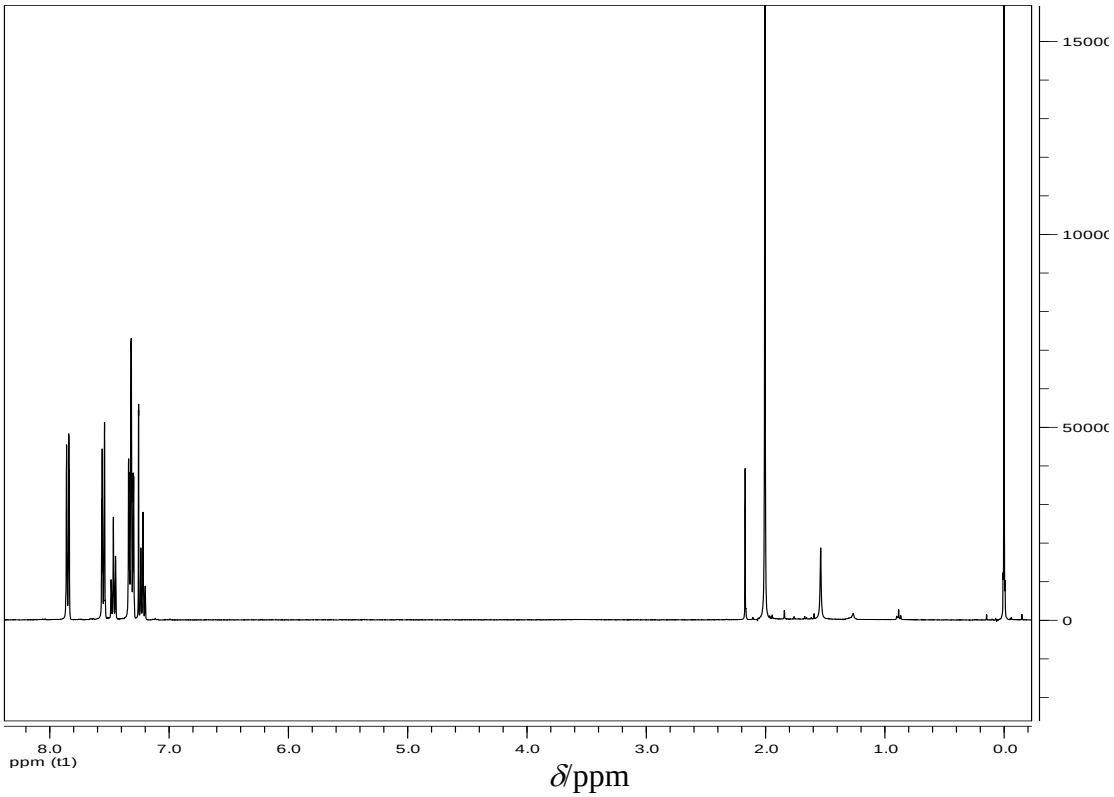

Figure 4.2 ^{1}HNMR spectrum of CDB

^{1}H-NMR ($CDCl_3$) δ(ppm):2.00 (6 H) is assigned to the methane; the phenyl is at 7.20-7.56(8H), 7.84-7.86(2H) respectively(Figure 4.2). Derived from the electroabsorption of C=S, the *o,p*-H in aromatic ring appears at a high field. Elements Analysis of CDB: C70.78%(70.49%), H5.97(5.88%), S23.25%(23.63%), the experimental value is given in the parenthesis.

4.2.2 Preparation and characterization of PGMA-POSS block copolymers.

Cumyl dithiobenzoate (CDB) as a RAFT agent has been proven to be a useful method to obtain information about additional mechanistic pathways of the RAFT process (Scheme 4.1). Reversible addition-fragmentation chain transfer (RAFT) polymerization is one of the most versatile techniques to produce complex polymer architectures (e.g., blocks, stars, and branched copolymers) with uniform chain length. The RAFT mechanism was first proposed by Zard and later confirmed by Rizzardo et al.[200]

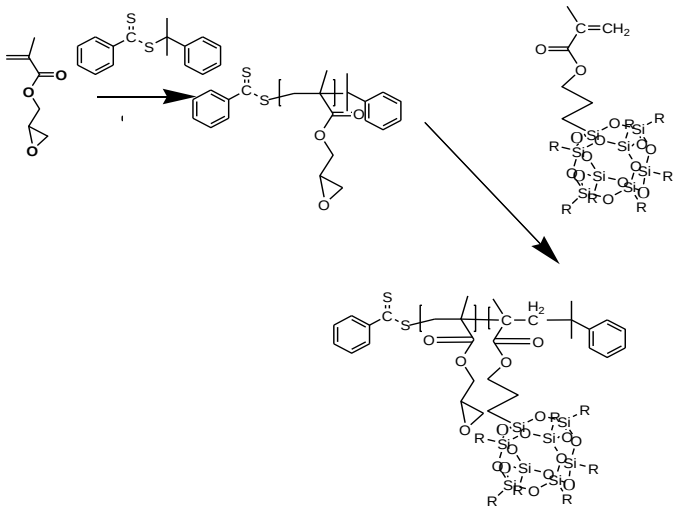

Scheme 4.1 The protocol of POSS-GMA block copolymers synthesis.

4.2.2.1 Preparation of PGMA macroinitiator

Typically, flask was charged with Glycidyl methacrylate, GMA (0.3g, mmol), the AIBN solution (0.01 mmol in toluene), CDB solution (0.3 mmol in toluene) were injected by syringe. The mixture was degased – charged argon three times, and then was immersed in 65 °C oil bath. With the processing polymerization, monomer as solvent of macro-initiator is consumed, which resulted in a growing viscosity. At a high conversion, it formed a gel of PGMA, which leads to an increasing *PDI* of bulk polymerization. The product was diluted by anisole and precipitated into cold methanol. Then the solid powder was re-dissolved in dioxane and precipitated into cold methanol twice.

4.2.2.2 Preparation of PGMA–POSS hybrid block copolymers

The designed PGMA-POSS copolymers are denoted as 10G10P(10k GMA and 10k POSS), 10G5P (10k GMA and 5k POSS). PGMA (0.1g) macro-initiator was dissolved in 0.5 ml THF in a round bottom flask with a magnetic stirring bar, and then MAPOSS(0.05g in 10G5P, 0.1g in 10G10P), AIBN (0.003mmol) was added. Then the flask was degassed and purged argon twice to keep it in an inert atmosphere.The mixture polymerized at 65 °C for 24 h. Afterwards, it was cooled to room temperature and was precipitated by methanol. Then, the fine powder was precipitated-dissolved again to remove the residual MAPOSS.

4.2.2.3Characterization of POSS copolymers

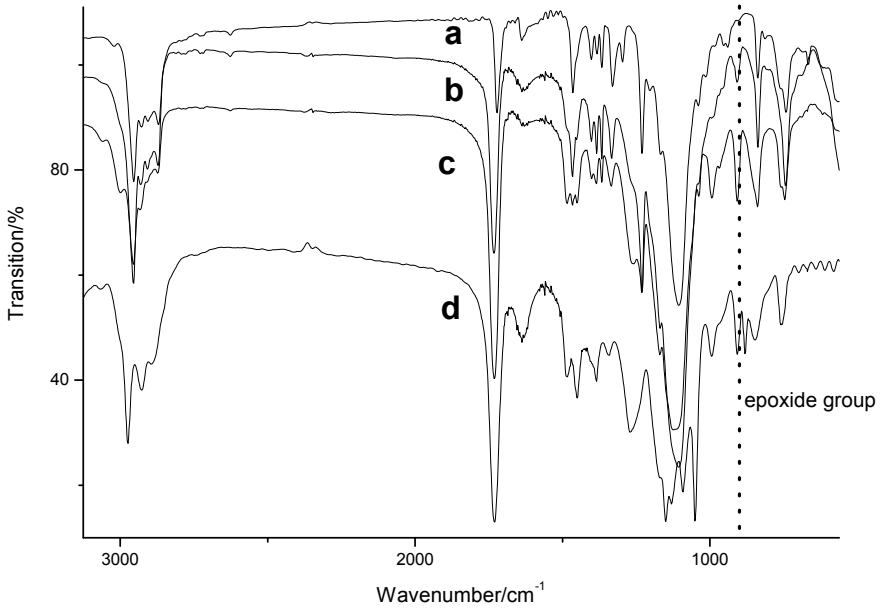

Figure 4.3 FTIR spectra of methacylate isobutyl POSS (a), 10G10P(b), 10G5P(c), PGMA(d)

The synthesized PGMA macro-CTA and PGMA-POSS copolymers are charaterized by FTIR(Figure 4.3): The vibration absorption peak of C=O appears at 1730 cm-1, peaks at >3000 cm-1 (phenyl group) and 760, 695 cm-1 (phenyl skeleton) are attributed to mono-functional phenyl group. The signal of epoxide ring structure at 907 cm-1 exists in all copolymers except POSS monomer. In POSS copolymers, Si-O-Si, Si-CH2 and Si-O-C absorption peaks are observed at around 1111–1120, 840 and 1233 cm-1, respectively. The absorption strength ratio of 907 and 840 cm-1 is

much more intensive in 10G10P than that of 10G5P in accordance with the fluctuation of POSS content [19, 42, 201].

The ^{1}HNMR spectra of the PGMA macro-CTA and the block POSS copolymer are different as shown in Figure 4.4, 4.5. The resonance signal at δ=0.9 ppm is assigned to the -CH3 protons, and at $\boldsymbol{\delta}$=1.6 ppm is ascribed to the -CH2- protons in the PGMA backbone. The signals of methylene group linking to chiral CH on epoxy group are observed at 3.7 ppm and 4.2 ppm. Resonance at δ=2.6 ppm, 2.8 ppm and 3.26 ppm are ascribed to hydrogens in the epoxy ring. After copolymerization of POSS, there are an additional methylene protons peak (δ=0.60 ppm) from Si-CH_2 in P(MA-POSS). Peak at δ=7.85 ppm is ascribed to o-H of phenyl in terminated dithioester group. The molecular weights are calculated from NMR follows:

$$DP_{PGMA}=A_{\delta=3.26}/A_{\delta=7.85}$$

$$Mn_{NMR}=M_{CDB}+M_{GMA}\times DP_{PGMA}+M_{POSS}\times(A_{\delta=0.60}/16A_{\delta=3.26})$$

The area of 7.85($A_{\delta=7.85}$) is ascribed to *o-H* of phenyl in CDB. The degree of copolymerization could be calculated from ^{1}HNMR by the ratio of polymerized POSS/ GMA. The area of $A_{\delta=0.60\ ppm}$/16 is the -CH_2- connecting with Si(16H per POSS),and that of $A_{\delta=3.26\ ppm}$(CH connecting with O atom of epoxide ring). To purify the free POSS, the circle of dissolving/ precipitating is repeated 3 times, though some still are residual. The residual POSS is observed at δ=6.13, 5.57 ppm in the sample 10G5P, so that the content of POSS corrected as the $A_{\delta=3.26\ ppm}$/16-$A_{\delta=6.13}$.

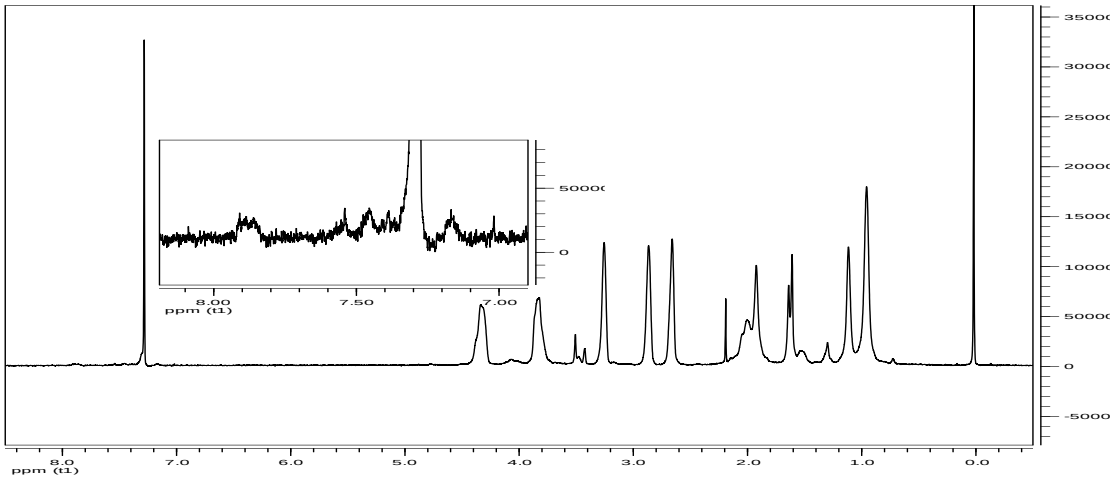

Figure 4.4 The macroinitiator, PGMA is characterized by 1HNMR

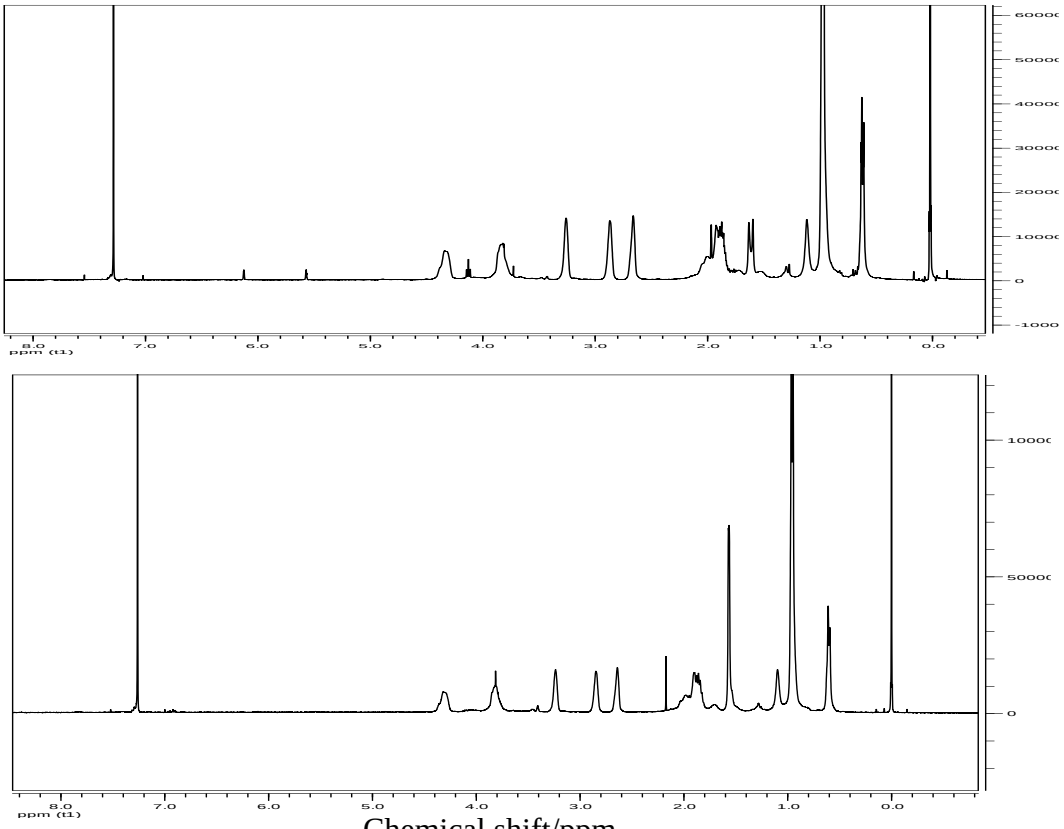

Figure 4.5 POSS block copolymer are characterized by ^{1}HNMR, 10G5P (upper), 10G10P (nether).

Table 4.1 The molar mass and index of polydisperisity(*PDI*)

Sample	Theoretical M_W	*Mn (NMR)*	*Mn (GPC)*	*PDI*
PGMA	10000	8520	8450	1.32
10PGMA-5POSS	15000	13107	12932	1.39
10PGMA-10POSS	20000	16396	15980	1.43

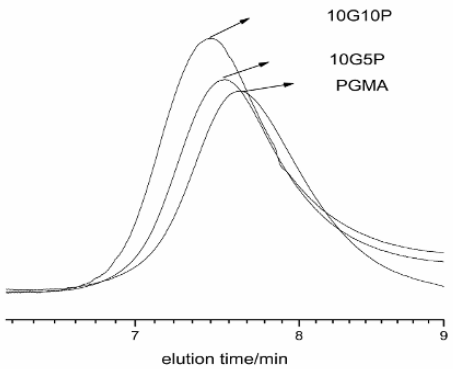

Figure 4.6 PGMA macroinitiator and POSS block copolymers are characterized by GPC.

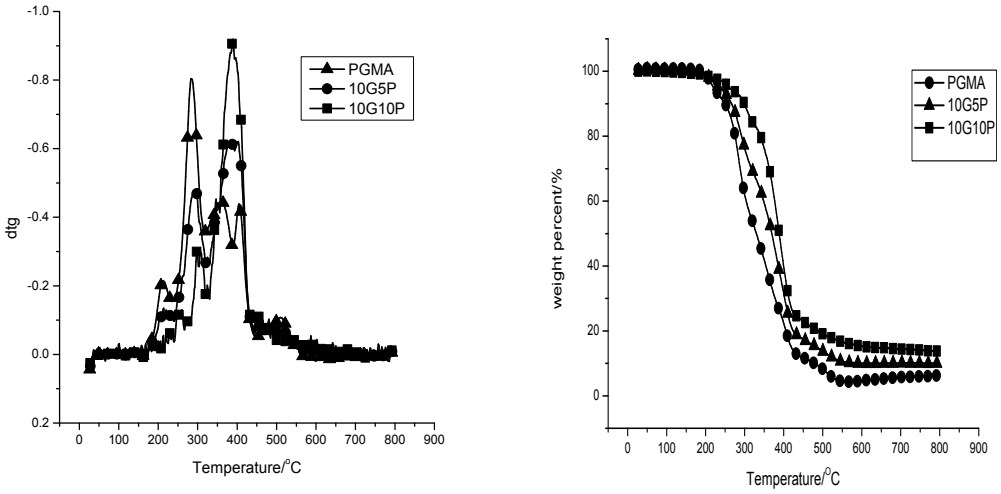

Figure 4.7 TGA trace of PGMA and block copolymers in the air, rate=10 °C

Table 4.2 The data of TGA trace

Sample	*T5*/°C	*T50*	*Tmax*/°C	Char product	Char product in theory
10G	218	328	284	5.9%	0
10G5P	236	368	386	10.3%	16%
10G10P	274	387	389	14.1%	25%

** the temperatures at which the sample lost 5%, 50% are denoted as T5, T50. Tmax is read from the peak of differential TG curve. Char productivity in theory is calculated from the SiO_2 after full oxidation of POSS.*

It is well known that, as a preceramic molecule, POSS can improve the thermostability which is attributed to the mechanism of the formation of silica and entrapment of radical[124, 125]. T5 (5 % weight loss temperature) and Tmax (maximum degradation temperature) of PGMA obtained from the TGA curves at about 218°C and 284°C respectively (Table 1, Figure 2), consistent with reference[202]. After the incorporation of POSS into PGMA, the initial degradation temperature (T5) of the block copolymer increases with increasing POSS content (~20 °C in 10G5P and ~66 °C in 10G10P). Moreover, the maximum degradation temperatures of POSS based copolymers (peak b, c) were higher than that of GMA homopolymer (Peak a, ~284°C). Probably, the covalent bonding severely reduces the volatile of POSS and enhances the thermal stability of polymers.

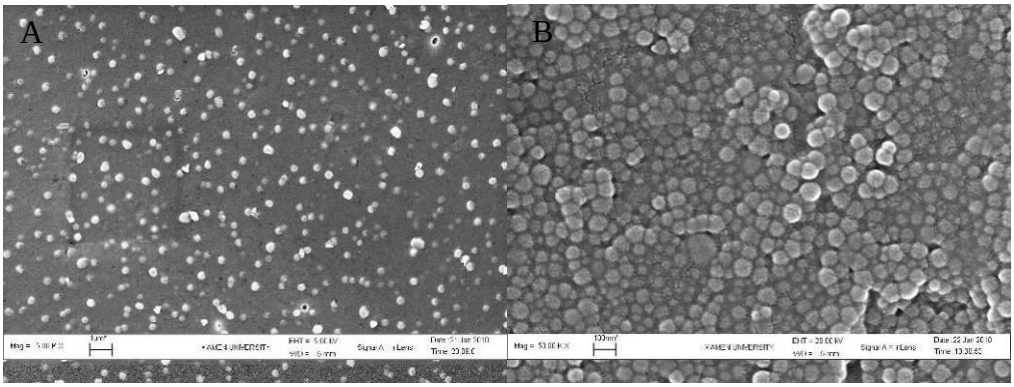

Figure 4.8 The selfassembly of block copolymers, 10G10P (A),10G5P(B).

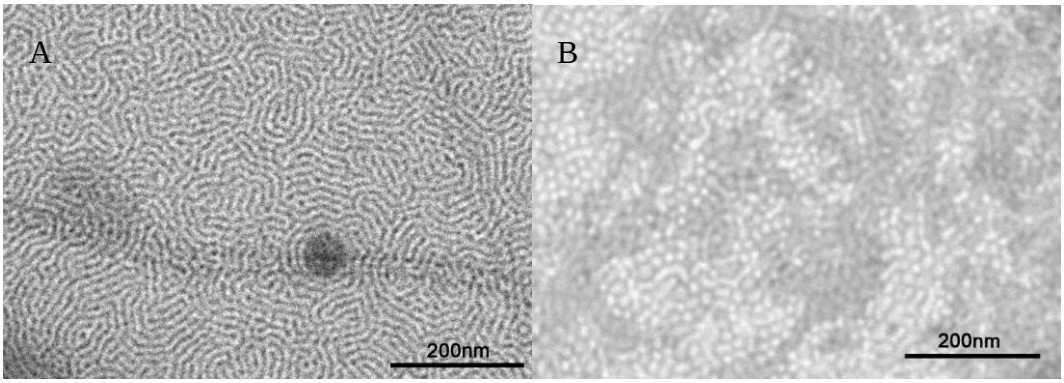

Figure 4.9 The morphology of copolymers observed from TEM, 10G5P(A),10G10P(B)**.**

Dioxane and hexane are selective solvents for our copolymers. The former is an excellent solvent for PGMA, and the latter for POSS. In 10G5P, unique dispersed spherules forms after selective solvent casting, which is similar with other block copolymer micelle. However, a part of them is larger than 100nm, which is larger than the term of "micelle" (Figure 4.8). Molar mass polydisperisty as a characteristic of polymer is relatively narrow via RAFT polymerization. Polymer with a small molar mass polydisperisty formed micelles during the evaporation of the selective solvent. Considering the experimental polydisperisty, a high POSS content copolymer forms larger diameter micelle. In case of short POSS chain sample (10G5P), the corona of GMA stabilizes the micelle efficiently in Dioxane. Only an opaque mixture of 10G5P is obtained in hexane, it is difficult to stabilize as a micelle in hexane. A longer POSS chain (in 10G10P) forms a micelle in hexane probably. Microscale particle is observed in cast 10G10P/ hexane sample (Figure 4.9).

To research the phase structure in POSS-GMA copolymer, films are prepareds by casting THF solution. In the POSS rich domain, Si with a higher atomic number element is dark in TEM. In 10G5P, lamallar structure of POSS and GMA is observed. Except that, some POSS/GMA shell/core fibers forms with a diameter of 20 nm, which is interested to achieve the nanofiber by casting a POSS block compolymer. It is a filamentous polymeric aggregation, so-called worm-like micelles or ‘‘filomicelles’’.

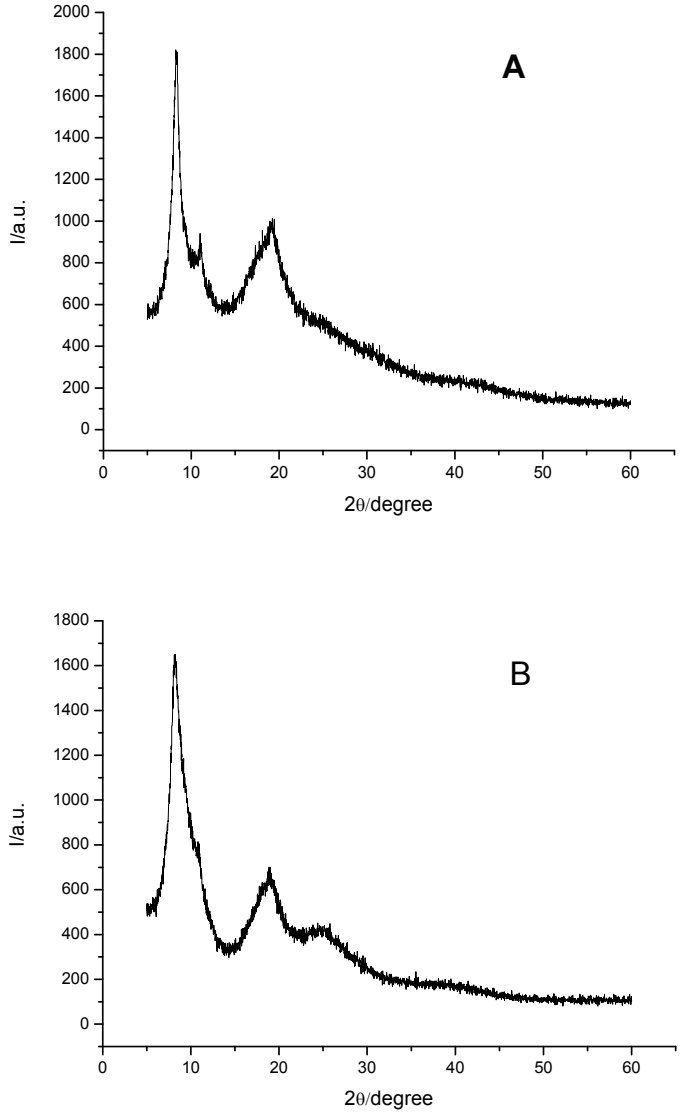

Figure 4.10 XRD spectra of 10G5P(A), 10G10P(B)

In linear diblock copolymers, composed of two immiscible blocks, A and B, they can adopt the equilibrium microphase morphologies, as spheres (S), cylinders (C or Hex), double gyroid (G or Gyr), lamellae (L or Lam)[203], which is related with the

composite. The filomicelle morphology of copolymer is related with the volume fraction of the blocks. There are three key effects determing the morphology of the micelle, namely the stretching of the core-forming chains, the core-corona interfacial energy and the repulsion among coronal chains[204, 205]. In the sight of these Gibbs energy related parameters, when the parameters vary, the micelles could become thermodynamically unstable and will modify their morphology in order to reach another stable state. The varying concentration of copolymer may be the reason to form the fiber of POSS copolymer, because the concentration changes with the procesure of solution evaporation and it affects the final phase in the phase diagram. On the other hand, in the view of THF, the condensated moisture dilutes the solution while the endothermic evaporation, leads to a filomicelle phase at an alternating concentration.

PGMA is a well-known amorphous polymer, no diffraction peak in the XRD spectrum, except for amorphous halo. In the block copolymers, consisting of a cubic POSS, a strong peak center of 8.3 ° reflects the POSS crystalline in the copolymer as the references, ascribed to (101) [153, 206](Figure 4.10) .

4.3 Bottom-up nanostucturation of POSS-PGMA in Epoxy

4.3.1 Preparation of POSS-GMA modified composites

4.3.1.1 Measurements

a. Scanning Electronic Microscopy (SEM).

The fracture of POSS-containing epoxy hybrids were characterized by a LEO 1530 scanning electron microscope (SEM). The samples of composites were fractured under cryogenic condition immersed in liquid nitrogen. The surfaces were etched in THF at room temperature for 30 min, which was an excellent solvent to POSS copolymer to remove all the residual POSS. The etched specimens were dried to remove the solvents. After that, a coating of gold about 100 Å was sprayed on the fracture surface (activation voltage=20 kV).

b.Dynamic Mechanical Thermal Analysis (DMTA).

DMTA was carried out on cured epoxy nanocomposites with a Rheometrics solid analyzer (RSA II) to obtain tensile dynamic mechanical spectra (storage modulus E’,

loss modulus E", and loss factor tan δ) between 25 and 220°C at a frequency of 1Hz in the linear viscoelastic domain.

c. Thermal Gravimetric Analysis (TGA).

A TA Q10 thermal gravimetric analyzer (TGA) was used to investigate the thermal stability of hybrid composites. The samples (about 10 mg) were heated from ambient temperature to 800 °C in the air, heating rate=10°C/min in all cases.

d.X-ray diffraction(XRD)

The degree of crystalline was carried out by x-ray diffraction (XRD), Philips X'Pert Pro Super X-ray diffractometer, Cu Kα radiation, at a 2 °min^{-1} scan rate. The PGMA-POSS copolymers were grinded as a fine powder, and the composites are films.

e. Transmission Electron Microscopy (TEM)

PGMA- POSS /THF solution was deposited on TEM copper grids coated with a thin amorphous carbon layer; JEM 2100 high-resolution transmission electron microscope was utilized at the accelerating voltage of 200 kV. These POSS composites were too hard to cut by glass knife of ultramicrotome. According to Li's method[207], ultra-thin samples were achieved by polishing and ion milling process, then were placed on a copper grids for observations.

4.2.1.2 Preparation of POSS-GMA modified composites

In all cases, we used POSS based copolymer to modify the epoxy network. For reactive modifier, desired amount of PGMA-POSS copolymer was dissolved in THF, then the epoxy (DGEBA, Dow 330) and curing agent MDEA were added under stirring. Based on the calculation of ^{1}HNMR, the epoxide value of PGMA-POSS was determined. MDEA is stoichiometric proportion of epoxy group in the blend of PGMA-POSS and DGEBA resin. The mixture was evaporated under vacuum to remove the solvent for 4 h at 60 °C. After that, it was poured into an aluminum mold (2 cm ×1 cm ×0.5 cm), which was cured at 135 °C for 4h and 190°C for 4h. Because of the difference in reaction rate between GMA and DGEBA[208], the GMA reacts with MDEA rapidly and self-assembles into a GMA corona - POSS core nanostructure before curing, which is stabilized and preserved after epoxy network forms. The samples were polished in 2cm×1cm×2mm for DMTA, and successively employed for SEM and TEM observation.

4.3.2 Characterization of core/shell POSS nanostructure in epoxy.

4.3.2.1 Morphology of POSS compolymer modified epoxy

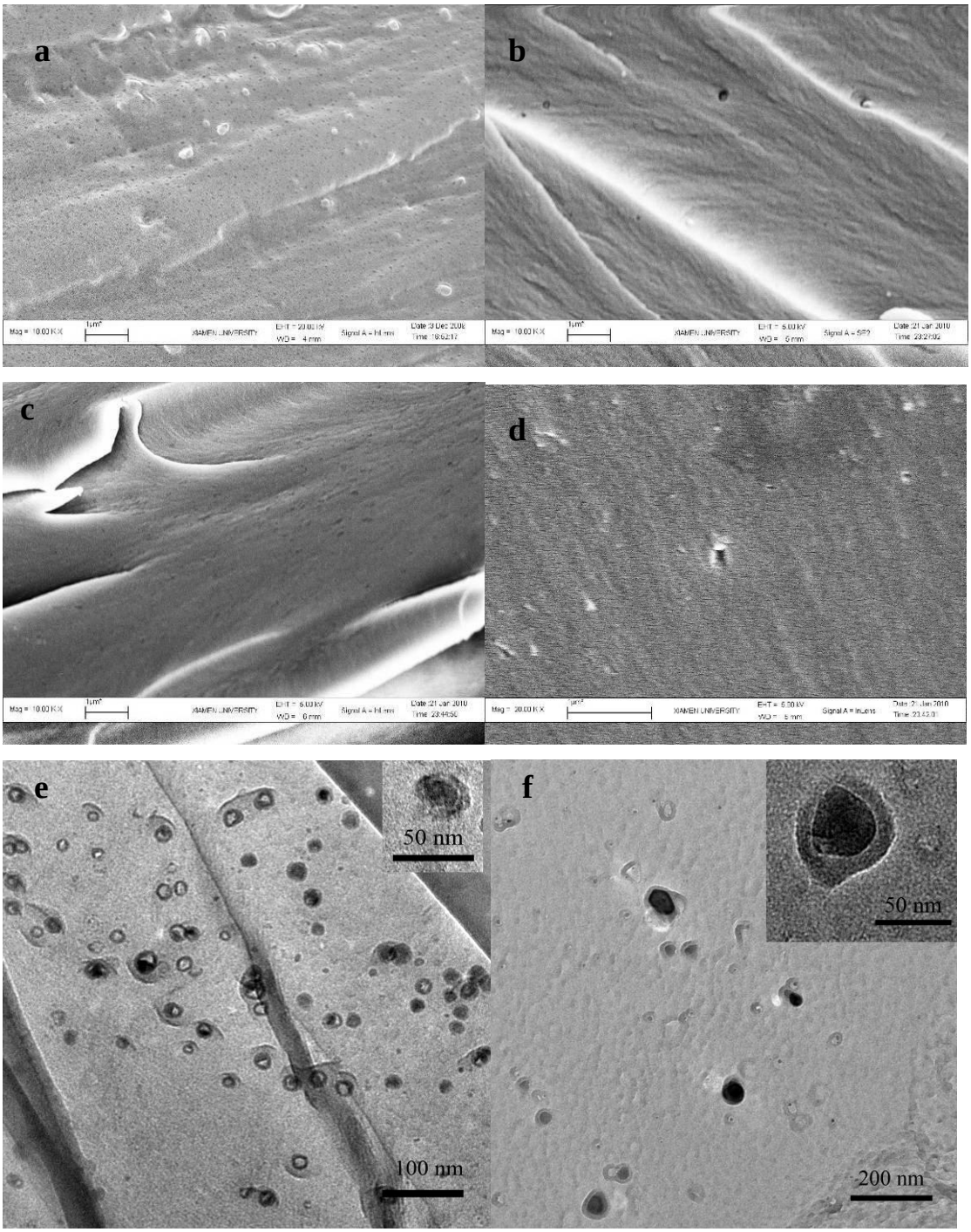

Figure 4.11 The morphology of PGMA-POSS copolymer hybrid epoxy, **a.10wt10G10P, b.20wt10G10P, c.10wt10G5P, d.20wt10G5P, e.10wt10G10P(TEM),f. 10wt10G5P(TEM)*

The morphology of POSS nano-built epoxy (Figure 4.11) after the postcure are characterized via SEM and TEM. Homogenously dispersed nanoparticles (<100nm)

and nanopores indicate the PGMA-POSS grafted into epoxy net-work successfully. Except that, a part of separated phase in 10G10P have a diameter of 100-200 nm, resulting from the inevitable molar mass polydispersity in block copolymer probably. Isobutyl POSS is incompatible with epoxy/network and forms large scale phase separation, because of the weak interaction epoxy networks.

The micelle distribution in the matrix relates with molar mass, PDI and content, but the size of micelle is relatively invariable before/after curing reaction[209]. Beside that, the energetic barriers to nucleation and growth of copolymer-rich regions occurs as network formation and the growth of epoxy molecular weight, which leads to the incompletely monodispersity possibly[210]. Further, TEM image shows that POSS block copolymer homogenously dispersed in epoxy matrix, which is in accordance with SEM results. Clusters of POSS composites are observed with a size of 30-50 nm. The inset of Figure 4.11E clearly performs a core/shell structure with dark POSS domain as core and GMA domain as shell. The similar morphology is also observed for 10G10P, in which the size of core/shell micelles is relatively larger than that of 10G5P (the inset of Figure 4.11F)

4.3.2.2 Thermostability of POSS hybrid composites

There is slightly improvement in thermostability of POSS modified epoxy composites compared with the neat epoxy matrix (Figure 4.12, 4.13). T5 and Tmax of composites perform as that of neat epoxy. However, the degradation takes place processes at a lower speed, confirmed by higher T50 in all composites than that in neat epoxy matrix. Char productivity increases in all composites as the degree of polymerization of POSS. All 10G10P composites get more char than 10G5P composites. Si forms a stable char familiar with ceramics, but the high oxidation temperature decides hardly astonishing improvement of thermodegradation in POSS modified composites. Zhang et al[94] observed the POSS hybrid epoxy and the inert layer formed after thermal treatment. Considering the insulating effect of silicate layer related with the micromorphology, the inert layer became looser and porous at high POSS loading, which explains POSS not always contributed to the thermostabiltiy positively. Except the silicate formation, evaporation or sublimation of POSS takes place[211] in inert atmosphere, especially in the alkyl-substituted POSS which is related with POSS molecular weight[212]. Methyl-POSS was recognized to undergo

almost complete sublimation, while longer chain POSS evaporate above melting temperature.

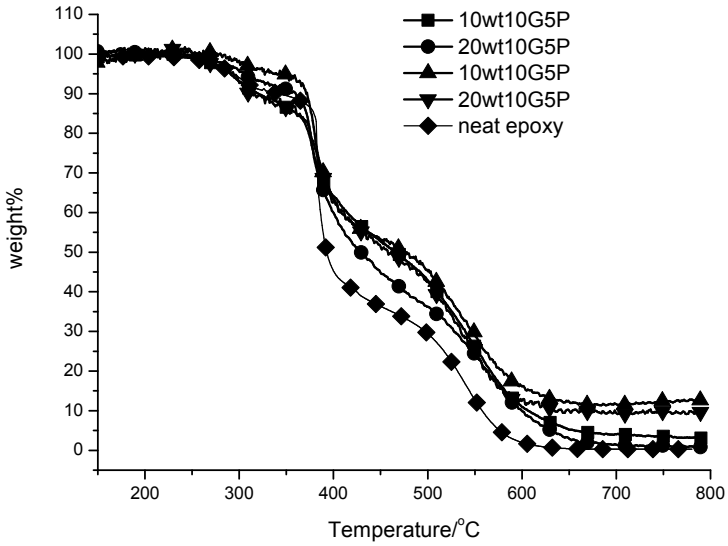

Figure 4.12 TGA curve of POSS composites in the air.

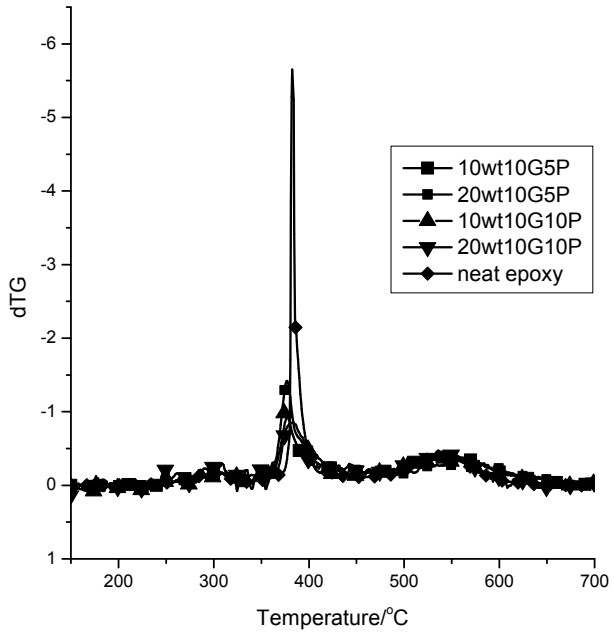

Figure 4.13 Differential TG curve of POSS composites in the air.

In the air, oxygen plays an active role in the degradation process, the competition of evaporation and oxidation decides the inert silicate layer formation. Except the

silicate formation, the carbonaceous residual of POSS composite improves the heat insulation too, resulting in fire retardency[122]. Subchain of POSS after peroxidation forms carbonaceous residual blending with silicate, which blocks the release of oxide products.[213, 214]

From the view of dilute, the reactive POSS copolymer is a reactive dilute. It probably increases the apparent activation energy and the kinetic exponent of thermodegradation[215]. Astonishingly, the char productivity decreases with the amount of addition in the same copolymer. 20 % addition of polymer gets less char than 10% loading sample. One explanation is that the incompletely cured network may wreck thermostability, because the formed micelle makes the reaction of the inner GMA difficult. The boundry of GMA-POSS micelle in matrix reacts with the curing agent amine easily, which modifies the compatibility of copolymer with matrix. In the inner micelle, reactive group is constrained by the boundary and the diffusion of a relative large MDEA, so it has a low reactive ability. The conversion of reactive group in micelle could relatively high, but complete reaction is difficult to reach even reacted with a small molecular [216]. In the matrix, excessive MDEA, even though a small amount is enough to break the stoichiometric of amine and epoxy. The unreacted ends of chain brought much free volume and decrease the curing density of network, leading to poor thermostablity. The functional-end micelle improves the miscibility of GMA block with the epoxy components in the curing process.

4.3.2.3 Thermodynamic performance of POSS hybrid epoxy.

Thermodynamic performance is interesting in the POSS hybrid epoxy composites. Compared with the neat epoxy, moduli and Tg are improved at small loading (10%) of POSS copolymers (Figure 4.14, 4.15). However, at high loading(20%), composites show weaker thermodynamic performance(Table 4.3). At the same copolymer loading, moduli *E'* and *Tg* are better in the high POSS percent copolymer (10G10P). Zheng etal[35] compared with the PCL and PCL-POSS copolymer nanostructured epoxy, Tg reduction is compressed. It is ascribed to that less PCL plasticizes epoxy network because of the constraint of PCL nanostructure formed. Zeng etal [135] obtains a decreased Tg with the increasing of POSS-PCL copolymer loading too. In those case, POSS copolymer influence matrix by second bonding effect such as van der waals force. From the view of toughening agent, the

above epoxy modified non-reactive POSS copolymer is analogues to epoxy modified via rubber[217], to enhance the toughness rather utilization temperature.

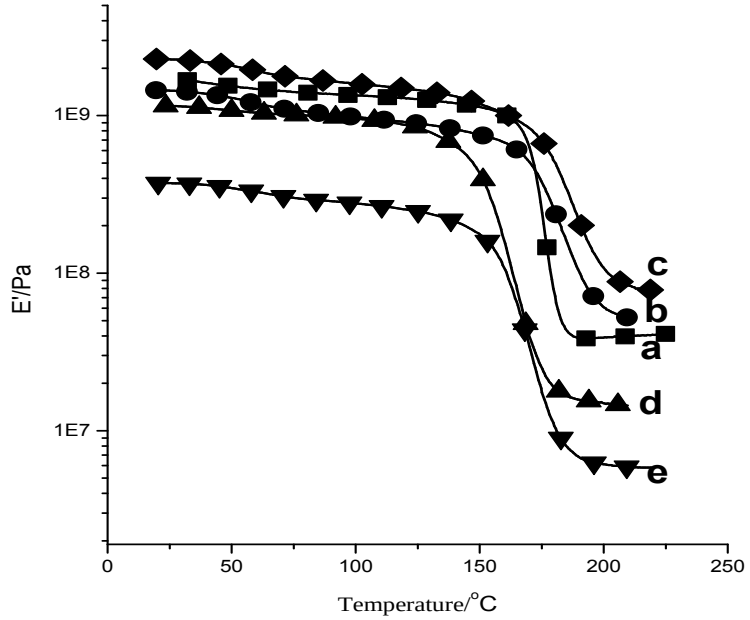

Figure 4.14 Storage moduli of composites, a. neat epoxy, b. 10wt10G5P, c. 10wt10G10P, d. 20wt10G10P, e.20wt10G5P

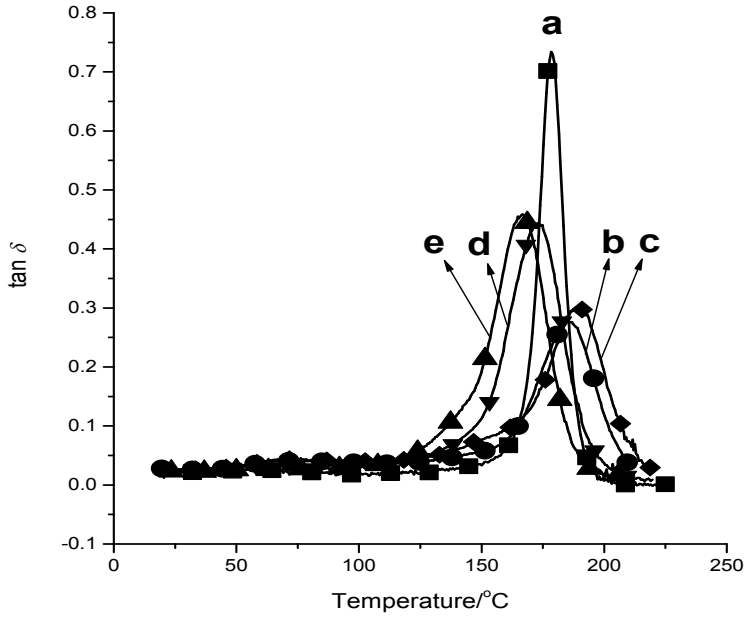

Figure 4.15 *tan δ* of composites, a. neat epoxy, b. 10wt10G5P, c. 10wt10G10P, d. 20wt10G10P, e.20wt10G5P

Table 4.3 the thermomechanical properties of composites are measured via DMTA, *Tg* is the temperature of main transition in *tan δ*.

sample	*Tg*	*E'r*(MPa)
DM	178	41
10wt10G5P	186	53
20wt10G5P	165	5
10wt10G10P	190	82
20wt10G10P	172	14

In this article, covalent bonding between POSS modifier and epoxy network, it is positive to the cohesive energy density compared with nonbonding POSS copolymer in Chapter 5. The higher is cohesive energy density, the higher is the moduli of composites [218, 219]. Moreover, covalent bonding of copolymer hinders the motion of segements in molecular scale. The crosslinking nanophase, with inert POSS core and reactive GMA shell, strengthens curing density compared with nonbonding modifier, which leads a higher Tg at small loading. It is known that moduli and glass transition temperature of epoxy/amine network are significantly affected by the variations of epoxy and curing agent stoichiometry[220]. In most cases reasonable predictions of Tg can be made using an empirical equation reported by L. E. Nielsen[221] together with the experimental Tg value of the stoichiometric network and statistical calculations of the concentration of elastic chains. It is stated that in these rigid networks the concentration of elastic chains is the main structural factor associated to the variations of Tg with stoichiometry[222] [223]. The steric barrier of GMA shell incompletely reacted would make curing agent excess. It is a probable explanation for lower Tg in 20% copolymer samples, in accordance with the TGA discussion. By the way, isobutyl side group is flexible, which increases the motion of main chains and decreases the energy barriers, namely "internal plasticization" of the flexible side group[132]. Whereas, Tg of 10G10P higher that of 10G5P at the same loading, meaning no obvious internal plasticization. One explanation is that the vertex group is embedded inside of micelle and constrained by the GMA shell, almost no plasticization of vertex group.

4.3.2.3 Crystalization of POSS compolymer hybrid epoxy.

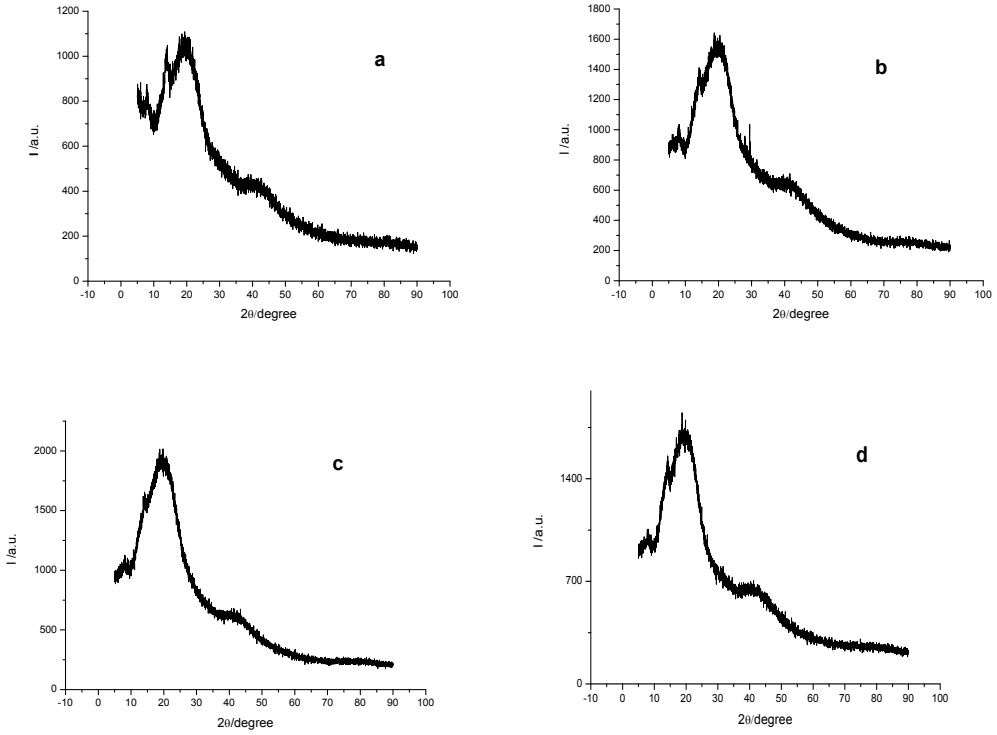

Figure 4.16 XRD spectra of 10wt10G5P(a), 20wt10G5P(b), 10wt10G10P(c), 20wt10G10P(d)

In the GMA-POSS modified epoxy composites, there is an additional shoulder peak center at 14.1 ° (Figure 4.16). That corresponds to 0.62 nm, which compares with polyacrylate amorphous peak from the early publishment[224]. It is different with the pure GMA chain. A small shoulder peak center at 7.8° reflects with crystallization of POSS in composite.

4.4 Conclusion

A reactive functional PGMA macroinitiator and PGMA-POSS copolymers were successfully synthesized via RAFT polymerization tuned by CDB. Molar masses were obtained as predicted, and the molar mass distributions were monomodal and acceptably narrow. The self-assembly of PGMA-POSS block copolymer indicated that the copolymer undergoes micelle in selective solvent. The thermostability of POSS-PGMA copolymers were improved than that of PGMA homopolymer. Introduced into epoxy precursor, homodispersed nano domaine of POSS copolymer successfully built in matrix and these preceramic POSS dots improved thermostability

of composites. Via the GMA block prereacted with one of monomer, hybrid composites could be constructed in step-growth polymerized matrix, which is possible to build POSS nanodomaine from this bottom-up method.

.

Chapter 5 Topology Influence of POSS-MMA Copolymers in Epoxy Network

5.1 Berief introduction of partial compatiable POSS copolymer modified epoxy

In general, introducing POSS into a polymer material follows two protocols, either "copolymerization" with organic monomers or "physical mixing" route. Whereas "physical mixing" is easy to carry on, the POSS cages remain generally undispersed and tend to agglomerate[225-227]. It is observed that, in most the cases, such POSS-based materials have very poor physical properties and often show a gradient composition over film thickness, as the surface is enriched with POSS cages compared to the bulk of the material [69, 70]. This behavior is associated with the poor compatibility of POSS with most of the polymers due to the nature of the organic ligands[75](isobutyl or cyclohexyl) or with the tendency to self-association in the case of strongly interactive ligands such as phenyl rings[103]. Although the invariant polarity of POSS monomer, POSS is copolymerized, then different comonomer tunes its compatibility with DGEBA network. For instance, the compatibility of block copolymer depends on the curing agent and epoxy precursors, PMMA is heterogeneous with DGEBA/4,4'-diaminodiphenyl sulfone (DDS) or 4,4'-methylene dianiline (MDA), however homogenous with DGEBA 4,4'-methylenebis(3-chloro2,6-diethylaniline) [134]. There are a few POSS copolymers were synthesized and obtain a nanostructure in epoxy network. Zheng et al[35] synthesized a POSS-capped PCL via ring-opening polymerization of ε-caprolactone with 3-hydroxypropylheptaphenyl POSS as the initiator, which was incorporated into epoxy resin to obtain hybrid thermosets. Zeng et al [135] synthesized hepta(3,3,3-trifluoropropyl) polyhedral oligomeric silsesquioxane (POSS)-capped poly(epsilon-caprolactone) (POSS-capped PCL) was synthesized via the ring-opening reaction of F-caprolactone, which was initiated by 3-hydroxypropylhepta(3,3,3-trifluoropropyl) POSS with stannous (II) octanoate [Sn(Oct)2] as the catalyst. Then the epoxy is cured in present of POSS copolymer via selfassembling in network.

In this part, partial compatible POSS copolymers, such as poly methacrylate isobutyl/cyclohexyl POSS-co-methyl methacrylate random, diblock and triple-block

copolymers, were characterized and modified into epoxy to obtain nanostructure, based on different topologies of POSS copolymer. To compare the vertex group, POSS with the isobutyl and cyclohexyl vertex group were nanobuilt in final morphology. Tg of epoxy at different conversion, was characterized and simulated with Couchman equation. In the composites, Tg was fitted with Gordon-Taylor equation and Kwei equation, which reflected with the interaction between modifier and DGEBA/MEDA/ epoxy/amine oligomers.

5.2 The same molar mass POSS-MMA copolymers with different topologies

5.2.1 POSS-MMA copolymers utilized.

5.2.1.1 Materials

3 sorts of isotuyl-POSS-MMA random copolymers (from Aldrich) containing 15%, 25%, 45 % *wt* POSS-monomer were chosen respectively. Furthermore 4 kinds of block copolymers (supported by Coll. D.Bertin-Uni Marseille) were utilized.

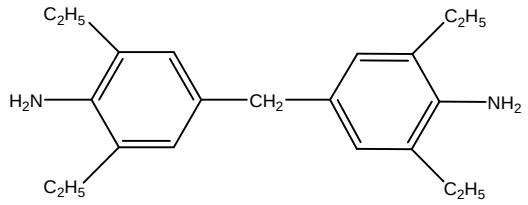

MDEA

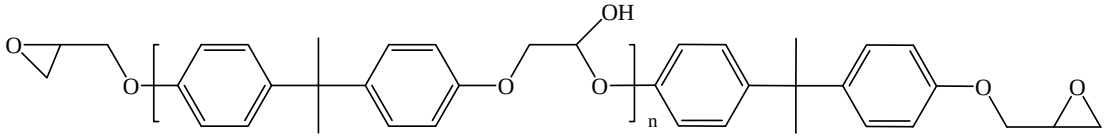

DGEBA 330,n=0.08, FW=180

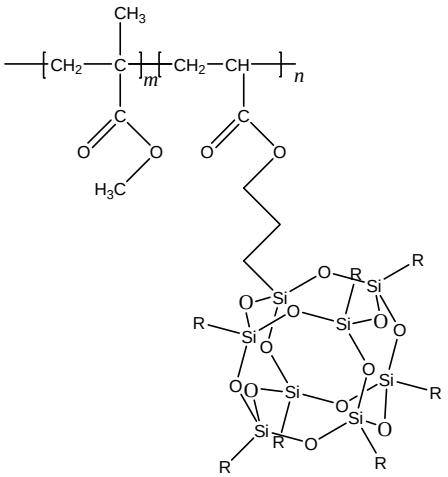

R=isobutyl, POSS-MMA copolymer (from Aldrich)

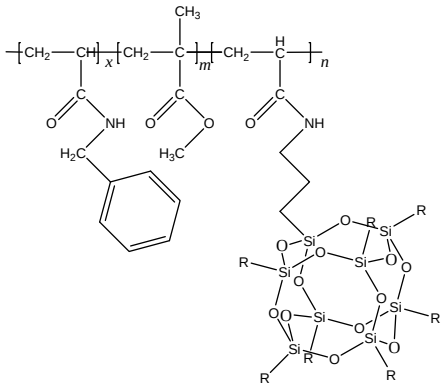

P(MMA-b-AM-b- isobutyl POSS) and P(MMA-b-AM-b- cyclohexyl POSS)

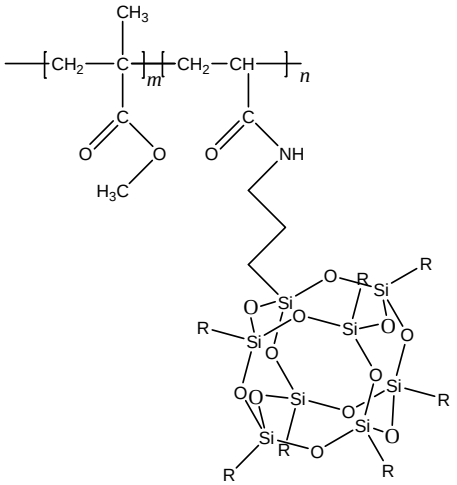

P(MMA-b- isobutyl POSS) and P(MMA-b- cyclohexyl POSS)

Scheme 5.1 Raw materials in this part.

5.2.1.2 Measurements:

a.Fourier Transform Infrared Spectroscopy (FTIR).

The FTIR measurements were performed on a Fourier transform spectrometer at room temperature (25 °C). Measurements were recorded at a resolution of 2 cm^{-1}, 64 scans on a KBr pellet.

b. Size Exclusion Chromatography (SEC)

Size Exclusion Chromatography (SEC) was performed using a Waters 510 device equipped with UV and refractive index detectors, 1 mL/min THF.Three Millipore microStyragel HR1, HR2, and HR3 columns were used. Number and weight average molar mass were calculated using calibration from polystyrene standards.

c. Thermal Gravimetric Analysis (TGA).

A TA Q10 Thermal Gravimetric Analyzer (TGA) was used to investigate the thermal stability of hybrid composites. The samples (about 10 mg) were heated from ambient temperature to 800 °C in the air and nitrogen atmospheres respectively, heating rate=10°C/min.

d. Differential Scanning Calorimeter (DSC)

A differential scanning calorimeter (DSC) (TA Q1000, TA Instruments) was employed to get Tg of POSS polymers.

e. X-Ray Diffraction(XRD)

The crystalline data were carried out in Bruker D8, 5-20°, Cu *Ka*=1.54Å, scanning rate 1°/min.

5.2.2 Characterization of the POSS-MMA copolymers

5.2.2.1 Molar of POSS copolymers.

Molar mass of epoxy modifiers (Figure 5.1) in this part are about 20k Dalton. In the series of random copolymers, molecular weights decrease with the percent of POSS cage(from 39.6k in P (MMA-15isobutylPOSS) to 2.39k Dalton in P (MMA-15isobutylPOSS)), arising from the steric hindrance. The decrease of polymer degree took place in the polymerization of MA cyclohexyl POSS [214] too. The large volume of POSS cage, compared with MMA monomer, confines the probability of chain-propagation. It is the reason why in free radical polymerization small molecular weight is obtained with increasing the POSS cage percent. Previous reports as far as we seen present difficulty of getting high molecular weight POSS copolymer.

Table 5.3 Molecular weight of polymer utilized, given *Mn* is afforded by the supplier.

	Mn	Given *Mn*	*Mw*	*d*	POSS%	MMA%
P (MMA-15isobutylPOSS)	39646		101198	2.553	15	85
PMMA-25isobutylPOSS)	17475		57850	3.310	25	75
P (MMA-45isobutylPOSS)	23904		53995	2.259	45	55
PMMA	24735		58733	1.842		
P(MMA-b-AM-b-isobutylPOSS	11406	20440	35131	3.080	35.2	52.3
P(MMA-b-AM-b-cyclohexyl POSS)	19211	25180	45231	2.354	46.4	42.5
P(MMA-b-isobutyl POSS)	14407	20950	23329	1.619	26	74
P(MMA-b-cyclohexyl POSS)	9495	30750	20796	2.90	46.9	53.1

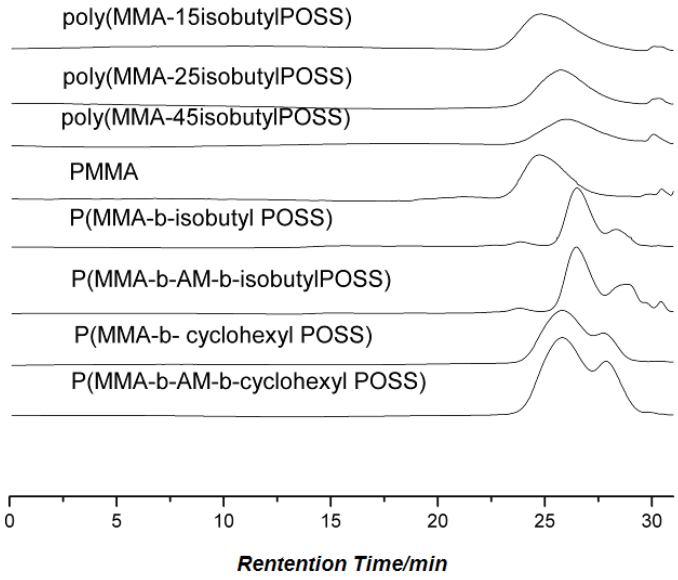

Figure 5.1 GPC retention volume of polymer utilized

It is interesting that the molar mass bimodal distributes in block copolymer from GPC, which may be caused by the coalescence of block copolymer in the composites. Another statement is that the *Br*- end macroinitiator reactivates more quickly than small halogen atom end macroinitiator (the value of the ATRP equilibrium constant for alkyl *Br*-type is of 1-2 orders of magnitude higher than the alkyl Chloride type with the same structure), because of the lower electronegativity (Figure 5.2). The *C–Br* bonds formed upon deactivation of the growing chain are reactivated faster, leading to a part of active center polymerizing at higher speed. It is why the halogen

exchange reaction effectively compress the polydispersity of *Br*-end macroinitiator via changing a low-atom-number halogen[228].

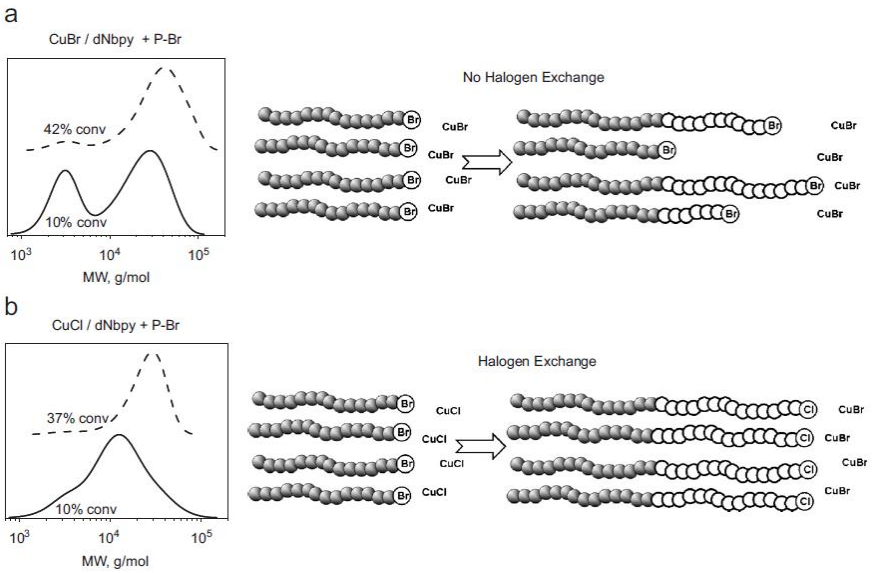

Figure 5.2 The above illustrations and GPC traces show chain extension of a polySty-Br macroinitiator with MMA using: (a) CuBr/dNbpy, and (b) CuCl/dNbpy as the catalyst. [MMA]:[polySt-Br]:[CuX]:[dNbpy] = 500:1:1:2; 75 °C[228]

5.2.2.2 Thermostability of POSS copolymers.

In the random copolymers, in P(MMA-15isobutylPOSS) and P(MMA-25isobutylPOSS), although the fraction of POSS cage increases, the degradation temperature decreases, probably caused by the defect of chains[229, 230]. Zhang etal[54] reported that in the POSS-co-polystyrenes, the onset thermal degradation temperature increases with the decease of the POSS content similarly. Moreover, higher molar mass is obtained at low POSS loading. For PMMA, there are 4 steps of weight loss[229]: 1) by the scission of head-to-head linkages at 170-180°C. The impurities and oligomers are able to generate free radicals to degrade the PMMA[230] 2 and 3) the scission at unsaturated ends results from the termination by disproportionation at 270-300°C: 4) random scissions of the polymer chains at higher than 370°C. The existence of POSS doesn't alternate the thermodegradation mechanism of PMMA in Figure 5.3. However, in triblock copolymers, the benzyl acylamide probably forms nitrile[231, 232] when elevating temperature, which is a radical trapper[233]. It assists the triblock copolymers to transform more carbonide layer (Figure 5.4, Table 5.3) and improves the thermostability.

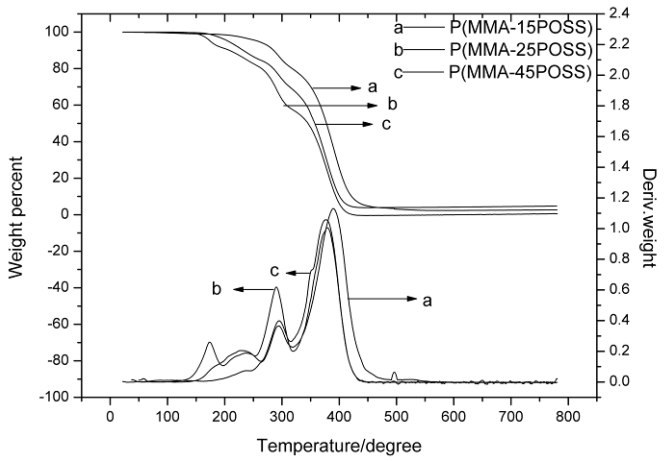

Figure 5.3 Random copolymer TGA in N_2, heating rate 10°C.

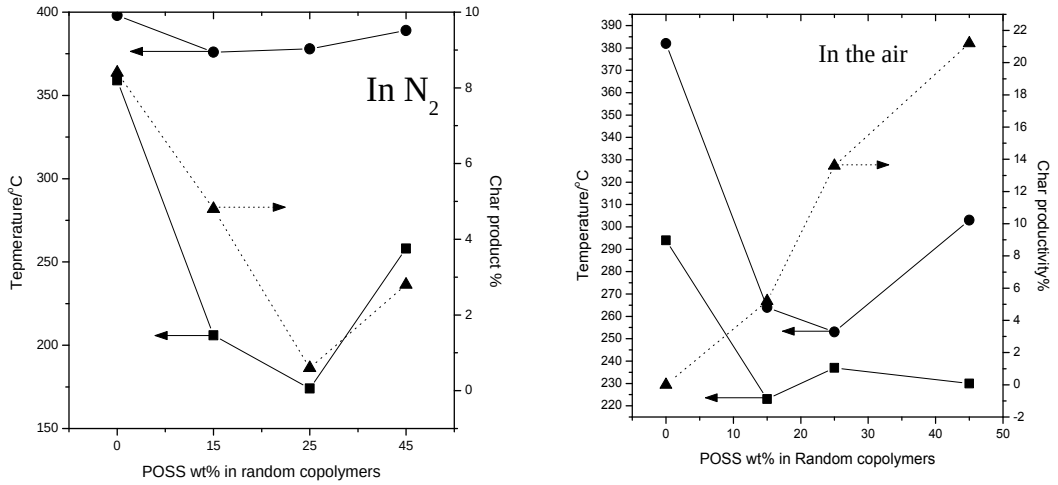

Figure 5.4 Plots of Random copolymer TGA data in N_2, heating rate 10°C. ●-*Tmax*, ▲-char productivity, ■-*T5*

Ferriola etal[229] concluded the degradation of PMMA chain to the chain defects, such as the head-head couple and disproportion reaction. Here, the copolymers of MMA-POSS obtain molar mass at a high POSS content, leading to more macromolecular tail. It means more defects in polymer chains, compresses the thermal stability. The samples prepared via radical controllable polymerization, has more regular structure. It can be apprehended easily why the block copolymers have better thermo stability. P(MMA-b-AM-b-cyclohexyl POSS), P(MMA-b-cyclohexyl POSS) degrades at 530 °C in the DTG curves. [234] There are two competitions in the thermodegradation of POSS/polymer: First is the release of POSS cage, which takes place at high temperature via sublimation or evaporation, before the fully oxidation. The release of POSS makes the formation of defect protective layer. It is the reason

why in some cases POSS doesn't have a positive effect on thermostability, due to POSS evaporation upon heating[212]. When POSS were polymerized into a macromolecule, its evaporation would be constrained because of the a convalent bonding[214]. POSS ceramisation is another important effect, which certainly improves the thermostability. POSS cage as a preceramic[3] precusor finally forms silica layer after fully oxidation. After the emission of organic group in POSS cage, silica layer seals the polymer, retards the oxidation of bulk polymer. On the other hand, POSS is a surface active moiety, tending to transport to the surface. As the term of "self healing"[235] described, it can be strengthen by energy or heating. The decomposited product acts as a protective barrier, limites the polymer volatilisation rate, obtains a high char productivity.

Table 5.2 Block copolymer TGA in the air.

Sample name	*T5* (°C)	*Tmax* (°C)	Char (%)	POSS (*wt*%)	MMA (*wt*%)
P(MMA-b-isobutylPOSS)	227	303	0.7%	26	74
P(MMA-b-cyclohexylPOSS)	255	409	3.8%	46.9	53.1
P(MMA-b-AM-b-isobutylPOSS)	258	409	3.0%	35.2	52.3
P(MMA-b-AM-b-cyclohexylPOSS)	249	413	7.8%	46.4	42.5
DM	359	398	8.4%	0	0

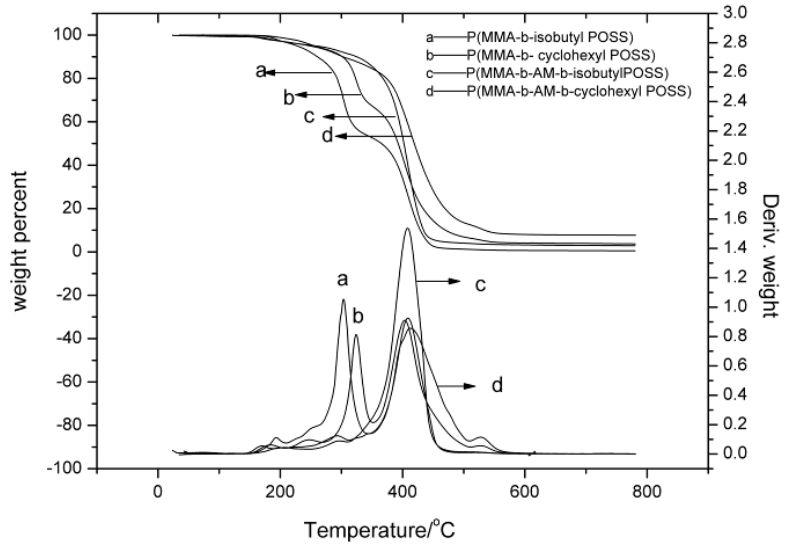

Figure 5.5 copolymer TGA in N2, heating rate 10°C.

Table 5.3 Block copolymer TGA in N_2

sample	*T5* (°C)	*Tmax* (°C)	char (%)
P(MMA-b-AM-b-isobutylPOSS)	225	382	16.9
P(MMA-b-AM-b-cyclohexylPOSS)	273	348	11.4
P(MMA-b-isobutylPOSS)	250	298	8.6
P(MMA-b-cyclohexylPOSS)	298	323	9.8
DM	294	382	0

5.2.2.3 The crystallization of POSS copolymers.

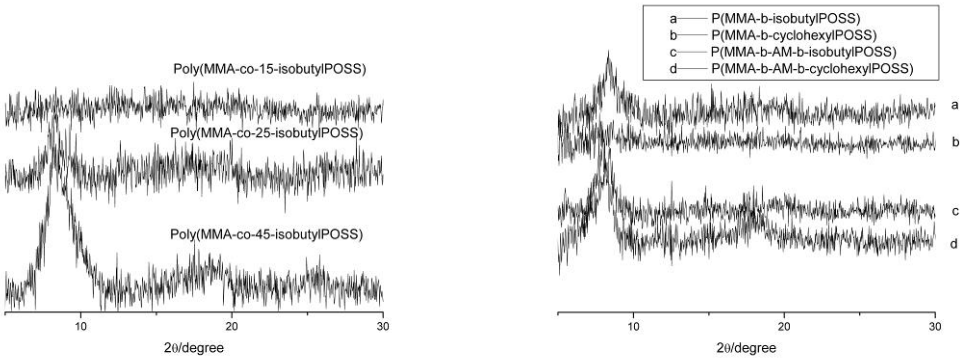

Figure 5.6 XRD for random and block copolymers.

In the copolymer, WAXS spectra show a diffractive peak at 2θ=8.2° in the isobutyl POSS and 2θ=7.8° in the cyclohexyl POSS polymer respectively (Figure 5.6). From the Brag law $n\lambda = 2d\sin\theta$, it indicates that the bigger *d* in the crystalline pattern resulted from the size of the cyclohexyl group. This diffractive peak corresponds to the strongest reflection of crystalline MA-POSS (101 hkl reflection associated to a characteristic distance of 1.12 nm)[196]. In the random copolymers, the degree of crystalline increases with POSS percent. XRD diffractive peak is observed hardly in P(MMA-b-AM-cyclohexyl POSS), but obviously in the its composites.

5.2.2.4 Tg of POSS copolymers.

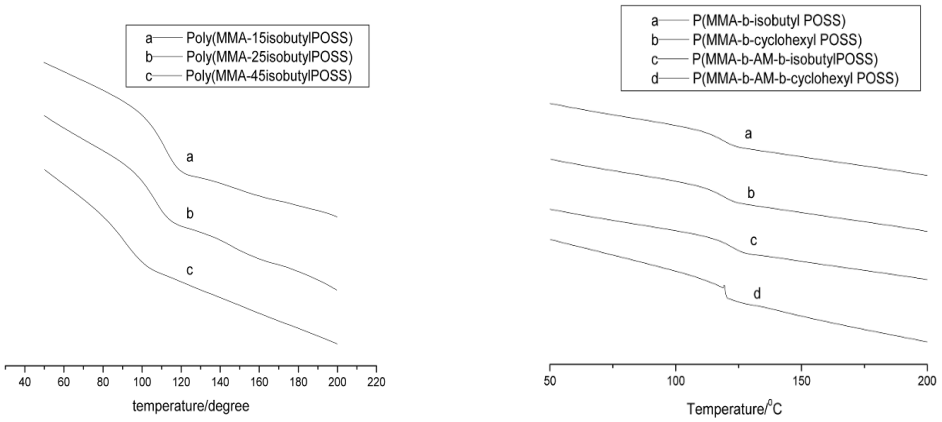

Figure 5.7 DSC second scaning of random and block copolymers**.**

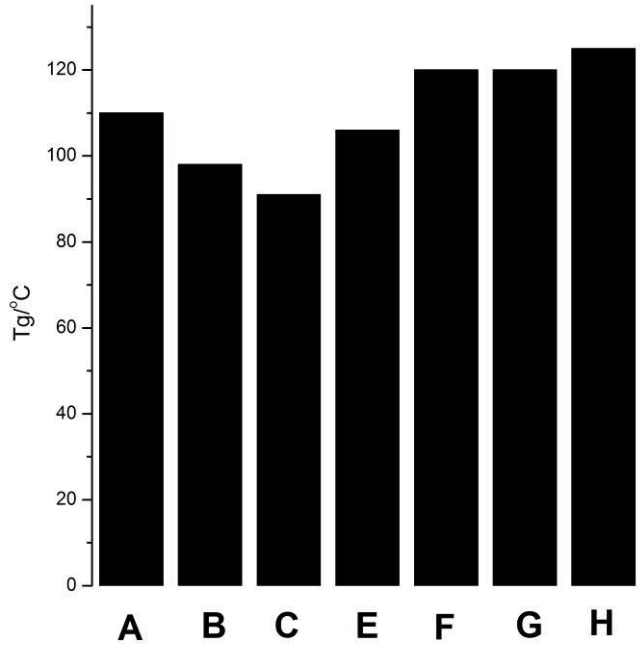

Figure 5.8 Plots of *Tg*.

- *A.P (MMA-15sobutylPOSS), B.P (MMA-25sobutylPOSS), C.P (MMA-45POSS), D.P(MMA-b-isobutylPOSS), E.P(MMA-b-cyclohexylPOSS), F.P(MMA-b-AM-b-isobutylPOSS) , G..P(MMA-b-AM-b-cyclohexylPOSS)*

From the second temperature ramping circle of DSC diagram, *Tg* of the random copolymers from Aldrich decrease with the POSS percentage, ascribing to free volume augment of POSS cage[11] (Figure 5.7, 5.8). The other factor can be

attributed to the molecular weight decrease with the POSS cage percent. It is considered that the molecular weight is an important factor to the vitrification.

According to Fox-Flory equation: $Tg=Tg_{\infty}-kM^{-1}$, molecular weight has inverse ratio with *Tg*, which is caused by the end of molecular chain as a source of free volume. The higher is free volumn, the easier is relaxation for macromolecular chain segaments. There is quite a large volumn in POSS cage (Φ=1.5-3nm) [2], larger than ordinary side group, leading to decreased *Tg*.

On the other hand, interaction between POSS-POSS cages and POSS-matrix are influenced by the vertex group of POSS cage. Namely, the shell structure properties decide the role of POSS as a plasticizer or an antiplasticizer. In a recent report[129], because of the weak interaction with each other in isobutyl POSS/St copolymer, isobutyl POSS plays a plasticizer-like role, contrary to cyclopentyl, cyclohextyl POSS. In the other two POSSs, stronger interaction leads to their outstanding rigidity. The rigid vertex group prevents molecule motion easily, resulting in *Tg* increase.

From the table of *Tg*, the samples containing cyclohexyl have higher Tg comparing with the ones containing isobutyl in the same series from Marseilles, which is similar with Bizet reported in MA-POSS copolymers resulting from stronger interaction of cyclohexyl group.[191]

Interaction between POSS cage and matrix molecules contributes to the final matrix thermo mechanical properties too. Unlike strong specific intermolecular interactions (also called supplementary valences, such as hydrogen bonding, ion-ion interactions, acid-base interactions), POSS-matrix interaction is relatively weak based on Van der Waales force in general. In cases, the most frequent interaction is hydrogen bonding which strengthen the interaction. Lee etal[236] introduced POSS into matrix containing amino group, and compared the hydrogen bonding via FTIR. It was found that the peak of relative absorption expending on weak hydrogen bonding. Hydrogen bonding broaden the utilization of composite, for instance a material will obtain higher moduli,when a higher cohesive energy density was produced by hydrogen bonding[237].

5.3 POSS nanostructurates in epoxy network.

5.3.1Materials and Measurement

Epoxy precursors loading desired amount of POSS copolymer were prepared at 135 °C with vigous mechanical stirring until homogenous. Afterward, curing agent, stoichiometric MDEA was poured into epoxy and mixed at 90 °C for 10 min. To obtain a fully network, this mixture was cured at 135°C 4h and 190°C 4h. The POSS modified epoxy samples were characterized by FTIR, DSC, TGA, SEM and TEM. All POSS modified epoxy samples were denoted as DM-m*wt*P(N).(m, weight percent of matrix ;N, POSS copolymers)

a.Fourier Transform Infrared Spectroscopy (FTIR).

FTIR measurements were performed on a Fourier transform spectrometer at room temperature (25 °C). Measurements were recorded at a resolution of 2 cm^{-1}, 64 scans on a KBr pellet.

b. Thermal Gravimetric Analysis (TGA).

A TA Q10 Thermal Gravimetric Analyzer (TGA) was used to investigate the thermal stability of hybrid composites. The samples (about 10 mg) were heated from ambient temperature to 800 °C in the air and nitrogen atmospheres respectively. The heating rate was 10°C/min.

c. Differential Scanning Calorimeter (DSC)

A differential scanning calorimeter (DSC) (TA Q1000, TA Instruments) was employed to get Tg of POSS composites. To monitor the conversion of epoxy, samples were heated in a glass tube. After a desired time, the samples were taken from the tube and put into an Al pan, which were heated in a nitrogen atmosphere afterward.

To calculate the activation energy, blend of epoxy/MDEA/POSS copolymer was heated in an aluminum pan at different rates: 5, 10, 15, 20 °C/min from -40 °C to 250 °C.

d. **Dynamic Mechanical Thermal Analysis (DMTA).**

DMTA was carried out on cured blends with a Rheometrics solid analyzer (RSA II) to obtain tensile dynamic mechanical spectra (storage modulus E', loss modulus E", and loss factor tan δ) between 25 and 220°C at a frequency of 1Hz in the linear viscoelastic domain.

e. Cloud point experiment

Samples in a small test tube were heated in a procedures controlling oven, then its transmittion was collected by a sensor and laser lamp.

f. Scanning Electron Microscope (SEM) and Transmission electron microscopy (TEM)

The morphology of POSS- containing epoxy hybrids was observed with a Philips XL 30 Scanning Electron Microscope (SEM). The samples were immersed in liquid nitrogen and then fractured. After that, a gold coating was sprayed on the fracture surface, (activation voltage=20 kV). Transmission electron microscopy (TEM) was performed on a Philips CM120 TEM at an acceleration voltage of 80 kV. Ultra-thin sections (ca. 70 nm in thickness) were cut using an ultramicrotome machine, and were placed on a 200 mesh copper grids for observation.

g. In Situ Rheological Measurements

The curing behavior of copolymer/epoxy systems was analyzed using a Rheometrics rheometer equipped with parallel plates of 50 diameters. Dynamic oscillatory shear measurements were performed at 135 °C as a function of curing time at frequency of 1, 3.16, 10, 31.6, 100 Hz. The gap between the plates was about 1 mm and the applied strain was changed during the experiment to ensure a linear viscoelastic response.

5.3.2 Interaction between POSS copolymers and epoxy

The interactions between modifier and matrix relates with the final morphology and performance of composite. POSS copolymers with Si-O-Si vertex group and carbonyl group possibly interact with epoxy matrix (hydroxyl group) by hydrogen bond. It is well known that the hydrogen bond can influence the wave number of C=O band, in which the occupied orbital of the donor overlaps with the vacant orbital of the acceptor and electron rearranges from the donor to the acceptor [238]. In random copolymers and their composites (Figure 5.9), no evident movements of carbonyl vibration in epoxy composite are observed, which is described to the aggregation morphology of POSS. In the composites of diblock copolymers, the peaks in FTIR switch to lower wave number which means the existence of hydrogen bond interactivity between C＝O and carboxyl group. It was reasonable attributing to the topology of macromolecular chain; the distinct distribution of MMA facilitates the formation of hydrogen bond.

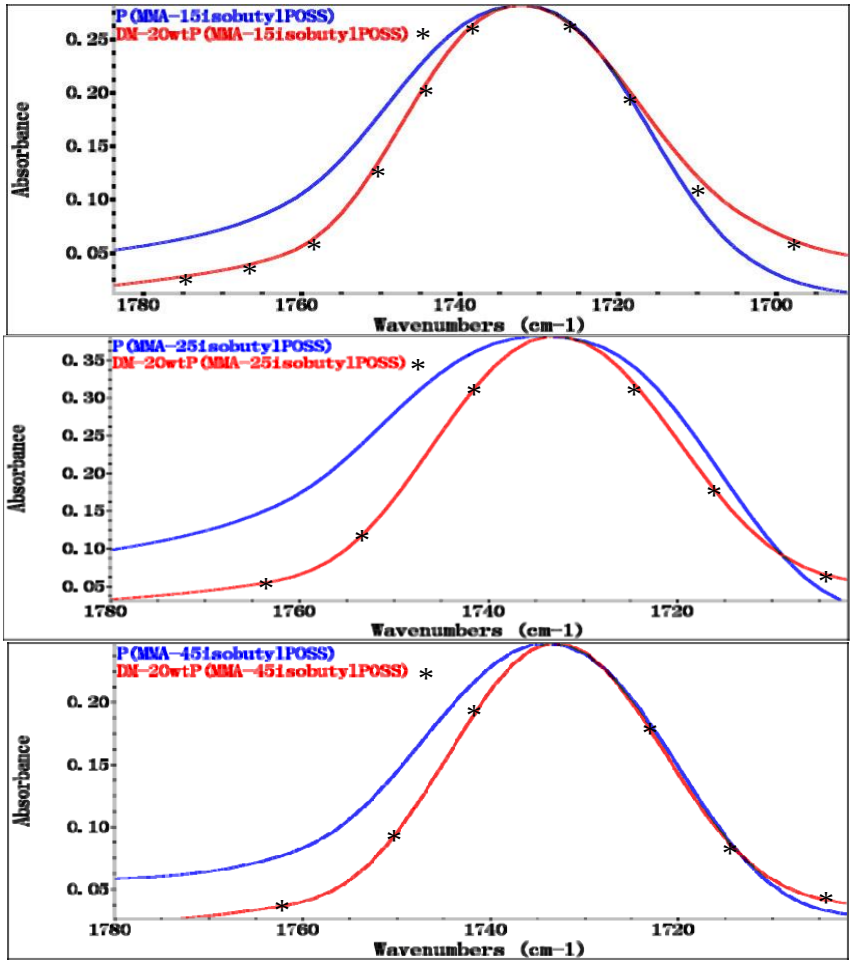

Figure 5.9 the vibration of C=O in POSS random copolymer and in epoxy composites

To check the interaction between amino MDEA and POSS, we characterized the light transparency of POSS polymer/epoxy blend before/after MDEA added. Figure 5.10 shows transparency of different mixtures with the temperature increasing. Pure DER 330 has the highest transparency, stronger than that of DER 330+MDEA. Introduction of isobutyl POSS–MMA copolymer into DER330 decreases the strength of transparency. Transparency descends with the increase of the POSS percent in the copolymer, indeed opaque in 45%POSS sample. It is interesting that the addition of MDEA makes the mixture containing POSS copolymer clearer. In fact, the signal differency of 25%POSS copolymer with/without MDEA is more obvious than that of 15%POSS copolymer. Because MDEA has a couple of amino, at the same time modifier containing oxygen from –COO- in MMA and and Si-O in POSS cage. It trends to form hydrogen bond before curing,[239, 240] that release the POSS self assembly. At high POSS content, POSS cages concentrate together, agglomerate decreasing the transparency. Hydrogen bond between MDEA and POSS cage decentralizes the concentrated domain.

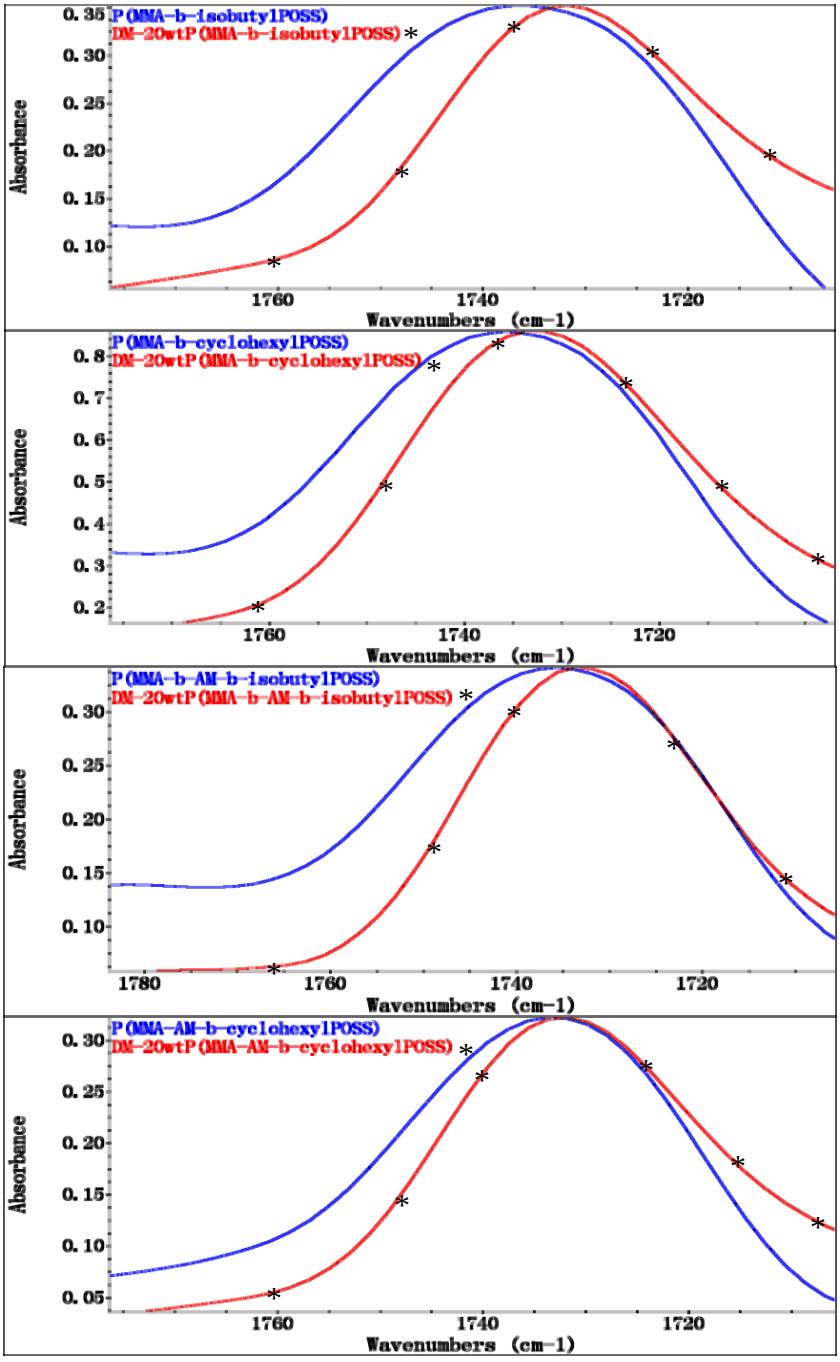

Figure 5.9 the vibration of C=O in POSS copolymer and in epoxy composites.

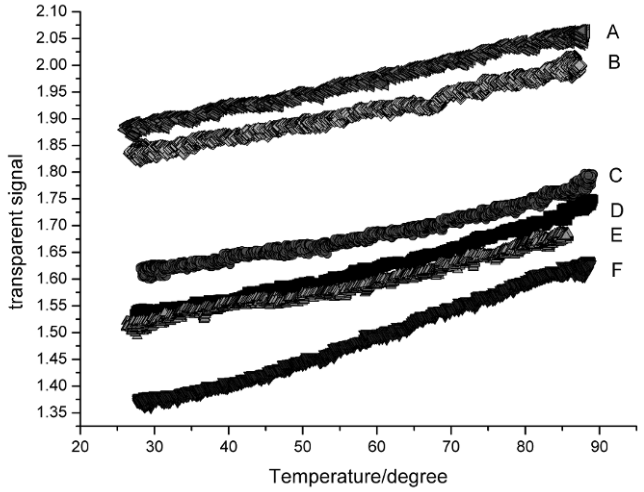

Figure 5.10 Transparency of different mixture.

** A.DER 330, B.DER 330+MDEA, C.DER 330+MDEA+15%isobutylPOSS-MMA (wt=5%), D. DER 330 +15%isobutylPOSS-MMA(wt=5%), E. DER 330+MDEA+ 25%isobutylPOSS-MMA(wt=5%), F. DER 330+15%isobutylPOSS-MMA(wt=5%)*

5.3.3 The relationship between morphology and performance.

5.3.3.1 Thermo mechanical behavior of composites

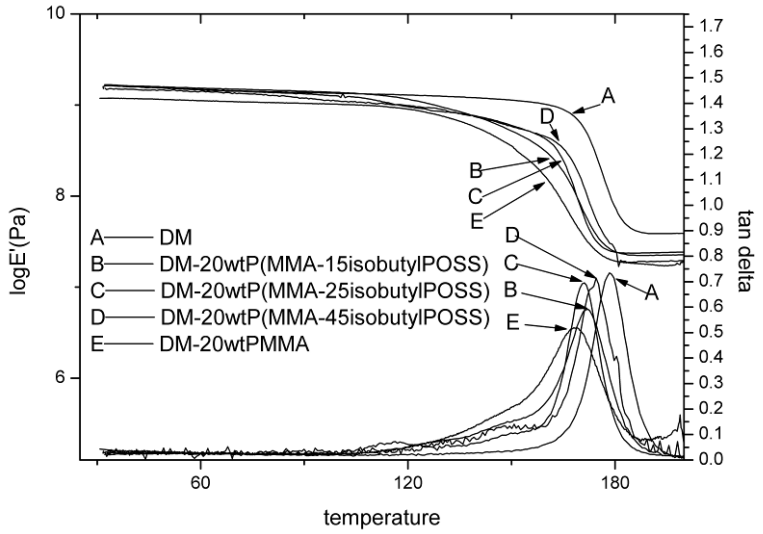

Figure 5.11 DMTA performances of random POSS modified composites.

In the rheology research, the storage modulus *E'* reflecting a certain degree of elasticity of the system, which is proportional to the energy storage in a cycle deformation. The loss modulus *E''* reflects a certain degree of viscosity of the system, which is proportional to the dissipation or loss energy. In the dynamic mechanic analysis diagram (Figure 5.11), the entire additive compresses the *Tg* than matrix epoxy/amine, because of the decrease of cross linking density. In other words, the introduction of thermoplastic macromolecules increases the free volume of the network matrix, which facilitates the motion of chain segments and decreases the glass state of composite. Relative free volume of composite can be regarded as:

$F_{vr}=w_1F_{vr1}+w_2F_{vr2}$

w_1,w_2 represent the weight fraction and F_{vr1}, F_{vr2} is the relative free volume of the component 1,2. In this case, the relative free volume was determined by the modifier because the same weight percentage of epoxy. Young's modulus of elasticity can be predicted from cohesive energy density[218, 219]. The main factor affecting Young's modulus is the cohesive energy density (*CED*) of the polymer network. Bizet reported cohesive energy density decrease as POSS was copolymerized with MMA, but in the same order of magnitude whatever the organic ligand nature is. POSS has lower cohesive energy with the matrix chains compared to that between the chain[241]

However, Williams etal[242]characterize the mechanical property in epoxy networks modified by POSS containing amine group, and found POSS modification was an increase in both the glassy and rubbery modulus explained, respectively, by the increase in cohesive energy and crosslink densities because of covalent bonding.

DM-20*wt*P(MMA-15isobutylPOSS) and DM-20wtP(MMA-25isobutylPOSS) have close storage module less than that of the matrix, and then DM-20wtP(MMA-45isobutylPOSS) and DM-20*wt*PMMA digressively. The module of glass state, DM-20wtP(MMA-15isobutylPOSS) is higher than DM matrix may be caused by the "nano-reinforcement" [243]of the POSS cage, which acts as a molecular scale reinforcement to the matrix[244]. The cocontinous phase separation was considered as a kind of state of high modules, [245, 246] which is the reason why DM-20*wt*P(MMA-25isobutylPOSS) has high modules compare with DM-20*wt*P(MMA-45isobutylPOSS). In DM-20*wt*P(MMA-45isobutylPOSS), there is a infect interface. In the particle phase separation, from the TEM and SEM photos, POSS cage enrichs on the interface of the particle, and forms a weak interface. From the FTIR, no evident hydrogen bonding exists in the random POSS copolymer and epoxy matrix, namely

low cohesive energy density between the compact matrix segment and POSS copolymer. It is reasonable to get lower moduli from DMTA characterization.

The rubber state E', were decrease in the order of DM, DM-20*wt*P(MMA-25isobutylPOSS), DM-20*wt*P(MMA-15isobutylPOSS), DM-20*wt*P(MMA-45isobutylPOSS), DM-20PMMA in order. It is interesting that Tg decreases with the increase of POSS percentage from DM-20*wt*P(MMA-15isobutylPOSS) to DM-20*wt*P(MMA-25isobutylPOSS), all lower than DM-20PMMA. The sample, DM-20*wt*P(MMA-25isobutylPOSS) has a closest vitrification temperature to DM matrix. In DM-20wtP(MMA-15isobutylPOSS) and DM-20*wt*P(MMA-25isobutylPOSS), the decrease of Tg can be regarded as POSS cage improve the free volume more effectively than PMMA chain dose. Isobutyl side group is a flexible group, which increases the motion of main chains and decreases the energy barriers, namely "internal plasticization" of the flexible side group[132]. In DM-20*wt*P(MMA-45isobutylPOSS), Tg is higher than the other POSS copolymers. With a view to the large phase separation from SEM photos, which owes to the low compatible between poly(MMA-45isobutylPOSS) and matrix, too little the residual plastic chains to decrease Tg evidently. On the other hand, from the TEM results, DM-20*wt*P(MMA-45isobutylPOSS) gets a complete phase separation, as all POSS polymer only can be found in the interface of particle phase. It means that the matrix is feckly improved or influence by POSS cage additive.

POSS introduced to the matrix is considered as special silicon which is a reason for decrease the interfacial strength. After phase separation, because the separated phase is soft polymer, it is difficult to play a role as modules hardener. However, the *Tg* of P (MMA-45isobutylPOSS) blend is not exactly the same with *Tg* of neat epoxy matrix and pure P (MMA-45isobutylPOSS), indicating that the two phases are all blends possible. Otherwise, it is resulted from the incompletely formation of network by phase separation. The strong interaction between amine curing agent[247] were afformed from infrared and Cloud point testing before, it makes the preferential immigration of amine into POSS polymer and the imbalance of epoxy/amine. The phenomenon results in the vitrification away from the pure matrix, when the molar ratio of precusors and curing agent fluctuate around the desired one. In addition, the glass transition of the mixtures precured are wider than that for the neat matrix, suggesting incomplete miscibility of these transparent mixtures[248]. For the transparent sample, P(MMA-15isobutylPOSS) blend, utilizing Fox equation, which is

often used to calculate vitrification of blend, caculated value 160 degrees is smaller than the measured one. It can be seen a result from the steric hinderance of POSS polymer.

5.3.3.2 The morphology of nanomodifed epoxy

From SEM (Figure 5.12), almost homogeneous the sample DM-20*wt*P(MMA-15isobutylPOSS) can be found. On the other hand, the full transparence of sample under visible light describes no macro phase separation in macroscale. From TEM, some aggregate particles by about 20-40 nm are observed, which can be seen as the nanostructuration of POSS cage.

From SEM and TEM images, the rough surface can be observed in DM-20*wt*P(MMA-25isobutylPOSS). Furthermore, bicontinuous phase separation, epoxy rich white phase and POSS rich black phase continuous phase, exists in this sample. The rough type fracture in the composites containing P(MMA-25isobutylPOSS) (Figure 5.13) and P(MMA-15isobutylPOSS) is familiar with the epoxy sample enhanced by thermoplastic. It absorbs the fracture energy via the relative large surface produced.

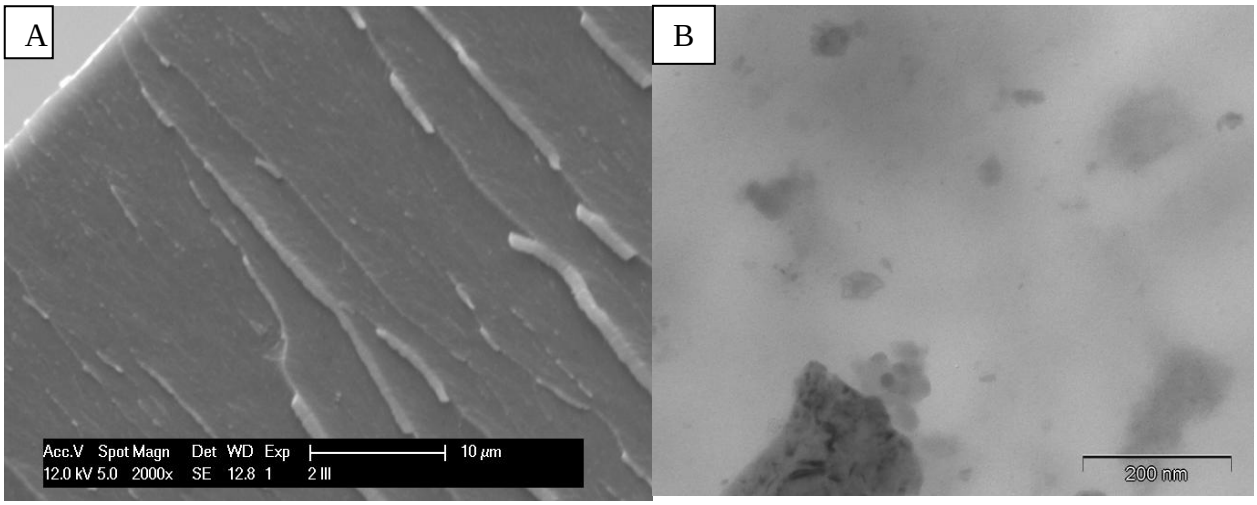

Figure 5.12 The electronic microscope images of DM - 20wtP(MMA-15isobutylPOSS) A.SEM,B.TEM

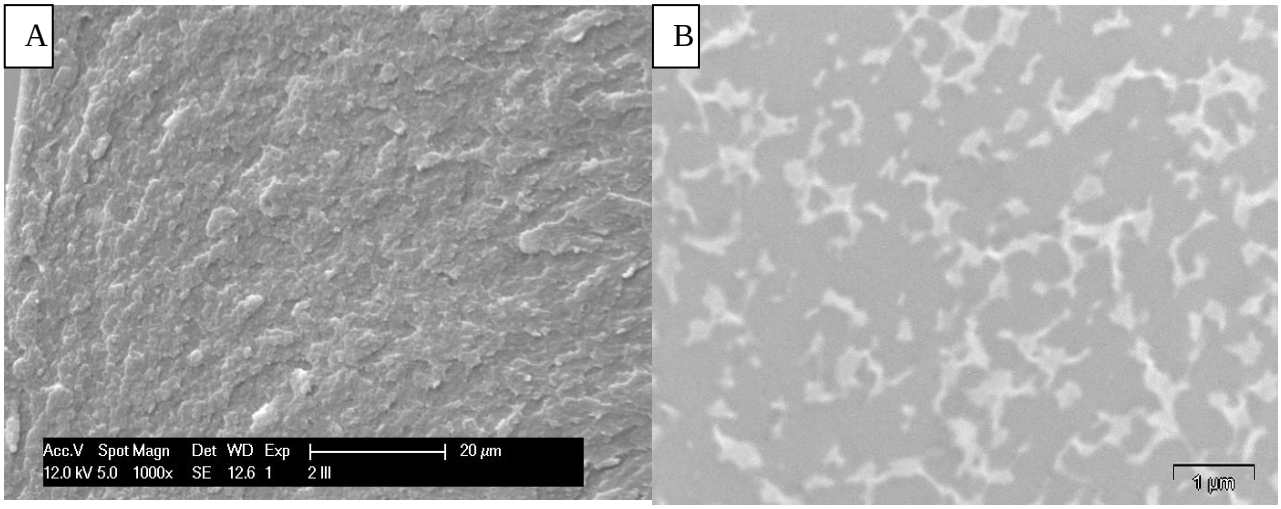

Figure 5.13 The electronic microscope images of DM−20wtP(MMA−25isobutylPOSS) A.SEM,B.TEM

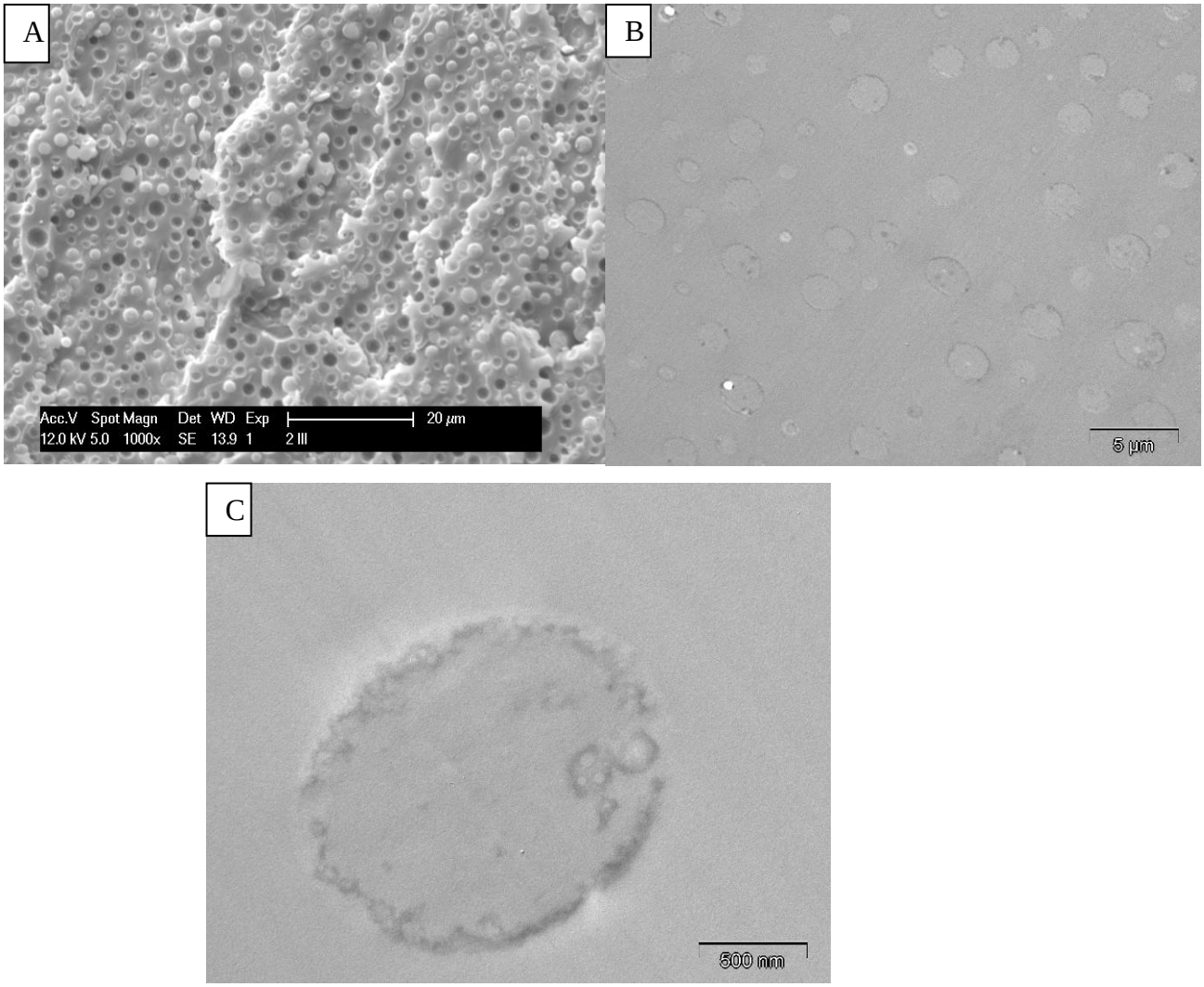

Figure 5.14 The electronic microscope images of DM-20wtP(MMA-45isobutylPOSS) A.SEM, B,C.TEM

The phase separation in DM-20*wt*P(MMA-45isobutylPOSS) takes place completely in macroscale(Figure 5.14). The separated phase is POSS rich, and the continuous phase is epoxy rich, POSS richening near by the interface of separated phase. From the SEM, except for the moved separated particles, there are vain holes, which means the particles weakly interact with matrix and could be removed easily.

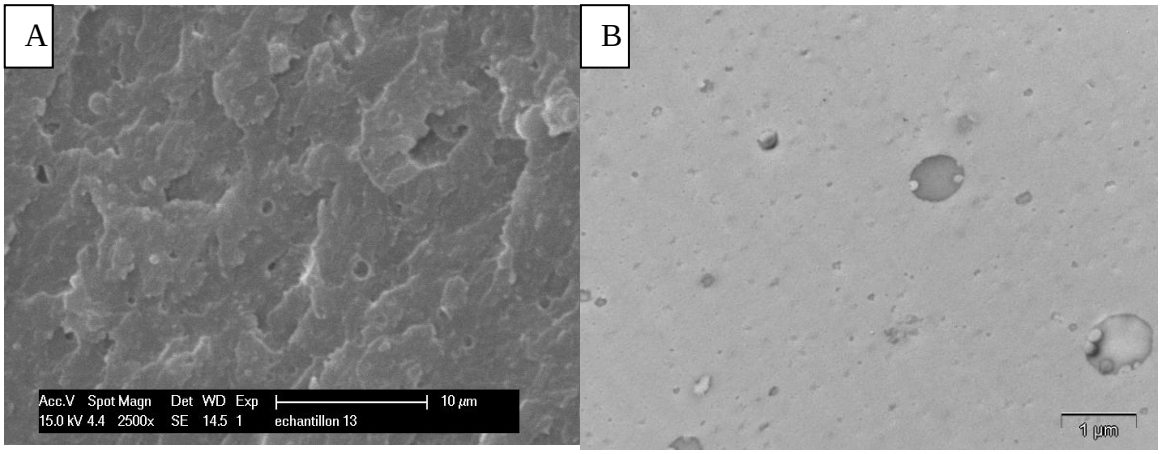

Figure 5.15 The electronic microscope images of DM-20*wt*P(MMA-b-isobutyl POSS),A.SEM, B.TEM

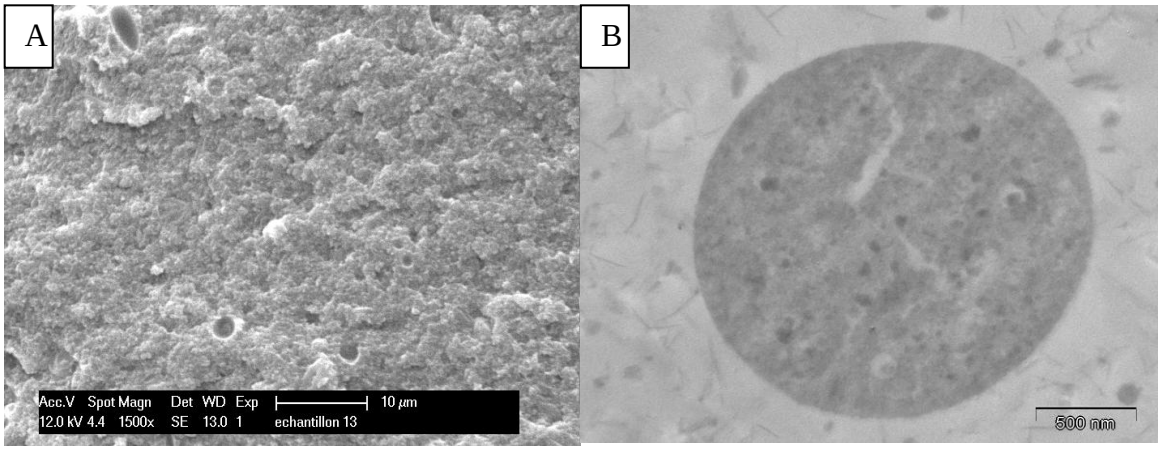

Figure 5.16 The electronic microscope images of DM-20*wt*P(MMA-b-cyclohexyl POSS),A.SEM, B.TEM

Three kinds of different phase separation depend on the interaction of matrix and the POSS copolymer, correlated to the amount of MMA concentration in POSS copolymer. DM-20*wt*P(MMA-15isobutylPOSS) has a tiny phase separation, (a diameter about 100-200nm), because plenteous PMMA segment assists the POSS-rich particle fabricating a PMMA shell. It is compatible with epoxy/amine when the phase separation begins. DM-20*wt*P(MMA-45isobutylPOSS) has a large diameter phase

separation, on account of the insufficient of MMA segment. The interface of the phase separation is weak coalescence, due to MMA chain too short to stable the interface.

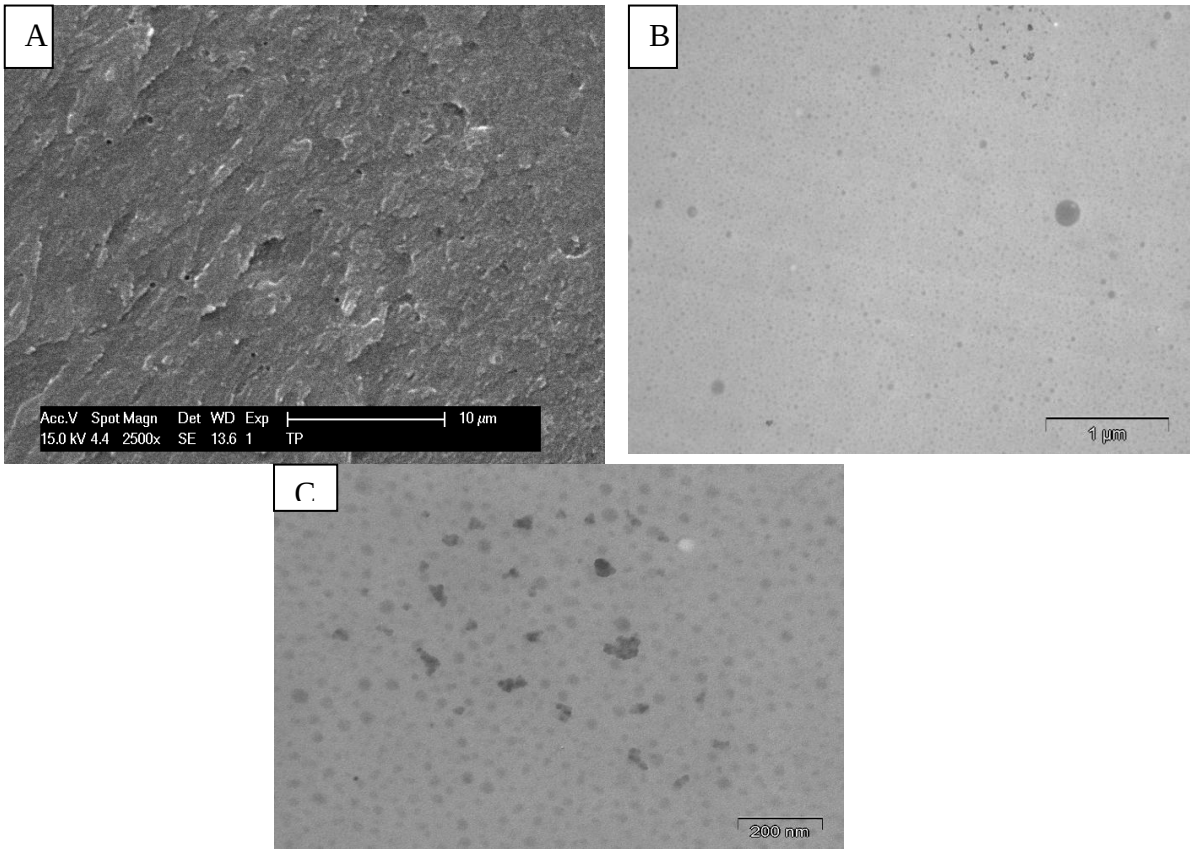

Figure 5.17 The electronic microscope images of DM-20*wt*P(MMA-b-AM-b-isobutyl POSS),A.SEM, B,C.TEM

In isobutyl and cyclohexyl POSS block copolymer modified composites (Figure 5.15, 5.16, 5.17, 5.18), there are bimodal distribution phase separations, diameter of 0.5-1 μm and 20-50 nm partcle at the same time. Because the bulky group capped POSS cage is quit large (1.5nm), calculating from the molecular weight, for instance P(MMA-b-AM-b- isobutyl POSS) has almost 17nm if the POSS cage packs each other together. So it is possible that the small separated phase contain several molecules of POSS polymer only.

In the sample containing cyclohexyl POSS (Figure 5.16, 5.18), whatever triblock or diblock copolymer, the phase separation contain some needle like or foliate like POSS rich phase. It's reasonable to conclude that it maybe derive from POSS, which tends to form raft or lamella structure at a high percentage, because the interaction between POSS-POSS vertex group[249]. It is in accordance with the high crystallization of cyclohexyl POSS polymer in epoxy network, which is stronger than isobutyl POSS on XRD.

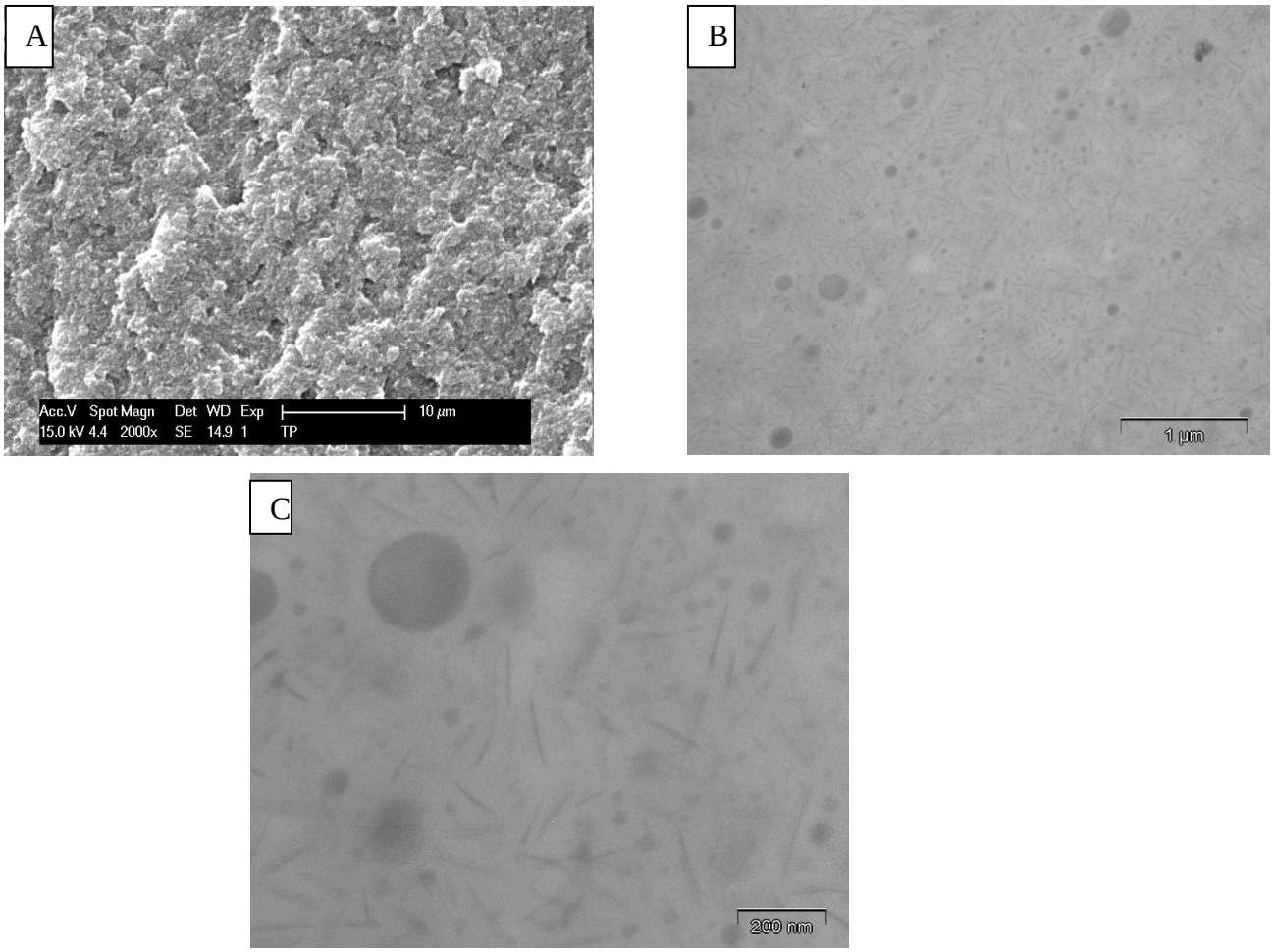

Figure 5.18 The electronic microscope images of DM-20*wt*P(MMA-b-AM-b-cyclohexyl POSS),A.SEM, B,C.TEM

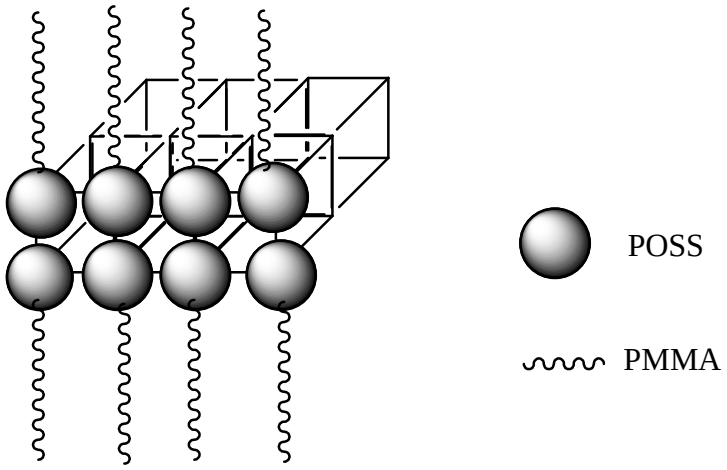

Scheme 5.2 Modal of foliate like POSS crystalline

Cloud point was utilized to monitor the phase separation in epoxy blends. From the original DM and DM-20PMMA curves, no obvious peak can be found (Figure 5.19). However, the transparency decreases obviously at 120 and 210 min for P(MMA-15isobutylPOSS). The first phase separation of DM-20*wt*P(MMA-15isobutylPOSS) was caused by the ripen of POSS macromolecules or the crystalline of POSS, caused by the decrease of "solvement". Then the second step is quit vite, can be caused by the thermodynamic inducing phase separation. The phase separation takes place earlier before gelation in DM-20*wt*P(MMA-25isobutylPOSS). The thermoplastic resin will be excluded to the epoxy/amine phase and enriched in the surface in thermoplastic/thermoset blend[250]. Moreover the process continues to form bicontinous phase seperation.

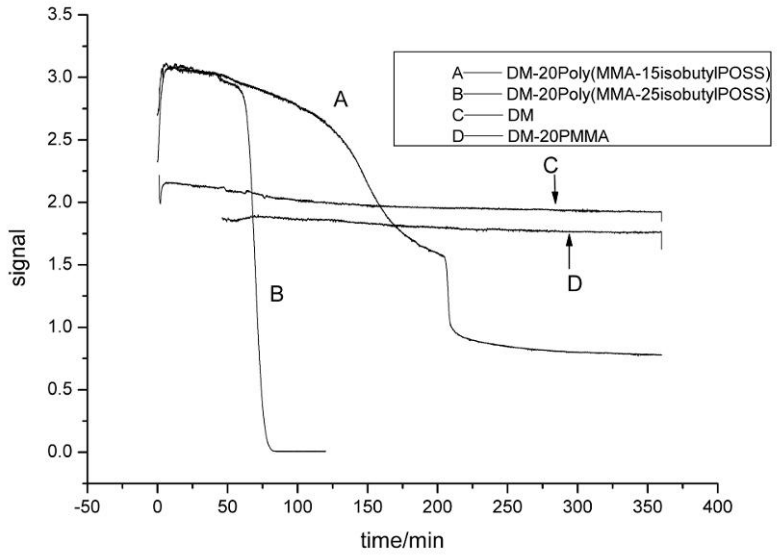

Figure 5.19 Transparency influenced by the polymerization-induced phase separation

In the above block copolymers not only ternary but binary after curing, all the blends of the epoxy precursors and the block copolymers are homogenous and transparent, in which no macroscopic phase separation occurred. But in the matrix of P(MMA-45isobutylPOSS) and P(MMA-25isobutylPOSS), the final product is opal, meaning to macro phase separation. However, the blend of precursors epoxy is opal with the former, whereas it is transparent with the latter before curing. It can be seen that in the mixture of P(MMA-25isobutylPOSS), reaction-induced phase seperature results in the final macro scales phase separation from homogeneous to opal.

Otherwise, P(MMA-45isobutylPOSS) is not compatible with epoxy matrix until the curing temperature 135 degrees. In this article, a series of polymers were utilized which have close molar mass, to eliminate the difference of kinetic parameter of viscosity, rheology, viscoelasticity in resulting from molecular weights as far as possible. The compatibility and phase separation influenced by the kinetic parameters. But it is impossible to get the same kinetic parameters, the different content of POSS which act as a lubricant, definitely more or less change the activity of phase separation. A direct result is to make the mixture viscosity decrease and phase separation more convenient. It is beyond this article, but an imaginable influence to the phase separation.

In general, thermoplastic moiety has a critical volume faction, it is dispersed thermoplastic phase separation before the critical point, otherwise bicontinuous or multilayer thermoplastic phase separation after that[251]. It is still controversial that the phase affects the performance positively or negatively, further, how to affect the performance. For instance, Some groups claim that the improvement of dispersability increases the fracture toughness[252] while others conclude that the morphology with largest microclusters can show the highest toughness [253].

This fact indicates that a secondary phase separation in the already separated domains of thermoplastic took place in a similar way to that reported by Oyanguren et al[254] for PSU modified epoxy mixtures.

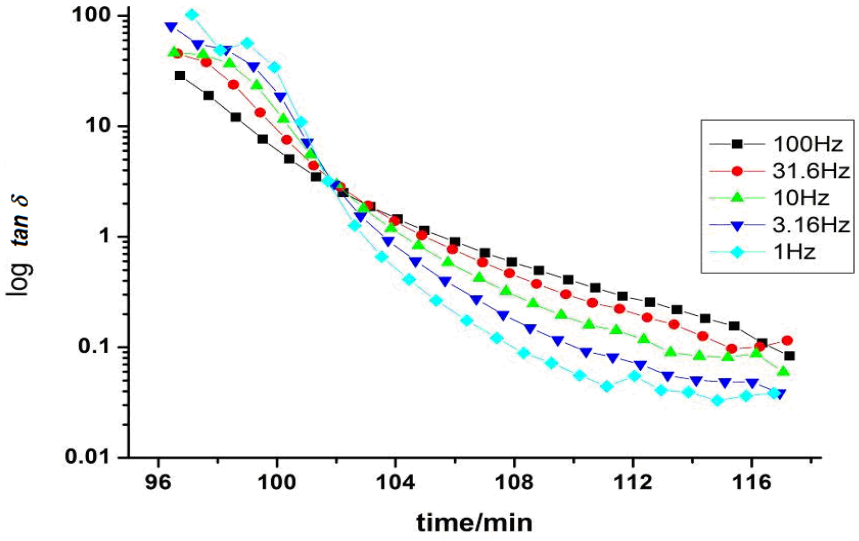

Figure 5.20 gelation time of DM,135 degrees, gel time=6121s

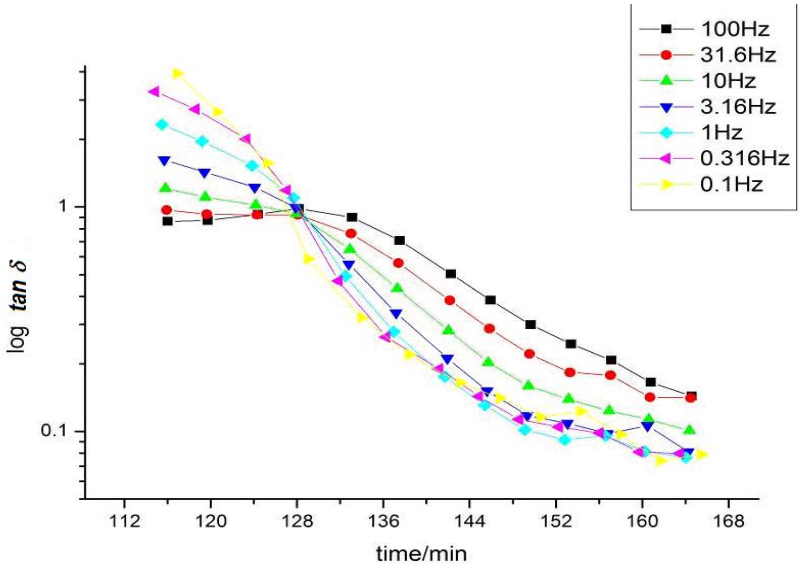

Figure 5.21 gelation time of DM-20wtP(MMA-25isobutylPOSS),135 degrees,gel time=7672s

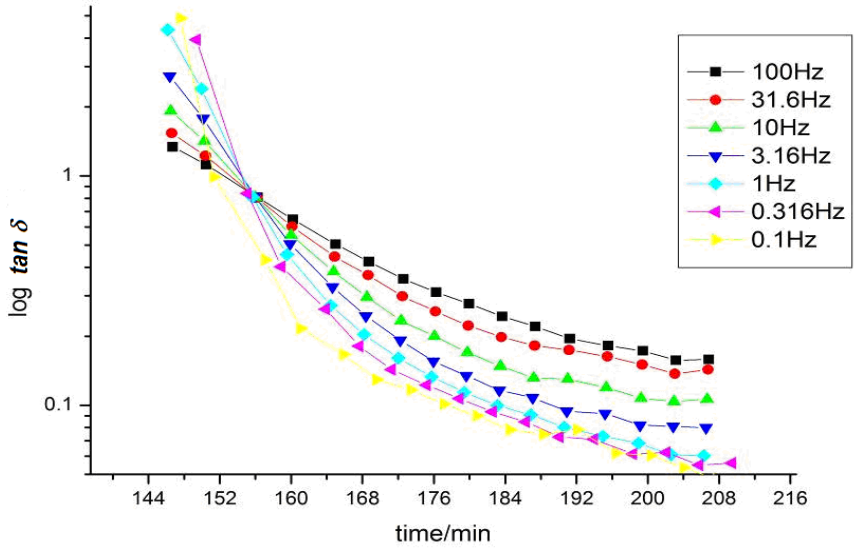

Figure 5.22 gelation time of DM-20wtP(MMA-15isobutylPOSS),135 degrees,gel time=9373s

The presence of thermoplastic or elastomer in the thermoset epoxy blend changes the gelation and virification properties (Figure 5.20, 5.21, 5.22). For instance, the addition of carboxyl-terminated copolymer of butadiene and acrylonitrile liquid rubber (CTBN) resulted in a decrease of both gel and vitrification time[255]. The nanostructure and macrostructure of POSS polymer modified epoxy network, forms a semi interpenetrating network in general. It is difficult to anticipate the gelation of IPN, because of kinetic parameters varied with the component. The fast gelation of

P(MMA-25isobutylPOSS) blend is influenced by the fast phase separation mainly which compresses the dilution effect of thermoplastic(Figure 5.21). POSS lubricating effect leads to a low friction in the composite, POSS separated from the matrix easily. On the other hand the compatible component, short PMMA chain leads to a thermodynamic instability, which is the reason why gelation takes place at a lower epoxy conversion. Moreover, the separated POSS domain connected with the compatible PMMA domains which embed in the matrix, act as a physical crosslinking point may elongate the gelation time.

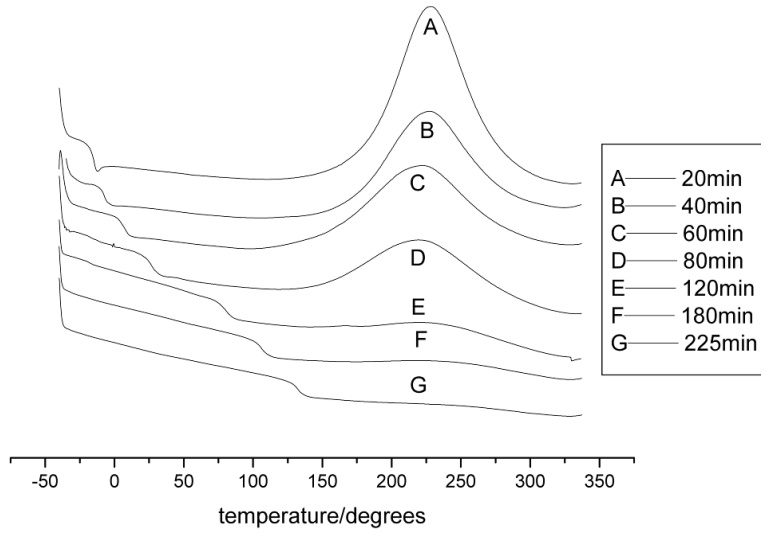

Figure 5.23 DSC of DM after heating at 135, rate=10degrees/min(20,40,60,80,120,189,225min)]

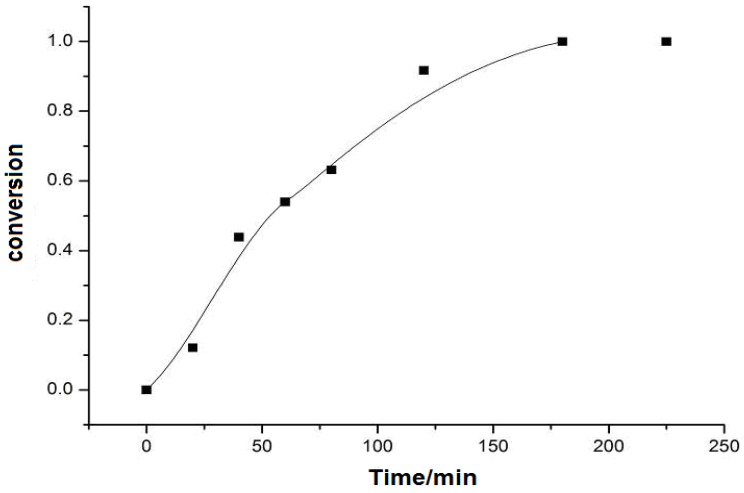

Figure 5.24 Conversion of DM heated at 135 degrees

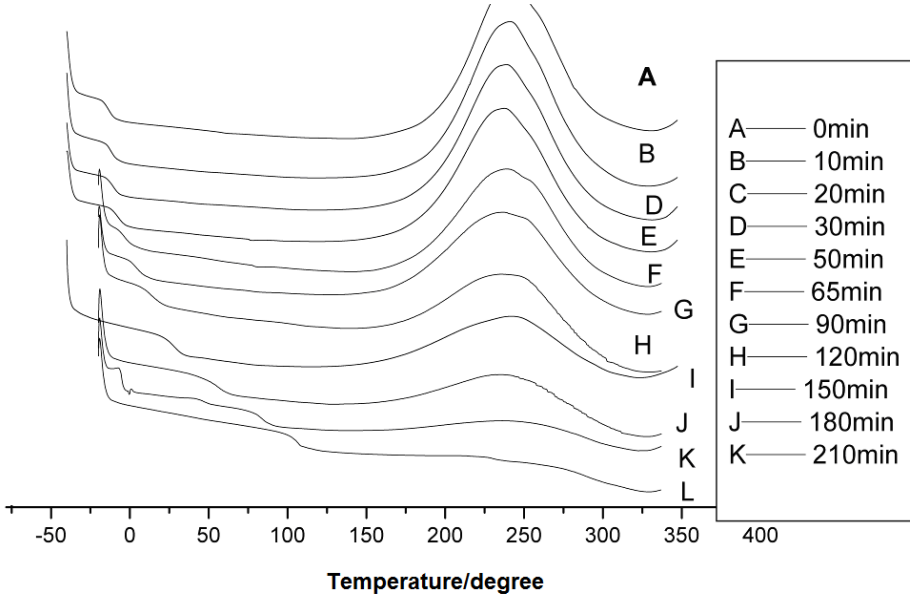

Figure 5.25 *ΔH* of DM-20wtP(MMA-15isobutylPOSS)after heating at 135, rate=10degrees/min

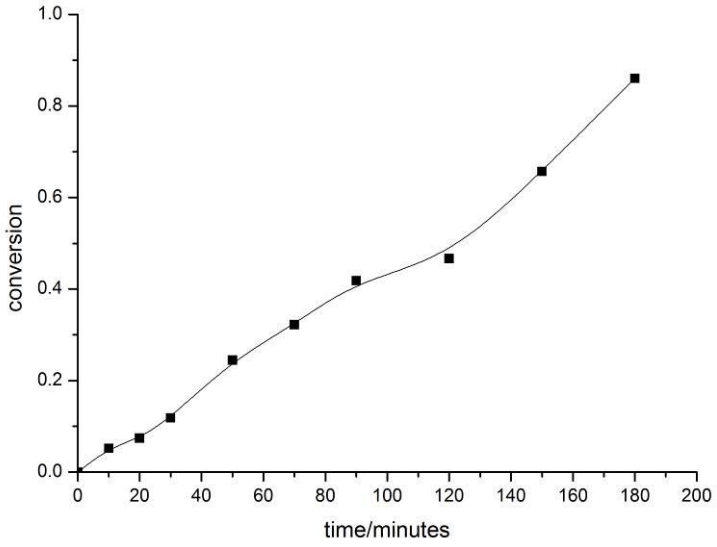

Figure 5.26 Conversion of DM-20wtP(MMA-15isobutylPOSS) heated at 135 degrees

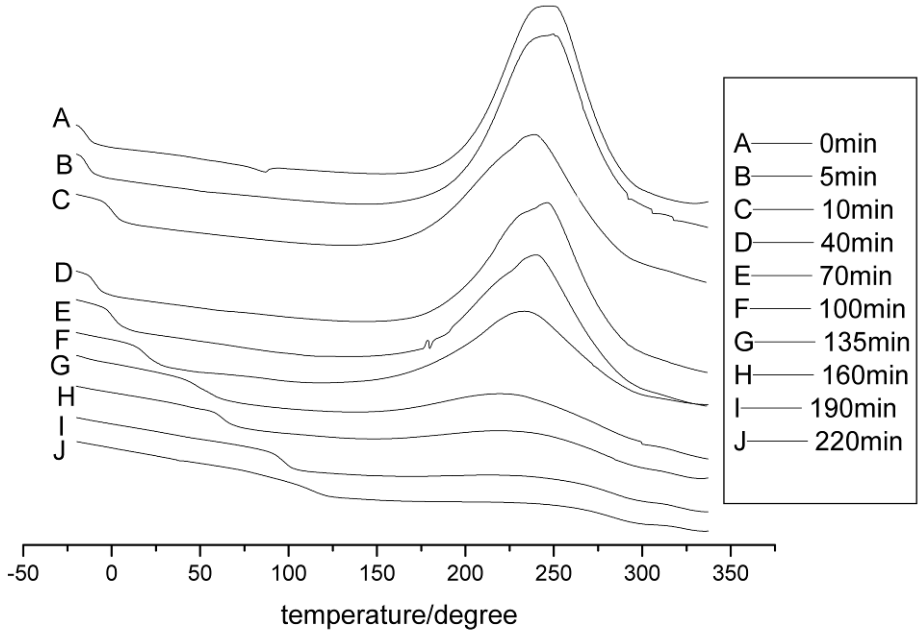

Figure 5.27 *ΔH* of DM-20wtP(MMA-25isobutylPOSS) after heating at 135, rate=10degrees/min

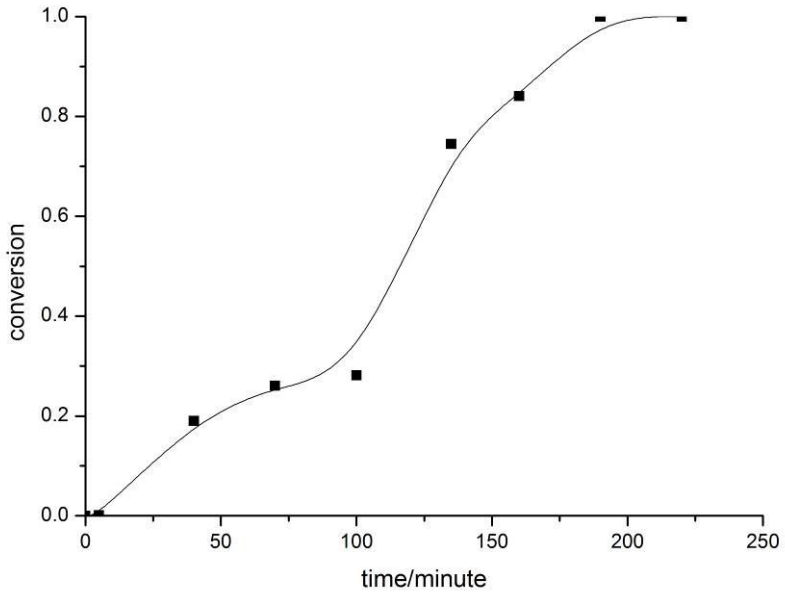

Figure 5.28 Conversion of DM-20*wt*P(MMA-25isobutylPOSS) heated at 135 degrees

Compared with the DGEBA/MDEA blend (Figure 5.23,5.24), the addition of POSS copolymer reduces the reaction rate, due to the dilution effect. In the conversion curve of DM-20wtP(MMA-25isobutylPOSS) (Figure 5.27, 5.28), on the

point of phase separation conversion is increase slowly, which is resulted from the phase separation retarding diffusion of oligomer and monomer of epoxy/amine. After the phase separation completely, the dilution effect of additive depreciates, accelarating the reaction. The conversion of the system was calculated by Conversion=1-$\Delta H/\Delta H_0$. Tg of this systems increasing with the heating time.

The reaction rate of DM-20wtP(MMA-15isobutylPOSS) is slower than the DM-DM-20wtP(MMA-25isobutylPOSS) (Figure 5.25, 5.26). In a word, our POSS copolymer/epoxy blend is a concentrated polymer solution[256, 257]. The entanglement of macromolecules takes place probably which increases the viscosity of blend and enlongates the reaction time[258]. However, phase separation happens in the DM-20wtP(MMA-25isobutylPOSS) blend, disentanglement[259] of POSS polymers compresses the dilution effect.

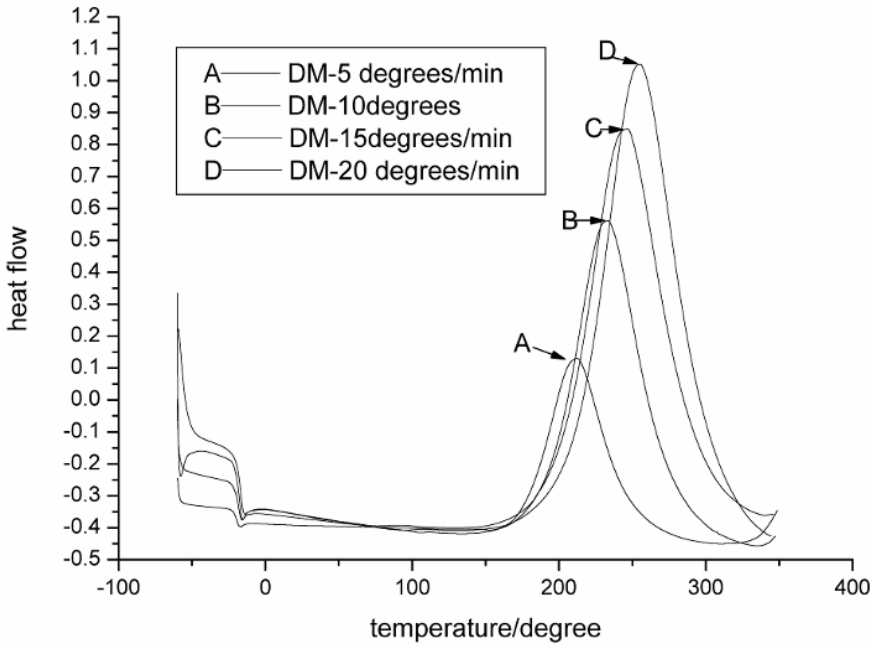

Figure 5.29 DSC at different scanning rate of DM

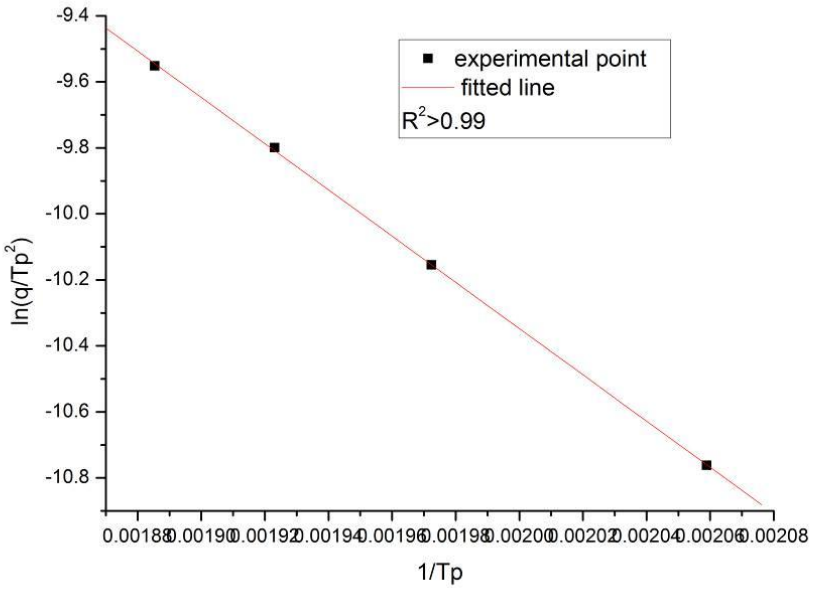

Figure 5.30 Utilizing Kissinger modal to calculate DM activation energy

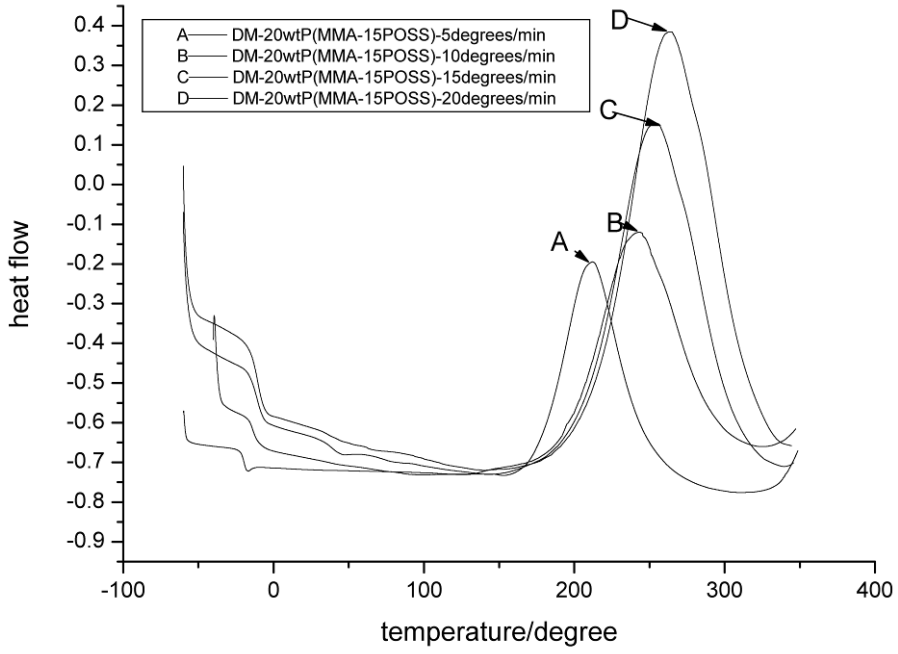

Figure 5.31 DSC at different scanning rate of DM-20wtP(MMA-15isobutylPOSS)

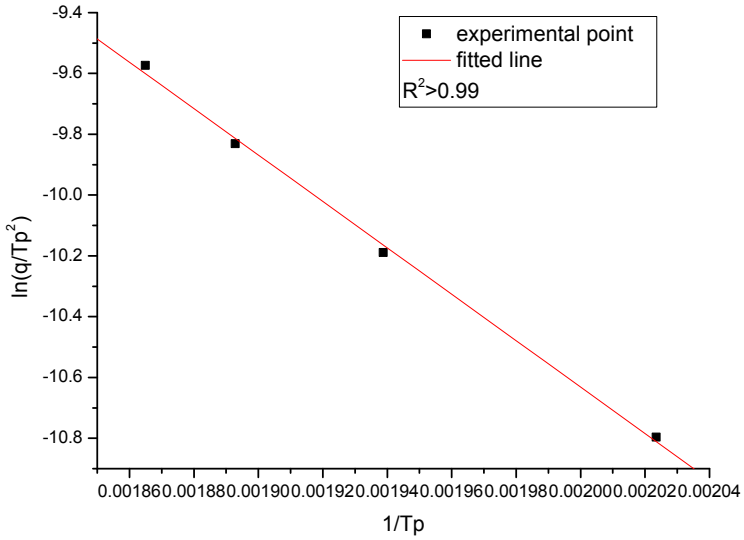

Figure 5.32 Utilizing Kissinger modal to calculate DM-20wtP(MMA-15isobutylPOSS)activation energy

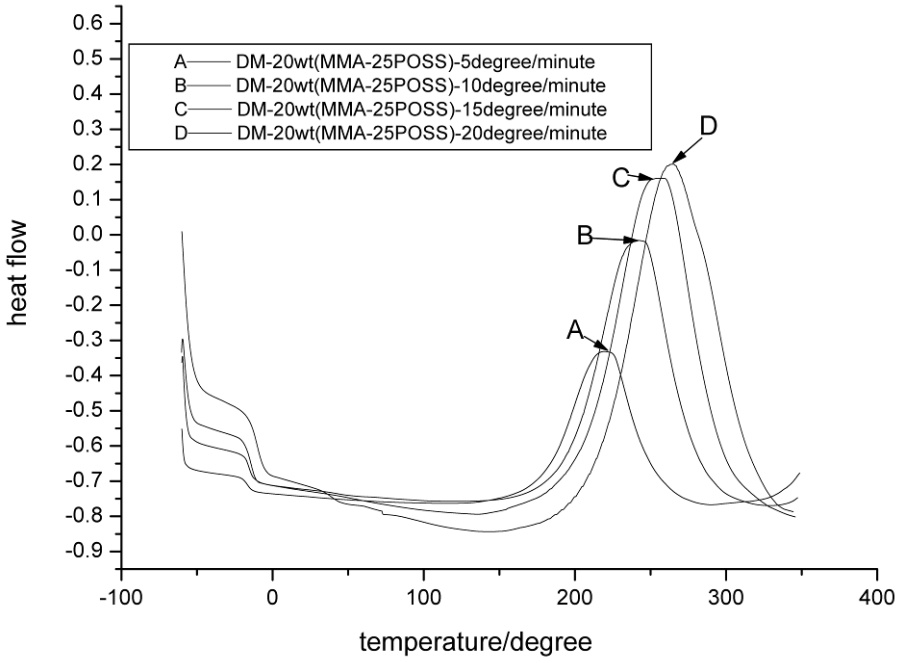

Figure 5.33 DSC at different scanning rate of DM-20wtP(MMA-25isobutylPOSS)

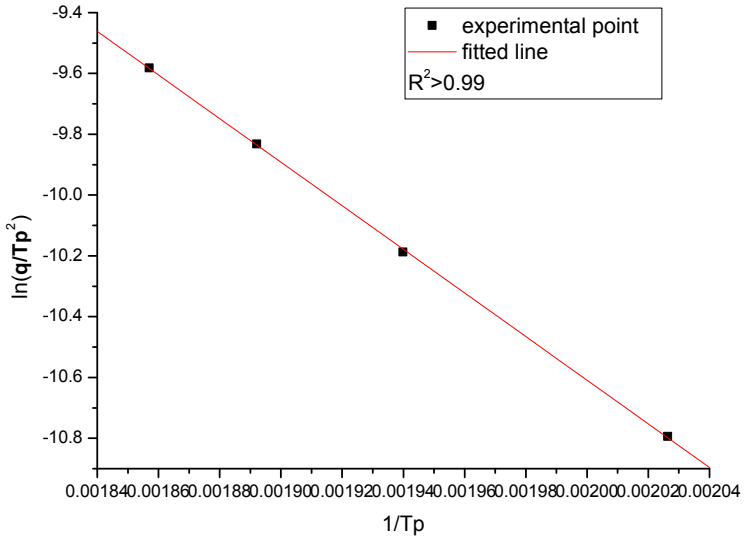

Figure 5.34 Utilizing Kissinger modal to calculate DM-20wtP(MMA-25isobutylPOSS) activation energy

Kinetic of epoxy curing process is quit complicated influenced by a lot of factors, in which many models are fitted. In general, the reaction rate of epoxy can be expressed as below:

$$\frac{d\alpha}{dt} = kf(\alpha)$$

The *k* is the constant of kinetic and the *f(α)* is function related to conversion. The *k* follows Arrhenius law:

$$k = A\exp(\frac{E}{RT})$$

Here, *A* is the activate energy and *R* is the universal gas constant. It can be determined:

$$\frac{d\alpha}{dt} = A\exp(\frac{E}{RT})f(\alpha)$$

According to the Kissinger method, the activation energy can be obtained from the maximum reaction rate, where *[d(da/dt)]/dt* is zero at a constant heating rate. Choosing the reaction maximum temperature *Tp* and increasing rate of temperature *q*, the reaction activate energy can be determined:

$$\frac{d\left[\ln\left(\frac{q}{T_p^2}\right)\right]}{d\left(\frac{1}{T_p}\right)} = -\frac{E}{R}$$

Table 5.4 The activation energy can read from the plot of $\ln(q/Tp^2)$ versus $1/Tp$. (See figure 5.29, 5.30, 5.31, 5.32, 5.33, 5.34).

sample	DM	DM-20*wt*P(MMA-15isobutylPOSS)	DM-20*wt*P(MMA-15isobutylPOSS)
Activation energy(kJ/mol)	58.23	63.48	59.59

In the case, the activation energy of net matrix is the lowest, whereas the introduction of POSS polymer increasing the activation energy. DM-20*wt* (MMA-15POSS) has higher activation energy than DM-20*wt*P(MMA- 25isobutylPOSS) (Table 5.4).

The activation energy of thermosetting system is influenced by paraments: The activation energy of DGEBA increases with the crosslinking density, namely decrease with the content of thermoplastic[255, 260]. The physical change in the network is resulted from the decrease of the distance between the polar groups in the components. The diffusion becomes difficult as crosslinking density increasing, Gupta[260] reported the activation energy enlarged from 34. 84 to 64.33 $KJmol^{-1}$ with DGEBA content from 50% to 80% in DGEBA. Further, in thermoplastic modified epoxy, the morphology influences the process of curing. Phase separation hinders the reaction between epoxy precursor and curing reagent, and induces a larger activation energy than that of the control epoxy[256, 262[255, 261]. However, the thermoplastic materials promotes the molecular mobility and to facilitates the curing reaction, compared with the rigid epoxy network, as reported by Calabrese etal [262] in CTBN/epoxy system.

Here, the activation energy of DM-20*wt*P(MMA-15isobutylPOSS) is resulted from joint effects: the thermoplastic polymer dilutes the control epoxy, enlarges the distance of polar group such as amine and epoxide, compresses the curing density; further, the thermoplastic polymer tackifies the control epoxy, hinders the diffusion of

precursor; moreover, the physical network forms by POSS-POSS interaction which leans to increase pseudo-curing density. However, for DM-20*wt*P(MMA-25isobutylPOSS), the decreased *Ea* is resulted from competition of these effects: free volume of bulky POSS is positive to the motion of precursor; dilution effect is compressed by phase separation, and the precursor diffused from the POSS rich phase more difficultly. The free volume reduction, because of the directional specific interchain, leads to a positive deviation of Tg composition curve which is approached by Schneider etal[263]. In our systems, POSS-POSS interaction results in a POSS rich domain self-aggregated, limiting the free volume introduced at the same time.

5.4 Simulating Vitrification v.s. the conversion of POSS composites

5.4.1 The model about vitrification

Vitrification was deeply researched as a mean to demonstrate the components interaction and variety of composites, especially in thermoset and thermoplastic mixture. The vitrification followed a powerful ruler of *Tg* and conversion in DGEBA blends with miscible component, which displayed the relation between vitrification and component. At a high conversion, the measurement deviated from the real value, because the reaction heat was inaccurate and uneasy to determine the baseline in DSC measurement. The test of vitrification temperature was relatively easy and high reliable through DSC measurement. It was a prospective candidate to resolve the difficulty in DSC, if the relationship can be confirmed. Vitrification of binary system was deeply researched and described through several models, especially in amorphous systems. At first, it was derived from the mixture of similar molecules, as the glass transition of polymer, and then developed in the system of different molecular weight polymers' blent with water and some solids. Several theories are utilized widely to simulate, such as Fox[264, 265], Gordon-Taylor[265, 266], Couchman[264, 265] [267]and Kwei[268, 269] equation. If we assumed that the vitrification was volumn additive completely, no special interaction between the components, the equation can be achieved as following:

$$T_g = \phi_1 Tg_1 + \phi_2 Tg_2$$

In this formula, Φ was the volumn fraction of each component. The relationship of Tg in blend was considered as a linear simple mixture. Thus, it can be related with

the thermo expansion coeffience changed at vitrification (Δα) and the density of the component (ρ), which was well known that $\phi_1 = \frac{\Delta\alpha w}{\rho}$ .It was possible to rewrite the relationship as:

$$Tg = \Delta\alpha w_1 Tg_1 / \rho_1 + \Delta\alpha w_2 Tg_2 / \rho_2$$

If we introduced $k=\Delta\alpha_1\rho_2/(\Delta\alpha_2\rho_1)$, the equation can be written as:

$$T_g = (w_1 T_{g1} + k w_2 Tg_2)/(w_1 + k w_2)$$

It was called as Gordon-Taylor equation. This equation can successfully describe the *Tg* behavior for miscible blends with positive or negative deviations if the parameter *k* is appropriately selected. It was an adjustable parameter in Gordon-Taylor equation, predicating the strength of component interaction. Kwei modified Gordon-Taylor equation by introducing a quadratic term qw_1w_2 (*q* is a constant), which is assumed to be proportional to the number of specific interactions between the two polymers[270].

$$T_g = \frac{(w_1 T_{g1} + k w_2 Tg_2)}{(w_1 + k w_2)} + q w_1 w_2$$

$$k = \frac{\rho_1 Tg_1}{\rho_2 Tg_2}$$

Weisse[271] treated the glass transition temperature as a process which consisted of vitrification of components, combining the Flory–Huggins interaction parameter with the Kwei equation.:

$$T_g = \frac{x_1 T_{g1} + k x_2 T_{g2}}{x_1 + x_2} - \frac{\chi R(Tg_2 - Tg_1)\phi_1\phi_2}{(x_1 + k x_2)(\Delta c_{p1} - x_2 \delta c_p^g)}$$

In the case of weak interactions between components and the *Tg* curve exhibits negative deviation from linear, an Gordon-Taylor uniform equation can be concluded from Weisse equation:

$$T_g = \frac{(w_1 T_{g1} + K' w_2 T_{g2})}{(w_1 + K' w_2)}$$

$$K' = \frac{\Delta c_{p1}}{\Delta c_{p2}} - \frac{\chi R(T_{g_1} - T_{g_2})\rho_2}{M_1 \rho_1 T_{g2} \Delta c_{p1}}$$

However, all the parameters in the equation were measurable from the experiment, without fitted. This equation utilized, glass transition temperature became

a powerful tool to determine interaction coefficient, except for ordinary melting point depression.

$$T_g = \frac{w_1 T_{g1} + k_0 w_2 T_{g2}}{w_1 + k_0 w_2} + \frac{\chi R (T_{g2} - T_{g1}) \rho_1 w_1 w_2}{(w_1 + \frac{\Delta c_{p2}}{\Delta c_{p1}} w_2)(w1 + w_2 \frac{M_2}{M_1})(w_1 + w_2 \frac{\rho_1}{\rho_2})\rho 2}$$

$$k_0 = \frac{\Delta c_{p2}}{\Delta c_{p1}}$$

Considering the determined character of the components as constant, the equation was changed into Kwei uniform equation.

Brostow etal [272]defined the deviation from simple vitrification temperature additive of :

$$\Delta T_g = T_g - T_g^{lin} = T_g - \left[x_1 T_{g1} + (1 - x_1) T_{g2} \right]$$

x_1 is defined as the molar ratio of component 1. Following a cubic polynomial centered on $2x_1-1=0$, at which the value is maximum was defined:

$$\Delta T_g = x_1 (1 - x_1) \left[a_0 + a_1 (2x_1 - 1) + a_2 (2x_1 - 1)^2 + a_3 (2x_1 - 1)^3 \right]$$

Thus *Tg* of composition is written as:

$$Tg = x_1 Tg_1 + (1 - x1) Tg_2 + x_1 (1 - x_1) \times \left[a_0 + a_1 (2x_1 - 1) + a_2 (2x_1 - 1)^2 + a_3 (2x_1 - 1)^3 \right]$$

From the definition, this method to calculate *Tg* was based on the mathematics simulation, that restricted the utilization of the equation in a miscible systems. However this multi-paraments equation was a versatile tool to simulate the behavior of curing, successfully approaching to data in some cases.

The majority of miscible binary polymer blends exhibited negative deviations of the glass temperature from the values predicted by the free volume or flexible bond additive rules. Some factors affected the accuracy of equation by increasing free volumn, such as induced interchain orientation by heterocontact between the components, the mobility in the neighborhood of the contacts, and the probability of related conformational entropy changes[273].

5.4.2 The relationship between conversion and Tg in POSS composites

In our systems, the quarternary blend consists of: amine, epoxy, epoxy/amine macromolecular precursors and POSS polymer, which is quite complicated to research the reciprocal interactions between components. Couchman equation,

developed by Di Benedetto equation and Pascault, was affirmed to approach the mechanism of epoxy curing process successfully. In Couchman equation,

$$\frac{Tg - Tg_0}{Tg_\infty - Tg_0} = \frac{\lambda x}{1-(1-\lambda)x}, \quad \lambda = \frac{\Delta Cp_\infty}{\Delta Cp_0}$$

In this case, the quarternary blend can be separated into a) additive,b) epoxy ternary mixture following Di Benedetto equation(Figure 5.35). According to the equation mentioned, the vitrification temperature of the epoxy ternary system can be approached when achieve the conversion of mixture, final network's and precusors' *Tg* (Tg_∞ and Tg_o respectively). Different equations approaching to the quarternary blend *Tg* was attempted in this part. The miscibility of polymer blends is often ascertained by measuring a single vitrification termperature, which is a function of composition. In partial crystalline blends, melting point *Tm* is pertinent with *Tg*, [274-276]. In our case, to avoid to involve with *Tm* into the system and to make the analysis simplify, thus the discussion is not extended to the effect of crystalline under *Tm* of POSS cage.

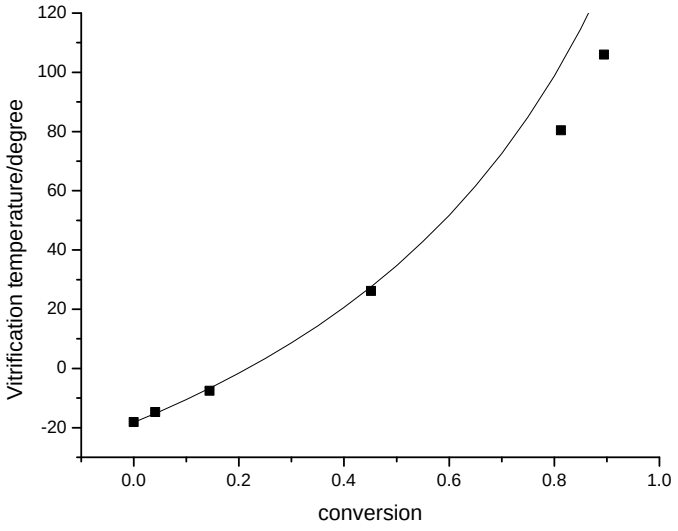

Figure 5.35 Tg of neat epoxy vs conversion, fitted with couchman equation.

Kovacs equation is based on the negligible excess volume upon mixing and ignores the attribution of interaction.

$$T_g = T_{g1} + f_{g2} / \alpha_1 (V_1 / V_2)$$

where *Vi* is the volume fractions, f_{g2} is the fractional free volume of component 2 at its *Tg*; and α_1 is the thermal expansion coefficient of component 1.

According to the free volume theory, the fractional free volume of polymers, a key parameter that is used to evaluate their molecular mobility, can be approximated to a universal value of ~0.025 at their glass transition temperatures. The predication of *Tg* with Pascault modified [277] Couchman equation is in accordance with the measured result, with deviation at high conversion for neat epoxy/amine.

A critical point in the Kovacs equation, Tc is necessarily higher then Tg, In our experiments, it is assumed that the volume fraction of epoxy-amine and POSS polymer is constant at *Tg*, whereas the universal value of 0.025 is utilized. The universal value, *fg2* in Kovacs equation is 0.025, which is a candidate to simulate *Tg* especially difficult to get Tg in a component probably. Therefore, vitrificaiton temperature of the blends is surprisingly just defined by the cubic thermal expansion coefficient and Tg of the polymer matrix. When the calculated Tg of epoxy-amine as X-axis and experimental Tg of blend as Y-axis, a line with a slope of 1 can be achieved. The thermal expansion coefficient can be read from the intercept of x-axis. The validity of the Kovacs equation for 3 mixture (r=0.96) reveals therefore that there is no appreciable excess volume upon POSS polymer and epoxy/amine system with the curing of epoxy. However, the fitted results is not very good in all system, especially in P(MMA-15isobutylPOSS-MMA) mixture.

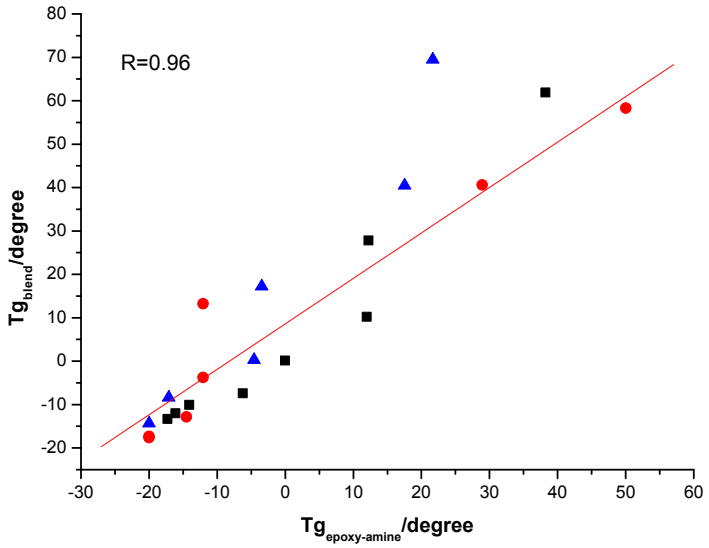

Figure 5.36 Kovacs equation demonstrates the *Tg* of blend and *Tg* of neat epoxy linearly.

The fitted result has a high confidence coefficient (R=0.96), with a slop=1.04 and the calculated thermal expansion of epoxy matrix is around $7.2*10^{-4}\ K^{-1}$, which is at the same order of magnitude as reported ($1.01\ *10^{-4}\ K^{-1}$)(Figure 5.36). The deviation was derived from the assumption a constant thermal expansion at different conversion potentially, which is reflect by the linear of experiment data is better at lower conversion. At low conversion, the blend of epoxy-amine matrix can be consider as a solution of epoxy and amine resolving with a small quantity of reacted precursors, which leads to the thermal expansion is consider as not far away from the constant. At high conversion, the variety of real thermal expansion is close to the final epoxy-amine network, which results in the deviation from linearity at high conversion

From the above discussion, the interaction and thermal expansion would not be ignored in the epoxy blend, to approach *Tg* with conversion precisely. The vitrification processes as a blending of completely cured and fully uncured epoxy. Generally, it is successful to simulate the binary or ternary system via the above equations. In our case, it is a quaternary system: epoxy precursor (DGEBA), curing agent (MDEA), fully cured epoxy and the thermal plastic polymer, which is impossible to deal directly via this equation. Here, it is hypothesis that the system could be treated as a blend of modifier and MDEA/epoxy/cured epoxy, which follows the Couchman equation. The inaccuracy is probably resulted from the difficulty in determination of base line at a high conversion in DSC. In this article, Fox, Gordon-Taylor equation and Weisse equation is attempted to simulate a correlation between conversion and *Tg*.

The Gordon-Taylor equation describes Tg of DM-20wtPMMA (Figure 5.37) and DM-20wtP(MMA-15isobutylPOSS) (Figure 5.38) composite with conversion exactly. The parameter *k*=0.084 in DM-20wt PMMA is less than the one of PMMA in DGEBA/ 4,4'-diamino-3,3'-dimethyldicyclohexyl-methane(3DCM,k=0.2), and in DGEBA/ Diethyltoluenediamine (DETDA) [278] which means the weaker interaction between PMMA and DM matrix than that of PMMA and DGEBA/3DCM, DGEBA/ DETDA, because of the different structural amine.

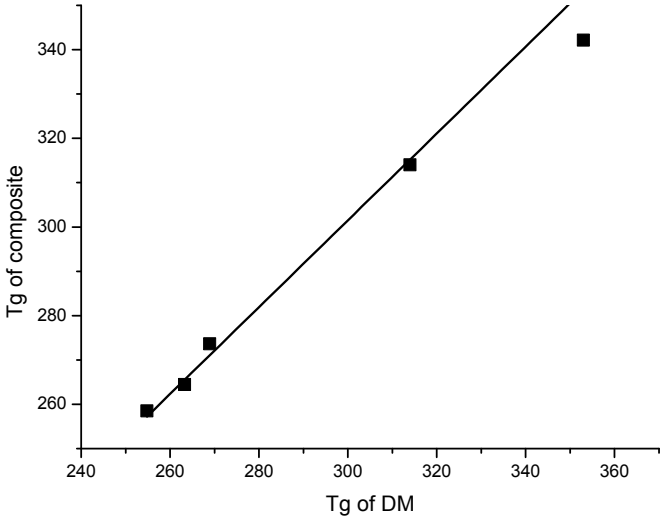

Figure 5.37 DM-20*wt*PMMA,R^2=0.97, *k*=0.084

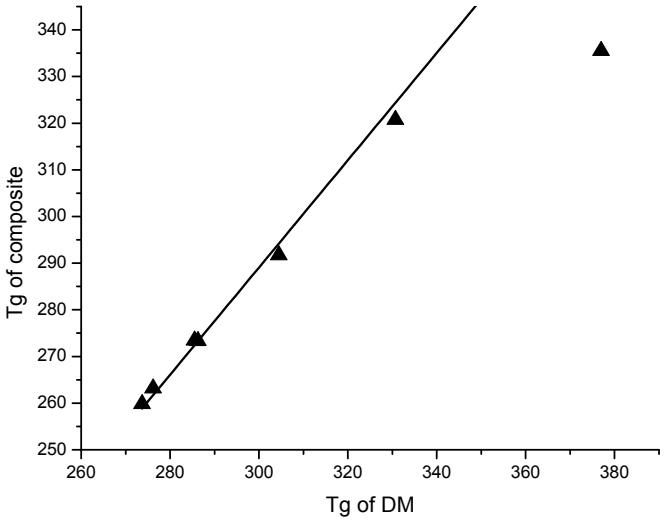

Figure 5.38 DM-20*wt*P(MMA-25isobutylPOSS), *k*=-0.052

The interaction of P(MMA-25isobutylPOSS) with epoxy network is weaker than the one of PMMA with matrix confirmed by the parameter k= -0.052(<k=0.084,PMMA). In the case of poly(MMA-15isobutylPOSS)(Figure 5.39), the confidence of simulated result is quite low (R^2>0.45) fitted with Gorden-Taylor equation. However, Weisse strong interaction equation, namely the Kwei's uniform equation simulated the data quite well, with a confidence of R^2>0.99. Parameter k=1.32 compares with the theoretical result appropriately, if we consider *k* of the

mixture in the scale of the fully cured and completely unreacted epoxy precursor, 0.6 <k<1.4($k_0 = \frac{\Delta c_{p2}}{\Delta c_{p1}}$).

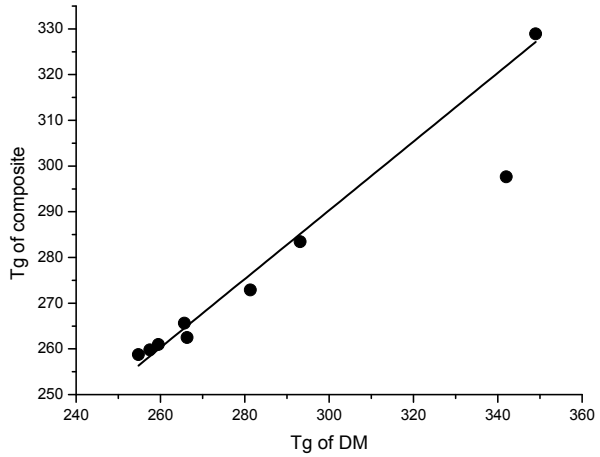

Figure 5.39 DM-20wtP(MMA-15isobutylPOSS), R2=0.99,k=1.32,k=-27.8

To determine the interaction parameter is difficult, because M_1 and M_2 is not defined for P(MMA-15isobutylPOSS). However, it is easy to conclude that the interaction parameter is negative from the simulation, because the other parameter in the uniform is positive. Generally, a negative interaction coefficient is observed in a strong interaction system for instance hydrogen bonding of carboxylic acid andhydroxyl groups, electron donor-acceptor complexes ionic interactions and transition metal complexe[279], which is in accordance with the presupposition of Weisse strong interaction. The strong interaction is assigned to the pseudo-network formed by the POSS-POSS interaction of POSS copolymer.

5.4 Conclusions:

1. Amphiphilic PMMA-POSS copolymers with the similar molar mass had been successfully introduced into DGEBA/MDEA. As a DGEBA compatible structure, percent of PMMA and its molecular topology determined the morphology of composites. In the random copolymers modified composites, the morphologies of samples changed from a homogenous to bicontinuous, until particle separated morphology according to the content of POSS increasing. In block copolymers composites, micelle formed and nanoparticle (less than 100 nm) dispersed in the

matrix, because of self-assembly of POSS block copolymers.

2. The mechanical properties of composites relates to the morphology of composites. All composites had lower *Tg* than the neat epoxy, attributed to free volumn of thermoplastic POSS copolymers. In 15% and 25% POSS samples, POSS plasticized the matrix and compress *Tg* of composites. However, the plasticizer effect was limited in full phase separated composite (45% POSS).

3. Introducing POSS into matrix improved the thermostability of composites within limits.

4. According to the investigation of rheoylogy, POSS polymers diluted DGEBA/MDEA mixture and enlongated the gelation time. In PMMA blend, the gelation took place more slowly than POSS copolymer, which could be assigned to the lubricant effect of POSS.

5. The relationship between *Tg* and conversion of DGEBA/MDEA was simulated with the Couchman equation. Here, to estimate the relationship between *Tg* and conversion, the POSS copolymers/DGEBA/MDEA blend was divided into binary systems, POSS copolymer and epoxy base matrix. The fitted result also showed a stronger interaction in the 15% POSS copolymer/epoxy blend.

Conclusions

The aim of this work is to nanostructure POSS into epoxy networks, via physical blend or chemical bonding. POSS is generally not distributed homogeneously and tends to agglomerate. Phase separation could occur between POSS and monomer(s) before and during polymerization depending on the chemical nature and functionality of the organic ligands of the POSS cages. **Reactive POSS analogue and partial compatible POSS copolymers** were synthesized and in-situ fabricated in nanocomposite when epoxy polymerization, namely the term of "**hybrid**".

In the first issue, **a reactive analogue of POSS**, named POSSMOCA was synthesized and characterized. After nanobuilding an epoxy network, it improved the thermostability, based on the synergic fire-retardent effect between silicon, nitrogen and halogen. **It is worthy notifying that POSSMOCA was amorphous** and crystallized after reacted with epoxy.

In the second issue, we attemptted to fabricate a hybrid POSS/epoxy by **another reactive analogue of POSS**. POSS-silanol reacted with DGEBA prepolymer via using different organic metal compounds as catalysts. To our knowledge these Cu and Co catalysts were not already described to catalyze POSS-OH and epoxy reactions. In this work, anhydride was considered as comonomer rather than a diamine, because the dependence with stoichiometric ratio between of epoxy and anhydride is relatively not important, compared with strickly stoichiometric amino hydrogen-to-epoxy in epoxy/amine systems. Hybrid O/I were prepared **with/without presence of moisture** and a mechanism of reactions involved, i.e. **competition between consumption of epoxy groups with anhydride and silanols** was proposed. Using model compounds, homopolymerisation of epoxy were confirmed via our chacterizations, which could explain some contradictory discussion on the influence of POSS-OH noticed in literature.

The ideal structure of POSS homogeneously dispersed in the matrix that is often desired, however frequently not achieved in practice due to the lack of compatibility of POSS with the matrix. The silicon nature of POSS constrains its compatibility with the matrix, although it's switchable with the vertex group. Although invariant the polarity of POSS monomer, POSS polymer copolymerized with other monomer, is able to tune the compatibility with DGEBA network. Even copolymer is compatible with the precursor, however aggregates resulting from the entropy of mixture decrease with the conversion of precursor, which means **the**

reaction induced phase separation. There are a few $[POSS]_m[A]_y$ copolymers were synthesized and modified in epoxy network. **In the third issue, partial compatible POSS copolymer were obtained by two steps:1. To synthesize reactive POSS-PGMA copolymer,** PGMA was homopolymerized via reversible addition-fragmentation transfer polymerization utilizing CDB as a chain transferring agent, to obtain a dioester terminated macro-initiator. Then the second POSS block was polymerized with PGMA macroinitiator at different ratio. The molar mass distributions were **monomodal and acceptably narrow**. The self-assembly of PGMA-POSS block copolymer indicated that the copolymer underwent micelle in selective solvent. 2. **To tail the compatibility** of the block copolymer with matrix and **to form nanostructure in a step-growth polymerization matrix**. We supposed that the curable **POSS block copolymer self-assembles** into micelle and **formed POSS core/intercrossing GMA-MDEA corona** in the epoxy base. After introduction into epoxy precursor, homodispersed nano domaine of POSS copolymer successfully formed effectively and improved the thermostability, which would be a preceramic role POSS played. Because the epoxide group has universal ring open agent, for instance acid, amine, anhydride, isocyanates and coordinating polymer.

In the last issue, POSS-PMMA copolymers are blent with the DGEBA/MDEA and observed their performances. Owing to the interaction between PMMA with DGEBA/MDEA via hydrogen bonding, POSS-PMMA formed sorts of morphologies, which depend on the **POSS concentration and topology of POSS-MMA copolymers**.

In this work, **amphiphilic PMMA-POSS copolymers** with the similar molar mass had been successfully **introduced into DGEBA/MDEA**. As a DGEBA compatible structure, percent of PMMA and its molecular topology determined the morphology of composites. In the random copolymers modified composites, the morphologies changed form a homogenous to bicontinuous, until particle separated morphology according to the content of POSS increasing. In block copolymers composites, micelle formed and nanoparticle (less than 100 nm) dispersed in the matrix, because of self-assembly of POSS block copolymers. The mechanical performance of composites related with the morphology of composites. **POSS plasticized** the matrix in partial compatible system; however it **is limited in fully phase separation composite.** Here, to estimate the relationship between Tg and conversion in POSS copolymers/DGEBA/MDEA blend, the blend is divide into binary systems, POSS copolymer and epoxy base matrix successfully.

The author would like to recommend, **as perspective research,** POSS-GMA block copolymer to structure a nanophase easily in UV curing resins, optical waveguide devices. GMA corona not only intercrosses with each segment, but covalently bond into network. PA, PAI, PU, PC, PET and PUA are possible nanostructurated via this “bottom-up” method. Moreover, other elemental hybrid POSS should be synthesized, such as Ti-POSS chelated with P ligand, could be a candidate for high performance fireproofing materials.

References

1. Nanko, M., *Definitions and Categories of Hybrid Materials.* Advances in Technology of Materials and Materials Processing, 2009. **11**(1): p. 1-8.
2. Li, G., et al., *Polyhedral Oligomeric Silsesquioxane (POSS) Polymers and Copolymers: A Review.* Journal of Inorganic and Organometallic Polymers, 2001. **11**(3): p. 123-154.
3. Mantz, R.A., et al., *Thermolysis of Polyhedral Oligomeric Silsesquioxane (POSS) Macromers and POSS-Siloxane Copolymers.* Chemistry of Materials, 1996. **8**(6): p. 1250-1259.
4. Zheng, L., et al., *Polymer Nanocomposites through Controlled Self-Assembly of Cubic Silsesquioxane Scaffolds.* Macromolecules, 2004. **37**(23): p. 8606-8611.
5. Skaria, S. and S.R. Schricker, *Synthesis and Characterization of Inorganic-Organic Hybrid Materials Derived from Polysilsesquioxanes (POSS)*, Taylor & Francis. p. 381 - 391.
6. Hurd, C.B., *Studies on Siloxanes. I. The Specific Volume and Viscosity in Relation to Temperature and Constitution.* Journal of the American Chemical Society, 1946. **68**(3): p. 364-370.
7. Hay, M.T., et al., *A Novel Linear Titanium(IV)-POSS Coordination Polymer.* Macromolecules, 2010. **43**(5): p. 2108-2110.
8. Yang, B., et al., *Poly(vinyl pyrrolidone-co-octavinyl polyhedral oligomeric silsesquioxane) hybrid nanocomposites: Preparation, thermal properties, and Tg improvement mechanism.* Journal of Applied Polymer Science, 2009. **111**(6): p. 2963-2969.
9. Xu, H., et al., *Glass transition temperatures of poly(hydroxystyrene-co-vinylpyrrolidone-co-isobutylstyryl polyhedral oligosilsesquioxanes).* Polymer, 2002. **43**(19): p. 5117-5124.
10. Seurer, B. and E.B. Coughlin, *Ethylene–Propylene–Silsesquioxane Thermoplastic Elastomers.* Macromolecular Chemistry and Physics, 2008. **209**(12): p. 1198-1209.
11. Haddad, T.S., B.D. Viers, and S.H. Phillips, *Polyhedral Oligomeric Silsesquioxane (POSS)-Styrene Macromers.* Journal of Inorganic and Organometallic Polymers, 2001. **11**(3): p. 155-164.
12. Markovic, E., et al., *Synthesis of POSS-Methyl Methacrylate-Based Cross-Linked Hybrid Materials.* Macromolecules, 2008. **41**(5): p. 1685-1692.
13. Yang, B.H., et al., *Synthesis and characterization of poly(methyl methacrylate-co-polyhedral oligomeric silsesquioxane) hybrid nanocomposites.* Chinese Chemical Letters, 2007. **18**(8): p. 960-962.
14. Tegou, E., et al., *Polyhedral oligomeric silsesquioxane (POSS) acrylate copolymers for microfabrication: properties and formulation of resist materials.* Microelectronic Engineering, 2004. **73-74**: p. 238-243.
15. Jeon, H.G., P.T. Mather, and T.S. Haddad, *Shape memory and nanostructure in poly(norbornyl-POSS) copolymers.* Polymer International, 2000. **49**(5): p. 453-457.

16. Xu, H., et al., *Characterization of poly(vinyl pyrrolidone-co-isobutylstyryl polyhedral oligomeric silsesquioxane) nanocomposites.* Journal of Applied Polymer Science, 2004. **91**(4): p. 2208-2215.
17. Xu, H., et al., *Poly(acetoxystyrene-co-isobutylstyryl POSS) Nanocomposites: Characterization and Molecular Interaction.* Journal of Polymer Research, 2002. **9**(4): p. 239-244.
18. Odian, G., *Principles of Polymerization.* Wiley:New York,, 1991.
19. Kotal, A., et al., *Synthesis of semitelechelic POSS-polymethacrylate hybrids by thiol-mediated controlled radical polymerization with unusual thermal behaviors.* Journal of Polymer Science Part A: Polymer Chemistry, 2008. **46**(3): p. 1111-1123.
20. Hutchinson, J.M., *Physical aging of polymers.* Progress in Polymer Science, 1995. **20**(4): p. 703-760.
21. Castelvetro, V., et al., *Synthesis and surface properties of microphase separated or nanostructured coatings based on hybrid and fluorinated acrylic copolymers.* Macromolecular Symposia, 2002. **187**(1): p. 165-176.
22. Castelvetro, V., et al., *Hybrid Nanocomposite Films from Mono- and Multi-Functional POSS Copolyacrylates in Miniemulsion.* Macromolecular Rapid Communications, 2006. **27**(8): p. 619-625.
23. Kwon, Y. and K.-H. Kim, *Synthesis of Norbornene Block Copolymers Containing Polyhedral Oligomeric Silsesquioxane by Sequential Ring-Opening Metathesis Polymerization.* Macromolecular Research, 2006. **14**(4): p. 424-429.
24. Carroll, J.B., et al., *"plug and Play" Polymers. Thermal and X-ray Characterizations of Noncovalently Grafted Polyhedral Oligomeric Silsesquioxane (POSS)-polystyrene Nanocomposites.* Macromolecules, 2003. **36**(17): p. 6289-6291.
25. Fu, B.X., A. Lee, and T.S. Haddad, *Styrene-butadiene-styrene Triblock Copolymers Modified with Polyhedral Oligomeric Silsesquioxanes.* Macromolecules, 2004. **37**(14): p. 5211-5218.
26. Miao, J., et al., *Self-Assembly and Chain-Folding in Hybrid Coil-Coil-Cube Triblock Oligomers of Polyethylene-b-Poly(ethylene oxide)-b-Polyhedral Oligomeric Silsesquioxane.* Macromolecules, 2007. **40**(15): p. 5460-5470.
27. Kim, B.-S. and P.T. Mather, *Morphology, Microstructure, and Rheology of Amphiphilic Telechelics Incorporating Polyhedral Oligosilsesquioxane.* Macromolecules, 2006. **39**(26): p. 9253-9260.
28. Kim, J.K., et al., *Morphology and rheological behaviors of poly(ethylene terephthalate) nanocomposites containing polyhedral oligomeric silsesquioxanes.* Journal of Applied Polymer Science, 2008. **107**(1): p. 272-279.
29. Kim, G.M., et al., *Hybrid epoxy-based thermosets based on polyhedral oligosilsesquioxane: Cure behavior and toughening mechanisms.* Journal of Polymer Science Part B: Polymer Physics, 2003. **41**(24): p. 3299-3313.
30. Yoon, K.H., et al., *Properties of poly(ethylene terephthalate) containing epoxy-functionalized polyhedral oligomeric silsesquioxane.* Polymer International, 2005. **54**(1): p. 47-53.
31. Iyer, S. and D.A. Schiraldi, *Role of Specific Interactions and Solubility in the Reinforcement of Bisphenol A Polymers with Polyhedral Oligomeric Silsesquioxanes.* Macromolecules, 2007. **40**(14): p. 4942-4952.
32. Sáchez-Soto, M., D.A. Schiraldi, and S. Illescas, *Study of the morphology and properties of melt-mixed polycarbonate-POSS nanocomposites.* European Polymer Journal, 2009. **45**(2): p. 341-352.

33. Kim, K.-M., D.-K. Keum, and Y. Chujo, *Organic-Inorganic Polymer Hybrids Using Polyoxazoline Initiated by Functionalized Silsesquioxane.* Macromolecules, 2003. **36**(3): p. 867-875.
34. Lee, K.M., et al., *Polycaprolactone-POSS Chemical/Physical Double Networks.* Macromolecules, 2008. **41**(13): p. 4730-4738.
35. Ni, Y. and S. Zheng, *Nanostructured Thermosets from Epoxy Resin and an Organic-inorganic Amphiphile.* Macromolecules, 2007. **40**(19): p. 7009-7018.
36. Ni, Y. and S. Zheng, *Supramolecular inclusion complexation of polyhedral oligomeric silsesquioxane capped poly(ε-caprolactone) with α-cyclodextrin.* Journal of Polymer Science Part A: Polymer Chemistry, 2007. **45**(7): p. 1247-1259.
37. Wu, F., T. Xie, and G. Yang, *Characterization of PBT/POSS nanocomposites prepared by in situ polymerization of cyclic poly(butylene terephthalate) initiated by functionalized POSS.* Journal of Polymer Science Part B: Polymer Physics. **48**(16): p. 1853-1859.
38. Liu, L. and W. Wang, *Synthesis and characterization of poly(methyl methacrylate) using monofunctional polyhedral oligomeric silsesquioxane as an initiator.* Polymer Bulletin, 2009. **62**(3): p. 315-325.
39. Wang, W., et al., *Synthesis and characterization of star-shaped block copolymers with polyhedral oligomeric silsesquioxane (POSS)core via ATRP.* Polymer Bulletin. **65**(9): p. 863-872.
40. Kessler, D., C. Teutsch, and P. Theato, *Synthesis of Processable Inorganic-Organic Hybrid Polymers Based on Poly(silsesquioxanes): Grafting from Polymerization Using ATRP.* Macromolecular Chemistry and Physics, 2008. **209**(14): p. 1437-1446.
41. Pyun, J., et al., *ABA triblock copolymers containing polyhedral oligomeric silsesquioxane pendant groups: synthesis and unique properties.* Polymer, 2003. **44**(9): p. 2739-2750.
42. Fei, M., et al., *Synthesis and characterization of AB block copolymers based on polyhedral oligomeric silsesquioxane.* Journal of Polymer Research, 2010. **17**(1): p. 19-23.
43. Ohno, K., et al., *Living Radical Polymerization by Polyhedral Oligomeric Silsesquioxane-Holding Initiators: Precision Synthesis of Tadpole-Shaped Organic/Inorganic Hybrid Polymers.* Macromolecules, 2004. **37**(23): p. 8517-8522.
44. Hirai, T., et al., *Hierarchical Nanostructures of Organosilicate Nanosheets within Self-Organized Block Copolymer Films.* Macromolecules, 2008. **41**(13): p. 4558-4560.
45. Hirai, T., et al., *Hierarchical Self-Assembled Structures from POSS-Containing Block Copolymers Synthesized by Living Anionic Polymerization.* Macromolecules, 2009. **42**(22): p. 8835-8843.
46. Lai, J.T., D. Filla, and R. Shea, *Functional Polymers from Novel Carboxyl-Terminated Trithiocarbonates as Highly Efficient RAFT Agents.* Macromolecules, 2002. **35**(18): p. 6754-6756.
47. Shim, S.E., H. Lee, and S. Choe, *Synthesis of Functionalized Monodisperse Poly(methyl methacrylate) Nanoparticles by a RAFT Agent Carrying Carboxyl End Group.* Macromolecules, 2004. **37**(15): p. 5565-5571.
48. Lima, V., et al., *Synthesis and characterization of telechelic polymethacrylates via RAFT polymerization.* Journal of Polymer Science Part A: Polymer Chemistry, 2005. **43**(5): p. 959-973.
49. Moad, G., et al., *Advances in RAFT polymerization: the synthesis of polymers with defined end-groups.* Polymer, 2005. **46**(19): p. 8458-8468.

50. Vijayakrishna, K., et al., *Synthesis by RAFT and Ionic Responsiveness of Double Hydrophilic Block Copolymers Based on Ionic Liquid Monomer Units.* Macromolecules, 2008. **41**(17): p. 6299-6308.
51. Lowe, A.B. and C.L. McCormick, *Reversible addition-fragmentation chain transfer (RAFT) radical polymerization and the synthesis of water-soluble (co)polymers under homogeneous conditions in organic and aqueous media.* Progress in Polymer Science, 2007. **32**(3): p. 283-351.
52. Zhang, W., et al., *Synthesis and self-assembly of tadpole-shaped organic/inorganic hybrid poly(N-isopropylacrylamide) containing polyhedral oligomeric silsesquioxane via RAFT polymerization.* Journal of Polymer Science Part A: Polymer Chemistry, 2008. **46**(21): p. 7049-7061.
53. Zhang, X.-Z. and R.-X. Zhuo, *Dynamic Properties of Temperature-Sensitive Poly(N-isopropylacrylamide) Gel Cross-Linked through Siloxane Linkage.* Langmuir, 2000. **17**(1): p. 12-16.
54. Zhang, W., et al., *Preparation and characterization of organic/inorganic hybrid polymers containing polyhedral oligomeric silsesquioxane via RAFT polymerization.* Reactive and Functional Polymers, 2009. **69**(2): p. 124-129.
55. Zhang, W., et al., *Synthesis via RAFT Polymerization of Tadpole-Shaped Organic/Inorganic Hybrid Poly(acrylic acid) Containing Polyhedral Oligomeric Silsesquioxane (POSS) and Their Self-assembly in Water.* Macromolecules, 2009. **42**(7): p. 2563-2569.
56. Zhang, W. and A.H.E. Muller, *Synthesis of tadpole-shaped POSS-containing hybrid polymers via "click chemistry".* Polymer, 2010. **51**(10): p. 2133-2139.
57. López, J., et al., *Blends of acrylonitrile–butadiene–styrene with an epoxy/cycloaliphatic amine resin: Phase-separation behavior and morphologies.* Journal of Applied Polymer Science, 2002. **85**(6): p. 1277-1286.
58. Hwang, J.W., et al., *Phase separation behavior of cyanate ester resin/polysulfone blends.* Journal of Applied Polymer Science, 1999. **74**(1): p. 33-45.
59. Goossens, S. and G. Groeninckx, *Mutual Influence between Reaction-Induced Phase Separation and Isothermal Crystallization in POM/Epoxy Resin Blends.* Macromolecules, 2006. **39**(23): p. 8049-8059.
60. Brooker, R.D., A.J. Kinloch, and A.C. Taylor, *The Morphology and Fracture Properties of Thermoplastic-Toughened Epoxy Polymers*, Taylor & Francis. p. 726 - 741.
61. Xu, Z. and S. Zheng, *Reaction-Induced Microphase Separation in Epoxy Thermosets Containing Poly(e-caprolactone)-block-poly(n-butyl acrylate) Diblock Copolymer.* Macromolecules, 2007. **40**(7): p. 2548-2558.
62. Yang, X., et al., *Morphology and mechanical properties of nanostructured blends of epoxy resin with poly([var epsilon]-caprolactone)-block-poly(butadiene-co-acrylonitrile)-block-poly([var epsilon]-caprolactone) triblock copolymer.* Polymer, 2009. **50**(16): p. 4089-4100.
63. Thio, Y.S., J. Wu, and F.S. Bates, *Epoxy Toughening Using Low Molecular Weight Poly(hexylene oxide)-Poly(ethylene oxide) Diblock Copolymers.* Macromolecules, 2006. **39**(21): p. 7187-7189.
64. Girard-Reydet, E., et al., *Polyetherimide-modified epoxy networks: Influence of cure conditions on morphology and mechanical properties.* Journal of Applied Polymer Science, 1997. **65**(12): p. 2433-2445.
65. Guo, Q., et al., *Phase separation, porous structure, and cure kinetics in aliphatic epoxy resin containing hyperbranched polyester.* Journal of Polymer Science Part B: Polymer Physics, 2006. **44**(6): p. 889-899.

66. Gerard, P., et al., *Toughness Properties of Lightly Crosslinked Epoxies Using Block Copolymers.* Macromolecular Symposia, 2007. **256**(1): p. 55-64.
67. Rebizant, V., et al., *Chemistry and Mechanical Properties of Epoxy-Based Thermosets Reinforced by Reactive and Nonreactive SBMX Block Copolymers.* Macromolecules, 2004. **37**(21): p. 8017-8027.
68. Li, G.Z., et al., *Viscoelastic and Mechanical Properties of Epoxy/Multifunctional Polyhedral Oligomeric Silsesquioxane Nanocomposites and Epoxy/Ladderlike Polyphenylsilsesquioxane Blends.* Macromolecules, 2001. **34**(25): p. 8686-8693.
69. Weickmann, H., et al., *PMMA nanocomposites and gradient materials prepared by means of polysilsesquioxane (POSS) self-assembly.* Journal of Materials Science, 2007. **42**(1): p. 87-92.
70. Misra, R., B.X. Fu, and S.E. Morgan, *Surface energetics, dispersion, and nanotribomechanical behavior of POSS/PP hybrid nanocomposites.* Journal of Polymer Science Part B-Polymer Physics, 2007. **45**(17): p. 2441-2455.
71. Zucchi, I.A., et al., *Monofunctional epoxy-POSS dispersed in epoxy-amine networks: Effect of a prereaction on the morphology and crystallinity of POSS domains.* Macromolecules, 2007. **40**(4): p. 1274-1282.
72. Ni, Y., S. Zheng, and K. Nie, *Morphology and thermal properties of inorganic-organic hybrids involving epoxy resin and polyhedral oligomeric silsesquioxanes.* Polymer, 2004. **45**(16): p. 5557-5568.
73. Matejka, L., et al., *Epoxy Networks Reinforced with Polyhedral Oligomeric Silsesquioxanes (POSS). Structure and Morphology.* Macromolecules, 2004. **37**(25): p. 9449-9456.
74. Zhang, C. and R.M. Laine, *Silsesquioxanes as synthetic platforms. II. Epoxy-functionalized inorganic-organic hybrid species.* Journal of Organometallic Chemistry, 1996. **521**(1-2): p. 199-201.
75. Mya, K.Y., et al., *Preparation and thermornechanical properties of epoxy resins modified by octafunctional cubic silsesquioxane epoxides.* Journal of Polymer Science Part a-Polymer Chemistry, 2004. **42**(14): p. 3490-3503.
76. Huang, J.C., et al., *Organic-inorganic nanocomposites from cubic silsesquioxane epoxides: direct characterization of interphase, and thermomechanical properties.* Polymer, 2005. **46**(18): p. 7018-7027.
77. Gao, J., D. Kong, and S. Li, *Preparation of BPA Epoxy Resin/POSS Nanocomposites and Nonisothermal Co-curing Kinetics with MeTHPA.* 2008, Taylor & Francis. p. 940 - 956.
78. Montero, B., et al., *Effect of an epoxy octasilsesquioxane on the thermodegradation of an epoxy/amine system.* Polymer International, 2009. **59**(1): p. 112-118.
79. Takala, M., et al., *Thermal, mechanical and dielectric properties of nanostructured epoxy-polyhedral oligomeric silsesquioxane composites.* Dielectrics and Electrical Insulation, IEEE Transactions on, 2009. **15**(5): p. 1224 - 1235.
80. Moon, J.H., et al., *Direct fabrication of 3D silica-like microstructures from epoxy-functionalized polyhedral oligomeric silsesquioxane (POSS).* Journal of Materials Chemistry, 2009. **19**(27): p. 4687-4691.
81. Tucker, S.J., et al., *Ambient cure POSS-epoxy matrices for marine composites.* Composites Part A: Applied Science and Manufacturing, 2010. **41**(10): p. 1441-1446.
82. Ramírez, C., et al., *Thermal behaviour of a polyhedral oligomeric silsesquioxane with epoxy resin cured by diamines.* Journal of Thermal Analysis and Calorimetry, 2003. **72**(2): p. 421-429.

83. Zhang, L., et al., *An Efficient Hybrid, Nanostructured, Epoxidation Catalyst: Titanium Silsesquioxane–Polystyrene Copolymer Supported on SBA-15*. Chemistry – A European Journal, 2007. **13**(4): p. 1210-1221.
84. Chiu, Y.-C., et al., *The POSS side chain epoxy nanocomposite: Synthesis and thermal properties.* Journal of Polymer Science Part B: Polymer Physics. **48**(6): p. 643-652.
85. Wu, K., et al., *Synthesis and characterization of a functional polyhedral oligomeric silsesquioxane and its flame retardancy in epoxy resin.* Progress in Organic Coatings, 2009. **65**(4): p. 490-497.
86. Huang, J.-M., et al., *Preparation and characterization of epoxy/polyhedral oligomeric silsesquioxane hybrid nanocomposites.* Journal of Polymer Science Part B: Polymer Physics, 2009. **47**(19): p. 1927-1934.
87. Matejka, L. and O. Dukh, *Organic-inorganic hybrid networks.* Die Makromolekulare Chemie. Macromolecular symposia, 2001. **171**: p. 181-188.
88. Cook, R.D., et al., *Dispersion characteristics of polyhedral oligomeric silsesquioxane nanostructured chemicals into a biphenol-A epichlorohydrin/3,3'' DDS epoxy system.* Polymer Preprints (American Chemical Society, Division of Polymer Chemistry), 2009. **50**(1): p. No pp given.
89. Kar, S. and J.S. Wiggins, *Rheological behavior and morphology of polyhedral oligomeric silsesquioxane (POSS) epoxy nanocomposites.* Polymer Preprints (American Chemical Society, Division of Polymer Chemistry), 2009. **50**(1): p. No pp given.
90. Zhang, Z., et al., *Using Octa(aminpropyl)silsesquioxane as the Curing Agent for Epoxy Resin*. 2007. p. 1665-1670.
91. Perrin, F.X., N. Chaoui, and A. Margaillan, *Effects of octa(3-chloroammoniumpropyl)octasilsesquioxane on the epoxy self-polymerisation and epoxy-amine curing.* Thermochimica Acta, 2009. **491**(1-2): p. 97-102.
92. Nakas, G.I. and C. Kaynak, *Use of different alkylammonium salts in clay surface modification for epoxy-based nanocomposites.* Polymer Composites, 2009. **30**(3): p. 357-363.
93. Mohan, T.P., M. Ramesh Kumar, and R. Velmurugan, *Rheology and curing characteristics of epoxy–clay nanocomposites.* Polymer International, 2005. **54**(12): p. 1653-1659.
94. Zhang, Z., et al., *Thermo-oxygen degradation mechanisms of POSS/epoxy nanocomposites.* Polymer Degradation and Stability, 2007. **92**(11): p. 1986-1993.
95. Hoque, M.A., Y.H. Cho, and Y. Kawakami, *High performance holographic gratings formed with novel photopolymer films containing hyper-branched silsesquioxane.* Reactive and Functional Polymers, 2007. **67**(11): p. 1192-1199.
96. Fu, J., et al., *Epoxy nanocomposites containing mercaptopropyl polyhedral oligomeric silsesquioxane: Morphology, thermal properties, and toughening mechanism.* Journal of Applied Polymer Science, 2008. **109**(1): p. 340-349.
97. Jothibasu, S., et al., *Synthesis and Characterization of a POSS-Maleimide Precursor for Hybrid Nanocomposites*. 2008. p. 67-85.
98. Ni, Y. and S.X. Zheng, *Epoxy resin containing octamaleimidophenyl polyhedral oligomeric silsesquioxane.* Macromolecular Chemistry and Physics, 2005. **206**(20): p. 2075-2083.
99. Xu, Y., et al., *Morphology and thermal properties of organic-inorganic hybrid material involving monofunctional-anhydride POSS and epoxy resin.* Materials Chemistry and Physics. **125**(1-2): p. 174-183.

100. Yu, D., et al., *Preparation of benzoxazine-containing silsesquioxanes and nanocomposites produced thereby*. 2007, (Beijing University of Chemical Technology, Peop. Rep. China). Application: CN
CN. p. 11pp.
101. Ni, C., et al., *The preparation of inorganic/organic hybrid nanomaterials containing silsesquioxane and its reinforcement for an epoxy resin network.* Colloid & Polymer Science, 2009. **288**(4): p. 469-477.
102. Herman Teo, J.K., et al., *Epoxy/polyhedral oligomeric silsesquioxane (POSS) hybrid networks cured with an anhydride: Cure kinetics and thermal properties.* Polymer, 2007. **48**(19): p. 5671-5680.
103. Zucchi, I.A., et al., *Monofunctional Epoxy-POSS Dispersed in Epoxy-amine Networks: Effect of a Prereaction on the Morphology and Crystallinity of POSS Domains.* Macromolecules, 2007. **40**(4): p. 1274-1282.
104. GAO, J.-G., et al., *Isothermal Curing Kinetics of POSSER and 4,4'-Diaminodiphenylsulfone System.* CHINESE JOURNAL OF APPLIED CHEMISTRY, 2008. **25**(7): p. 787-791.
105. Zhang, Z., et al., *Curing behavior of epoxy/POSS/DDS hybrid systems.* Polymer Composites, 2008. **29**(1): p. 77-83.
106. Lligadas, G., et al., *Bionanocomposites from Renewable Resources:Epoxidized Linseed Oil Polyhedral Oligomeric Silsesquioxanes Hybrid Materials.* Biomacromolecules, 2006. **7**(12): p. 3521-3526.
107. Schiraldi, D.A., et al., *Transparent nanocomposites of polyhedral oligomeric silsesquioxanes (POSS).* Polymer Preprints (American Chemical Society, Division of Polymer Chemistry), 2004. **45**(1): p. 642-643.
108. Jones, I.K., et al., *Effect of polyhedral-oligomeric-sil-sesquioxanes on thermal and mechanical behavior of SC-15 epoxy*. eXPRESS Polymer Letters, 2008. **2**(7): p. 494-501.
109. Di Luca, C., et al., *In-Situ Generation of a Dispersion of POSS Crystalline Platelets in an Epoxy Matrix Induced by Polymerization.* Macromolecules, 2010. **43**(21): p. 9014-9021.
110. Zhang, Z., et al., *Epoxy/POSS organic–inorganic hybrids: Viscoelastic, mechanical properties and micromorphologies.* Polymer Composites, 2007. **28**(2): p. 175-179.
111. Zhang, Z.-p., et al., *Study on the curing kinetics and properties of polyhedral oligomeric silsesquioxane (POSS)/epoxy hybrid resin system.* Zhongguo Jiaonianji, 2007. **16**(9): p. 1-4.
112. Camino, G., A. Fina, and D. Tabuani, *POSS as fire retardants.* High Performance Fillers for Polymer Composites 4th, Barcelona, Spain, Mar. 4-5, 2009: p. Paper 15/1-Paper 15/6.
113. Dong, S., et al., *Research on high temperature resistant anaerobic adhesive modified with polyhedral oligomeric silsesquioxane.* Zhanjie, 2007. **28**(3): p. 1-3, 12.
114. Gao, J.-g., et al., *Preparation and the curing kinetics of heat-resistant anaerobic adhesive containing-POSS.* Zhongguo Jiaonianji, 2007. **16**(10): p. 1-5.
115. Lichtenhan, J.D., et al., *High use temperature nanocomposite resins*. 2008, (Hybrid Plastics, Inc., USA). Application: US
US. p. 21 pp , Cont -in-part of U S Ser No 166,008.
116. Jiang, C.-j., J.-g. Gao, and X.-j. Zhang, *Synthesis and characterization of silsesquioxanes cage epoxy resin.* Reguxing Shuzhi, 2007. **22**(1): p. 5-8.
117. Zhang, C., B. Wang, and Z. Liang, *Fabrication of fire retardant materials with nanoadditives*. 2009, (Florida State University Research Foundation, USA). US. p. 17pp.

118. Pittman, C.U., Jr., et al., *Hybrid organic resin/POSS and resin/carbon nanofiber composites.* Abstracts of Papers, 225th ACS National Meeting, New Orleans, LA, United States, March 23-27,, 2003: p. MTLS-008.
119. Liu, Y.L., et al., *Epoxy/polyhedral oligomeric silsesquioxane nanocomposites from octakis(glycidyldimethylsiloxy)octasilsesquioxane and small-molecule curing agents.* Journal of Polymer Science Part A: Polymer Chemistry, 2006. **44**(12): p. 3825-3835.
120. Franchini, E., et al., *Influence of POSS structure on the fire retardant properties of epoxy hybrid networks.* Polymer Degradation and Stability, 2009. **94**(10): p. 1728-1736.
121. Wu, Q., et al., *Combustion and thermal properties of epoxy/phenyl-trisilanol polyhedral oligameric silsesquioxane nanocomposites.* SAMPE Conference Proceedings, 2008. **53**: p. 303/1-303/18.
122. Xu, Y., X. Zhu, and S. Yang, *Fabrication of 3D silica-like structures with high fidelity through interference lithography of epoxy functionalized polyhedral oligomeric silsesquioxanes (POSS).* Polymer Preprints (American Chemical Society, Division of Polymer Chemistry), 2009. **50**(1): p. No pp given.
123. Jeon, H., P. Mather, and T. Haddad, *Shape memory and nanostructure in poly(norbornyl-POSS) copolymers.* Polymer International, 2000. **49**(5): p. 453-457.
124. Wu, Q., et al., *Combustion and thermal properties of epoxy/phenyltrisilanol polyhedral oligomeric silsesquioxane nanocomposites.* Journal of Thermal Analysis and Calorimetry, 2010. **100**(3): p. 1009-1015.
125. Wang, X., et al., *Thermal degradation behaviors of epoxy resin/POSS hybrids and phosphorus-silicon synergism of flame retardancy.* Journal of Polymer Science, Part B: Polymer Physics, 2010. **48**(6): p. 693-705.
126. Xu, H., et al., *Synthesis and characterization of organic–inorganic hybrid polymers with a well-defined structure from diamines and epoxy-functionalized polyhedral oligomeric silsesquioxanes.* Journal of Applied Polymer Science, 2006. **101**(6): p. 3730-3735.
127. Xu, H., et al., *Characterization of poly(vinyl pyrrolidone-co-isobutylstyryl polyhedral oligomeric silsesquioxane) nanocomposites.* Journal of Applied Polymer Science, 2004. **91**(4): p. 2208-2215.
128. Abad, M.J., et al., *Epoxy networks containing large mass fractions of a monofunctional polyhedral oligomeric silsesquioxane (POSS).* Macromolecules, 2003. **36**(9): p. 3128-3135.
129. Wu, J., T.S. Haddad, and P.T. Mather, *Vertex Group Effects in Entangled Polystyrene-Polyhedral Oligosilsesquioxane (POSS) Copolymers.* Macromolecules, 2009. **42**(4): p. 1142-1152.
130. Choi, J., A.F. Yee, and R.M. Laine, *Organic/Inorganic Hybrid Composites from Cubic Silsesquioxanes. Epoxy Resins of Octa(dimethylsiloxyethylcyclohexylepoxide) Silsesquioxane.* Macromolecules, 2003. **36**(15): p. 5666-5682.
131. Cho, H., et al., *Synthesis, Morphology, and Viscoelastic Properties of Polyhedral Oligomeric Silsesquioxane Nanocomposites with Epoxy and Cyanate Ester Matrices.* Journal of Inorganic and Organometallic Polymers and Materials, 2005. **15**(4): p. 541-553.
132. Wu, J., et al., *Rheological Behavior of Entangled Polystyrene-Polyhedral Oligosilsesquioxane (POSS) Copolymers.* Macromolecules, 2007. **40**(3): p. 544-554.
133. Liu, H.Z., S.X. Zheng, and K.M. Nie, *Morphology and thermomechanical properties of organic-inorganic hybrid composites involving epoxy resin and an incompletely condensed polyhedral oligomeric silsesquioxane.* Macromolecules, 2005. **38**(12): p. 5088-5097.

134. Ritzenthaler, S., E. Girard-Reydet, and J.P. Pascault, *Influence of epoxy hardener on miscibility of blends of poly(methyl methacrylate) and epoxy networks.* Polymer, 2000. **41**(16): p. 6375-6386.
135. Zeng, K., et al., *Self-assembly behavior of hepta(3,3,3-trifluoropropyl) polyhedral oligomeric silsesquioxane-capped poly(epsilon-caprolactone) in epoxy resin: Nanostructures and surface properties.* Polymer, 2009. **50**(2): p. 685-695.
136. Franchini, E., et al., *c on the fire retardant properties of epoxy hybrid networks.* Polym. Degrad. Stab., 2009. **94**(10): p. 1728-1736.
137. Glodek, T.E., et al., *Properties and performance of fire resistant eco-composites using polyhedral oligomeric silsesquioxane (POSS) fire retardants.* Composites Science and Technology, 2008. **68**(14): p. 2994-3001.
138. Lu, S.-Y. and I. Hamerton, *Recent developments in the chemistry of halogen-free flame retardant polymers.* Progress in Polymer Science, 2002. **27**(8): p. 1661-1712.
139. Fina, A., et al., *Metal functionalized POSS as fire retardants in polypropylene.* Polymer Degradation and Stability, 2006. **91**(10): p. 2275-2281.
140. Carniato, F., et al., *Synthesis and Characterisation of Metal Isobutylsilsesquioxanes and Their Role as Inorganic–Organic Nanoadditives for Enhancing Polymer Thermal Stability.* European Journal of Inorganic Chemistry, 2007. **2007**(4): p. 585-591.
141. Bourbigot, S., S. Duquesne, and C. Jama, *Polymer Nanocomposites: How to Reach Low Flammability?* Macromolecular Symposia, 2006. **233**(1): p. 180-190.
142. Devaux, E., M. Rochery, and S. Bourbigot, *Polyurethane/clay and polyurethane/POSS nanocomposites as flame retarded coating for polyester and cotton fabrics.* Fire and Materials, 2002. **26**(4-5): p. 149-154.
143. Vlase, T., et al., *Thermooxidative stabilization of a MDI.* Journal of Thermal Analysis and Calorimetry. **99**(3): p. 973-979.
144. Nanda, A.K., et al., *Nanostructured Polyurethane/POSS Hybrid Aqueous Dispersions Prepared by Homogeneous Solution Polymerization.* Macromolecules, 2006. **39**(20): p. 7037-7043.
145. Li, C.Y., W.Y. Chiu, and T.M. Don, *Preparation of polyurethane dispersions by miniemulsion polymerization.* Journal of Polymer Science Part a-Polymer Chemistry, 2005. **43**(20): p. 4870-4881.
146. Zierkiewicz, W., D. Michalska, and T. Zeegers-Huyskens, *Molecular structures and infrared spectra of p-chlorophenol and p-bromophenol. Theoretical and experimental studies.* Journal of Physical Chemistry A, 2000. **104**(50): p. 11685-11692.
147. Bryan, G., A. Stephen, and H. Michael, *Hydrogen Bonding Interactions in Amorphous Salicyl Salicylate13.* Angewandte Chemie, 2000. **39**(20): p. 3601-3604.
148. Xu, H., et al., *Preparations, Thermal Properties, and Tg Increase Mechanism of Inorganic/Organic Hybrid Polymers Based on Polyhedral Oligomeric Silsesquioxanes.* Macromolecules, 2002. **35**(23): p. 8788-8793.
149. Jean-Hong, C. and C. Young-Di, *Crystallization behavior and morphological development of isotactic polypropylene blended with nanostructured polyhedral oligomeric silsesquioxane molecules.* Journal of Polymer Science Part B: Polymer Physics, 2006. **44**(15): p. 2122-2134.
150. Waddon, A.J. and E.B. Coughlin, *Crystal Structure of Polyhedral Oligomeric Silsequioxane (POSS) Nano-materials: A Study by X-ray Diffraction and Electron Microscopy.* Chemistry of Materials, 2003. **15**(24): p. 4555-4561.
151. Li, G., et al., *Cyanate Ester/Polyhedral Oligomeric Silsesquioxane (POSS) Nanocomposites: Synthesis and Characterization.* Chemistry of Materials, 2005. **18**(2): p. 301-312.

152. Miao, J.J. and L. Zhu, *Topology Controlled Supramolecular Self-Assembly of Octa Triphenylene-Substituted Polyhedral Oligomeric Silsesquioxane Hybrid Supermolecules.* Journal of Physical Chemistry B. **114**(5): p. 1879-1887.
153. Sheen, Y.-C., et al., *Synthesis and characterization of amorphous octakis-functionalized polyhedral oligomeric silsesquioxanes for polymer nanocomposites.* Polymer, 2008. **49**(18): p. 4017-4024.
154. Strachota, A., et al., *Formation of nanostructured epoxy networks containing polyhedral oligomeric silsesquioxane (POSS) blocks.* Polymer, 2007. **48**(11): p. 3041-3058.
155. Muench, V. and W. Frank, *Fire-retarding foams containing polyurethane and/or polyisocyanurate groups*. 1983, (BASF A.-G., Fed. Rep. Ger.). Application: EP
EP. p. 31 pp.
156. Zhang, L.L., A.H. Liu, and X.R. Zeng, *Flame-retardant epoxy resin from a caged bicyclic phosphate quadridentate silicon complex.* Journal of Applied Polymer Science, 2009. **111**(1): p. 168-174.
157. Cartier, H. and A. Chopin, *Halogen-free flame retardant thermoplastic compositions*. 2010, (Sabic Innovative Plastics IP B.V., USA). US. p. 8pp.
158. Camino, G., et al., *Fire Retardant Halogen-Antimony-Clay Synergism in Polypropylene Layered Silicate Nanocomposites.* Chemistry of Materials, 2001. **14**(1): p. 189-193.
159. Zeng, K. and S.X. Zheng, *Synthesis and Characterization of Organic/Inorganic Polyrotaxanes from Polyhedral Oligomeric Silsesquioxane and Poly(ethylene oxide)/alpha-Cyclodextrin Polypseudorotaxanes via Click Chemistry.* Macromolecular Chemistry and Physics, 2009. **210**(9): p. 783-791.
160. Liu, H., S. Zheng, and K. Nie, *Morphology and thermomechanical properties of organic-inorganic hybrid composites involving epoxy resin and an incompletely condensed polyhedral oligomeric silsesquioxane.* Macromolecules, 2005. **38**(12): p. 5088-5097.
161. Lee, A. and J.D. Lichtenhan, *Viscoelastic Responses of Polyhedral Oligosilsesquioxane Reinforced Epoxy Systems.* Macromolecules, 1998. **31**(15): p. 4970-4974.
162. Lichtenhan, J.D., et al., *The next generation of silicon-based plastics: polyhedral oligomeric silsesquioxane (POSS) nanocomposites.* Polymer Preprints (American Chemical Society, Division of Polymer Chemistry), 1998. **39**(1): p. 489-490.
163. Kim, Y.H. and R. Beckerbauer, *Role of End Groups on the Glass Transition of Hyperbranched Polyphenylene and Triphenylbenzene Derivatives.* Macromolecules, 1994. **27**(7): p. 1968-1971.
164. Zhang, X., et al., *Morphology, hydrogen-bonding and crystallinity of nano-hydroxyapatite/polyamide 66 biocomposites.* Composites Part A: Applied Science and Manufacturing, 2007. **38**(3): p. 843-848.
165. Kang, S.O., V.W. Day, and K. Bowman-James, *The Influence of Amine Functionalities on Anion Binding in Polyamide-Containing Macrocycles.* Organic Letters, 2009. **11**(16): p. 3654-3657.
166. Ma, X. and J. Yu, *The plastcizers containing amide groups for thermoplastic starch.* Carbohydrate Polymers, 2004. **57**(2): p. 197-203.
167. Borba, A., et al., *Low Temperature Infrared Spectroscopy Study of Pyrazinamide: From the Isolated Monomer to the Stable Low Temperature Crystalline Phase.* The Journal of Physical Chemistry A, 2009. **114**(1): p. 151-161.

168. Guo, Q., R. Thomann, and W. Gronski, *Synthesis and fractionated crystallization of organic-inorganic hybrid composite materials from an amphiphilic polyethylene-block-poly(ethylene oxide) diblock copolymer.* Polymer, 2007. **48**(14): p. 3925-3929.
169. Gardon, J.L., *Emulsion polymerization. VI. Concentration of monomers in latex particles*. 1968. p. 2859-2879.
170. Sulaiman, S., et al., *Silsesquioxane epoxy resins with low coefficient of thermal expansion.* Abstracts of Papers of the American Chemical Society, 2005. **230**: p. 358-PMSE.
171. Takahashi, K., et al., *New aminophenylsilsesquioxanes - Synthesis, properties, and epoxy nanocomposites.* Australian Journal of Chemistry, 2006. **59**(8): p. 564-570.
172. Choi, J., S.G. Kim, and R.M. Laine, *Organic/Inorganic Hybrid Epoxy Nanocomposites from Aminophenylsilsesquioxanes.* Macromolecules, 2003. **37**(1): p. 99-109.
173. Jothibasu, S., S. Premkumar, and M. Alagar, *Synthesis and characterization of a POSS-maleimide precursor for hybrid nanocomposites.* High Performance Polymers, 2008. **20**(1): p. 67-85.
174. Villanueva, M., et al., *Thermal study of an epoxy system DGEBA (n=0)/mXDA modified with POSS.* Journal of Thermal Analysis and Calorimetry, 2009. **96**(2): p. 575-582.
175. Zhang, Z., G. Liang, and X. Wang, *The effect of POSS on the thermal properties of epoxy.* Polymer Bulletin, 2007. **58**(5): p. 1013-1020.
176. Lee, Y.J., et al., *Syntheses, thermal properties, and phase morphologies of novel benzoxazines functionalized with polyhedral oligomeric silsesquioxane (POSS) nanocomposites.* Polymer, 2004. **45**(18): p. 6321-6331.
177. Soong, S.Y., et al., *The effects of thermomechanical history and strain rate on antiplasticization of PVC.* Polymer, 2008. **49**(6): p. 1440-1443.
178. Gao, J., Y. Du, and C. Dong, *Rheological behavior and mechanical properties of PVC/MAP-POSS nanocomposites.* Polymer Composites, 2010. **31**(10): p. 1822-1827.
179. Lu, T.L., T. Chen, and G.Z. Liang, *Synthesis, thermal properties, and flame retardance of the epoxy-silsesquioxane hybrid resins.* Polymer Engineering and Science, 2007. **47**(3): p. 225-234.
180. Musto, P., et al., *A study by Raman, near-infrared and dynamic-mechanical spectroscopies on the curing behaviour, molecular structure and viscoelastic properties of epoxy/anhydride networks.* Polymer, 2007. **48**(13): p. 3703-3716.
181. Guerrero, P., et al., *Influence of cure schedule and stoichiometry on the dynamic mechanical behaviour of tetrafunctional epoxy resins cured with anhydrides.* Polymer, 1996. **37**(11): p. 2195-2200.
182. Park, W.H. and J.K. Lee, *A study on isothermal cure behavior of an epoxy-rich/anhydride system by differential scanning calorimetry*. Journal of Applied Polymer Science, 1998. **67**(6): p. 1101-1108.
183. Templin, M., U. Wiesner, and H.W. Spiess, *Multinuclear solid-state-NMR studies of hybrid organic-inorganic materials.* Advanced Materials, 1997. **9**(10): p. 814-817.
184. Fu, B.X., M. Namani, and A. Lee, *Influence of phenyl-trisilanol polyhedral silsesquioxane on properties of epoxy network glasses.* Polymer, 2003. **44**(25): p. 7739-7747.
185. Zheng, Y., et al., *Study on the curing reaction, dielectric and thermal performances of epoxy impregnating resin with reactive silicon compounds as new diluents.* Journal of Applied Polymer Science, 2008. **107**(5): p. 3127-3136.

186. Giuffrida, S., et al., *Photochemical Mechanism of the Formation of Nanometer-Sized Copper by UV Irradiation of Ethanol Bis(2,4-pentandionato)copper(II) Solutions.* Chemistry of Materials, 2004. **16**(7): p. 1260-1266.
187. Hayase, S., et al., *Polymerization of cyclohexene oxide with aluminum complex-silanol catalysts. Part III. Dependence of catalytic activity on bulkiness of silanol and its intramolecular hydrogen bond.* Journal of Polymer Science, Polymer Chemistry Edition, 1981. **19**(11): p. 2977-85.
188. Hortschansky, P. and G. Heublein, *A study of interface reaction during composite formation between polybutadiene epoxide and highly dispersed silica or alumina.* Die Makromolekulare Chemie, 1991. **192**(7): p. 1535-1540.
189. Hayase, S., et al., *Polymerization of cyclohexene oxide with aluminum complex/silanol catalyst. VI. Oligomer and polymer effects.* Journal of Polymer Science: Polymer Chemistry Edition, 1983. **21**(2): p. 467-477.
190. Ni, Y., S.X. Zheng, and K.M. Nie, *Morphology and thermal properties of inorganic-organic hybrids involving epoxy resin and polyhedral oligomeric silsesquioxanes.* Polymer, 2004. **45**(16): p. 5557-5568.
191. Bizet, S., J. Galy, and J.F. Gerard, *Structure-property relationships in organic-inorganic nanomaterials based on methacryl-POSS and dimethacrylate networks.* Macromolecules, 2006. **39**(7): p. 2574-2583.
192. Levchik, S.V., et al., *Mechanistic study of thermal behaviour and combustion performance of carbon fibre-epoxy resin composites fire retarded with a phosphorus-based curing system.* Polymer Degradation and Stability, 1996. **54**(2-3): p. 317-322.
193. Levchik, S.V. and E.D. Weil, *Thermal decomposition, combustion and flame-retardancy of epoxy resins—a review of the recent literature.* Polymer International, 2004. **53**(12): p. 1901-1929.
194. Fina, A., et al., *Polypropylene metal functionalised POSS nanocomposites: A study by thermogravimetric analysis.* Polymer Degradation and Stability, 2006. **91**(5): p. 1064-1070.
195. Livage, J., M. Henry, and C. Sanchez, *Sol-gel chemistry of transition metal oxides.* Progress in Solid State Chemistry, 1988. **18**(4): p. 259-341.
196. Kopesky, E.T., et al., *Thermomechanical Properties of Poly(methyl methacrylate)s Containing Tethered and Untethered Polyhedral Oligomeric Silsesquioxanes.* Macromolecules, 2004. **37**(24): p. 8992-9004.
197. Bonnet, A., et al., *Epoxy-diamine thermoset/thermoplastic blends. 1. Rates of reactions before and after phase separation.* Macromolecules, 1999. **32**(25): p. 8517-8523.
198. Pyun, J. and K. Matyjaszewski, *The Synthesis of Hybrid Polymers Using Atom Transfer Radical Polymerization: Homopolymers and Block Copolymers from Polyhedral Oligomeric Silsesquioxane Monomers.* Macromolecules, 1999. **33**(1): p. 217-220.
199. Xu, Y., J. Yuan, and A.H.E. Muller, *Single-molecular hybrid nano-cylinders: Attaching polyhedral oligomeric silsesquioxane covalently to poly(glycidyl methacrylate) cylindrical brushes.* Polymer, 2009. **50**(25): p. 5933-5939.
200. Moad, G., E. Rizzardo, and S.H. Thang, *Radical addition-fragmentation chemistry in polymer synthesis.* Polymer, 2008. **49**(5): p. 1079-1131.
201. Lo Schiavo, S., et al., *Novel propylmethacrylate-monofunctionalized polyhedral oligomeric silsesquioxanes homopolymers prepared via radical bulk free polymerization.* European Polymer Journal, 2007. **43**(12): p. 4898-4904.

202. Sabaa, M.W., Z.R. Farag, and N.A. Mohamed, *Thermal degradation behavior of poly(vinyl chloride) in the presence of poly(glycidyl methacrylate).* Journal of Applied Polymer Science, 2008. **110**(4): p. 2205-2210.
203. Rychkov, I., *Block Copolymers Under Shear Flow.* Macromolecular Theory and Simulations, 2005. **14**(4): p. 207-242.
204. Zhang, L. and A. Eisenberg, *Multiple Morphologies and Characteristics of "Crew-Cut" Micelle-like Aggregates of Polystyrene-b-poly(acrylic acid) Diblock Copolymers in Aqueous Solutions.* Journal of the American Chemical Society, 1996. **118**(13): p. 3168-3181.
205. Fustin, C.-A., et al., *Multiple micellar morphologies from tri- and tetrablock copoly(2-oxazoline)s in binary water–ethanol mixtures.* Journal of Polymer Science Part A: Polymer Chemistry. **48**(14): p. 3095-3102.
206. Fina, A., et al., *POSS grafting on PPgMA by one-step reactive blending.* Polymer, 2009. **50**(1): p. 218-226.
207. Li, S., et al., *Preparation of thin ceramic monofilaments for TEM observation with novel embedding processes.* Ultramicroscopy. **111**(2): p. 117-122.
208. Lin, K.F. and Y.D. Shieh, *Core-shell particles designed for toughening the epoxy resins. II. Core-shell-particle-toughened epoxy resins.* Journal of Applied Polymer Science, 1998. **70**(12): p. 2313-2322.
209. Nagasaki, Y., et al., *The Reactive Polymeric Micelle Based on An Aldehyde-Ended Poly(ethylene glycol)/Poly(lactide) Block Copolymer.* Macromolecules, 1998. **31**(5): p. 1473-1479.
210. Grubbs, R.B., et al., *Reactive Block Copolymers for Modification of Thermosetting Epoxy.* Macromolecules, 2000. **33**(26): p. 9522-9534.
211. Calzaferri, G. and R. Hoffmann, *The symmetrical octasilasesquioxanes X8Si8O12: electronic structure and reactivity.* Journal of the Chemical Society, Dalton Transactions, 1991(issue S): p. 917 - 928.
212. Fina, A., et al., *Polyhedral oligomeric silsesquioxanes (POSS) thermal degradation.* Thermochimica Acta, 2006. **440**(1): p. 36-42.
213. Schartel, B., et al., *Layered silicate epoxy nanocomposites: formation of the inorganic-carbonaceous fire protection layer.* Polymers for Advanced Technologies: p. n/a-n/a.
214. Amir, N., A. Levina, and M.S. Silverstein, *Nanocomposites through copolymerization of a polyhedral oligomeric silsesquioxane and methyl methacrylate.* Journal of Polymer Science Part A: Polymer Chemistry, 2007. **45**(18): p. 4264-4275.
215. Montserrat, S., J. Malek, and P. Colomer, *Thermal degradation kinetics of epoxy-anhydride resins: II. Influence of a reactive diluent.* Thermochimica Acta, 1999. **336**(1-2): p. 65-71.
216. Hruby, M., et al., *Thermoresponsive, Hydrolytically Degradable Polymer Micelles Intended for Radionuclide Delivery.* Macromolecular Bioscience, 2009. **9**(10): p. 1016-1027.
217. Maazouz, A., H. Sautereau, and J.F. Gérard, *Toughening of epoxy networks using pre-formed core-shell particles or reactive rubbers.* Polymer Bulletin, 1994. **33**(1): p. 67-74.
218. Roberts, R.J., R.C. Rowe, and P. York, *The relationship between Young's modulus of elasticity of organic solids and their molecular structure.* Powder Technology, 1991. **65**(1-3): p. 139-146.
219. Roberts, R.J., R.C. Rowe, and P. York, *The relationship between the fracture properties, tensile strength and critical stress intensity factor of organic solids and*

their molecular structure. International Journal of Pharmaceutics, 1995. **125**(1): p. 157-162.
220. Palmese, G.R. and R.L. McCullough, *Effect of epoxy–amine stoichiometry on cured resin material properties.* Journal of Applied Polymer Science, 1992. **46**(10): p. 1863-1873.
221. Nielsen, L.E., *Effects of Chemical Heterogeneity in Copolymers on Some Physical Properties.* Journal of the American Chemical Society, 1953. **75**(6): p. 1435-1439.
222. Vallo, C.I., P.M. Frontini, and R.J.J. Williams, *The glass transition temperature of nonstoichiometric epoxy–amine networks.* Journal of Polymer Science Part B: Polymer Physics, 1991. **29**(12): p. 1503-1511.
223. Fernandez-Nograro, F., et al., *Dynamic and mechanical properties of DGEBA/poly(propylene oxide) amine based epoxy resins as a function of stoichiometry.* European Polymer Journal, 1996. **32**(2): p. 257-266.
224. Kopesky, E.T., et al., *Miscibility and viscoelastic properties of acrylic polyhedral oligomeric silsesquioxane-poly(methyl methacrylate) blends.* Polymer, 2005. **46**(13): p. 4743-4752.
225. Li, S., G.P. Simon, and J.G. Matisons, *Morphology of blends containing high concentrations of POSS nanoparticles in different polymer matrices.* Polymer Engineering & Science, 2010. **50**(5): p. 991-999.
226. Lee, Y.J., et al., *Synthesis and characterization of polybenzoxazine networks nanocomposites containing multifunctional polyhedral oligomeric silsesquioxane (POSS).* Polymer, 2006. **47**(12): p. 4378-4386.
227. Soong, S.Y., et al., *Rate-Dependent Deformation Behavior of POSS-Filled and Plasticized Poly(vinyl chloride).* Macromolecules, 2006. **39**(8): p. 2900-2908.
228. Tsarevsky, N.V., et al., *Halogen exchange in atom transfer radical polymerization as a route to well-defined block copolymers.* Polymer Preprint (Am Chem Soc, Div Polym Chem), 2005. **46**: p. 249–250.
229. Ferriol, M., et al., *Thermal degradation of poly(methyl methacrylate) (PMMA): modelling of DTG and TG curves.* Polymer Degradation and Stability, 2003. **79**(2): p. 271-281.
230. Manring, L.E., *Thermal degradation of poly(methyl methacrylate). 4. Random side-group scission.* Macromolecules, 1991. **24**(11): p. 3304-3309.
231. Kabiri, K., H. Mirzadeh, and M.J. Zohuriaan-Mehr, *Undesirable effects of heating on hydrogels.* Journal of Applied Polymer Science, 2008. **110**(6): p. 3420-3430.
232. Leung, W.M., D.E. Axelson, and J.D. Van Dyke, *Thermal degradation of polyacrylamide and poly(acrylamide-co-acrylate).* Journal of Polymer Science Part A: Polymer Chemistry, 1987. **25**(7): p. 1825-1846.
233. Fraser-Reid, B., et al., *Novel Reactions of Carbohydrates Discovered En Route to Natural Products.* Bulletin des Sociétés Chimiques Belges, 1992. **101**(7): p. 617-626.
234. Kim, B.-S. and P.T. Mather, *Amphiphilic Telechelics Incorporating Polyhedral Oligosilsesquioxane:1. Synthesis and Characterization.* Macromolecules, 2002. **35**(22): p. 8378-8384.
235. Tomczak, S.J., et al., *Properties and Improved Space Survivability of POSS (Polyhedral Oligomeric Silsesquioxane) Polyimides.* Edwards AFRL , Air Force ,technical paper.
236. Lee, L.H. and W.C. Chen, *Organic-inorganic hybrid materials from a new octa(2,3-epoxypropyl)silsesquioxane with diamines.* Polymer, 2005. **46**(7): p. 2163-2174.
237. Pellice, S.A., D.P. Fasce, and R.J.J. Williams, *Properties of epoxy networks derived from the reaction of diglycidyl ether of bisphenol A with polyhedral oligomeric*

silsesquioxanes bearing OH-functionalized organic substituents. Journal of Polymer Science Part B-Polymer Physics, 2003. **41**(13): p. 1451-1461.
238. Ning, L., W. De-Ning, and Y. Sheng-Kang, *Hydrogen bonding between urethane and urea: band assignment for the carbonyl region of FTi.r. spectrum.* Polymer, 1996. **37**(14): p. 3045-3047.
239. Lin, H.M., et al., *Polyhedral Oligomeric Silsesquioxane Containing Copolymers for Negative-Type Photoresists.* Macromolecular Rapid Communications, 2006. **27**(18): p. 1550-1555.
240. Zhang, Y., et al., *Phenolic Resin/Octa(aminophenyl)-T8-Polyhedral Oligomeric Silsesquioxane (POSS) Hybrid Nanocomposites: Synthesis, Morphology, Thermal and Mechanical Properties.* Journal of Inorganic and Organometallic Polymers and Materials, 2007. **17**(1): p. 159-171.
241. Tang, Y. and M. Lewin, *Migration and surface modification in polypropylene (PP)/polyhedral oligomeric silsequioxane (POSS) nanocomposites.* Polymers for Advanced Technologies, 2009. **20**(1): p. 1-15.
242. dell'Erba, I. and R. Williams, *Epoxy networks modified by multifunctional polyhedral oligomeric silsesquioxanes (POSS) containing amine groups.* Journal of Thermal Analysis and Calorimetry, 2008. **93**(1): p. 95-100.
243. Liu, Y., Y. Ni, and S. Zheng, *Polyurethane Networks Modified with Octa(propylglycidyl ether) Polyhedral Oligomeric Silsesquioxane.* Macromolecular Chemistry and Physics, 2006. **207**(20): p. 1842-1851.
244. Huang, F., et al., *Organic/inorganic hybrid bismaleimide resin with octa(aminophenyl)silsesquioxane.* Polymer Engineering & Science, 2008. **48**(5): p. 1022-1028.
245. Willemse, R.C., et al., *Tensile moduli of co-continuous polymer blends.* Polymer, 1999. **40**(24): p. 6645-6650.
246. Nielsen, L.E., *Morphology and the elastic modulus of block polymers and polyblends.* Rheologica Acta, 1974. **13**(1): p. 86-92.
247. Mondragon, I., et al., *Viscoelastic behaviour of epoxy resins modified with poly(methyl methacrylate).* Polymer International, 1998. **47**(2): p. 152-158.
248. Remiro, P.M., et al., *Design of morphology in PMMA-modified epoxy resins by control of curing conditions. I. Phase behavior.* Journal of Applied Polymer Science, 1999. **74**(4): p. 772-780.
249. Zheng, L., et al., *X-ray Characterizations of Polyethylene Polyhedral Oligomeric Silsesquioxane Copolymers.* Macromolecules, 2002. **35**(6): p. 2375-2379.
250. Meynie, L., et al., *Limitation of the Coalescence of Evolutive Droplets by the Use of Copolymers in a Thermoplastic/Thermoset Blend.* Macromolecular Materials and Engineering, 2005. **290**(9): p. 906-911.
251. Fine, T. and J.-P. Pascault, *Structured Thermoplastic/Thermoset Blends Using Block Copolymers.* Macromolecular Symposia, 2006. **245-246**(1): p. 375-385.
252. Qian, J.Y., et al., *The role of dispersed phase morphology on toughening of epoxies.* Polymer, 1997. **38**(1): p. 21-30.
253. Huang, Y., et al., *Particle-Matrix Interfacial Bonding*, in *Toughened Plastics I*. 1993, American Chemical Society. p. 189-210.
254. Oyanguren, P.A., et al., *Phase separation induced by a chain polymerization: Polysulfone-modified epoxy/anhydride systems.* Journal of Polymer Science Part B: Polymer Physics, 1998. **36**(8): p. 1349-1359.
255. Calabrese, L. and A. Valenza, *Effect of CTBN rubber inclusions on the curing kinetic of DGEBA-DGEBF epoxy resin.* European Polymer Journal, 2003. **39**(7): p. 1355-1363.

256. Aharoni, S.M., *Dilute and concentrated solution properties of zigzag polymers comprising long rodlike segments with freely rotating joints.* Macromolecules, 1987. **20**(4): p. 877-884.
257. Jansen, J.C., et al., *Rheological evaluation of the influence of polymer concentration and molar mass distribution on the formation and performance of asymmetric gas separation membranes prepared by dry phase inversion.* Polymer, 2005. **46**(25): p. 11366-11379.
258. Soong, D. and M. Shen, *Shear-rate-dependent viscosity of non-Newtonian suspensions and entangled polymer systems.* Polymer Engineering & Science, 1980. **20**(17): p. 1177-1180.
259. Xie, M. and H. Li, *Viscosity reduction and disentanglement in ultrahigh molecular weight polyethylene melt: Effect of blending with polypropylene and poly(ethylene glycol).* European Polymer Journal, 2007. **43**(8): p. 3480-3487.
260. Gupta, A., R. Singhal, and A.K. Nagpal, *Reactive blends of epoxy resin (DGEBA) crosslinked by anionically polymerized polycaprolactam: Process of epoxy cure and kinetics of decomposition.* Journal of Applied Polymer Science, 2004. **92**(2): p. 687-697.
261. Thomas, R., et al., *Cure kinetics, morphology and miscibility of modified DGEBA-based epoxy resin - Effects of a liquid rubber inclusion.* Polymer, 2007. **48**(6): p. 1695-1710.
262. Atarsia, A. and R. Boukhili, *Relationship between isothermal and dynamic cure of thermosets via the isoconversion representation.* Polymer Engineering and Science, 2000. **40**(3): p. 607-620.
263. Bouslah, N., et al., *Study of the miscibility of poly(ethyl methacrylate-co-4-vinylpyridine)/poly(styrene-co-cinnamic acid) blends.* Polymer Bulletin, 1999. **42**(6): p. 701-708.
264. Cortázar, M., et al., *Glass transition temperatures of plasticized polyarylate.* Polymer Bulletin, 1987. **18**(2): p. 149-154.
265. An, L., et al., *Effects of molecular weight and interaction parameter on the glass transition temperature of polystyrene mixtures and its blends with polystyrene/poly (2,6-dimethyl-p-phenylene oxide).* European Polymer Journal, 1997. **33**(9): p. 1523-1528.
266. Schneider, H.A., *The Gordon-Taylor equation. Additivity and interaction in compatible polymer blends.* Die Makromolekulare Chemie, 1988. **189**(8): p. 1941-1955.
267. Yang, J., L. An, and T. Xu, *The glass transition temperatures of PS/PPO blends: Couchman volume-based equation and its verification.* Polymer, 2001. **42**(18): p. 7887-7892.
268. Hsu, W.-P., *Phase behavior and a modified Kwei equation for ternary polymer blends containing stereoregular PMMA.* Thermochimica Acta, 2006. **441**(2): p. 137-143.
269. Slark, A.T., *Application of the Kwei equation to the glass transition of dye solute-polymer blends.* Polymer, 1999. **40**(8): p. 1935-1941.
270. Cicala, G., et al., *Synthesis and thermal characterization of some novel ABA block copolymers.* Macromolecular Materials and Engineering, 2007. **292**(5): p. 588-597.
271. Lu, X. and R.A. Weiss, *Relationship between the glass transition temperature and the interaction parameter of miscible binary polymer blends.* Macromolecules, 1992. **25**(12): p. 3242-3246.
272. Brostow, W., et al., *Prediction of glass transition temperatures: Binary blends and copolymers.* Materials Letters, 2008. **62**(17-18): p. 3152-3155.

273. Schneider, H.A., *Conformational Entropy Contributions to the Glass Temperature of Blends of Miscible Polymers Volume.* Journal of Research of the National Institute of Standards and Technology, 1997. **102**(2): p. 229-248.
274. Harris, J.E., et al., *Miscible binary blends containing the polyhydroxy ether of bisphenol-a and various aliphatic polyesters.* Journal of Applied Polymer Science, 1982. **27**(3): p. 839-855.
275. Sakka, S. and J.D. Mackenzie, *Relation between apparent glass transition temperature and liquids temperature for inorganic glasses.* Journal of Non-Crystalline Solids, 1971. **6**(2): p. 145-162.
276. Lee, W.A. and G.J. Knight, *Ratio of the glass transition temperature to the melting point in polymers.* British Polymer Journal, 1970. **2**(1): p. 73-80.
277. Eloundou, J.P., et al., *Modeling complex permittivity of an epoxy-amine system using simultaneous kinetic and microdielectric studies.* Macromolecular Chemistry and Physics, 2002. **203**(13): p. 1974-1982.
278. Mounif, E., et al., *Poly(methyl methacrylate)-modified epoxy/amine system for reactive rotational moulding: crosslinking kinetics and rheological properties.* Polymer International, 2009. **58**(8): p. 954-961.
279. Lu, X. and R.A. Weiss, *Relationship between the glass transition temperature and the interaction parameter of miscible binary polymer blends.* Macromolecules, 1992. **25**(12): p. 3242-6.

Nanostructuration of Epoxy Networks by Using Polyhedral Oligomeric Silsesquioxanes POSS and Its Copolymers

Abstract

A series of hybrid component based on reactive polyhedral oligomeric silsesquioxane(POSS) precusors and its reactive copolymers of PGMA were synthesized and utilized to nanobuild in epoxy. Reactive POSS and copolymer dispersed in homogenous in matrix, overcomed POSS-POSS interaction, which resulted in macroscale phase separation. The nanocomposites obtained were analyzed by Scanning electron microscopy, Transmission electron microscopy, X-ray scattering and dynamic mechanical.

An analogue of POSS (denoted as POSSMOCA) was synthesized via addition reaction, which had reactive amino group bonding into epoxy network and improved the thermostability, because of the structural silicon, nitrogen and halogen. Epoxy/polyhedral oligomeric silsesquioxanes (POSS) hybrid composites were prepared from prereaction between trifunctional silanol POSS-OH and diglycidyl ether of bisphenol A (DGEBA) via silanol and the oxirane group.

Reactive POSS-PGMA was polymerized via Reversible addition-fragmentation transfer polymerization. It was easy to tail the compatibility of the epoxide block copolymer with a step-growth polymerized matrix, to form nanostructure via reaction with PGMA segements. In the case of inert POSS-PMMA copolymers modified epoxy, topology of copolymer defined the final morphology and interaction between epoxy and them, because of directional hydrogen bonding and dilution effect. *Tg* of different epoxide conversion, obeyed of Gordon-Taylor equation and Kwei equation, *k* which reflected the interaction of modifier and DGEBA/MEDA and epoxy/amine oligomers, was consistent of the reology and dynamic results.

Mots-Clés : POSS, nanostructurate, epoxy, copolymer, hybrid

Abréviations et symboles

a.u.	Arbitrary Unity
AIBN	AzobisIsoButyroNitrile
ATRP	Atom Transfer Radical Polymerization
BCPs	block copolymers
CED	Cohesive Energy Density
Cp	CycloPentyl
CpPOSS	CycloPentyl-POSS, POSS bearing Cy substituents
Cy	CycloHexyl
CyPOSS	CycloHexyl-POSS, POSS bearing Cy substituents
DGEBA	Diglycidyl Ether of Bishenol A
DMSO	dimethyl sulfoxide
DP	Degree of polymerization
E	Young Modulus (expressed in Pa)
E’	Storage Modulus (expressed in Pa)
Isobutyl POSS	Heptaisobutyl-propylmethacrylate-POSS
NCO	isocyanate
Tg	glass transition temperature
Tmax	temperature of the main degradation event
Tanδ	loss factor
T5	the temperature at at which there is 5% weight loss
Tα (peak)	temperature of the α-transition
THF	TetraHydroFurane
PA	Polyamide
PU	Poly Urethane
PUA	Polyurea
ROMP	Ring-opening metathesis copolymerization
PI	polyimide
OAPS	octaaminophenyl POSS
WAXS	Wide Angle X-ray Scattering

FOLIO ADMINISTRATIF

THESE SOUTENUE DEVANT L'INSTITUT NATIONAL DES SCIENCES APPLIQUEES DE LYON

NOM :Jiangfeng DATE de SOUTENANCE : 2012

Prénoms : Chen

TITRE :
NANOSTRUCTURATION OF EPOXY NETWORKS BY USING POLYHEDRAL OLIGOMERIC SILSESQUIOXANES POSS AND ITS COPOLYMERS

NATURE : Doctorat Numéro d'ordre : 2012-ISAL-

Ecole doctorale : Matériaux de Lyon

Spécialité : Matériaux Polymères et Composites

Cote B.I.U. - Lyon : T 50/210/19 / et bis CLASSE :

RESUME : Une série de composant hybride basée sur réactives polyédriques oligomères silsesquioxane (POSS) precusors et ses copolymères réactifs de PGMA ont été synthétisés et utilisés pour nanobuild en époxy. POSS réactifs et de copolymères en dispersion dans la matrice homogène dans, au délà de POSS-POSS interaction, ce qui a entraîné la séparation de phase macroscopique. Les nanocomposites obtenus ont été analysés par microscopie électronique à balayage, microscopie électronique à transmission, diffusion des rayons X et l'analyse mécanique dynamique.

Un analogue de POSS (notée POSSMOCA) a été synthétisé par réaction d'addition, qui a réactive liaison groupe amino dans le réseau époxy et d'améliorer la stabilité thermique, en raison du silicium, d'azote et un atome d'halogène structurel. Époxy / polyédriques silsesquioxanes oligomères (POSS) composites hybrides ont été préparés à partir de pré-réaction entre l'éther de silanol POSS-OH et diglycidylique trifonctionnel de bisphénol A (DGEBA) par l'intermédiaire du silanol et un groupe oxiranne.

Réactif POSS-PGMA a été polymérisé par polymérisation par transfert de réversible par addition-fragmentation. Il est facile à queue de la compatibilité du copolymère séquencé époxyde avec une matrice de l'étape de croissance-polymérisé, pour former par réaction avec nanostructure segements PGMA. Dans le cas d'inertes POSS-PMMA copolymères modifiés époxy, topologie de copolymère défini la morphologie finale et l'interaction entre époxy et entre eux, en raison de la liaison hydrogène directionnelle à effet de dilution. *Tg* de conversion époxyde différente, obéi de Gordon-Taylor équation et l'équation Kwei, *k* qui reflète l'interaction de modificateur et les oligomères DGEBA / MEDA et époxy / amine, était cohérente de la rhéologie et les résultats dynamiques.

Mots-Clés : POSS, nanostructurate, époxy, copolymère, hybride.

Laboratoire (s) de recherche : Ingenierie des Matériaux Polymères (IMP)
UMR 5223 INSA de Lyon

Directeurs de thèse:Professor Jean-François GERARD, Professor DAI Lizong

Président de jury :

Composition du jury :

Prof. LU	Canzhong	Fujian Institute of Structure of Matter, CAS	– Rapporteur
Prof. CHEN	Xudong	Sun Yat-sen University	– Rapporteur
Prof.GERARD	Jean-François	INSA Lyon	–Directrice de thèse
Prof DAI	Lizong	Xiamen University	– Directrice de thèse
Prof. Wu	Huihuang	Xiamen University	– Examinateur
Dr. XU	Yiting	Xiamen University	– Examinateur